



ERNEST ORLANDO LAWRENCE
BERKELEY NATIONAL LABORATORY

A Total Cost of Ownership Model for Solid Oxide Fuel Cells in Combined Heat and Power and Power-Only Applications

Roberto Scataglini, Ahmad Mayyas¹, Max Wei, Shuk Han Chan², Timothy Lipman¹, David Gosselin², Anna D'Alessio², Hanna Breunig, Whitney G. Colella³, and Brian D. James³

Environmental Energy Technologies Division

December 2015

¹University of California, Berkeley, Transportation Sustainability Research Center, Berkeley, California

²University of California, Berkeley, Laboratory for Manufacturing and Sustainability, Department of Mechanical Engineering, Berkeley, California

³Strategic Analysis, Inc. (SA), Energy Services Division, 4075 Wilson Blvd., Suite 200, Arlington VA 22203

This work was supported by the U.S. Department of Energy, Office of Energy Efficiency and Renewable Energy (EERE) Fuel Cells Technologies Office (FCTO) under Lawrence Berkeley National Laboratory Contract No. DE-AC02-05CH11231

DISCLAIMER

This document was prepared as an account of work sponsored by the United States Government. While this document is believed to contain correct information, neither the United States Government nor any agency thereof, nor The Regents of the University of California, nor any of their employees, makes any warranty, express or implied, or assumes any legal responsibility for the accuracy, completeness, or usefulness of any information, apparatus, product, or process disclosed, or represents that its use would not infringe privately owned rights. Reference herein to any specific commercial product, process, or service by its trade name, trademark, manufacturer, or otherwise, does not necessarily constitute or imply its endorsement, recommendation, or favoring by the United States Government or any agency thereof, or The Regents of the University of California. The views and opinions of authors expressed herein do not necessarily state or reflect those of the United States Government or any agency thereof, or The Regents of the University of California.

Ernest Orlando Lawrence Berkeley National Laboratory is an equal opportunity employer.

ACKNOWLEDGEMENTS

The authors gratefully acknowledge the U.S. Department of Energy, Office of Energy Efficiency and Renewable Energy (EERE) Fuel Cells Technologies Office (FCTO) for their funding and support of this work.

The authors would like to thank the following individuals and companies for their expert input on SOFC system designs, system specifications, and manufacturing equipment and processes.

- Brian Borglum, Fuel Cell Energy
- SOFCpower, Mezzolombardo, Italy
- Minh Nguyen, University of California, San Diego
- Professor Massimo Santarelli, Polytechnic University of Turin, Italy
- Professor Jack Brouwer, University of California, Irvine
- Patricia Irving, InnovaTek
- Jim W. Dennis, HED international, Inc.
- Dixita Bhat, Bionics Scientific Technologies Pvt. Ltd.
- Mathias Rachau, FuelCon AG
- Alexey Peshkovsky, Industrial Sonomechanics, LLC
- Martin De Moya, Haiku Tech, Inc.
- Edward Stone, Manncorp
- Charles H. Birks, Keith Company
- Fabio Pagnotta, Aurel Automation S.p.A
- Donald Wang, Ph.D., Inframat Advanced Materials
- Nickle Shang, Qingdao Terio Corporation
- Dick Wildman, Dowd and Guild Inc.
- Chris Betz, CHEMPOINT Inc.
- Matthew Dickerson, American Chemical Inc.
- Christian Ames, Univar USA

Executive Summary

A total cost of ownership model (TCO) is described for emerging applications in stationary fuel cell systems. Solid oxide fuel cell systems (SOFC) for use in combined heat and power (CHP) and power-only applications from 1 to 250 kilowatts-electric (kWe¹) are considered. The total cost of ownership framework expands the direct manufacturing cost modeling framework of other studies to include operational costs and life-cycle impact assessment of possible ancillary financial benefits during operation and at end-of-life. These include credits for reduced emissions of global warming gases such as carbon dioxide (CO₂) and methane (CH₄), reductions in environmental and health externalities, and end-of-life recycling.

System designs and functional specifications for SOFC fuel cell systems (FCS) for CHP and power-only applications were developed across the range of system power levels above. Bottom-up cost estimates were made based on currently installed fuel cell systems for balance of plant (BOP) costs, and detailed design-for-manufacturing-and-assembly² (DFMA) cost analysis was carried out to estimate the direct manufacturing costs for key fuel cell stack components. The costs of the fuel processor subsystem are also based on a DFMA analysis (James et. al., 2012). The development of high throughput, automated processes achieving high yield are estimated to push the direct manufacturing cost per kWe for the SOFC fuel cell stack to \$370/kWe and \$180/kWe for a 10-kWe system at 1,000 units per year and 50,000 units per year, respectively. The sub-\$200/kWe stack cost projection is below the high volume \$238/kWe stack cost target set by the National Energy Technology Laboratory (NETL 2013). Overall system costs including a 50% corporate markup are estimated to be \$2380/kWe and \$1660/kWe for a 10-kWe system, again at 1000 units per year and 50,000 units per year, respectively. The high volume system cost meets the U.S. Department of Energy's (DOE) 2020 target of \$1700/kWe for 10-kWe fuel cell CHP systems (DOE 2014).

At high production volume, material costs make up the largest component of stack costs (up to 59% of overall stack direct cost at highest modeled volume). Based on the decline in stack costs at moderate to larger production volumes, we find that BOP costs (including the fuel processor) dominate overall system direct costs for CHP systems and are thus a key area for further cost reduction. For CHP systems at low power, the fuel processing and electrical power subsystems are the largest cost contributor of total non-stack costs. At high power, the electrical power subsystem is the dominant cost contributor.

In this round of cost estimates, a DFMA analysis was not applied to the non-fuel processor balance of plant components and cost estimates were based on industrial price quotes. It is expected that a full DFMA analysis of the non-fuel processor balance of plant components could show a greater trend towards cost reduction with increases in production volume.

Life-cycle or use-phase modeling and life cycle impact assessment (LCIA) were carried out for two building types (small hotels and hospitals) in six U.S. cities. At an annual production volume of 100 MWe (e.g., 10-kWe systems at 10,000 units per year or 50-kWe system at 2,000 units per year), life cycle costs for SOFC systems are competitive with grid-based electricity and conventional heating in many parts of the country with the modeled SOFC costs here as an input. In regions in the U.S. with

¹ In this report, units of kWe stand for net kW electrical power unless otherwise noted.

² DFMA is a registered trademark of Boothroyd, Dewhurst, Inc. and is the combination of the design of manufacturing processes and design of assembly processes for ease of manufacturing and assembly and cost reduction.

high-carbon intensity electricity from the grid³, total cost of ownership credits can further reduce the levelized cost of electricity for buildings with fuel cell CHP. TCO costs for fuel cell CHP systems are dependent on several factors such as the cost of natural gas, utility tariff structure, amount of waste heat utilization, carbon intensity of displaced electricity and conventional heating, carbon price, and valuation of health and environmental externalities. These factors typically depend on geographic location of the CHP installation. For example, a fuel cell CHP system that displaces a large quantity of fossil heating fuel such as heating oil will have a larger environmental benefit than one that displaces natural gas heating fuel. As with CHP systems in general, regions with a higher spark spread are more economically favorable⁴. Quantification of externality damages to the environment and public health utilized earlier environmental impact assessment work and datasets available at LBNL.

Overall, this type of total cost of ownership analysis quantification is important to identify key opportunities for direct cost reduction, to fully value the costs and benefits of fuel cell systems in stationary applications, and to provide a more comprehensive context for future potential policies.

³ In this work, different marginal emissions factors for CO₂, NO_x, and SO₂ from grid-based electricity are assumed for each of the eight North American Electric Reliability Corporation (NERC) regions in the United States (Siler-Evans et al. 2012).

⁴ Spark spread is defined as follows: $SS = \text{Price of Electricity} - [(\text{Price of Gas}) * (\text{Heat Rate})] = \$/\text{MWh} - [(\$/\text{MMBtu}) * (\text{MMBtu} / \text{MWh})]$, or equivalently, the theoretical gross margin of a gas-fired power plant from selling a unit of electricity. Heat rate is often taken as 2.0 by convention for gas-fired plants. CHP systems powered by natural gas are more economically favorable in regions with large spark spread.

Table of Contents

1	Introduction.....	1
1.2	Emerging applications.....	3
1.3	Total Cost of Ownership Modeling	3
2.	System design and Functional specs	5
2.1	System and Component Lifetime	5
2.2	System Design	5
2.2.1	System Design for SOFC CHP.....	5
2.2.2	System Design for SOFC non-CHP.....	7
2.3	System Functional Specifications	7
2.3.1	Functional specifications for SOFC CHP system	7
2.3.2	Functional specifications for SOFC non-CHP system	9
3.	Costing Approach and Considerations	11
3.1.	DFMA Costing Model Approach	13
3.2.	Non-Product Costs	16
3.3.	Manufacturing Cost Analysis - Shared Parameters.....	17
3.4.	Factory model.....	19
3.5.	Yield Considerations.....	19
3.6.	Initial Tool Sizing	20
3.7.	Time-frame for Cost Analysis.....	20
4.	Direct Manufacturing Cost Analysis of Stack Components.....	21
4.1.	Electrode-Electrolyte Assembly (EEA) Manufacturing Cost Analysis	21
4.2.	Interconnect Manufacturing Cost Analysis.....	71
4.3.	Frame Manufacturing Cost Analysis.....	86
4.4.	EEA Cell-to-Frame Seal Cost Analysis	95
4.5.	Stack Assembly and Testing Analysis.....	113
4.6.	FC Stack Manufacturing Cost Results	132
5.	Balance of Plant Costs.....	153
5.1.	Overview.....	153
5.2.	Costing Approach.....	153
5.3.	System Terminology	154
5.4.	Balance of Plant Results	157
5.4.1.	CHP System with Reformate fuel	157
5.4.2	Electricity Only System with Reformate fuel.....	160

5.5.	Conclusions.....	161
6.	Total System Costs	163
7	Life Cycle Assessment (LCA) Model.....	168
7.1	Life Cycle Assessment (LCA) Model.....	168
7.1.1	Use-phase Model	169
7.1.2	Results and Discussion	172
7.2	Conclusions for Use-Phase Model.....	177
7.3	Life Cycle Impact Assessment (LCIA) Modeling	177
7.4	Total Cost of Ownership Modeling Results	178
7.	Conclusions.....	184
	Bibliography and References	185

1 Introduction

As the world moves toward a more carbon-constrained economy, a better understanding of the costs and benefits of “cleaner” technology options such as fuel cells are critically needed as industry and governments make research, development, and deployment funding decisions and as organizations and individuals make long term investment decisions. Fuel cell systems are being considered for a range of stationary and specialty transport applications due to their ability to provide reliable power with cleaner direct emissions profiles than fossil fuel combustion-based systems. Existing and emerging applications include primary and backup power, combined heat and power (CHP), materials handling applications such as forklifts and pallet trucks, and auxiliary power applications.

As a chemical energy conversion device, fuel cells have intrinsically higher efficiency and much lower criteria pollutant emissions than coal or gas combustion-based plants. In addition, fuel cells can serve as a reliable source of baseload power in comparison to intermittent wind or solar photovoltaic supply sources. If fuel cells were to displace coal plants they could improve public health outcomes due to the elimination of coal-fired air pollutants such as fine particulate matter, and they might also displace nuclear plants and avert the disposal issues associated with nuclear waste. Fuel cell systems also can qualify as distributed generation systems and as power supply sources close to load, they do not trigger transmission line construction or line losses. Natural gas supplied fuel cell systems result in lower overall CO₂-equivalent (CO₂-e) emissions than the average U.S. grid emissions, and biomass gasification sources offer low to zero emissions in the future (e.g., Doherty et al. 2015)).

Over the last decade, the U.S. Department of Energy (DOE) has supported several cost analysis studies for fuel cell systems for both automotive (e.g., James 2010, Sinha 2010) and non-automotive systems (e.g., Mahadevan 2010, James 2012). While these and other cost studies and cost projections as a function of manufacturing volume have been done for specific fuel cell stack technologies and for automotive fuel cell systems, fewer cost studies have been done for stationary fuel cell applications. The limited studies available have primarily focused on the manufacturing costs associated with fuel cell system production (e.g., James 2012). This project expands the scope and modeling capability from existing direct manufacturing cost modeling in order to quantify more fully the broader economic benefits of fuel cell systems by taking into account the full production and use lifecycle, and air pollutant impacts. The full value of fuel cell systems cannot be captured without considering the full range of total cost of ownership (TCO) factors. TCO modeling provides valuable data and information in a carbon-constrained economy and in a context where health and environmental impacts are increasingly valued.

This report provides TCO estimates based around direct manufacturing cost modeling of CHP and power-only systems in the 1 to 250 kWe range for solid oxide fuel cell (SOFC) systems, including a detailed breakdown of fuel cell stack, balance of plant, and fuel subsystem component costs. Table 1.1 provides a depiction of the system sizes and production volumes considered. CHP systems assume reformate fuel with natural gas as the input fuel. Life-cycle costs of CHP systems are estimated for two commercial building types (small hotels and hospitals) in different geographical regions of the U.S. A health and environmental impact assessment is provided for fuel cell-based CHP systems compared to a baseline of grid-based electricity and fossil fuel-based heating (e.g., natural gas, fuel oil, wood, etc., or some combination thereof). This is not meant to be a market penetration study, although promising CHP market regions of the country are identified. Rather, the overriding context is to assume that this market is available to fuel cell systems and to address what range of costs can be achieved and under what assumptions.

Table 1.1. Application space for this work. CHP are Studied at various production volumes and system sizes.

Application	Size [kW]	Production volume (units/year)			
		100	1000	10,000	50,000
Stationary Power (P); Combined Heat and Power (C)	1	C	C	C	C
	10	P, C	P, C	P,C	P,C
	50	P,C	P,C	P,C	P,C
	100	P,C	P,C	P,C	P,C
	250	P,C	P,C	P,C	P,C

Detailed cost studies provide the basis for estimating cost sensitivities to stack components, materials, and balance of plant components and identify key cost component limiters. Other key outputs of this effort are manufacturing cost sensitivities as a function of system size and annual manufacturing volume. Such studies can be compared to DOE fuel cell system cost targets or highlight key requirements for DOE targets to be met. Insights gained from this study can be applied toward the development of lower-cost, higher-volume manufacturing processes that can meet DOE combined heat and power system equipment cost targets.

1.1 Technical Targets and Technical Barriers

For stationary applications, DOE has set several fuel cell system cost and performance targets (DOE 2014). For example, a 10-kWe residential combined heat and power system in 2020 should have an equipment cost below \$1700/kWe, electrical generation efficiency greater than 45%, durability in excess of 60,000 hours, and system availability at 99%. Table 1.2 shows a summary of equipment cost targets for natural gas based systems excluding installation costs.

Table 1.2. DOE Multiyear plan system equipment cost targets for 10-kWe and 100-250-kWe system sizes for 2015 and 2020.

System Type	2015 Target	2020 Target
10-kWe CHP System	\$1900/kWe	\$1700/kWe
100-250-kWe, CHP System	\$2300/kWe	\$1000/kWe
Stack Cost at high production volume (NETL 2013)⁵	\$238/kWe	

Stationary fuel cell systems are not deployed in high volumes today due to their still high initial capital costs, lack of familiarity, concerns with hydrogen as a fuel source, and other new technology adoption barriers (see for example, DOE 2012 and EPA 2015). Among the identified barriers to more rapid deployment of fuel cells are:

- Reservations about new technology;
- Concerns about supply chains and component availability;
- Administration/transactional costs;

⁵ Stack Cost target is quoted for “Nth of a kind DG SOFC unit (1 GW cumulative installed capacity)” assumed to be achieved in 2030 (NETL 2013). The target in US2011\$ is \$225/kWe, or \$238/kWe in US2015\$.

- Demonstration of long-lifetime systems needed for power applications;
- Uncertain/unproven reliability can make cost planning difficult – e.g., outages can trigger electricity demand charges in addition to fuel cell capital costs; and
- Unfamiliarity with working with hydrogen fuel in the case of backup power or forklifts (for proton-exchange membrane type fuel cells).

These barriers make clear the need for an increased understanding of the full costs of fuel cell system implementation, especially in emerging applications with increasing manufacturing volumes.

This project further addresses key technical barriers from the “Technical Plan - Fuel Cells and Technical Plan – Manufacturing” sections of the *Fuel Cell Technologies Program Multi-Year Research, Development and Demonstration Plan* (DOE 2014), including:

- Fuel-cell cost: Expansion of cost envelope to total cost of ownership including full life cycle costs and externalities
- Lack of High-Volume Membrane Electrode Assembly Processes
- Lack of High-Speed Bipolar Plate Manufacturing Processes

1.2 Emerging applications

The key markets for this study are CHP and power-only applications. Cost, system reliability and system utilization are key drivers. A recent report from Oak Ridge National Laboratory (Greene 2011) reports technology progress ratio data with a doubling of fuel cell output production in megawatts leading to 20-30% cost reduction. Recent studies have highlighted backup power systems and material handling systems as key market opportunities (Greene et al. 2011, Mahadevan 2007). Depending on energy costs and policy environments, there may be opportunities for “micro-CHP” (1-5 kWe) as well, for example in large expensive homes in cold climates (Greene et al. 2011). Cogeneration of power and heat for commercial buildings may be another opportunity, and has been highlighted as a market opportunity for California commercial buildings (e.g., in Stadler 2011). Some buildings may have requirements greater than 250 kWe but these could be served by several fuel cell units of less than or equal to 250 kWe.

Internationally, stationary fuel cell systems are enjoying an increase in interest with programs in Japan, South Korea and Germany but all markets are still at a cost disadvantage compared to incumbent technologies. Japan has supported residential fuel cell systems of 0.7-1 kWe for co-generation with generous subsidies. The recent nuclear reactor accident in Fukushima has prompted consideration of a range of hydrogen powered systems as alternatives to nuclear energy.

1.3 Total Cost of Ownership Modeling

This work estimates the total cost of ownership (TCO) for emerging fuel cell systems manufactured for stationary applications. The TCO model includes manufacturing costs, operations and end of life disposition, life cycle impacts, and externality costs and benefits. Other software tools employed include commercially available Boothroyd Dewhurst Design for Manufacturing and Assembly (DFMA) software, existing life-cycle analysis (LCA) database tools, and LBNL exposure and health impact models. Figure 1.1 shows the overall research and modeling approach.

The approach for direct manufacturing costs is to utilize DFMA techniques to generate system design, materials and manufacturing flow for lowest manufacturing cost and total cost of ownership. System designs and component costs are developed and refined based on the following: (1) existing cost studies where applicable; (2) literature and patent sources; (3) industry and national laboratory advisors.

Life-cycle or use-phase cost modeling utilizes existing characterization of commercial building electricity and heating demand by geographical region, and references earlier CHP modeling work by one of the authors (Lipman 2004). Life cycle impact assessment is focused on use-phase impacts from energy use, carbon emissions, and pollutant emissions (see Van Rooijen 2006 for discussion) —with a significant focus on particulate matter (PM) emissions since PM is the dominant contributor to life-cycle health impacts (NRC 2010). Health impact from PM is characterized using existing health impact models (Muller and Mendelsohn 2007) available at LBNL. Life-cycle impact assessment is characterized as a function of fuel cell system adoption by building type and geographic location. This approach allows the quantification of externalities (e.g. CO₂ and particulate matter) for FC system market adoption in various regions of the U.S.

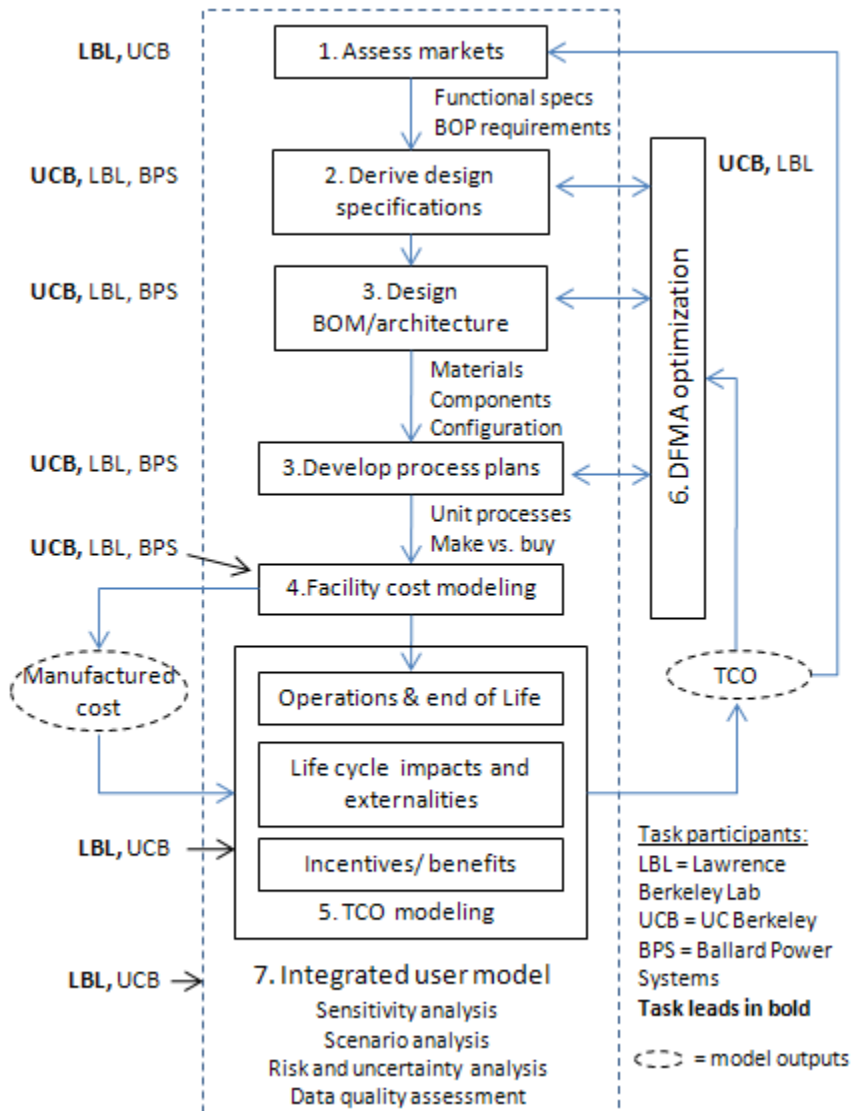


Figure 1.1. Research and modeling approach. (UCB= University of California, Berkeley, LBL = Lawrence Berkeley Laboratory, BPS = Ballard Power Systems (for earlier PEM work), BOM=bill of materials, BOP = balance of plant, TCO=total cost of ownership)

2. System design and Functional specs

For this report, SOFC system designs and functional specifications have been developed for a range of system sizes including (1) CHP systems with reformat fuel from 1-250 kWe, and (2) SOFC electricity only (non-CHP) systems from 10-250 kWe with reformat fuel. These choices are based upon a search of relevant fuel cell literature and patents, industry system spec sheets as well as industry and academic advisor input.

The choice of these system designs and functional specifications allowed the research team to define the operational parameters for each respective fuel cell system and to define the system components or balance of plant (BOP) that will be the basis for cost estimates. Functional requirements for the stack further define the stack geometries and stack sizing (number of cells per stack) for the DFMA direct manufacturing cost analysis presented below.

The functional specifications are referenced to the rated power of the system. Operating at partial load would result in slightly higher efficiency across most of the turndown ratio of the system. System designs are meant to be “medium fidelity” designs that are representative of actual fuel cell systems to provide the basis for the costing estimates that are the main focus of this work. As such, the project is not scoped with process modeling or optimization of the system design in terms of detailed pressure management, flow rates, or detailed thermal balances. However, the designs provide a reasonable starting point for costing based on feedback from industry advisors and for showing key system components, sub-systems, and interconnections that are important for understanding system “topography” for analysis and costing purposes.

2.1 System and Component Lifetime

System and component lifetime assumptions are shown in Table 2.1 and 2.2 for CHP and non-CHP applications, respectively. These specifications are shared across the system power range for each application. In the application of TCO to both CHP and non-CHP systems, overall system life is assumed to be approximately 15 years currently and anticipated to increase to 20 years in the future (2015-2020 timeframe). Stack life is assumed to be 20,000 hours in the near term and projected to double to 40,000 hours per industry and DOE targets. Subsystem component lifetimes are assumed to vary from 5-10 years, with longer lifetimes around 20 years expected in the future. The system turndown ratio is defined as the ratio of the system peak power to its lowest practical operating point (e.g., running at 33 kWe for a 100-kWe system is a turndown ratio of 3 to 1). Direct air and off-gas cooling strategy is utilized for stack cooling for cost savings and BOP design specifications.

Overall system specs are similar for non-CHP applications (Table 2.2) but BOP subsystem lifetimes are assumed to be slightly higher for non-CHP systems due to a more simplistic system design, thus reducing the amount of flow streams for some of the BOP components and increasing their lifetime.

2.2 System Design

System designs for both a SOFC CHP and SOFC non-CHP system operating on reformat fuel will be shown in this section. System design rationale and operations will be discussed in greater detail.

2.2.1 System Design for SOFC CHP

Figure 2.1 shows the system design for a SOFC CHP system operating on reformat fuel. Delineation into subsystems is provided for modularity of design and also to facilitate the tracking and classification of balance of plant components and costing. The CHP systems are subdivided further into

subsystems as follows: (1) fuel cell stack, (2) fuel supply system, (3) water recirculation, (4) power conditioning, (5) coolant subsystem, and (6) controls and meters.

Table 2.1 Specifications and assumptions for SOFC CHP system

CHP Application - SOFC	Near-Term	Future	
System life	15	20	years
Stack life	20,000	40,000	hours
Reformer life (if app.)	5	10	years
Compressor/blower life	7.5	10	years
WTM sub-system life	7.5	10	years
Battery/startup system life	7.5	10	years
Turndown % (>50 kW)	0	25	percent
Turndown % (<50 kW)	25	50	percent
Expected Availability	96	98	percent
Stack cooling strategy	Air+off gas	Air+off gas	cooling

Table 2.2 Specifications and assumptions for SOFC non-CHP system

Stationary - No CHP	Near-Term	Future	
System life	15	20	years
Stack life	20,000	40,000	hours
Reformer life (if app.)	5	10	years
Compressor/blower life	8	10	years
WTM sub-system life	8	10	years
Battery/startup system life	8	10	years
Turndown (>50 kW)	0	25	percent
Turndown (<50 kW)	25	50	percent
Expected Availability	96	98	percent
Stack cooling strategy	Air+off gas	Air+off gas	cooling

To improve fuel utilization, the CHP system with reformat fuel has a fuel burner to utilize cathode tail gas fuel to provide heating for the incoming air supply. The burner exhaust is also used for CHP applications for improved thermal and overall efficiency of the system.

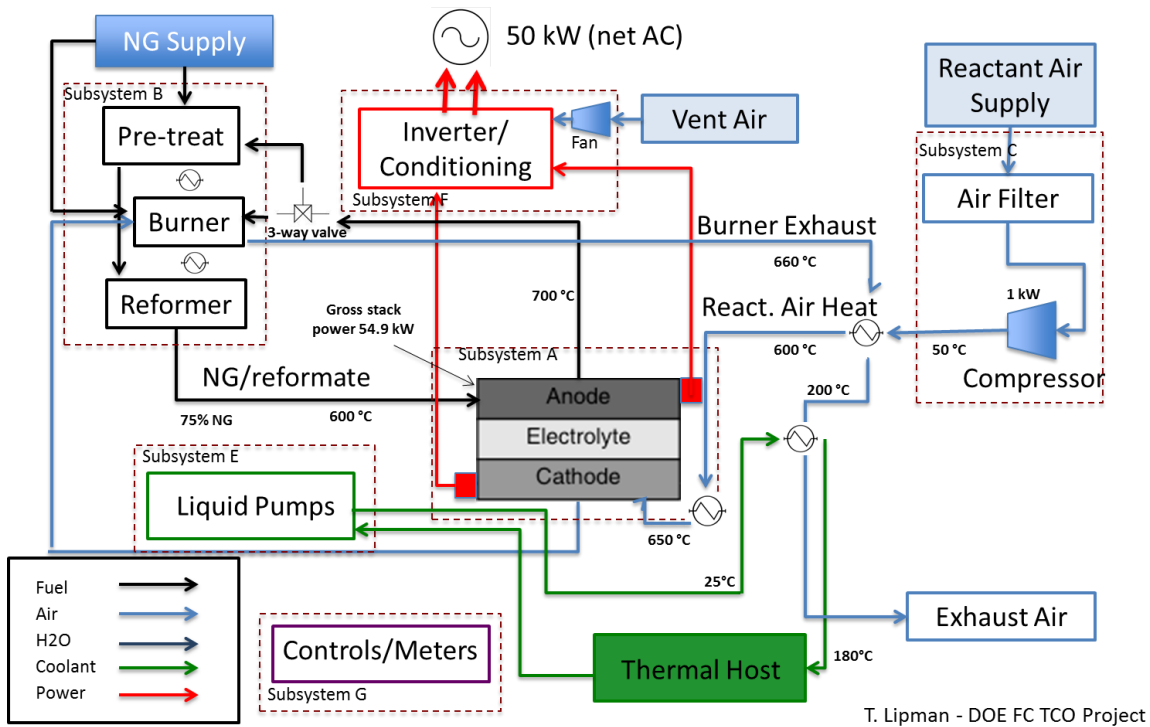


Figure 2.1 SOFC CHP system design schematic

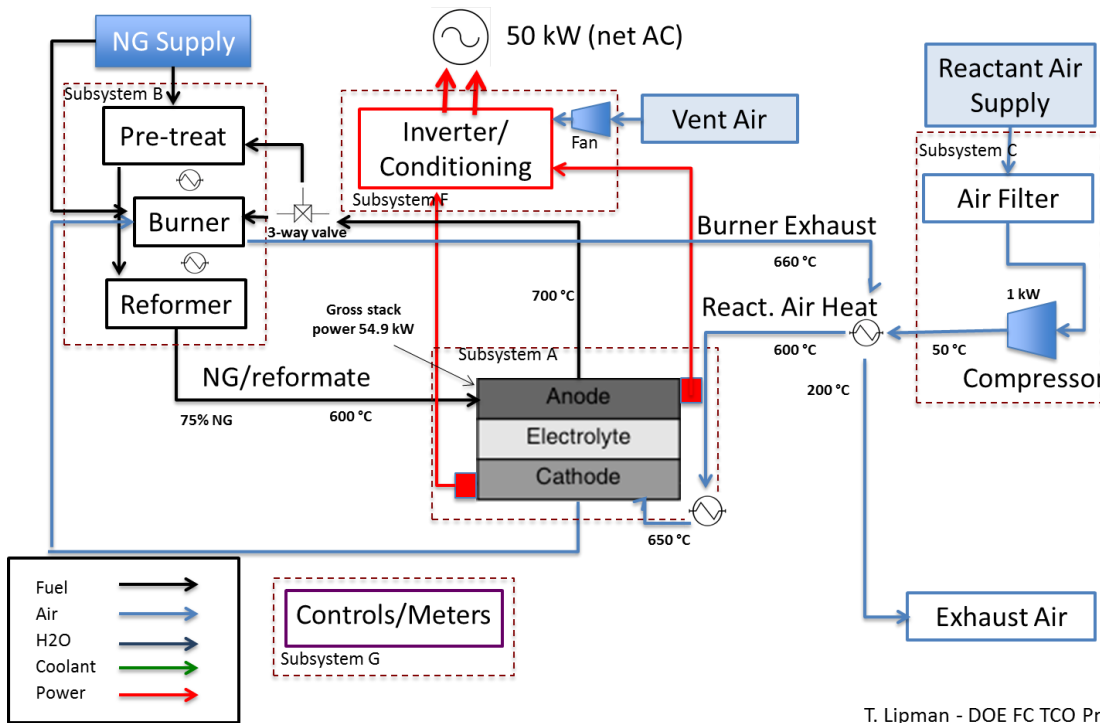
2.2.2 System Design for SOFC non-CHP

Figure 2.2 shows the system design for a SOFC non-CHP (e.g. electricity production only) system. The overall system design is similar to the SOFC CHP case, with the exception of the absence of a thermal host system. In the CHP case, the burner exhaust is utilized for CHP applications while for the non-CHP case, the burner exhaust is directed out of the system.

2.3 System Functional Specifications

2.3.1 Functional specifications for SOFC CHP system

Functional specifications for the 10 kWe and 50 kWe CHP systems with reformat fuel are shown in Table 2.3 below. These functional specifications were developed based on a variety of industry sources and literature and include calculated parameters for stack and system efficiencies for an “internally consistent” set of reference values. A detailed description of the functional specification focused on the 10-kWe and 50-kWe system sizes follows below. The determination of gross system power reflects about 10% overall parasitic power at 10 kWe and about 9.7% at 100 kWe, including losses through the inverter. DC to AC inverter efficiency is assumed to be 95% and constant across the system power ranges. Additional parasitic losses are from compressors, blowers and other parasitic loads and are assumed to be direct DC power losses from the fuel cell stack output power.



T. Lipman - DOE FC TCO Project

Figure 2.2. SOFC non-CHP system design schematic

The waste heat grade from the coolant system is taken to be 220°C for all system sizes although a range of other temperatures are possible, mostly over the range of 50-70°C. The heat exchanger configuration can also depend on the demand temperatures for the heating streams, and the exact cooling and heating loops will be location and system specific. In the use-phase cost model described later in the report, hot water and space heating are generated as the main waste heat application with enhancement to absorption chilling as an additional possibility. Additional waste heat streams from the anode and cathode exhaust can be routed to the fuel processor reactor burner.

At the reference cell voltage of 0.8 volts, the net electrical efficiency is 59% (lower heating value, or LHV) for the reformate systems. These overall electrical efficiency levels are similar to those reported in the literature (James et al. 2012). The total overall CHP system efficiency of 84% is viewed as a benchmark value for the case where a large reservoir of heat demand exists and represents the maximal total efficiency of the system. Actual waste heat utilization and total efficiency will be highly dependent on the site and heating demands. For example, a smaller overall heat efficiency can result if waste heat utilization is confined to building water heating and the building has a relatively low demand for hot water.

There is a well-documented tradeoff of peak power and efficiency. The functional specifications are defined for operation at full rated power. Moving away from the peak power point to lower current density, the cell voltage increases and thus the stack efficiency improves somewhat. Partial load operation thus has higher efficiency but less power output.

Total fuel cell plate area is taken to be 540 cm². Active catalyzed area is about 61% of this area due to plate border regions and manifold openings. Single cell active area has an additional 10% area loss due to the frame sealing process. (More details of this process are described in Chapter 4).

Table 2.3 Functional specifications for CHP system operating on reformat fuel

Parameter	10kWe CHP system reformat fuel	50kWe CHP system with reformat fuel	Units
Gross system power	11.0	54.9	kW DC
Net system power	10	50	kW AC
Electrical output	220V AC	480V AC	Volts AC or DC
DC/AC inverter efficiency	95	95	%
Waste heat grade	220	220	Temp. °C
Fuel utilization % (overall)	N/A	N/A	%
Net electrical efficiency	59	59	% LHV
Thermal efficiency	24	24	% LHV
Total efficiency	84	84	Elect.+thermal (%)
Stack power	11.0	54.9	kW
Total plate area	540	540	cm ²
Actively catalyzed area	329	329	cm ²
Single cell active area	299	299	cm ²
Gross cell inactive area	45	45	%
Cell amps	105	105	A
Current density	0.35	0.35	A/cm ²
Reference voltage	0.8	0.8	V
Power density	0.28	0.28	W/cm ²
Single cell power	84	84	W
Cells per stack	130	130	cells
Stacks per system	1	5	stacks
Parasitic loss	0.5	2.5	kW AC

2.3.2 Functional specifications for SOFC Power-Only system

Table 2.4 displays the functional specifications for a SOFC power-only system operating on reformat. The power-only SOFC system achieves cost reduction through reduction of balance of plant components used for thermal management application. The total efficiency (also equal to electrical efficiency for the power-only case) is lowered than the previous case because the waste heat from the stack is not re-used. Stack parameters remain the same as CHP case from above.

Table 2.4 Functional specifications for power-only system operating on reformat fuel

Parameters	10-kWe system reformat fuel	50-kWe system with reformat fuel	Units
Gross system power	11.0	54.9	kW DC
Electrical output	220V AC	480V AC	Volts AC or DC
DC/AC inverter effic.	95	95	%
Waste heat grade	N/A	N/A	Temp. °C
Fuel utilization % (overall)	N/A	N/A	%
Net electrical efficiency	59	59	% LHV
Total efficiency	59	59	Elect.+thermal (%)
Thermal efficiency	N/A	N/A	%
Stack power	10.97	54.86	kW
Total plate area	540	540	cm ²
Actively catalyzed area	329	329	cm ²
Single cell active area	299	299	cm ²
Gross cell inactive area	45	45	%
Cell amps	105	105	A
Current density	0.35	0.35	A/cm ²
Reference voltage	0.8	0.8	V
Power density	0.28	0.28	W/cm ²
Single cell power	84	84	W
Cells per stack	130	130	cells
Stacks per system	1	5	stacks
Parasitic loss	0.5	2.5	kW AC

3. Costing Approach and Considerations

The aim of this chapter is to present the LBNL overall costing approach used in this study and in the recent work “A Total Cost of Ownership Model for Low Temperature PEM Fuel Cells in Combined Heat and Power and Backup Power Applications” (Wei, et al., 2014).

Table 3.1 below presents a schematic description of the costing approach. The starting point is system definition and identification of key subsystems and components. System definition includes the key subsystems and components of the complete fuel cell system and also includes formulation of functional specifications of stack parameters and stack and system operating characteristics.

Manufacturing strategy is then defined to determine which components to purchase and which to manufacture in-house (i.e., the “make or buy” decision). A detailed parts list is assembled for purchased components and detailed DFMA costing is done for in-house manufactured components. In this work, non-stack components are assumed to be purchased while stack components are assumed to be manufactured in-house.

Direct manufacturing costs for the stack are thus captured in the DFMA costing, and a further markup of stack and other system components will include non-manufacturing costs such as General and Administrative, Sales and Marketing, and profit margin to determine the final “factory gate” price to the customer.

The general guidelines for purchased-versus-made components or “make or buy” are whether the part is readily available as a commodity item or off-the-shelf part. If this is the case, there is little reason to manufacture in-house (e.g. pumps, compressors, electronic components). One informal criterion for purchasing components is whether or not there is an “active market” of buyers and sellers for the component. For example an active market might be defined as one in which there are at least three suppliers and three purchasers, and one in which suppliers do not have undue market power or monopoly power.

Clearly there are gray areas where there may be off-the-shelf components available but a high degree of manual assembly is required, and the development of subassemblies available for purchase would be more economical. These would probably require more standardized designs or interfaces for both the supplier industry and fuel cell system providers to leverage over time. Similarly, in many cases, a fuel cell supplier will find it cost effective to subcontract the design, manufacturing and/or assembly of a subsystem component to an appropriate manufacturing partner. This work employs a relatively simplified approach of “made vs. bought” components, but these considerations do enter into cost estimates of this study. For example, labor associated with system assembly is assumed to drop with increasing volume with both learning-by-doing and the implicit assumption that there is greater availability of subassemblies.

In this analysis, balance of plant components are largely assumed to be purchased components, and stack components are largely manufactured in-house, with end-plates and stack compression springs the key exceptions. Note that a bottom-up DFMA costing was not done for non-stack components and thus further cost reduction may be possible for those components.

Vertical integration is assumed for stack manufacturing, i.e. a fuel cell manufacturer is assumed to manufacture all stack components as described below. This assumption is geared toward the case of high volume production. At lower production volume some purchase of finished or partially finished

stack components may be cost beneficial because at very low volumes the investment costs for vertical integration is prohibitive and equipment utilization is inefficient.

Table 3.1. Generalized roll-up steps for total system cost; (b) scope of direct manufacturing costs for components produced in-house.

<u>Step</u>		<u>Key Outcome</u>	<u>Direct Manufacturing Costs</u>
System definition	System Design 	Identification of subsystems and components	Capital costs
	↓		Labor costs
Manufacturing strategy	Make/Buy Decisions 	Differentiation between purchased and made components	Materials costs
	↓		Consumables
Detailed parts list and costs	Multi-level BOM 	Estimation of total system "materials" costs, DFMA costing	Scrap / yield losses
	↓		Factory costs
Est. of final system cost	Rolled-Up Factory Cost 	Estimation of final factory gate price incl. labor, G&A, and corporate costs + profit	Global Assumptions
			Discount rate, inflation rate
			Tool lifetimes
			Costs of energy, etc.
			<u>Other Costs</u>
			R&D costs, G&A, sales, marketing
			Product warranty costs

The DFMA analysis includes the following items shown in Table 3.1 for direct manufacturing costs, global cost assumptions and other non-product costs. For each manufactured component, first a patent and literature search was done and industry advisor input elicited. This was followed by selection of a base manufacturing process flow based on these inputs, an assessment of current industry tooling and direction, and engineering judgment as to which process flows can support high volume manufacturing in the future.

Direct manufacturing costs include capital and operational costs, labor, materials, scrap (waste material and yield loss) and factory building costs, subject to global assumptions such as discount rate, inflation rate and tool lifetimes. This methodology follows other cost studies (James, Spisak, & Colella, 2012).

For each major electrode-electrolyte assembly (EEA) functional cell processing module (e.g. tape casting, or co-firing process), a machine rate is computed corresponding to an annual production volume, where the machine rate comprises capital, operational and building costs and has units of cost

per hour for operating a given module. “Process cost” per module is then the product of machine rate and annual operation hours of the tool. Total annualized manufacturing cost is the sum of process cost per module plus required labor and required materials and consumable materials.

Overall manufacturing costs are then quoted as the sum of all module or component costs normalized to the annual equivalent production volume in kWe. Direct manufacturing costs are quoted in cost per kWe of production, or, cost per meter squared of material can be quoted similarly for roll-to-roll goods such as EEA. Other costs such as G&A and sales and marketing are added to determine the final factory gate price.

3.1. DFMA Costing Model Approach

This chapter discusses economic analysis used in developing DFMA costing model. This model was adopted from an ASHRAE handbook publication (Haberl, 1994).

Below are the definitions of terms used in developing economic equations:

C_e = cost of energy to operate the system for one period

C_f = floorspace (building) cost

C_{labor} = labor rate per hour

$C_{s, assess}$ = initial assessed system value

$C_{s, salvage}$ = system salvage value at the end of its useful life in constant dollars

$C_{s init}$ = initial system cost

C_y = annualized system cost in constant dollars

$D_{k,sl}$ or $D_{k,SD}$ = amount of depreciation at the end of period k depending on the type of depreciation schedule used, where $D_{k,sl}$ is the straight line depreciation method and $D_{k,SD}$ represents the sum-of-digits depreciation method in constant dollars

F = future value of a sum of money

$i_m P_k$ = interest charge at the end of period k

$i' = (j_d - j)/(1 + j)$ = effective interest rate adjusted for inflation rate j and discount rate j_d ; sometimes called the real rate

$i'' = (j_d - j_e)/(1 + j_e)$ = effective interest rate adjusted for energy inflation j_e

I = annual insurance costs

ITC = investment tax credit for energy efficiency improvements, if applicable

j = general inflation rate per period

j_d = discount rate

j_{br} = building depreciation rate

j_e = general energy inflation rate per period

j_m = average mortgage rate (real rate + general inflation rate)

k = end if period(s) in which replacement(s), repair(s), depreciation, or interest is calculated

M = periodic maintenance cost

n = number of period(s) under consideration

P = a sum of money at the present time, *i.e.*, its present value

P_k = outstanding principle of the loan for Cs,init at the end of period k in current dollars

R_k = net replacement(s), repair cost(s), or disposals at the end of period k in constant dollars

T_{inc} = (state tax rate + federal tax rate) -(state tax rate X federal tax rate) where tax rates are based on the last dollar earned, *i. e.*, the marginal rates

T_{prop} = property tax rate

T_{br} = salvage value of the building

For any proposed capital investment, the capital and interest costs, salvage costs, replacement costs, energy costs, taxes, maintenance costs, insurance costs, interest deductions, depreciation allowances, and other factors must be weighed against the value of the services provided by the system.

Present value or present worth is a common method for analyzing the impact of a future payment on the value of money at the present time. The primary underlying principle is that all monies (those paid now and in the future) should be evaluated according to their present purchasing power. This approach is known as discounting.

The future value F of a present sum of money P over n periods with compound interest rate i can be calculated as following:

$$F = P(1 + i)^n$$

The present value or present worth P of a future sum of money F is given by:

$$P = F / (1 + i)^n = F \times PWF(i, n)$$

where $PWF(i, n)$ the worth factor, is defined by:

$$PWF(i, n) = 1 / (1 + i)^n$$

Inflation is another important economic parameter that accounts for the rise in costs of a commodity over time. Inflation must be accounted for in an economic evaluation, either by being explicitly included or excluded through the use of "constant dollars." One way to account for inflation is to use effective interest rates that can also account for varying rates of inflation.

The effective interest rate i' , sometimes called the real rate, accounts for the general inflation rate j and the discount rate j_d , and can be expressed as follows (Haberl, 1994):

$$i' = \frac{1+j_d}{1+j} - 1 = \frac{j_d - j}{1+j}$$

However, this expression can be adapted to account for energy inflation by considering the general discount rate j_d and the energy inflation rate j_e , thus:

$$i'' = \frac{1+j_d}{1+j_e} - 1 = \frac{j_d - j_e}{1+j_e}$$

When considering the effects of varying inflation rates, the above discount equations can be revised to get the following equation for the future value F , using constant currency of an invested sum P with a discount rate j_d under inflation j during n periods:

$$F = P \left[\frac{1 + j_d}{1 + j} \right]^n = P(1 + i')^n$$

The present worth P , in constant dollars, of a future sum of money F with discount rate j_d under inflation rate j during n periods is then expressed as:

$$P = F / \left[\frac{1 + j_d}{1 + j} \right]^n$$

In constant currency, the present worth P of a sum of money F can be expressed with an effective interest rate i' , which is adjusted for inflation by:

$$P = F / (1 + i')^n = F \times PWF(i', n)$$

where the effective present worth factor is given by:

$$PWF(i', n) = 1 / (1 + i')^n$$

Table 3.2. Cost components and their corresponding mathematical formulas

$(C_{s,init} - ITC) * CRF(i', n)$	Capital and Interest
$C_{s,salv} * PWF(i', n) * CRF(i', n) * (1 - T_{salv})$	Salvage Value
$\sum_{k=1}^n [R_k PWF(i', k)] * CRF(i', n) * (1 - T_{inc})$	Replacement or Disposal
$C_e * \left[\frac{CRF(i', n)}{CRF(i'', n)} \right] * (1 - T_{inc})$	Operating Energy
$C_{br} = CRF_m * c_{fs} * j_{br}$	Building Cost
$C_{s,assess} T_{prop} (1 - T_{inc})$	Property Tax
$M(1 - T_{inc})$	Maintenance
$I(1 - T_{inc})$	Insurance
$T_{inc} * \sum_{k=1}^n [j_m P_{k-1} PWF(i_d, k)] CRF(i', n)$	Interest Tax Deduction
$T_{inc} * CRF(i', n) * \sum_{k=1}^n [D_k * PWF(i_d, k)]$	Depreciation
$P_k = (C_{i,init} - ITC) * \left[(1 + j_m)^{k-1} + \frac{(1 + j_m)^{k-1} - 1}{(1 + j_m)^{-n} - 1} \right]$	Principle P_k during year k at market mortgage rate i_m

Another important economic concept is the recovery of capital as a series of uniform payments or “depreciation”. Using “straight line” (i.e. equal over time) a simple capital recovery factor (CRF) can be used. The CRF is commonly used to describe periodic uniform mortgage or loan payments. S is defined as the ratio of the periodic payment to the total sum being repaid. The discounted sum S of such an annual series of payments P_{ann} invested over n periods with interest rate i is given by:

$$S = P_{ann}[1 + (1 + i)^{-n}]/i$$

$$P_{ann} = (S \times i)/[1 + (1 + i)^{-n}/i]$$

$$CRF(i, n) = \frac{i}{[1 - (1 + i)^{-n}]} = \frac{i(1 + i)^n}{(1 + i)^n - 1}$$

Table 3.2 above summarizes the primary mathematical formulae used in calculating these cost components.

The discount rate is expected to have a range of parameters depending on several financial factors including the “investment risk” reflected in the respective cost of equity and debt for a manufacturing company and the company’s debt to equity ratio.

For the fuel cell industry, given the current market environment (post 2007-2008 “financial crisis”) the weighted average cost of capital is expected to be in the range of 10-15%. Here we use the lower end of this range based on industry inputs and previous SOFC manufacturing cost model (James, Spisak, & Colella, 2012). Also note that the discount rate, along with several other key global parameters, is varied for sensitivity analysis.

3.2. Non-Product Costs

The DFMA cost estimates in Chapter 4 refer to direct manufacturing costs and exclude profit, research and development (R&D) costs, and other corporate costs (sales and marketing, general and administrative, warranty, etc.).

To better quantify these other non-product costs, financial statements from four publicly traded fuel cell companies were analyzed for the 2008-2011 period (Fuel Cell Energy, Proton Power, Plug Power, and Ballard). Excluding Plug Power, which showed much higher non-product costs than the other companies, median “General and Administrative” (G&A) and “Sales and Marketing” costs were 40% of the total “Cost of Product and Services,” and median R&D costs were 38% of this total. Based on these publically available financial statements, gross margins were 20% for Ballard but negative for the other three companies. All four recorded a net loss for all years in this period.

Thus, a 100% markup in the sales price of a fuel cell system above the manufacturing cost would achieve a slightly positive operating income taking both G&A/Sales and Marketing, and R&D into account. These historical numbers for Sales and Marketing and R&D could be on the high side since these companies are building a market presence and these costs can be expected to drop over time with greater market penetration.

A typical sales markup of 50% is expected to approximately cover the G&A/Sales portion of operating expenses for current fuel cell vendors but not R&D expenses. Gross margin product markup is also expected to be slim given the existence of highly cost competitive alternative technologies for CHP applications and the available financial data. These other factors can be seen to increase the direct manufacturing costs by 50% to 100% including profit margin.

Note that fuel cell system shipping and delivery costs are not split out separately, but that there is an additional 33% markup assumed for installation costs and all other fees.

3.3. Manufacturing Cost Analysis - General Parameters

General parameters for the cost analysis are summarized below, with these values being shared among all cases and others being more specific to certain system sizes and types. Table 3.3 shows the cell and stack configurations for CHP system based on the functional specifications described above. The number of cells per system are used to compute total active area and component volumes in the DFMA section below. Similarly, the plate (interconnect) area and EEA cell area are shown in Table 3.4. These cell areas could be expected to change for different applications for optimized product configuration and performance, but at the same time, it is beneficial for manufacturing cost control to have a consolidated cell size in multiple products and that approach was adopted here.

Table 3.3. Summary of cell and stack configuration for CHP systems with reformat fuel

System Power [kWe]	Cells/ stack	Stacks/System	Cells/ system	Single cell power [W]	Gross Power [kWe]
1	13	1	13	85.1	1.11
10	130	1	130	84	11
50	130	5	650	84	54.9
100	130	10	1300	84	109.7
250	130	25	3250	84	274.3

Table 3.4. Plate and EEA area for CHP SOFC system

Parameter	CHP SOFC system	Unit
Total plate area	540	cm ²
EEA cell area	329	cm ²

General manufacturing cost parameters are summarized in Table 3.5. References are shown in the table and are a mixture of general industry numbers (e.g. annual operating days, inflation rate, tool lifetime) together with fuel cell specific industry assumptions (discount rate, hourly wage).

An annualized cost of tool approach is adopted from Haberl (1994). The annualized cost equation can be expressed in constant currency as follows:

$$C_y = C_c + C_r + C_{oc} + C_p + C_{br} + C_i + C_m - C_s - C_{int} - C_{dep}$$

Table 3.5. Manufacturing cost general parameters

Parameter	Symbol	Value	Units	Comments
Operating hours	t_{hs}	varies	Hours	8 hours base shift; (2-3 shifts per day)
Annual Operating Days	t_{dy}	240	Days	52wks*5days/wk-10 vacation days-10 holidays
Avg. Inflation Rate	j	0.023		US avg. for past 10 years (Phillips, 2008)
Avg. Mortgage Rate	j_m	0.051		(Trading Economics , 2015)
Discount Rate	j_d	0.1		
Energy Inflation Rate	j_e	0.056		US avg of last 3 years (Phillips, 2008)
Income Tax	i_i	0		No net income
Property Tax	i_p	0.01035		US avg from 2007 (Tax-rates.org, 2015)
Assessed Value	i_{av}	0.4		
Salvage Tax	i_s	0.5		
EOL Salvage Value	k_{eol}	0.02		Assume 2% of end-of-life value
Tool Lifetime	T_t	15	Years	Typical value in practice
Energy Tax Credits	ITC	0	Dollars	
Energy Cost	c_e	0.1	\$/kWh	e.g., the cost of electricity in the industrial sector was \$0.109/kWh in New England, and \$0.102/kWh in the Pacific contiguous states in October 2014 (https://www.eia.gov/electricity/monthly/epm_table_grapher.cfm?t=epmt_5_6_a , accessed 29 December 2015))
Floor space Cost	c_{fs}	1291	\$/m ²	US average for factory (Selinger, 2011)
Building Depreciation	j_{br}	0.031		BEA rates (U.S. Department of commerce, 2015)
Building Recovery	T_{br}	31	Years	BEA rates (U.S. Department of commerce, 2015)
Building Footprint	a_{br}	Varies	m ²	
Line Speed	v_l	Varies	m/min	
Hourly Labor Cost	c_{labor}	29.81	\$/hr	Hourly wage per worker

where

C_y is the total annualized cost
 C_c is the capital/system cost (with interest)

C_r is the replacements or disposal cost

C_{oc} is the operating costs (e.g. electricity) excluding labor

C_p is the property tax cost

C_{br} is the building or floor space cost

C_i is the tool insurance cost

C_m is the maintenance cost

C_s is the end-of-life salvage value

C_{int} is the deduction from income tax

C_{dep} is the deduction due to tool depreciation

In the current version of the model C_r , the replacements or disposal cost, and C_i , the tool insurance cost, are assumed to be zero. We assume no net profit for fuel cell manufacturers, as is currently the case for SOFC manufacturers, and thus income tax credits such as interest tax credits do not factor into the calculations but can easily be added for future scenarios.. The machine rate quoted above can be easily found from these annualized cost components (capital cost component, operating cost, and building cost

3.4. Factory model

Two approaches were pursued: first, a global factory model with total area dependent on overall volume and including factors for non-production factory space, and also a second method to incrementally add factory area associated with each specific process module.

It is difficult to keep all of the process modules coordinated in the first case, so the approach has shifted to adopting the second, simpler approach. Factory cost contributions in both cases are found to be very small factors in general, especially as production volumes exceed 1,000 systems per year.

Process module footprint is computed using the following formula:

$$\text{Process module footprint (m}^2\text{)} = \# \text{ of machines} * \text{machine size (m}^2\text{)} * 2.8$$

where the 2.8 space correction factor is taken from (Verrey, 2006).

Also note that the “building cost” element is amortized with building depreciation and building life (estimated at 31 years).

3.5. Yield Considerations

As in other costing studies ((Borglum B. , 2009); (Carlson, Yang, & Fulton, 2004); (Woodward, 2003)) and as will be detailed in the DFMA analysis below, this work assumes that high yield is achieved at high manufacturing volumes. This stems from several implicit assumptions:

- Learning by doing over the cumulative volume of fuel cell component production and greater process optimization will drive yield improvement both within a given vendor, and from vendor to vendor through industry interactions (conferences, IP, cross vendor personnel transfers, etc.);
- Inline inspection improvement with greater inspection sensitivity and more accurate response to defects and inline signals;

- Greater development and utilization of “transfer functions” (Manhattan Projection 2011), e.g., development of models that relate inline metrics and measurements to output responses and performance, and resultant improvement in inline response sensitivity and process control;
- Utilization of greater feedback systems in manufacturing processing such as feed-forward sampling, for real time adjustment of process parameters (for example, doctor-blade coating thickness and process parameter control); and
- Systematic, integrated analysis to anticipate and prepare for yield excursions e.g., FMEA (failure modes and effect analysis).

Consideration of yield limiting mechanisms or FMEA-type analysis as a function of process tooling assumptions are out of scope here and would be very challenging in this type of analysis project without access to detailed manufacturing data.

3.6. Initial Tool Sizing

The choice of initial tool sizing was governed by several factors. In some cases it was made on the basis of tool availability and in other cases it was dependent on the choice of batch sizes with smaller batch sizes leading to smaller tools. In general however, tooling decisions were made to support medium to high volume manufacturing of greater than 10 kWe and 1,000 systems per year. This choice was made on the basis of assuming that vertically integrated manufacturing would not be done for small volumes e.g. 10 kWe of total production a year. A cost-optimized process for low volume manufacturing would have a very different mix of automated versus manual production lines as well as in-house manufactured versus purchased components. A detailed optimization study of low volume manufacturing was not a key priority for this work. Production volumes might also be expected to grow due to “exogenous factors” such as if sales of other types of SOFC systems (e.g., auxiliary power units (APUs) for transportation applications) drive increased demand for common SOFC stack components.

3.7. Time-frame for Cost Analysis

The cost analysis utilizes largely existing manufacturing equipment technologies and existing materials. The analysis is thus a “potential cost reduction” study for future costs with existing tools and mostly existing materials. The study assumes that higher overall volumes will drive significant improvements in yield, but it is not a market adoption or market penetration study and therefore timelines will vary according to the assumptions made for market adoption. Stationary fuel cell system cost reductions may also benefit from growth in the transportation sector, such as through commercialization of APUs, and for other “long duty cycle” applications..

4. Direct Manufacturing Cost Analysis of Stack Components

4.1. Electrode-Electrolyte Assembly (EEA) Manufacturing Cost Analysis

An electrode-electrolyte assembly functional cell (EEA) is made from several layers, but the major functional layers are the anode layer, cathode layer and electrolyte layer (Figure 4.1). Two other layers are also made and called anode supporting layer and cathode supporting layer which are designed to support cathode and anode functional layers. A process flow for making these functional cells is shown on Figure 4.2.

Based on the functional specifications from Chapter 2, each single cell has a size of 18.15x18.15 cm² and a active area of 329 cm². Bills of materials for anode, cathode and electrolyte layers are shown below (Table 4.1).

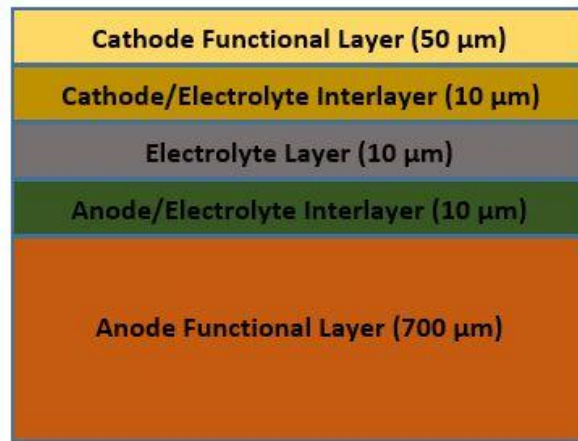


Figure 4.1. Schematic of a single anode supported cell (electrode-electrolyte assembly; EEA)

Table 4.1. Bill of materials for electrode-electrolyte assembly (EEA) cells

Component	Materials	Thickness (μm)	Process
Anode	Ni/YSZ	700	Tape casting
Anode Electrolyte Interlayer	50%YSZ+50%NiO	10	Screen printing
Electrolyte	YSZ	10	Screen printing
Electrolyte/Cathode Interlayer	50%YSZ+50%LSM	10	Screen printing
Cathode	LSM	50	Screen printing

EEA Manufacturing Process Flow

Figure 4.2 shows the flow of EEA manufacturing process. In the anode supported cell design, anode layer provides the structural support for the electrically-active components. The anode layer is designed to handle the high operating temperatures in the cell and is tape cast from a slurry containing yttria-stabilized zirconia (YSZ) and nickel particles.

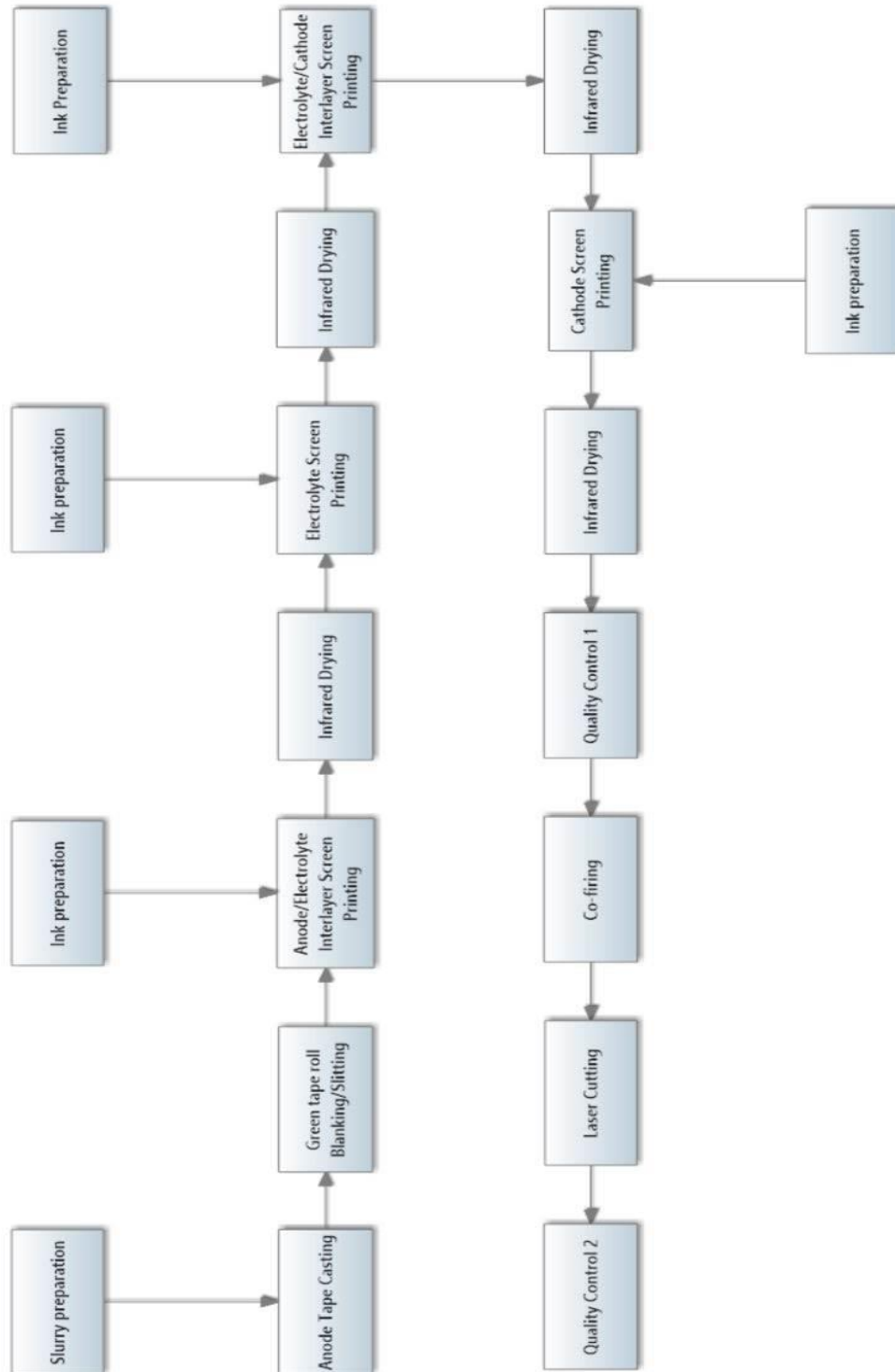


Figure 4.2. Process flow for making functional cell (EEA)

Tape casting starts with preparation of a slurry containing the ceramic powders, dispersant, binder, plasticizer and solvents. The batch is blended in a ball mill for about 24 hours to ensure homogeneity and proper viscosity is achieved. After ball milling is finished, the slurry is sent through a sieve (in

order to separate it from grinding media and unbroken agglomerates) and poured to an open mouth container.

Prior to tape casting, air bubbles must be removed from the slurry. In this analysis slurry de-airing is performed by means of high amplitude ultrasonic processors instead of the more common method of using a vacuum chamber. Inserting the container in a vacuum chamber it is possible to eliminate air bubbles and obtain a de-aired slurry (Thorel, 2010), but this analysis has found ultrasonic processing to a more cost-effective approach.

Finally, the de-aired and homogenized slurry is pumped to the tape casting machine reservoir to make the cast anode tape. Bulk anode layers can be made through single or multiple passes depending on the viscosity of the paste and thickness of the green cast layer. After that, the wet cast layer passes through a tape casting machine drying chamber in which the solvents evaporate, leaving the flexible yet hard tapes (700µm).

The dried green tape is then rolled in a take-up roll and moved to a cutting station where the roll is cut into stripes and each stripe is blanked into sheets. These sheets are moved to screen printing stations where each subsequent layer (anode-electrolyte interlayer, electrolyte, cathode-electrolyte interlayer and cathode layer) is deposited successively in the same fashion. An infrared drying process (using infrared conveyor ovens) is always required after each deposition layer.

Following the screen printing processes, a first quality control analysis is performed in order to measure layer thicknesses and detect the presence of surface defects. The mini-stack of five layers is then bonded together by placing it in a furnace at elevated temperature (~1300-1400°C) for 24 hours (Schafbauer, Menzler, & Buchkremer, 2014); (Thorel, 2010).

Finally each EEA cell is laser cut to the proper dimensions (18.15x18.15 cm²) using a laser cutter and a second quality control analysis is performed. In this case, a vacuum leak test is also conducted.

EEA Manufacturing Line Process Parameters

Ideally, the equipment should run at its required rate and produce high quality products. In practice, downtime occurs or inferior quality products are made.

These losses caused by machine malfunctioning and process, can be divided into these categories (Iannone & Nenni, 2013):

- “Down time” losses: most common unscheduled down-time losses occur when a malfunction arises, an unplanned maintenance task must be done. Scheduled down time can occur due to regular maintenance and inspections, to perform tool upgrades or tool softwares revisions
- Speed losses: the equipment is running, but it is not running at its maximum designed speed. Most common speed losses happen when equipment speed decreases but is not zero. These events can occur due to various malfunctions, small technical imperfections such as stuck packaging, start-up of the equipment after a maintenance task, or an equipment setup.
- Quality losses: the equipment is producing products that do not fully meet the specified quality requirements. These can occur because of equipment instability, an incorrect functioning of the machine, process defects, or because process parameters are not tuned to optimal processing conditions.

These losses can be classified according to three different measurable components (Iannone & Nenni, 2013):

1. Availability (percentage of time that equipment is available to run during the total possible planned production up-time);
2. Line Performance (measure of how well the machine runs within its designed operating time); and
3. Process Yield or Quality (measure of the number of parts that meet specification compared to how many were produced).

In order to know these process parameters it would be necessary to obtain private data collected by fuel cell manufacturers since these values are not available online or in the literature. In addition, each fuel cell manufacturer uses different toolsets and different manufacturing techniques and when different volumes of production and different machines sizes are analyzed, it is even more difficult to understand all these factors. What can be expected is that process yield and line availability are both functions of annual production volume since level of automation and number of manufacturing lines increase with volume.

Under these assumptions, line availability was assumed to be 80% and process yield to be 85% at low volumes (< 100,000 EEA cells/year). At the highest volumes (>10,000,000 EEA cells/year), line availability and process yield were estimated to be 95%. For volumes between 100,000 and 10,000,000 EEA cells/year, the process parameters were found through exponential interpolation.

Line performance was assumed to be 89% for manual configuration and 95% for semi-automatic and automatic configurations. The process parameters are shown in Table 4.2.

Table 4.2. EEA manufacturing line process parameters for all annual production volumes

Power	Systems/year	Process Yield (%)	Availability (%)	Line Performance (%)
1	100	85.00%	80.00%	89.00%
	1,000	88.00%	80.00%	89.00%
	10,000	91.00%	80.79%	95.00%
	50,000	92.00%	85.79%	95.00%
10	100	88.00%	80.00%	89.00%
	1,000	91.00%	80.79%	95.00%
	10,000	92.00%	88.04%	95.00%
	50,000	93.00%	93.49%	95.00%
50	100	90.00%	80.00%	89.00%
	1,000	92.00%	85.79%	95.00%
	10,000	93.00%	93.49%	95.00%
	50,000	94.00%	95.00%	95.00%
100	100	91.00%	80.79%	95.00%
	1,000	92.00%	88.04%	95.00%
	10,000	94.00%	95.00%	95.00%
	50,000	95.00%	95.00%	95.00%
250	100	91.00%	83.60%	95.00%
	1,000	93.00%	91.10%	95.00%
	10,000	94.00%	95.00%	95.00%
	50,000	95.00%	95.00%	95.00%

A sensitivity analysis was also performed ($\pm 20\%$ change of availability, performance and process yield) in order to understand how much these factors affected the EEA cells manufacturing cost (see section 5.1.5).

EEA Manufacturing Processes Cost Analysis

Ceramic Slurry Volume

Slurry batch volume depends on the part size, casting width and layer thickness. Unlike the other layers, a larger area (366 cm^2) was considered for anode slurry volume evaluation because the tape casting process required a 1 cm margin on each size of the layer. Table 4.3 shows slurry compositions of each layer and corresponding characteristics.

Table 4.3. Slurry composition of each layer of EEA cell

Anode Layer	Weight (gm/366 cm²)	Density (g/cm³)	Weigth (%)	Volume (cm³)	Appearance/ function
Nickel Oxide (70% wt)	93.0006	8.91	50.82%	10.438	solid
YSZ (30% wt)	27.7794	6.1	15.18%	4.554	solid
Carbon Black	7.3200	1.8	4.00%	4.067	pore former
Santicizer 160 (DBP)	10.9800	1.1	6.00%	9.982	plasticizer
Butvar-76 (PVB)	10.9800	1.08	6.00%	10.167	binder
n-Butylacetate	32.940	0.88	18.00%	37.432	solvent
Total weight (g)	183.000	2.387		76.639	

Anode/Electrolyte Interlayer	Weight (gm/329 cm²)	Density (g/cm³)	Weigth (%)	Volume (cm³)	Appearance/ function
Nickel Oxide (50% vol)	1.6450	8.91	26.50%	0.185	solid
YSZ (50% vol)	1.6450	6.1	26.50%	0.270	solid
Methocel A4M	1.8623	0.85	30.00%	2.191	binder
2-Butoxyethanol	1.0553	0.9	17.00%	1.173	solvent
Total	6.208	1.625		3.818	

Cathode Layer	Weight (gm/329 cm²)	Density (g/cm³)	Weigth (%)	Volume (cm³)	Appearance/ function
LSM	6.580	6.521	53.00%	1.009	solid
Methocel A4M	3.725	0.85	30.00%	4.382	binder
2-Butoxyethanol	2.111	0.9	17.00%	2.345	solvent
Total	12.415	1.604		7.736	

Cathode/Electrolyte Interlayer	Weight (gm/329 cm ²)	Density (g/cm ³)	Weight (%)	Volume (cm ³)	Appearance/function
LSM (50% vol)	1.645	6.521	26.50%	0.252	solid
YSZ (50% vol)	1.645	6.1	26.50%	0.270	solid
Methocel A4M	1.862	0.85	30.00%	2.191	binder
2-Butoxyethanol	1.055	0.9	17.00%	1.173	solvent
Total	6.208	1.597		3.885	

Electrolyte Layer	Weight (gm/329 cm ²)	Density (g/cm ³)	Weight (%)	Volume (cm ³)	Appearance/function
YSZ	3.290	6.1	70.00%	0.539	solid
Santicizer 160 (DBP)	0.282	1.1	6.00%	0.256	Plasticizer
Butvar-76 (PVB)	0.282	1.08	6.00%	0.261	binder
n-Butylacetate	0.846	0.88	18.00%	0.961	solvent
Total	4.700	2.328		2.018	

Cathode and electrolyte material composition are adopted from those used in an earlier TIAX report (Carlson, Yang, & Fulton, 2004). Interlayer compositions used in this study were 50%YSZ-50%LSM for the cathode/electrolyte interlayer and 50%YSZ-50%NiO for the anode/electrolyte interlayer (Reitz & Xiao, 2006). The same solvents as those used for the cathode slurry were utilized. The anode is formed mixing NiO powder and 8YSZ powder in the common volume ratio 70:30 (Kishimoto, Miyawaki, Iwai, Saito, & Yoshida, 2013). Binders most commonly used for Ni/YSZ anode organic slurry are polyvinyl butyral (PVB) or methyl ethyl ketone (MEK) while in the case of screen printing the most diffused are ethyl cellulose or polyvinyl butyral (Shanefield, 2013).

The quantity of binder in the ceramic slurry is between 1% and 20% by weight, and commonly between 2% and 10% by weight relative to the total weight of said ceramic slurry (Delahaye & Rieu, 2012). The plasticizers most frequently used are dibutyl phthalate (DBP) and polyethylene glycol (PEG). The quantity of plasticizer in the ceramic slurry is between 1% and 20% by weight, and commonly between 2% and 10% by weight relative to the total weight of said ceramic slurry (Delahaye & Rieu, 2012).

According to (Sanson, Pinasco, & Roncari, 2008), the most favorable pore formers for SOFC anode tape casting are rice starch and carbon black. Their influence on the amount of porosity and on the pore dimensions and shape is much higher compared to other pore formers. Based on these considerations, it was decided to use the same slurry composition of electrolyte slurry (6%wt binder, 6%wt plasticizer, 18%wt solvent) and to add ~ 5% in weight of carbon black (Weimar, Chick, & Whyatt, 2013) necessary to reach a final anode porosity of 30-40% .

The first step of slurry preparation consists of mixing powder with solvent in a ball mill for 12 hours without the presence of binder and plasticizer. In the second stage milling, binder and plasticizer are added and slurry is ball milled for another 12 hours.

Ceramic Slurry Material Cost

Material cost of each layer was calculated using the weight of the slurry constituents multiplied by the corresponding material cost (\$/kg). Most materials were priced from several suppliers who supply high-quality materials for SOFC. These suppliers are based in Japan, USA, and China. Materials were priced based on delivery to the center of the United States.

The prices from Chinese suppliers were also evaluated against prices from some US distributors to determine whether their prices were competitive or significantly underpriced. It was found that Chinese suppliers provide high quality materials at competitive prices relative to some US-based suppliers. Material prices used in this study are shown in Table 4.4.

Table 4.4. Anode-supported cell material prices

Vendor/Country	Material	Order quantity (kg)	Price (\$/kg)	Comments
AIICHI JITSUGYO (Japan)	Nickel Oxide	1000	68.5	CIF USA by sea
		5000	42.5	CIF USA by sea
		10000	37	CIF USA by sea
		20000	34	CIF USA by sea
AIICHI JITSUGYO (Japan)	8YSZ (8mol%YSZ)	100	78	CIF USA by sea
		1000	68	CIF USA by sea
		5000	63	CIF USA by sea
Daiichi (Japan)	8YSZ (8mol%YSZ)	10	97	CIF USA by sea
		100	95	CIF USA by air
		1000	83	CIF USA by sea
Inframat Advanced Materials (USA)	8YSZ (8mol%YSZ)	1	139.2	by rail or truck
		5	115.8	by rail or truck
		10	94.5	by rail or truck
		50	71.6	by rail or truck
		100	49.7	by rail or truck
		1000	35.2	by rail or truck
Inframat Advanced Materials (USA)	LSM powder	100	170	by rail or truck
		1000	95	by rail or truck
		10000	70	by rail or truck
Qingdao Terio Corporation (China)	LSM powder	10	250	CIF USA by air
		100	150	CIF USA by air
		200	125	CIF USA by air
		500	105	CIF USA by air
		1000	80	CIF USA by air
		2000	75	CIF USA by air
		5000	60	CIF USA by air

CIF = price including cost, insurance and freight

Table 4.5. Binders, plasticizers, pore formers and solvents prices

Vendor/Country	Material	Order quantity (kg)	Price (\$/kg)	Comments
Jiangsu Xiangcanghongrun Trade Co.,Ltd (China)	N-butyl acetate 99,5%	100	4.34	CIF USA by sea
		1000	1.516	CIF USA by sea
		10000	1.29	CIF USA by sea
ChemPoint Inc (USA)	Methocel A4M	1-45400	18,5-29,6	CIF price
Dowd & Guild, Inc. (CA)	Butvar B-76	63.5	23.37	by rail or truck
		200	21.42	by rail or truck
		500	19.47	by rail or truck
		1000	18.36	by rail or truck
		2000	17.14	by rail or truck
		5000	16.07	by rail or truck
Univar USA	Santicizer 160	Contact Univar USA for a current price quote		
Cancarb Limited (USA)	Thermax® N990 Thermal Carbon Black	Contact Cancarb for a current price quote		
Jinan Shijitongda Chemical Co., Ltd. (China)	2- Butoxyethanol	1000	3.07	CIF USA
		10000	3.07	CIF USA
		100000	2.53	CIF USA
		1000000	2.32	CIF USA
		10000000	2.29	CIF USA

CIF = price including cost, insurance and freight

As shown on Table 4.4 and Table 4.5, material costs depend on the annual production volume, especially for ceramic materials used in the fabrication of the EEA cells.

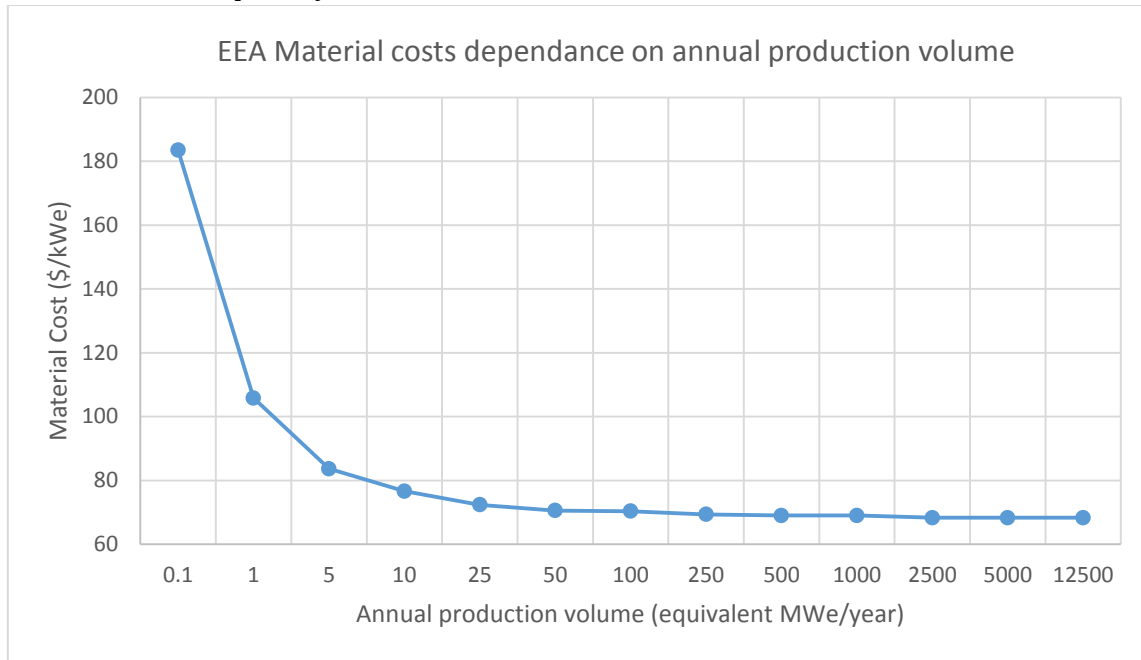


Figure 4.3. Material costs dependence on annual production volume (\$/kWe)

Since material quotations were provided by vendors mainly for quantity varying from 1 to 50,000 kg, materials costs (\$/kWe or \$/part) tend to *become constant* at levels of annual productivity higher than 25 MW (325000 EEA cells/year) as shown on Figure 4.3 and Figure 4.4.

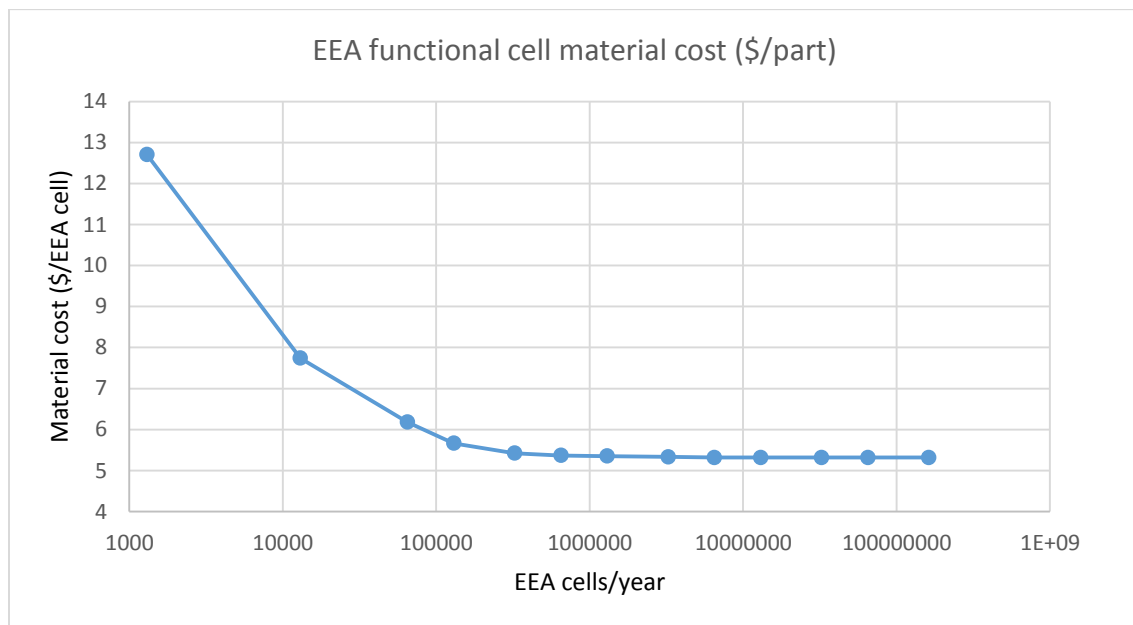


Figure 4.4. EEA functional cell material cost in \$/EEA cell

Generally speaking, anode materials in anode supported cell design contribute to about 75-82% of the EEA material cost (because of the thickness of this layer) followed by the cathode, leaving a small fraction for remaining layers (<9% for electrolyte and interlayers). Figure 4.5 below show layers material cost contribution on total EEA material cost at an annual production volume of 50 MW (650,000 cells/year).

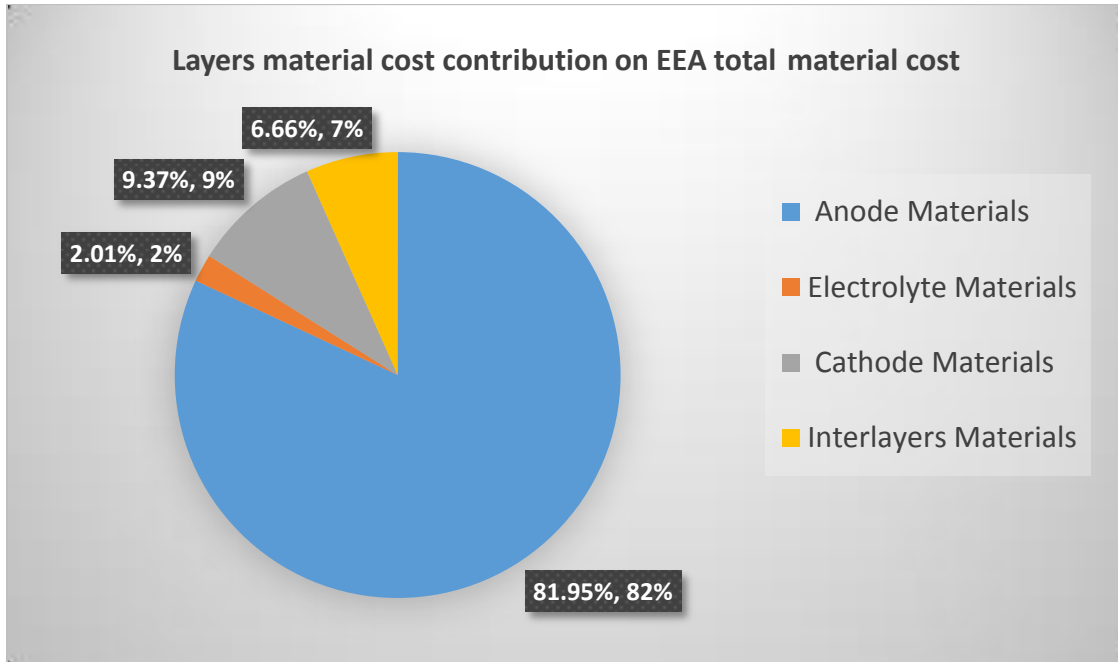


Figure 4.5. Layer material cost contribution on total EEA material cost (%) at an annual production volume of 50MW.

Ceramic Slurry Drying Time

In the EEA coating and deposition processes (tape casting and screen printing), ceramic slurry is dried in a tunnel dryer by radiant heating (infrared heating). In order to estimate the required tape casting under-bed heater length and infrared oven tunnel length it was necessary to calculate the drying time after each deposition process.

The drying stage comprises three steps (Burggraaf & Cot, 1996):

1. Solvent diffuses through the slurry to the surface;
2. Solvent evaporates at the surface; and
3. Solvent is removed from the surface by a counter-flow of air.

Such a drying process can result in a very slow process since the drying temperature must be kept below the solvent boiling temperature otherwise there would be an inevitable formation of air bubbles (Burggraaf & Cot, 1996). In practical situations the evaporation rate of organic solvents are not absolute values because they depend upon various factors such as temperature, airflow, humidity, exposed surface area and the presence of resin (binders) and pigment (Koleske, 1995).

For example, the presence of resin retards solvent evaporation. Usually, the evaporation rate of organic solvents are estimated empirically or using appropriate software able to model solvency and

evaporation rates of solvents taking into account chemical interactions between slurry components (Koleske, 1995).

In this analysis non-aqueous slurries were also considered but it is well known that water evaporates more slowly than most organic solvents such as n-butyl acetate or 2-butoxyethanol (Brock, Groteklaes, & Mischke, 2000). Hence it was decided to be conservative and use the average evaporation rate value of aqueous slurry suggested by (Mistler, Runk, & Shanefield, 1978) as done in a recent Battelle report (Battelle Memorial Institute, 2014). In reality, evaporation rates may be expected to be faster than the ones estimated in this study and these would result in shorter drying times. Assuming that the ratio of the freshly deposited layer thickness to the dried tape thickness is two (i.e., 2:1) (Burggraaf & Cot, 1996), and multiplying this freshly deposited layer thickness by its corresponding liquid density it was possible to obtain the quantity of liquid removed per unit area.

Drying tunnel length required was estimated for three different casting speeds considering an average evaporation rate of the solvent equal to 2.22×10^{-5} g/(cm² sec) at room temperature for an air flow rate of 75 l/min (Mistler, Runk, & Shanefield, 1978). Table 4.6 shows the obtained results.

Table 4.6. Estimated Quantity of Liquid removed per unit area and corresponding Drying Time for each EEA layer

ANODE SLURRY			ELECTROLYTE SLURRY		
Liquid density (g/cm ³)	Liquid removed/unit area(g/cm ²)	Drying time (min)	Liquid density (g/cm ³)	Liquid removed/unit area(g/cm ²)	Drying time (min)
0.264588	0.029633856	24.69	0.28716	0.00057432	0.48

CATHODE SLURRY			INTERLAYERS SLURRY		
Liquid density (g/cm ³)	Liquid removed/unit area(g/cm ²)	Drying time (min)	Liquid density (g/cm ³)	Liquid removed/unit area(g/cm ²)	Drying time (min)
0.26775	0.0026775	2.23	0.26775	0.0005355	0.45

Tape Casting

In this treatment, the tape casting machine represents the “bottleneck machine” and limits throughput, and all the other machines in the production line (as screen printers, infrared ovens, ball mills etc.) were sized depending on tape casting machine production capacity and considering a continuous production process for all different production volumes.

This means that all machines in the production line will operate for a number of hours per year equal to the annual operating hours of casting machine except for ball mills, co-firing kilns, laser cutters and the quality control system after co-firing step since they have different daily operating hours due to their longer cycle times. In this analysis tape casting machines from HED International were chosen (Figure 4.6).

	PRO CAST		TCM Series Tape Casting Machines
Model No.	Casting Length	Casting Width	Suggested Application Description
TC-71LC	2.1M	300mm	Ideal for R&D Lab Table-Top
TC-121	3.7M	300mm	Designed for Lab-scale studies
TC-251	7.7M	300mm	Versatile Pilot Plant Size
TC-501	15.4M	300mm	Medium Scale Production
TC-252	7.7M	600mm	Double Wide Pilot Plant Size
TC-502	15.4M	600mm	Double Wide Scale Production
TC-1002	30.8M	600mm	Double Wide Volume Production
TC-504	15.4M	1200mm	Quad Wide Scale Production
TC-1004	30.8M	1200mm	Quad Wide Volume Production

*Specifications are approximate and subject to change without notice.

Figure 4.6. Tape casting machine specification from HED International.

The factors taken into account in the tape casting process analysis in order to estimate the annual production capacity and the required size of the tape casting machine were:

- Casting width (which determines the number of pieces casted simultaneously)
- Drying time (together with casting speed determines the drying tunnel length required)
- Casting speed (which determines also the number of parts casted with respect to time)

The choice of an appropriate casting speed was extremely difficult since it depends upon the length of drying chamber (or under-bed heater), the required thickness of the tape and solvent used (Terpstra, Pex, & de Vries, 1995). Since casting speed values are proprietary and not revealed by fuel cell manufacturers, a literature research about Ni/YSZ anode tape casting was conducted.

It was found that in case of low scale production (laboratory and pilot plant), typical casting speeds are around 0.15-0.6 m/min (Schafbauer, Menzler, & Buchkremer, 2014; Moreno, Bernardino, & Hotza, 2014; Battelle Memorial Institute, 2014; Moreno R. , 2012), depending on the thickness of the tape, the length of tape casting machine and the solvent volatility. Similar to our case, one recent reference (Schafbauer, Menzler, & Buchkremer, 2014) assumed a speed of 0.25 m/min for an organic solvent based slurry and a desired green tape thickness of about 600 μm .

For medium and high volume production, typical industrial casting speeds (for 350 μm anode thickness) can reach 1.2-1.5 m/min as found in two reports (National Energy Technology Laboratory , 2007) and (Carlson, Yang, & Fulton, 2004). In addition, (Weimar, Chick, & Whyatt, 2013) considered a casting rate of 3 m/min for a 30 m long machine and a drying time of 10 minutes and (Carter & Norton, 2013) declared that for quick-drying compositions, casting speed can be as high as 2 m/min.

Reflecting on these results, it is apparent that increasing the annual production volume (and so the grade of manufacturing automation) there was a tendency of using longer machines in order to reduce cycle time and production costs. For this reason, the approach in this analysis was to choose three possible values of casting speed to use for three different ranges of annual production volume starting from estimated drying time and available machine lengths. Then, a casting speed sensitivity analysis ($\pm 20\%$ casting speed change) was conducted to understand how much the production rate (m/min) affected the EEA cells manufacturing cost (see paragraph 5.1.5).

The speed values chosen were:

- 0.25 m/min for low production volumes (≤5 MWe)
- 0.5 m/min for production volumes from 10 to 100 MWe
- 1 m/min for high production volumes (>100 MWe)

The required drying tunnel lengths (shown on Table 4.7) were obtained multiplying the casting speed by the drying time assuming a fixed dryer temperature setting.

Table 4.7. Estimated required tunnel length for different casting speed values

Tape casting machine required tunnel length (m)		
0.25 m/min speed	0.5 m/min speed	1 m/min speed
6.17	12.35	24.69

The number of pieces cast simultaneously was obtained dividing the maximum casting width of each machine by the anode layer size including a 1 cm margin.

The required casting length to cover the desired annual production volume was determined with the “max carrier length” formulae shown below.

$$\text{Required carrier length} \left(\frac{m}{\text{year} * \text{line}} \right) = \frac{\text{cell size (m)} * \frac{\text{cells required}}{\text{year}}}{\frac{\text{Process Yield}}{\text{\# of cells casted simultaneously}}}$$

Setup consists of loading and threading the casting substrate and maintenance operations. The numbers of setups per year were estimated using an approach from Battelle (Battelle Memorial Institute, 2014). As mentioned in their study, Mylar roll stock in 50 μm thickness cost approximately \$2.00/m² in bulk. Considering a 1000 m long bulk roll stock the number of setups required were determined as (Battelle Memorial Institute, 2014):

$$\text{\# of setups} \left(\frac{\text{setups}}{\text{year}} \right) = \text{roundup} \left[\frac{\text{required carrier length (m)}}{\text{roll length(m)}} \right]$$

Since number of setups per year corresponds to the number of Mylar rolls needed per year, Mylar film cost is equal to:

$$\text{Mylar film cost} \left(\frac{\$}{\text{year}} \right) = \frac{\text{\# of setups}}{\text{year}} * (\text{roll length(m)} * \text{casting width(m)}) * 2 \left(\frac{\$}{\text{m}^2} \right)$$

Assuming a value of two hour as setup time, 16 operational hours per day and 240 operational days (48 operating weeks) per year the maximum casting length achievable with one machine is:

$$\frac{\text{Max carrier length(m)}}{\text{line} * \text{day}} = \text{speed} \left(\frac{m}{h} \right) * \text{Line Performance} * \left[\frac{\text{op. hours}}{\text{day} * \text{line}} - \frac{\text{req carr length}}{\text{day} * 1000} \right]$$

$$\frac{\text{Max carrier length}(m)}{\text{line} * \text{year}} = \text{speed} \left(\frac{m}{h} \right) * \text{Line Performance} * \left[\frac{\text{op. hours}}{\text{year} * \text{line}} - \frac{\text{setups}}{\text{year}} \right] * \text{Availability}$$

This corresponds to a number of cells casted per day and per week equal to:

$$\frac{\# \text{ of cells casted}}{\text{day} * \text{line}} = \frac{\text{Max carrier length} \left(\frac{m}{\text{day} * \text{line}} \right) * \# \text{ of cells casted simultaneously}}{\text{cell size} (m)}$$

$$\frac{\# \text{ of cells casted}}{\text{day}} = \frac{\# \text{ of cells casted}}{\text{day} * \text{line}} * \# \text{ of lines}$$

$$\frac{\# \text{ of cells casted}}{\text{week} * \text{line}} = \frac{\# \text{ of cells casted}}{\text{day} * \text{line}} * 5 \frac{\text{operational days}}{\text{week}}$$

$$\frac{\# \text{ of cells casted}}{\text{week}} = \frac{\# \text{ of cells casted}}{\text{week} * \text{line}} * \# \text{ of lines}$$

Then the number of casting machines necessary to guarantee the annual production volume and the corresponding percentage utilization was:

$$\# \text{ of casting lines} = \frac{\text{Required carrier length}(m/\text{year})}{\text{Max carrier length} \left(\frac{m}{\text{line} * \text{year}} \right)}$$

$$\text{Line utilization} (\%) = \frac{\text{Required carrier length}(m/\text{year})}{\text{Max carrier length} \left(\frac{m}{\text{line} * \text{year}} \right) * \# \text{ of lines}}$$

The annual operating hours including setup time were estimated as:

$$\text{Annual operating hours} = \frac{\text{Required carrier length} \left(\frac{m}{\text{year}} \right)}{\text{casting speed} \left(\frac{m}{h} \right) * \text{Line Performance}} + \text{Number of setups} \left(\frac{\text{hours}}{\text{year}} \right)$$

$$\frac{\text{Annual operating hours}}{\text{line}} = \frac{\text{Annual operating hours}}{\# \text{ of casting lines}}$$

From this it is possible to obtain the total labor cost for casting process considering 2 workers per casting line:

$$\text{Labor Cost} \left(\frac{\$}{\text{year}} \right) = \text{Annual operating hours} * \# \text{ of lines} * \frac{\text{workers}}{\text{line}} * \text{worker rate} \left(\frac{\$}{\text{hour}} \right)$$

Table 4.8 shows estimated tape casting process parameters and corresponding machine rates for 50-kWe systems at all production volumes.

Table 4.8. Tape casting machine rates and manufacturing parameters for 50-kWe systems at all production volume

System size (kWe)	50			
	100	1000	10000	50000
Systems/year	100	1000	10000	50000
Casting Machine Model	TC251	TC502	TC1002	TC1004
Casting Width (m)	0.30	0.60	0.60	1.20
Casting Speed (m/min)	0.25	0.50	1.00	1.00
Number of Lines	1	1	3	6
EEA cells required/year	65000	650000	6500000	32500000
Casting Line Utilization (%)	34.09%	49.24%	76.77%	93.51%
No of cells casted simultaneously	1	3	3	6
Required roll length(m)	13830.56	45099.64	446146.95	1103501.77
Max No of cells/year/line	211870	478280	3034724	6162180
# of setups / year	14	46	447	1104
Mylar film cost (\$/year)	8400	55200	536400	2649600
Annual Operating Hours (+setup)	1064.00	1674.44	8721.14	21567.68
Workers/casting line	2	2	2	2
Labor cost(\$)	63435.5	99830.3	519954.3	1285865.1
Maintenance factor	0.10	0.10	0.10	0.10
Auxiliary Costs Factor	0.00	0.00	0.00	0.00
Power Consumption	24	50	210	540
Machine Footprint (m2)	30	90	510	1680
Initial Capital (\$)	316,000	512,000	2,160,000	7,070,000
Initial System Cost (\$)	348,000	563,000	2,380,000	7,780,000
Annual Depreciation (\$/yr)	20,600	33,500	141,000	462,000
Annual Cap Payment (\$/yr)	39,400	63,900	270,000	883,000
Auxiliary Costs (\$/yr)	0.00	0.00	0.00	0.00
Maintenance (\$/yr)	3585.86	5809.99	24510.91	80273.23
Salvage Value (\$/yr)	120.74	195.62	825.28	2702.81
Energy Costs (\$/yr)	3184.58	10440.97	76132.79	242073.03
Property Tax (\$/yr)	1308.24	2119.68	8942.40	29286.36
Building Costs (\$/yr)	2525.06	7575.18	42926.00	141403.30
Interest Tax Deduction (\$/yr)	0.00	0.00	0.00	0.00
Machine Rate (\$/h)	46.92	53.55	48.31	63.68
Capital	36.96	38.05	30.82	40.82
Variable	14.26	42.67	73.05	137.80
Building	3.60	5.79	5.95	7.91

Sensitivity analysis was also conducted to see how casting speeds and casting width considered affected the size of the other machines in the production line, annual operating hours and consequently the EEA final cost (\$/kWe) for different annual production volumes. This was useful for

understanding which casting machine configuration is best for each annual production volume considered in this study.

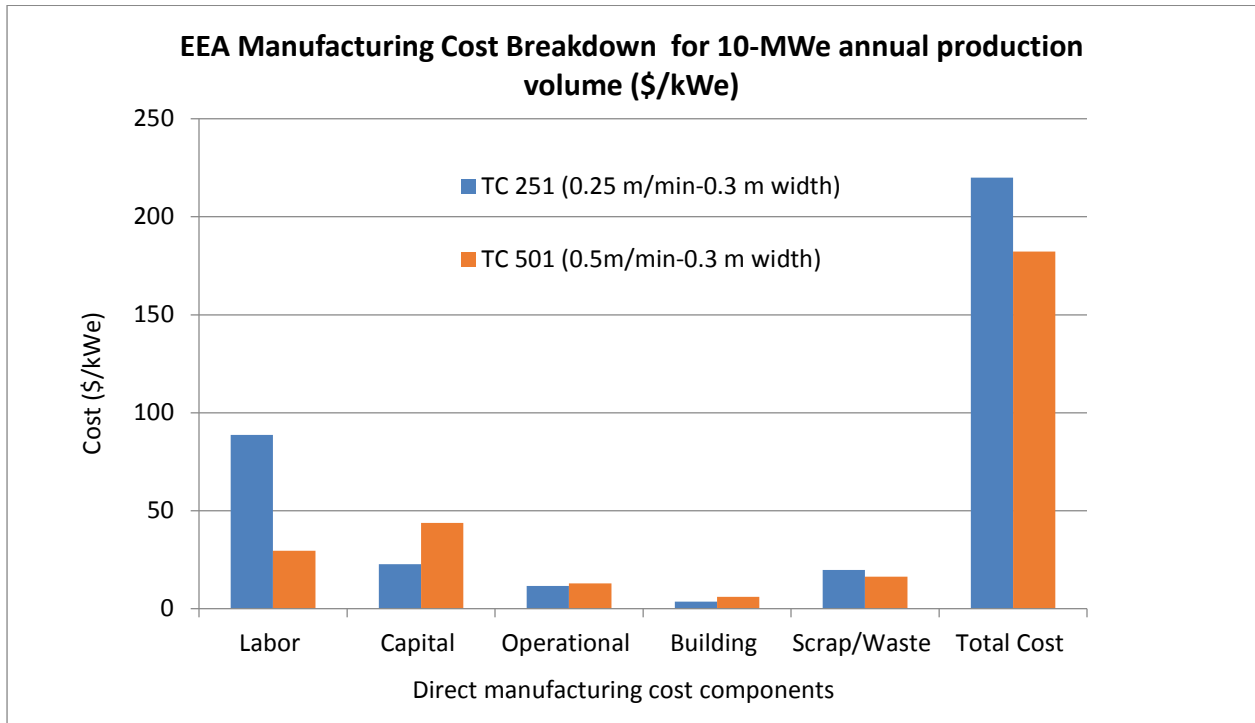


Figure 4.7. EEA Cost breakdown comparison for two different casting configurations at 10 MWe annual volume

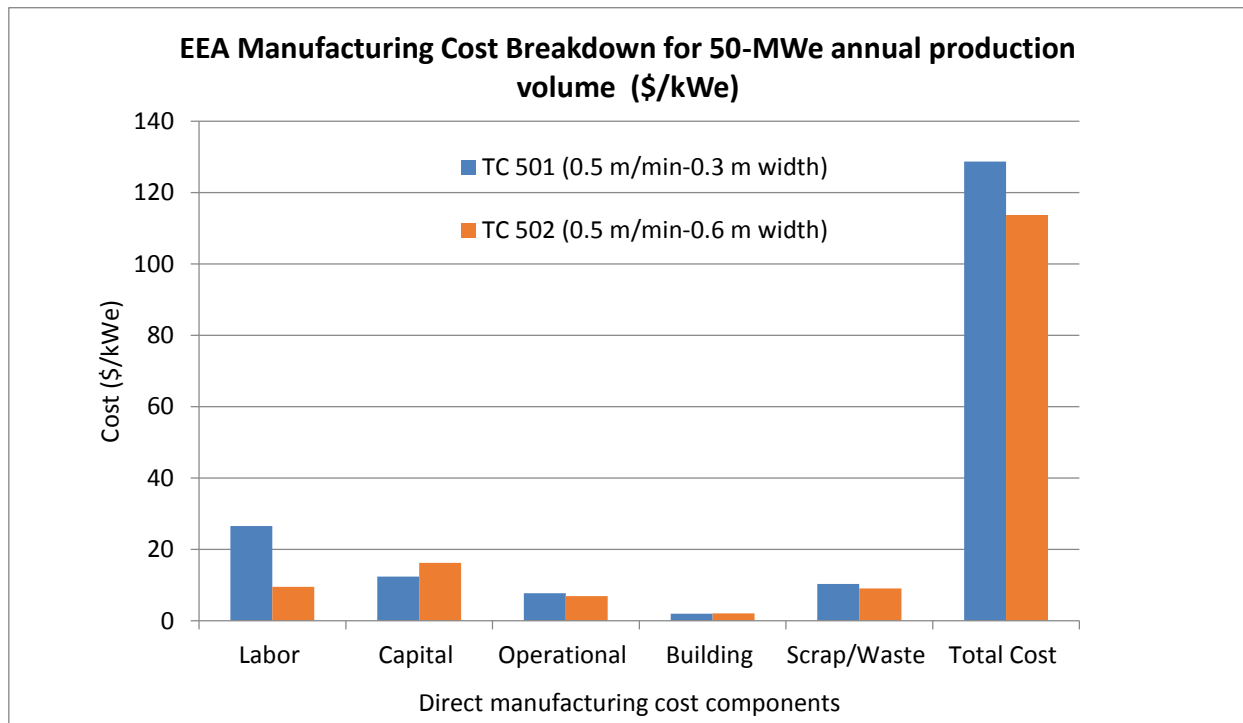


Figure 4.8. EEA manufacturing cost breakdown comparison for two different casting configurations at 50 MW annual volume

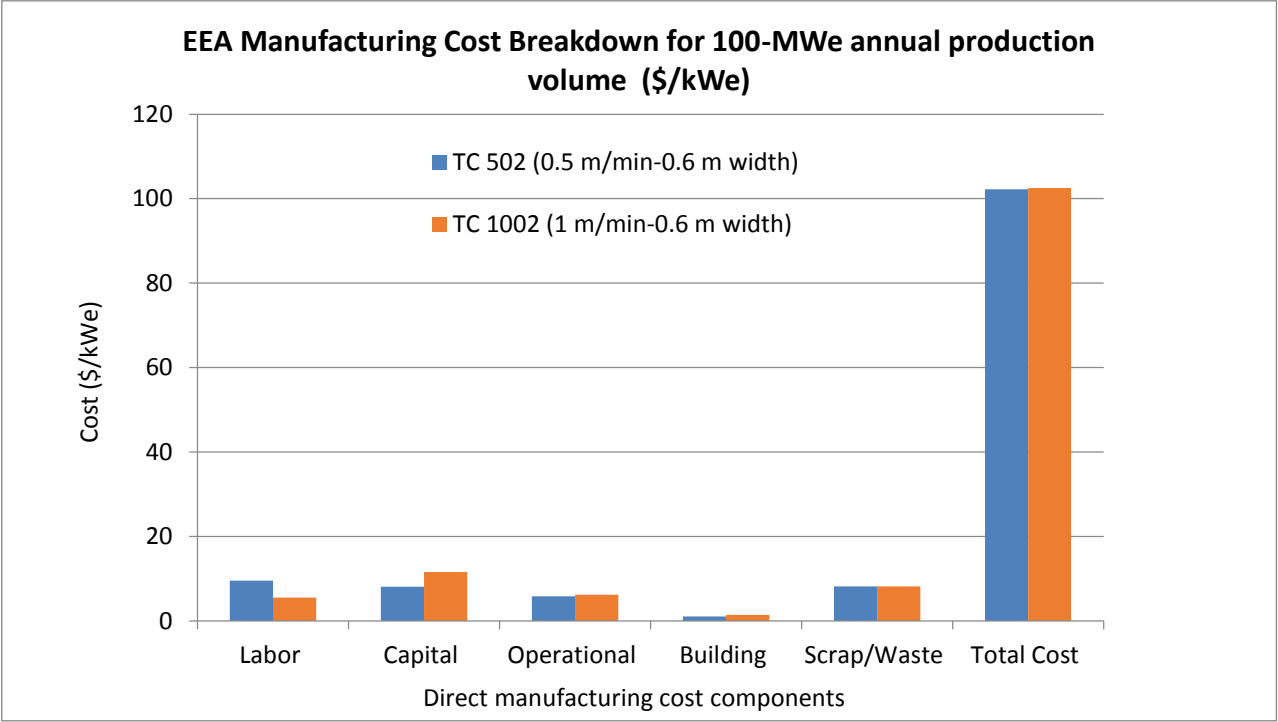


Figure 4.9. EEA manufacturing cost breakdown comparison for two different casting configurations at 100 MWe annual volume

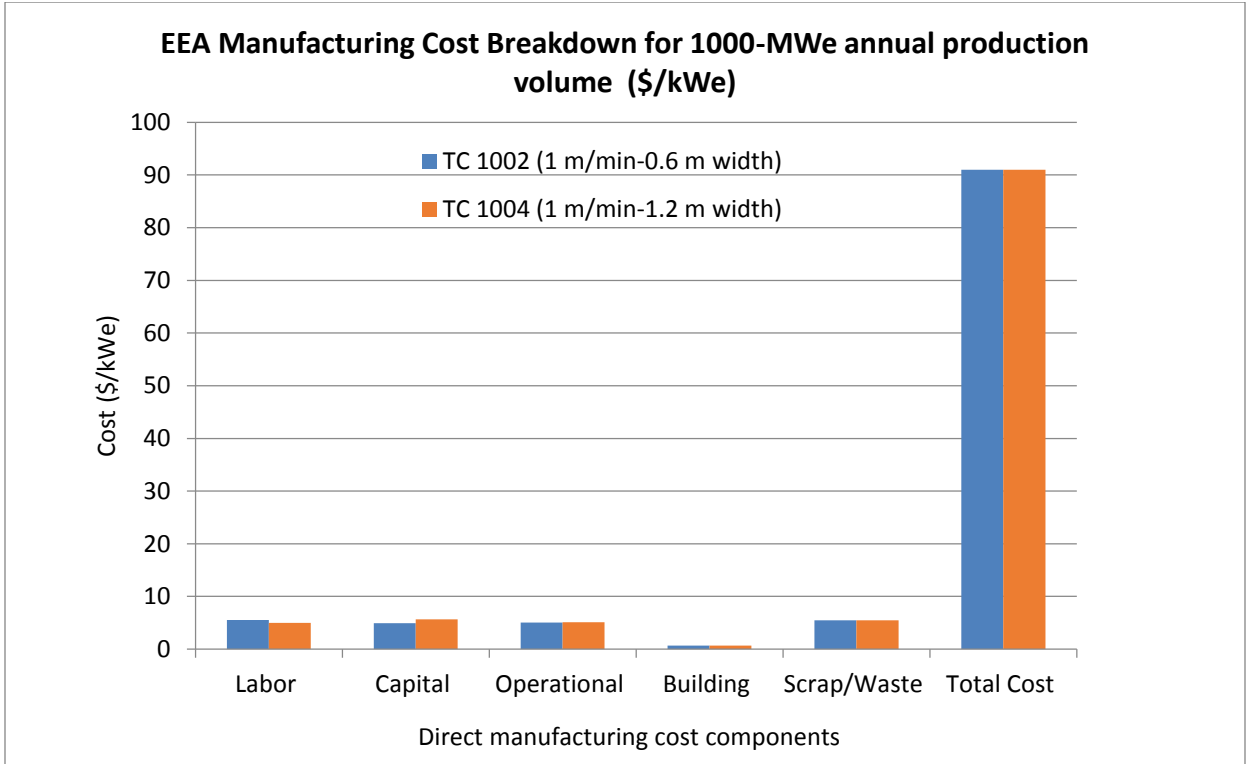


Figure 4.10. EEA manufacturing cost breakdown comparison for two different casting configurations at 1000 MWe annual volume

Referring to these results it was possible to choose the appropriate machines configurations:

- TC-251 with 0.25 m/min casting speed for production volumes ≤ 5 MWe
- TC-501 with 0.5 m/min casting speed for production volumes from 10 to 25 MWe
- TC-502 with 0.5 m/min casting speed for production volumes from 50 to 100 MWe
- TC-1002 with 1 m/min casting speed for production volumes from 250 to 500 MWe
- TC-1004 with 1 m/min casting speed for production volumes ≥ 1000 MWe

Ball Milling

Slurries are prepared by a two-step ball milling process. In the first step, solid powders are ball milled for 12 hours in solvent. In the second step, binder and plasticizer ingredients are added and then ball milled for another 12 hours (Liu, Fu, Chan, & Pasciak, 2011). Quantities of slurry to mill per day were estimated based on number of cells casted per day and slurry weight of each layer.

Ball mill sizes for anode and cathode layer slurries preparation were evaluated separately while the same size machines are assumed in the case of electrolyte layer and interlayer slurries since they are characterized by similar weights. We followed the rule of thumb that wet milling grinding balls should occupy 50% of the mill capacity and the slurry 40% of the mill capacity (Rahaman & Rahaman, 2006).

For low production volumes ball mills from Bionics Scientific Technologies (P) Ltd. were taken into account. Prices including grinding media and consumption are shown on the Table 4.9.

Table 4.9. Bionics Scientific Technologies Ltd. ball mills costs and specifications

Small scale ball mills		
Capacity (kg)	2	10
Consumption (KW)	0.3	0.8
Cost (\$)	567	1150

For high production volumes, prices and specifications of 5 ton ball mill was found in literature (Weimar, Chick, & Whyatt, 2013) while those of 0.5 ton, and 50 ton ball mills were found on from the Alibaba website.

Table 4.10. Industrial ball mills costs and consumptions

Industrial ball mills			
Capacity (ton)	0.5	5	50
Consumption (kW)	7.5	36.8	119
Cost (\$)	10000	44668,36	158490

In the case of small scale ball mills, approximate costs and dimensions of intermediate size ball mills were estimated with the modified version of “rule of six-tenth” (Whitesides, 2012) using 2 kg and 10 kg ball mills technical data as reference:

$$C_b = C_a * \left(\frac{S_b}{S_a}\right)^N$$

where

C_b = the approximate cost (\$) of equipment having size S_b

C_a = is the known cost (\$) of equipment having corresponding size S_a (same unit as S_b)

S_b/S_a is the ratio known as the size factor, dimensionless

N=process equipment size exponent

A process equipment size exponent for ball mill equal to 0.65 was found on Table 4.11 (Whitesides, 2012).

Table 4.11. Process equipment size exponent for common industrial equipment

PROCESS EQUIPMENT SIZE EXPONENT (N) - TABLE 1		
EQUIPMENT NAME	UNIT	SIZE EXPONENT (N)
Dryer, drum and rotatory	sq. ft.	0.45
Dust collector, cyclone	cfm	0.80
Dust collector, cloth filter	cfm	0.68
Dust collector, predpitator	cfm	0.75
Evaporator, forced circulation	sq. ft.	0.70
Evaporator, vertical and horizontal tube	sq. ft.	0.53
Fan	Hp	0.66
Filter, plate and press	sq. ft.	0.58
Filter, pressure leaf	sq. ft.	0.55
Heat exchanger, fixed tube	sq. ft.	0.62
Heat exchanger, U-tube	sq. ft.	0.53
Mill, ball and roller	ton/hr	0.65
Mill, hammer	ton/hr	0.85
Pump, centrifugal carbon steel	Hp	0.67
Pump, centrifugal stainless steel	Hp	0.70
Tanks and vessels, pressure, carbon steel	gallons	0.60
Tanks and vessels, horizontal, carbon steel	gallons	0.50
Tanks and vessels, stainless steel	gallons	0.68

As in the case of small scale ball mills, intermediate size and relative costs of industrial ball mills were also estimated with the rule of six tenth using 0.5, 5, and 50 ton ball mills (Whitesides, 2012) as reference.

Concerning raw materials handling, the first step is to weigh the materials out and place them in the mill. Once the process is complete, the slurry needs to be separated from the milling balls using sieves and poured into a container. In this, analysis sieves and containers were not explicitly costed. Then the ball mill must be cleaned by dumping a moderate amount of solvent into the mill, running it for one minute, and then dumping immediately to avoid settling out of solids. Several washes may be necessary to do the job (U.S. Stoneware, 2015).

For ball mill loads <= 50 kg, a manual process was considered, while for heavier loads, a robotic system with dosing machines was assumed. Handling time for manual process (measurement, mill loading and unloading, balls removal and mill cleaning) was assumed to be 0.5 hours.

Based on these assumptions, for each deposition process it was possible to estimate the following:

$$\frac{\text{Slurry}}{\text{day}} \left(\frac{\text{kg}}{\text{day}}\right) = \frac{\text{slurry}}{\text{cell}} \left(\frac{\text{kg}}{\text{cell}}\right) * \frac{\text{cells casted}}{\text{day}}$$

$$\frac{\text{Slurry} \left(\frac{\text{ton}}{\text{year}} \right)}{\text{year}} = \frac{\frac{\text{slurry} \left(\frac{\text{ton}}{\text{cell}} \right) * \frac{\text{cells required}}{\text{year}}}{\text{Process Yield}}}$$

$$\frac{\text{Cycles required}}{\text{year} * \text{machine}} = \text{roundup} \left(\frac{\left(\frac{\text{Slurry} \left(\frac{\text{kg}}{\text{year}} \right)}{\frac{\text{Slurry} \left(\text{Kg} \right)}{\text{day}}} \right)}{\left(\frac{\text{kg}}{\text{year}} \right) / \left(\frac{\text{day}}{\text{day}} \right)} \right)$$

$$\frac{\text{Max \# of Cycles}}{\text{year} * \text{machine}} = 240 = \frac{\text{operational days}}{\text{year}}$$

$$\text{Machine utilization (\%)} = \frac{\frac{\text{Cycles required}}{\text{year}}}{\frac{\text{Max \# of cycles}}{\text{year} * \text{machine}} * \# \text{ of machines required}}$$

$$\text{Annual Operating hours} \left(\frac{\text{hours}}{\text{year}} \right) = \frac{\text{cycles required}}{\text{year}} * \text{Milling time} \left(\frac{24 \text{ hours}}{\text{cycle}} \right)$$

Since manual labor is required only for load and unload machines, annual labor hours and cost were calculated as:

$$\text{Labor hours} \left(\frac{\text{hours}}{\text{year}} \right) = \frac{\text{Cycles required}}{\text{year}} * \text{load unload time} \left(\frac{0.5 \text{ hours}}{\text{cycle}} \right)$$

$$\text{Labor cost} \left(\frac{\$}{\text{year}} \right) = \frac{\# \text{ of workers}}{\text{kiln}} * \text{Labor hours} \left(\frac{\text{hours}}{\text{year}} \right) * \text{Worker rate} \left(\frac{\$}{\text{hour}} \right)$$

Table 4.12 and Table 4.13 show ball milling process estimated machine rates and corresponding costs for 50-kWe systems for anode slurry and cathode slurry, respectively. Electrolyte and interlayer slurry milling process cost are shown on Table 4.14.

Table 4.12. Machine rates for anode slurry ball milling process (50-kWe systems)

Ball Mill for Anode Slurry				
System size (kWe)	50			
Production volume (systems/year)	100	1000	10000	50000
Type of handling (load/unload)	automatic	automatic	automatic	automatic
No of ball mills	1	1	1	1
Workers/machine	0	0	0	0
Quantity of slurry to mill/day (kg)	169.09	2070.92	6212.75	24851.91
Max load capacity (kg)	500	5000	15000	50000
Max Load /cycle (kg/cycle)	250	2500	7500	25000
Max # of cycles/year/machine	240.00	240.00	240.00	240.00
# of cycles required/year/machine	66	53	173	214
Machine utilization (%)	18.60%	18.29%	59.71%	88.64%
Labor time (hours)	0.00	0.00	0.00	0.00
Annual operating hours (hours)	1551.00	1245.50	4065.50	5029.00
Labor cost(\$)	0.00	0.00	0.00	0.00
Maintenance factor	0.10	0.10	0.10	0.10
Auxiliary Costs Factor	0.00	0.00	0.00	0.00
Power Consumption/machine (KW)	7.5	36.8	68	150
Machine Footprint (m2)	32	89	146	250
Initial Capital (\$)	1.00E+04	4.47E+04	9.12E+04	2.00E+05
Initial System Cost (\$)	1.10E+04	4.91E+04	1.00E+05	2.20E+05
Annual Depreciation (\$/yr)	6.53E+02	2.92E+03	5.96E+03	1.31E+04
Annual Cap Payment (\$/yr)	1.25E+03	5.58E+03	1.14E+04	2.50E+04
Auxiliary Costs (\$/yr)	0.00	0.00	0.00	0.00
Maintenance (\$/yr)	113.48	506.88	1035.23	2269.53
Salvage Value (\$/yr)	3.82	17.07	34.86	76.42
Energy Costs (\$/yr)	1450.69	5716.00	34476.51	94074.81
Property Tax (\$/yr)	41.40	184.93	377.69	828.00
Building Costs (\$/yr)	2693.40	7491.01	12288.62	21042.16
Interest Tax Deduction (\$/yr)	0.00	0.00	0.00	0.00
Machine Rate (\$/h)	3.57	15.62	14.64	28.46
Capital	0.80	4.46	2.79	4.95
Variable	1.01	5.00	8.73	19.16
Building	1.76	6.16	3.12	4.35

Table 4.13. Machine rates for cathode slurry milling process (50-kWe systems)

Ball Mill for Cathode slurry	50			
System size (kWe)	50			
Production volume (systems/year)	100	1000	10000	50000
Type of handling (load/unload)	manual	automatic	automatic	automatic
No of ball mills	1	1	1	1
Workers/machine	1	0	0	0
Quantity of slurry to mill/year (ton)	627.65	6140.07	60740.52	300471.70
Quantity of slurry to mill/day (kg)	9.56	117.08	351.24	1405.00
Max load capacity (kg)	20	300	1000	3000
Max Load /cycle (kg/cycle)	10	150	500	1500
Max # of cycles/year/machine	240.00	240.00	240.00	240.00
# of cycles required/year/machine	66	53	173	214
Machine utilization (%)	26.29%	17.24%	50.64%	83.52%
Labor time (hours)	33.00	0.00	0.00	0.00
Annual operating hours (hours)	1723.33	1353.80	4371.51	5350.00
Labor cost(\$)	983.73	0.00	0.00	0.00
Maintenance factor	0.10	0.10	0.10	0.10
Auxiliary Costs Factor	0.00	0.00	0.00	0.00
Power Consumption	1	5	12	26.5
Machine Footprint (m2)	10	26	44	71
Initial Capital (\$)	1.81E+03	7.18E+03	1.57E+04	3.20E+04
Initial System Cost (\$)	1.99E+03	7.89E+03	1.73E+04	3.53E+04
Annual Depreciation (\$/yr)	1.18E+02	4.69E+02	1.03E+03	2.09E+03
Annual Cap Payment (\$/yr)	2.25E+02	8.96E+02	1.96E+03	4.00E+03
Auxiliary Costs (\$/yr)	0.00	0.00	0.00	0.00
Maintenance (\$/yr)	20.48	81.42	178.07	363.67
Salvage Value (\$/yr)	0.69	2.74	6.00	12.24
Energy Costs (\$/yr)	8.23	33.05	258.90	707.23
Property Tax (\$/yr)	7.47	29.70	64.96	132.68
Building Costs (\$/yr)	841.69	2188.38	3703.42	5975.97
Interest Tax Deduction (\$/yr)	0.00	0.00	0.00	0.00
Machine Rate (\$/h)	0.64	2.38	1.41	2.09
Capital	0.13	0.66	0.45	0.75
Variable	0.02	0.08	0.10	0.20
Building	0.49	1.64	0.86	1.14

Table 4.14. Machine rates for electrolyte and interlayers slurries milling process (50-kWe systems)

3 Ball Mills for screen printing (electrolyte and interlayers)				
System size (kWe)	50			
Production volume (systems/year)	100	1000	10000	50000
Type of handling (load/unload)	manual	automatic	automatic	automatic
No of ball mills	3	3	3	3
Workers/machine	1	0	0	0
Quantity of slurry to mill/year (ton)	313.83	3070.04	30370.26	150235.85
Quantity of slurry to mill/day (kg)	4.78	58.54	175.62	702.50
Max load capacity (kg)	10	300	500	2000
Max Load /cycle (kg/cycle)	5	150	250	1000
Max # of cycles/year/machine	240	240	240	240
# of cycles required/year/machine	66	53	173	214
Machine utilization (%)	26.29%	8.62%	50.64%	62.64%
Labor time(hours)	99.00	0.00	0.00	0.00
Annual operating hours (hours)	5170.00	4061.41	13114.52	16050.00
Labor cost(\$)	2951.19	0.00	0.00	0.00
Maintenance factor	0.10	0.10	0.10	0.10
Auxiliary Costs Factor	0.00	0.00	0.00	0.00
Power Consumption (KW)	2.4	15	22.5	54
Machines Footprint (m2)	21	78	96	177
Initial Capital (\$)	3450	21525	30000	73869
Initial System Cost (\$)	3.80E+03	2.37E+04	3.30E+04	8.13E+04
Annual Depreciation (\$/yr)	2.25E+02	1.41E+03	1.96E+03	4.83E+03
Annual Cap Payment (\$/yr)	4.31E+02	2.69E+03	3.74E+03	9.22E+03
Auxiliary Costs (\$/yr)	0.00	0.00	0.00	0.00
Maintenance (\$/yr)	39.15	244.26	340.43	838.24
Salvage Value (\$/yr)	1.32	8.22	11.46	28.22
Energy Costs (\$/yr)	19.75	99.14	485.43	1441.15
Property Tax (\$/yr)	14.28	89.11	124.20	305.82
Building Costs (\$/yr)	1767.54	6565.15	8080.19	14897.85
Interest Tax Deduction (\$/yr)	0.00	0.00	0.00	0.00
Machine Rate (\$/h)	0.44	2.38	0.97	1.66
Capital	0.08	0.66	0.28	0.57
Variable	0.01	0.08	0.06	0.14
Building	0.34	1.64	0.63	0.95

Slurry De-airing and Pumping System

This analysis assumes that slurry de-airing is performed using the high amplitude ultrasonic processing. Due to their high amplitude, these mixers can achieve higher production rates and better final product quality since ultrasonic cavitation also help to disperse particles effectively. Quotes of ultrasonic mixers were obtained from Industrial Sonomechanics LLC.

Three different mixers were considered depending on productivity (Liters/hour) as shown on Table 4.15 below:

Table 4.15. Ultrasonic mixer cost and consumption depending on productivity in (L/h)

Ultrasonic Mixers	Cost with gear pump (\$)	Consumption (kW)	Productivity (L/h)	
			min	max
Low scale processor	8425	1	0	1
Mid scale processor	17950	2	1	50
Industrial scale processor	36950	5	5	300

In order to choose appropriate mixers, slurry volumes to mix per hour were estimated as:

$$\frac{\text{slurry volume}}{\text{hour} * \text{line}} \left(\frac{L}{\text{hour}} \right) = \frac{\frac{\text{cells casted}}{\text{day} * \text{line}} * \frac{\text{slurry volume}}{\text{cell}} \left(\frac{L}{\text{cell}} \right)}{\frac{\text{operational hours}}{\text{day}} \left(\frac{\text{hours}}{\text{day}} \right)}$$

Since anode slurry volume per hour was much higher than those of other layers, three different configurations (with different scale mixers and pumps) were considered:

Table 4.16. Mixing and pumping system configurations

Mixing System Configuration	Low Scale	Medium Scale	High Scale
Anode Slurry	Mid Scale	Mid Scale	Industrial scale
Interlayer Slurry	Low Scale	Mid Scale	Mid Scale
Electrolyte Slurry	Low Scale	Mid Scale	Mid Scale
Interlayer Slurry	Low Scale	Mid Scale	Mid Scale
Cathode Slurry	Low Scale	Mid Scale	Mid Scale

A pumping and mixing system per tape-casting machine and per screen-printing machine was considered. Using expert judgment, one worker per mixer to move slurry from container to mixer and from mixer to tape casting machine reservoir (or screen printing machine) is assumed to be necessary only in the case of a low production volume configuration, while in other cases pumps are used and the number of workers per system depends on system configuration:

- Five workers per system in case of a low scale system (one worker per mixer)
- Two workers per system in case of a medium scale system
- One worker per system in case of a high scale system

Labor cost was evaluated as:

$$\text{Labor Cost} \left(\frac{\$}{\text{year}} \right) = \# \text{ of workers} * \text{Annual operating hours} \left(\frac{\text{hours}}{\text{year} * \text{line}} \right) * \text{Worker rate} \left(\frac{\$}{\text{hour}} \right)$$

where annual operating hours per line are equivalent to those of tape casting line.

Table 4.17 shows estimated machine rates and corresponding costs of slurry de-airing and pumping processes for 50-kWe systems.

Table 4.17. Machine rates for slurries de-airing and pumping system (50-kWe systems)

System size (kWe)	50			
Production volume (systems/year)	100	1000	10000	50000
Type of Mixer Configuration	low scale	high scale	high scale	high scale
Cast slurry volume/hour/line (L/hour)	6.57	75.02	68.84	135.49
Print slurry volume/hour (L/hour)	0.66	7.59	6.97	13.71
# of Workers	5	2	6	22
No of Mixers for anode slurry	1	1	3	6
Total No of Mixers	5	5	15	54
Labor hours	1064.00	883.22	2907.05	3594.61
Labor cost (\$)	158588.70	52657.68	519954.34	2357419.34
Maintenance factor	0.10	0.10	0.10	0.10
Auxiliary Costs Factor	0.00	0.00	0.00	0.00
Power Consumption/line (kW)	6.00	13.00	39.00	126.00
Machine Footprint (m2)	14.00	60.00	180.00	600.00
Initial Capital (\$)	5.17E+04	1.09E+05	3.26E+05	1.08E+06
Initial System Cost (\$)	5.68E+04	1.20E+05	3.59E+05	1.19E+06
Annual Depreciation (\$/yr)	3.37E+03	7.11E+03	2.13E+04	7.08E+04
Annual Cap Payment (\$/yr)	6.45E+03	1.36E+04	4.07E+04	1.35E+05
Auxiliary Costs (\$/yr)	0.00	0.00	0.00	0.00
Maintenance (\$/yr)	586.11	1234.06	3702.17	12292.90
Salvage Value (\$/yr)	19.73	41.55	124.65	413.90
Energy Costs (\$/yr)	796.14	1431.90	14138.95	56483.71
Property Tax (\$/yr)	213.83	450.23	1350.68	4484.86
Building Costs (\$/yr)	1178.36	5050.12	45451.06	303007.08
Interest Tax Deduction (\$/yr)	0.00	0.00	0.00	0.00
Machine Rate (\$/h)	1.73	4.91	2.41	2.63
Capital	1.21	3.06	0.93	0.69
Variable	0.26	0.60	0.41	0.35
Building	0.26	1.25	1.07	1.58

Green Tape Blanking

When a green tape roll⁷ is finished, it is unloaded from the tape casting machine and moved to a cutting station where the roll is blanked (cut) into sheets of the size needed for the fuel cell stack. The cells are cut somewhat larger than the desired ultimate dimension to account for the shrinkage associated with the co-firing process.

Keko Equipment makes a series of automatic green tape blankers. The SC-series of tape blankers are designed to automatically blank green ceramic sheets from a roll of green tape and transfers them to a magazine. There are two different models:

- SC 25MNC for carrier tapes up to 250 mm wide

⁷ A dried tape-cast ceramic film is often referred to as a green tape.

- SC 35MNC for carrier tapes up to 350 mm wide

Since these machines are suitable only for carrier tapes up to 350 mm wide, in the case of higher casting width (0.6-1.2 m) a slitting machine (Kunshan Furi Precision Machinery Co., Ltd.) was employed for this analysis in order to take the wider rolls, slit them into smaller rolls, and rewind the tapes into narrower rolls. The slitting process is very rapid since the machine has an average speed of 180 m/min and requires a setup time of 10 minutes.

The blanking machine has a maximum speed of 20 sheets/min (about 3 s/cell) and requires a setup time of 10 minutes per roll (about 3.11 s/cell, including setup time). The production rate of the tape casting machine (including a setup time of 2 hours per roll) was calculated as:

$$\frac{\text{Casting time}}{\text{cell}} \text{ (s)} = \frac{\frac{\text{roll length(m)}}{\text{casting speed} \left(\frac{\text{m}}{\text{min}}\right) * \text{Line Performance}} + \frac{\text{setup time}}{\text{roll}} \text{ (min)}}{\frac{\text{roll length(m)} * \text{cells casted simultaneously}}{\text{cell length (m)}}} * 60$$

Table 4.18 show production rates for every tape casting machine.

Table 4.18 Production rate of different tape casting machines

Casting Machine	Casting speed (m/min)	Casting width(m)	Casting time (s/cell)
TC251	0.25	0.3	53.02
TC501	0.5	0.3	25.57
TC502	0.5	0.6	8.52
TC1002	1	0.6	4.49
TC1004	1	1.2	2.24

For a tape casting width of 1.2 m and casting speed of 1 m/min, a row of 6 cells is cast in 13.44 seconds (1 piece every 2.24 seconds), and in this case two parallel blanking machines per casting line are required.

Under these assumptions three different machine configurations were taken into account:

- For green tape rolls 0.3 m wide, a SC 35MNC blanking machine is used (one per casting line) and slitting machine is not required.
- For green tape rolls 0.6 m wide, a SC 25MNC blanking machine (one per casting line) and a slitting machine (one per casting line) are used. The slitting machine cuts the roll into three smaller rolls 0.2 m wide.
- For green tape rolls 1.2 m wide, a SC 25MNC blanking machines (two per casting line) and a slitting machine (one per casting line) are used. The slitting machine cuts the roll into six smaller rolls 0.2 m wide.

In this analysis, recycling of cutting waste for powder preparation was not considered. Table 4.19 summarizes specifications of the three different configurations chosen.

Table 4.19. Green tape cutting machines configurations for different casting widths

Die cutting stations	0.3 m casting width	0.6 m casting width	1,2 m casting width
Tape Slitting machine			
# of machines/casting line	0	1	1
Footprint (m ²)	0	15	15
Consumption (kW)	0	5.5	5.5
Desired roll width(m)		0.2	0.2
Labor time/tape roll (min)	0	10	10
Green tape blanker			
Model	SC 35MNC	SC 25MNC	SC 25MNC
# of machines/casting line	1	1	2
Footprint (m ²)	20	20	20
Consumption (kW)	0.5	0.5	0.5
Labor time/tape roll (min)	0	30	60
Labor time/casting machine setup (min)	10	40	70

Labor time is required only for loading rolls on slitting and blanking machines. Labor cost was calculated assuming a setup time of 10 minutes to load a roll on the slitting or blanking machine.

As shown in Table 4.19, setup time (labor time) increases with casting width since the wider the roll, the higher the number of narrower rolls to load in the blanking machine. Considering the number of setups per year of the tape casting machines and a worker per line, the labor cost for machine setup was calculated as:

$$\text{Annual labor hours for setup} \left(\frac{\text{hours}}{\text{year}} \right) = \frac{\# \text{ of setups}}{\text{year}} * \frac{\text{Labor time}}{\text{casting machine setup}} \left(\frac{\text{hours}}{\text{setup}} \right)$$

$$\text{Labor cost for setup} \left(\frac{\$}{\text{year}} \right) = \text{Annual Labor hours} \left(\frac{\text{hours}}{\text{year}} \right) * \text{Worker rate} \left(\frac{\$}{\text{hour}} \right)$$

In addition, we assume that a worker for every five machines is necessary during operating hours to ensure that all the equipment is working properly.

$$\begin{aligned} \text{Labor cost} \left(\frac{\$}{\text{year}} \right) \\ = \# \text{ of machines} * \frac{0.2 \text{ workers}}{\text{machine}} * \text{Ann. oper. hours} \left(\frac{\text{hours}}{\text{year}} \right) * \text{Worker rate} \left(\frac{\$}{\text{hour}} \right) \end{aligned}$$

Table 4.20 shows estimated machine rates and corresponding costs for the green tape blanking process for 50-kWe systems.

Table 4.20. Machine rates for green tape blanker (50-kWe systems)

System size (kWe)	50			
Production volume (systems/year)	100	1000	10000	50000
No of slitting machines	1	1	3	6
No of blanking machines	1	1	3	12
No of workers/machine	1	1	1	1
Labor hours/setup	0.17	0.67	0.67	1.17
Labor hours	2.59	33.33	320.43	1370.21
Labor Cost	6420.83	6259.43	61547.46	298019.06
Maintenance factor	0.10	0.10	0.10	0.10
Auxiliary Costs Factor	0	0	0	0
Power Consumption/station (KW)	0.5	6	6	6.5
Machine Footprint/station (m2)	20	35	35	55
Initial Capital (\$)	Contact vendor	Contact vendor	Contact vendor	Contact vendor
Initial System Cost (\$)	Contact vendor	Contact vendor	Contact vendor	Contact vendor
Annual Depreciation (\$/yr)	3.92E+03	4.57E+03	1.37E+04	4.86E+04
Annual Cap Payment (\$/yr)	7.49E+03	8.74E+03	2.62E+04	9.29E+04
Auxiliary Costs (\$/yr)	0.00	0.00	0.00	0.00
Maintenance (\$/yr)	680.86	794.33	2383.00	8442.65
Salvage Value (\$/yr)	22.92	26.75	80.24	284.26
Energy Costs (\$/yr)	66.35	660.88	6525.67	17483.05
Property Tax (\$/yr)	248.40	289.80	869.40	3080.16
Building Costs (\$/yr)	1683.37	2945.90	8837.71	27775.65
Interest Tax Deduction (\$/yr)	0.00	0.00	0.00	0.00
Machine Rate (\$/h)	9.54	15.17	5.13	6.93
Capital	Contact vendor	Contact vendor	Contact vendor	Contact vendor
Variable	0.70	1.65	1.02	1.20
Building	1.82	3.66	1.11	1.43

Screen Printing

After the blanking process, sheets are moved to the screen printing stations by hand or by means of magazines. In a screen printing line, the bottleneck is the printing cycle time which consists of 3 different steps:

- Part load (manual/automatic)
- Printing operation (manual/automatic)
- Part unload (manual/automatic)

Manncorp, a stencil printer equipment supplier recommends three different kinds of machines (Table 4.21):

Table 4.21. Screen printers technical information

MODEL	Printable area dimensions (m)		Cycle time (s)	Automation	Cost (\$)	Power (kW)	Printed pieces per cycle
PB2300	0.48	0.4	35	Semi-automatic	20000	3	1
AP430	0.4	0.5	12	Automatic	60000	3	1
AP660	0.58	0.58	12	Automatic	80200	3	3

Since the PB2300 stencil printer is a semi-automatic machine, it was used only in the case of low production rates (casting speeds <0.33 m/min) and manual handling was assumed. A worker loads the printer, unloads it and then moves each printed piece to a conveyor positioned before the dryer. In the other cases pieces are moved by means of conveyors, loaders and un-loaders.

For casting speed higher than 0.33 m/min the following equipment was used:

- AP430 printer in case of casting width of 0.3 m
- AP660 printer for larger casting widths (0.6-1.2 m)

According to the vendor, the AP660 is able to print a maximum of three parts in 12 seconds with the use of a carrier, so in case of a casting width of 1.2 m (TC1004 tape caster) two parallel printing lines for each casting line were required (as for blanking machines), while for casting widths of 0.3 and 0.6m, only a printing line per casting machine was considered.

Following deposition, the ceramic slurry is dried by means of an infrared dryer positioned directly after the deposition step. As with casting machines, drying tunnel lengths of infrared ovens for each deposition process were estimated by multiplying the casting speed (since it corresponds to the EEA manufacturing line speed) by the estimated drying time of printed slurry. In order to simplify the calculations, the estimated printed cathode layer drying time (2.23 minutes) was considered as a reference for all deposition processes (cathode, interlayers and electrolyte depositions) since all these thin layers were characterized by a small drying time.

Table 4.22 shows the estimated conveyor length for the three different casting speeds considered in this study.

Table 4.22. Infrared Oven required conveyor length for three different casting speed

IR Required conveyor length (m)		
0.25 m/min speed	0.5 m/min speed	1 m/min speed
0.56	1.12	2.23

CR-3000 and CR-4000 ovens have a tunnel width of 0.33 and 0.5 m respectively while CR-5000 and CR-8000 ovens have a width of about 0.57 m. For this reason, ovens were chosen depending on casting width and casting speed as:

- CR-3000 in case of casting width of 0.3 m and casting speed of 0.25 m/min
- CR-4000T in case of casting width of 0.3 m and casting speed of 0.5 m/min
- CR-5000 in case of casting width of 0.6 m and casting speed of 0.5 m/min

- CR-8000 in case of casting width of 0.6 m and casting speed of 1 m/min

Table 4.23 shows manual and automatic printing station configurations and characteristics.

Table 4.23. Manual and automatic printing station configurations and characteristics.

Manual Station	Length(m)	Width(m)	Cost (\$)	Consumption (kW)
Screen printer(PB-2300)	0.745	0.96	20000	3
Reflow oven (CR-3000)	1.8	0.855	10000	10
PCB conveyor (BC-100X-W1)	1.2	0.8	3595	0.1
Total	6	0.96	33595	13.1

Automatic Station (AP430)	Length(m)	Width(m)	Cost (\$)	Consumption (kW)
PCB Loader (BL-460W-ST)	1.75	0.96	10695	0.3
Screen Printer (AP430)	1.45	1.12	60000	3
PCB conveyor (BC-100X-W1)	1.2	0.8	3595	0.1
Reflow oven (CR-4000)	2	1.2	25000	15
PCB unloader (UL-460W-ST)	2.1	0.96	10375	0.3
6 Magazine for PCBs			3600	
Total	9	1.2	113265	18.7

Automatic Station (AP660)	Length(m)	Width(m)	Cost (\$)	Consumption (kW)
PCB Loader (BL-460W-ST)	1.75	0.96	10695	0.3
Screen Printer (AP660)	1.13	0.89	80200	3
PCB conveyor (BC-100X-W1)	1.2	0.8	3595	0,1
Reflow oven (CR-5000)	3	1.51	35000	22
PCB unloader (UL-460W-ST)	2.1	0.96	10375	0,3
6 Magazine for PCBs			3600	
Total	9.2	1.51	143465	25.7

Automatic Station (AP660)	Length(m)	Width(m)	Cost (\$)	Consumption (kW)
PCB Loader (BL-460W-ST)	1.75	0.96	10695	0.3
Screen Printer (AP660)	1.13	0.89	80200	3
PCB conveyor (BC-100X-W1)	1.2	0.8	3595	0.1
Reflow oven (CR- 8000)	4.8	1.51	50000	40
PCB unloader (UL-460W-ST)	2.1	0.96	10375	0.3
6 Magazine for PCBs			3600	
Total	11	1.51	158465	43.7

The vendor suggested one worker per station for the labor cost calculation. Since there are four deposition processes, each printing line is composed of four stations and needs four workers. Under these assumptions, the following manufacturing calculations were evaluated:

$$\frac{\text{Max \# of cells printed}}{\text{year} * \text{line}} = \frac{\text{\# of cells printed simultaneously} * \left(\frac{\text{Ann. oper. hours}}{\text{year}}\right) * \text{Availability}}{\text{Cycle time}}$$

$$\text{Line Utilization (\%)} = \frac{\frac{\text{\# of cells required}}{\text{year}}}{\text{\# of printing lines} * \frac{\text{Max \# of cells}}{\text{year} * \text{line}}}$$

$$\text{Labor Cost} \left(\frac{\$}{\text{year}}\right) = \text{Ann. oper. hours} \left(\frac{\text{hours}}{\text{year}}\right) * \text{\# of lines} * \frac{\text{workers}}{\text{line}} * \text{worker rate} \left(\frac{\$}{\text{hour}}\right)$$

where annual operating hours are equivalent to those of tape casting line.

Table 4.24. Machine rate for screen printing line infrared ovens (50-kWe systems)

System size (kWe)	50			
Production volume (systems/year)	100	1000	10000	50000
Oven Model	CR-3000	CR-8000	CR-8000	CR-8000
Required conveyor speed (m/min)	0.25	1.00	1.00	1.00
drying time (min)	2.23	2.23	2.23	2.23
Required tunnel length(m)	0.56	2.23	2.23	2.23
required conveyor width(m)	0.19	0.57	0.57	0.57
Total No. of ovens	4	4	12	48
Annual operating hours/oven	1064.00	883.22	2907.05	3594.61
Max No of cells/oven/year	270704	3320647	3356741	3392835
Oven utilization (%)	34.09%	25.25%	76.77%	93.51%
Maintenance factor	0.10	0.10	0.10	0.10
Auxiliary Costs Factor	0.00	0.00	0.00	0.00
Initial Capital (\$)	4.00E+04	2.00E+05	6.00E+05	2.40E+06
Initial System Cost (\$)	4.40E+04	2.20E+05	6.60E+05	2.64E+06
Annual Depreciation (\$/yr)	2.61E+03	1.31E+04	3.92E+04	1.57E+05
Annual Cap Payment (\$/yr)	4.99E+03	2.50E+04	7.49E+04	3.00E+05
Auxiliary Costs (\$/yr)	0.00	0.00	0.00	0.00
Maintenance (\$/yr)	453.91	2269.53	6808.59	27234.34
Salvage Value (\$/yr)	15.28	76.42	229.25	916.98
Energy Costs (\$/yr)	5307.63	17623.42	174017.80	860704.11
Property Tax (\$/yr)	165.60	828.00	2484.00	9936.00
Building Costs (\$/yr)	0.00	0.00	0.00	0.00
Interest Tax Deduction (\$/yr)	0.00	0.00	0.00	0.00
Machine Rate (\$/h)	2.56	12.91	7.40	6.93
Capital	1.17	7.04	2.14	1.73
Variable	1.35	5.63	5.18	5.15
Building	0.04	0.23	0.07	0.06

Table 4.25. Machine rates for screen printing line (50-kWe systems)

System size (kWe)	50			
Production volume (systems/year)	100	1000	10000	50000
Machine model	manual PB2300	Auto AP660	Auto AP660	Auto AP660
No of printing Lines	1	1	3	12
Cycle time	35	12	12	12
Cycle time required (s/row)	53.02	13.47	13.47	13.47
No of screen printers/printing line	4	4	4	4
Annual operating hours (h)/line	1064.00	883.22	2907.05	3594.61
Max # of cells/year/line	281219	2816583	3069300	3119040
Machine utilization (%)	23.11%	23.08%	70.59%	86.83%
No of cells printed/cycle	1	3	3	3
No of workers/printing line	4	4	4	4
Labor Cost (\$)	126870.96	105315.36	1039908.68	5143460.38
Maintenance factor	0.10	0.10	0.10	0.10
Auxiliary Costs Factor	0.00	0.00	0.00	0.00
Total Power Consumption (KW)	12.40	14.80	44.40	177.60
Total machines Footprint (m2)	68	188	564	2256
Initial Capital (\$)	9.44E+04	4.23E+05	1.27E+06	2.54E+06
Initial System Cost (\$)	1.04E+05	4.65E+05	1.40E+06	2.79E+06
Annual Depreciation (\$/yr)	6.17E+03	2.76E+04	8.29E+04	1.66E+05
Annual Cap Payment (\$/yr)	1.18E+04	5.28E+04	1.58E+05	3.17E+05
Auxiliary Costs (\$/yr)	0.00	0.00	0.00	0.00
Maintenance (\$/yr)	1070.99	4800.73	14402.20	28804.40
Salvage Value (\$/yr)	36.06	161.64	484.92	969.85
Energy Costs (\$/yr)	1645.37	1630.17	16096.65	79615.13
Property Tax (\$/yr)	390.73	1751.47	5254.41	10508.81
Building Costs (\$/yr)	5723.47	15823.70	47471.11	189884.44
Interest Tax Deduction (\$/yr)	0.00	0.00	0.00	0.00
Machine Rate (\$/h)	19.34	86.79	27.65	14.48
Capital	11.04	59.61	18.11	7.32
Variable	2.55	7.28	3.50	2.51
Building	5.75	19.90	6.05	4.65

EEA Quality Control prior co-firing process

Inspection and testing procedures before co-firing process included in this analysis were:

- Infrared imaging (to detect defects on the surface or close to the surface)
- Ultrasonic spectroscopy (to detect defects on the surface or under the surface)

Costs, cycle times and laborers required for each testing procedure (see Table 4.26) were obtained from a TIAX study (Carlson, Yang, & Fulton, 2004).

Table 4.26 Cost, cycle time and laborers required for each testing procedure

Infrared inspection	Cost (\$)	Cycle time(s)	No of workers/station
manual	50000	15	1
Automatic	150000	5	0.5
Ultrasound inspection	Cost (\$)	Cycle time(s)	No of workers/station
Manual	20000	15	1
Automatic	150000	5	0.5

Manual inspection was considered for annual production volume ≤ 10 MWe where manufacturing processes have a cycle time higher than 15 seconds and annual operating hours are not so high as to result in high labor costs. For 25 MWe of annual production, automatic inspection resulted in lower total costs, and the use of robotic loading instead of manual labor is adopted (see Figure 4.11).

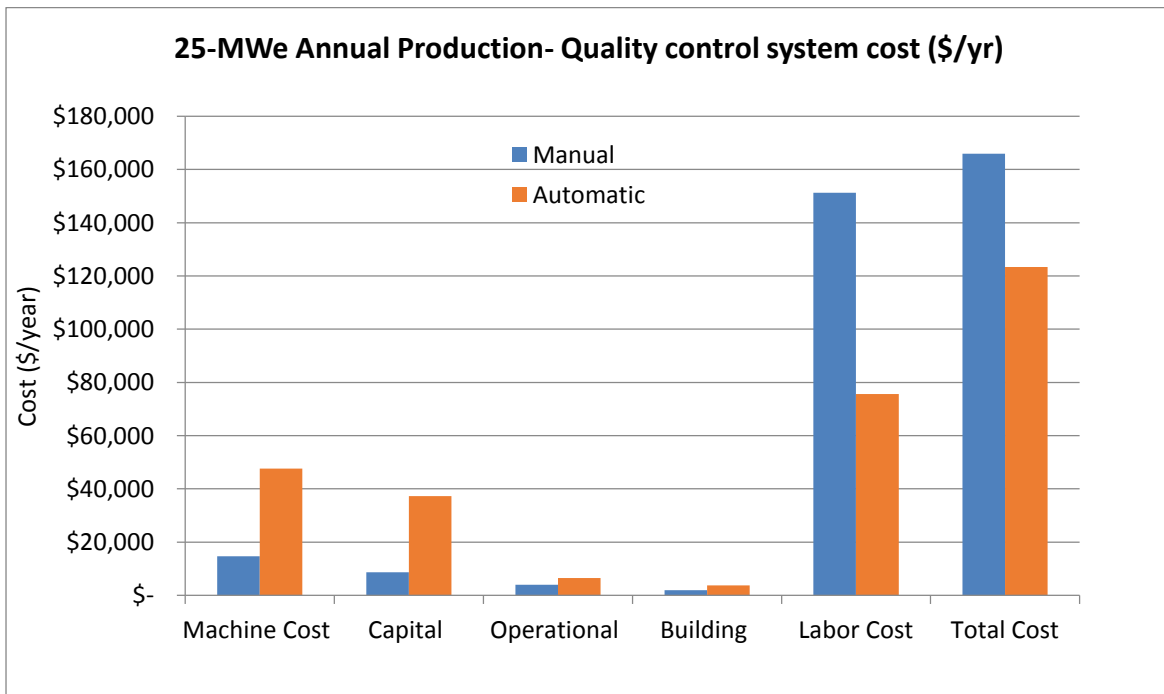


Figure 4.11. Manual and automatic quality control system cost comparison for a production rate of 325000 cells/yr

The maximum number of EEA cells tested per week is estimated as:

$$\frac{\text{Max \# of cells tested per week}}{\text{machine}} = \frac{\text{Operating hours (including setup)} * 3600 \left(\frac{s}{\text{hour}}\right)}{\text{week} * \text{machine} * \text{Cycle time (s)}}$$

The number of testing stations required was estimated starting from the maximum number of EEA cells tested per week and the number of EEA cells casted per week as:

$$\# \text{ of machines required} = \frac{\# \text{ of cells casted per week}}{\frac{\text{Max \# of cells tested per week}}{\text{machine}}}$$

As expected, this resulted in a number of machines equal to the number of tape casting lines since they are both characterized by same cycle time (s/piece).

Finally labor cost was calculated as:

$$\text{Labor cost} \left(\frac{\$}{\text{year}} \right) = \frac{\# \text{ of workers}}{\text{machine}} * \# \text{ of machines} * \text{Ann. op. hours} \left(\frac{\text{hours}}{\text{year}} \right) * \text{Worker rate} \left(\frac{\$}{\text{hour}} \right)$$

where annual operating hours are those of tape casting lines.

Table 4.27 show machine rates estimated for quality control systems in the case of 50-kWe systems.

Table 4.27. Machine rates for quality control system prior co-firing process (50-kWe systems)

System size (kWe)	50			
Production volume (systems/year)	100	1000	10000	50000
Type of handling and inspection	manual	automatic	automatic	automatic
No of machines	1	1	3	12
Max cells tested/week/machine	17280	66240	66960	67680
Annual operating hours	1064.00	883.22	8721.14	21567.68
Labor Cost (\$)	63435.48	26328.84	259977.17	1285865.10
Maintenance factor	0.10	0.10	0.10	0.10
Auxiliary Costs Factor	0	0	0	0
Power Consumption/machine (KW)	10	10	10	10
Machine Footprint (m2)	20	30	90	360
Initial Capital (\$)	7.00E+04	3.00E+05	9.00E+05	3.60E+06
Initial System Cost (\$)	7.70E+04	3.30E+05	9.90E+05	3.96E+06
Annual Depreciation (\$/yr)	4.57E+03	1.96E+04	5.88E+04	2.35E+05
Annual Cap Payment (\$/yr)	8.74E+03	3.74E+04	1.12E+05	4.49E+05
Auxiliary Costs (\$/yr)	0.00	0.00	0.00	0.00
Maintenance (\$/yr)	794.33	3404.29	10212.88	40851.51
Salvage Value (\$/yr)	26.75	114.62	343.87	1375.47
Energy Costs (\$/yr)	1326.91	1101.46	10876.11	26897.00
Property Tax (\$/yr)	289.80	1242.00	3726.00	14904.00
Building Costs (\$/yr)	1683.37	2525.06	7575.18	30300.71
Interest Tax Deduction (\$/yr)	0.00	0.00	0.00	0.00
Machine Rate (\$/h)	12.04	51.64	16.56	26.01
Capital	8.19	42.27	12.84	20.77
Variable	1.99	5.10	2.42	3.14
Building	1.85	4.27	1.30	2.10

One-Step Co-firing

Co-firing kilns for solid oxide fuel cells produced by Keith Company were chosen. The vendor provided costs including installation costs (see Figure 4.12) for a small front loading kiln (for low volume production) and an envelope kiln (for high volume production) and suggested the use of a logarithmic curve to estimate approximate costs for intermediate size kilns. The vendor also suggested an amount equal to the 20% of kiln purchase cost as the maintenance cost per year.



Figure 4.12 Kiln cost with respect to kiln load capacity

Load capacity of each kiln was estimated based on these assumptions:

- In order to enable loading pieces on more than one level, kiln furniture is used. This consists of shelves and posts positioned in the kiln firing chamber
- Each EEA can be set in kiln furniture in columns consuming a vertical space (y axis) of approximately 18 mm. This is based upon setting each EEA on a 6 mm high temperature recrystallized silicon carbide (ReSic) slab with another 1 mm slip of material used to isolate the finished product from the furniture to avoid contamination and providing enough clear space to allow uniform heating and to allow volatile organic compounds to escape during a de-binding process.
- Loading in the x and z dimensions can be calculated using the linear dimensions of the part and adding post dimension of 125 mm in one axis (see Table 4.28)

Table 4.28. EEA cell dimensions including margins used for kiln loading estimation

EEA dimensions	
EEA cell height (mm)	18
EEA cell width (mm)	181.5
EEA cell length(mm)	306.5

Knowing the internal dimensions of the kiln it was possible to calculate the number of parts per load that each kiln is able to accommodate. In the case of manual loading, envelope kilns are used and each kiln needs at least 2 workers in order to load 4 parts per minute. In case of large production sizes and high production rates, a shuttle kiln with fully automated robotic systems is utilized.

Shuttle kilns have fixed position heating chambers and one or more ware cars that are moved into the kiln for firing. The robotic loading system consists of pick and place robots that move parts from the conveyor to a carrier and loading robots that move parts from carrier to a kiln car. Cars facilitate loading and unloading operations, especially in large production sizes.

Although shuttle kilns with robotic loading have a higher price (~\$2.2 M) and require about 1/3 more floor space than comparably sized envelope kilns, the robotic loading system allows the elimination of labor cost at the expenses of an additional power consumption to reach a loading speed of approximately 32 parts per minute.

Each kiln (envelope or shuttle) includes two firing bases so that one can be unloaded and reloaded while the other is firing. Kilns are assumed to be capable of running continuously without the presence of workers since a control system is assumed to be available (per the vendor's input) that can stop the machine and place an automatic phone call to process engineers in case of any problems.

From these assumptions, cycle time (including load and unload) and maximum number of cycles per week per machine were estimated. Table 4.29 shows specifications of kilns including load capacity per cycle, prices, total cycle time, maximum number of cycles per week and maximum annual production.

Table 4.29. Co-firing kiln costs and specifications for different load capacities

Co-Firing Kiln	low volume kiln	mid volume kiln	high volume kiln	high volume kiln
Model	envelope	envelope	envelope	shuttle
type of load	manual	manual	Manual	robotic
Kiln capacity (parts/cycle)	256	2000	4960	4960
Furniture cost (\$)	30000	146000	200000	200000
Cost + installation (\$)	150000	730000	1000000	2000000
Furnace total cost (\$)	180000	876000	1200000	2200000
Load/unload time (hours/cycle)	2.2	16.7	48	6
Sintering time (hours)	24	24	24	24
Total cycle time (hours)	26.2	40.7	72	30
Average consumption (kW)	50	240	300	320
Max no. of cycles/week (including setup)	5	4	2	6
Annual operating weeks	48	48	48	48
Max no. of cycles/year	240	192	96	288
Max annual production (fired pieces/year)	61440	384000	476160	1428480

Knowing the number of cells cast per week, the maximum number of cycles per week and per year for each machine can be found as follows:

$$\frac{\text{Cycles required}}{\text{week}} = \frac{\frac{\text{\# of cells casted}}{\text{week}}}{\frac{\text{kiln capacity}}{\text{cycle}}}$$

$$\frac{\text{Cycles required}}{\text{year}} = \frac{\frac{\text{\# of cells required}}{\text{year}}}{\frac{\text{Process Yield}}{\frac{\text{\# of cells casted}}{\text{week}}}} * \frac{\text{cycles required}}{\text{week}}$$

$$\text{\# of kilns required} = \frac{\frac{\text{\# of cells casted}}{\text{week}}}{\frac{\text{Max \# of cycles}}{\text{week * kiln}} * \frac{\text{kiln capacity}}{\text{cycle}}}$$

$$\text{Kiln utization (\%)} = \frac{\frac{\text{cycles required}}{\text{year}}}{\frac{\text{Max \# of cycles}}{\text{year * kiln}} * \text{\# of kilns required}}$$

$$\text{Annual Operating hours} \left(\frac{\text{hours}}{\text{year}} \right) = \frac{\text{Cycles required}}{\text{year}} * \text{Sintering time} \left(\frac{\text{hours}}{\text{cycle}} \right)$$

Since manual labor is required only for load and unload kilns, annual labor hours and cost were calculated as:

$$\text{Labor hours} \left(\frac{\text{hours}}{\text{year}} \right) = \frac{\frac{\text{\# of cells required}}{\text{year}}}{\frac{\text{Process Yield}}{\text{loaded parts}} \cdot \frac{\text{hour}}{\text{hour}}} * 2 \text{ (to count load \& unload)}$$

$$\text{Labor cost} \left(\frac{\$}{\text{year}} \right) = \frac{\text{\# of workers}}{\text{kiln}} * \text{\# of kilns} * \text{Labor hours} \left(\frac{\text{hours}}{\text{year}} \right) * \text{Worker rate} \left(\frac{\$}{\text{hour}} \right)$$

A low volume kiln was used for a production volume of 1,300 cells/year (1-kW system, 100 units per year) while mid-volume kilns were used in the case of a casting speed of 0.25 m/min. This corresponds to a maximum number of cells cast per week of less than 7,000 pieces.

We note that in case of manual loading, the labor cost (see Figure 4.13) increases dramatically with the annual production rate because of higher number of furnaces required and higher number of cycles per week. For this reason, a comparison of annualized processing costs of both types of kilns with the same load capacity (shuttle and envelope high volume kilns) was conducted in order to understand when it was favorable to use an automatic loading system.

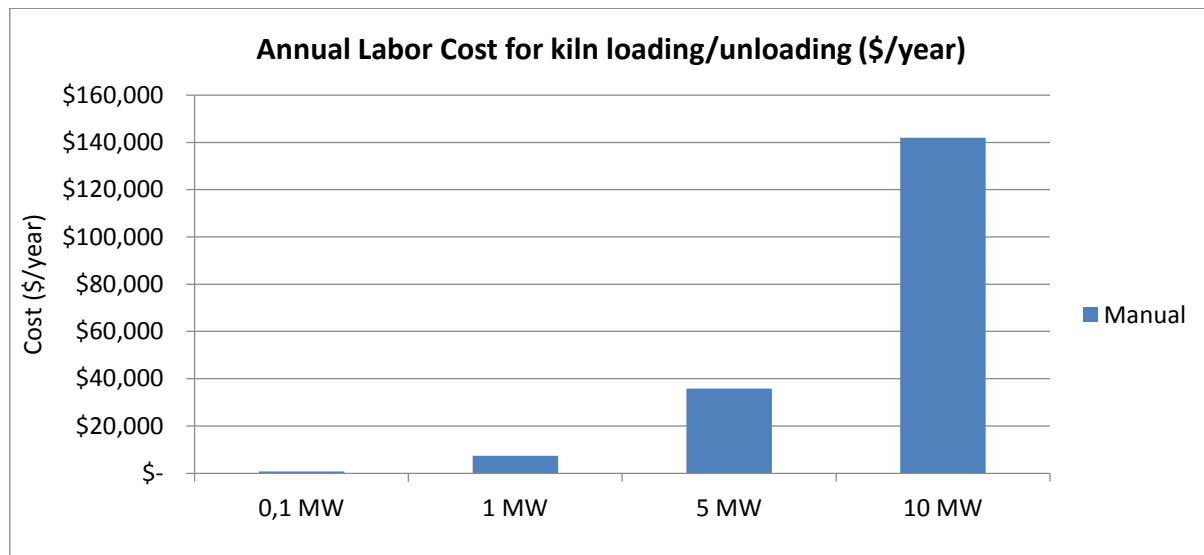


Figure 4.13. Kiln loading labor cost in (\$/yr) at different annual production volume

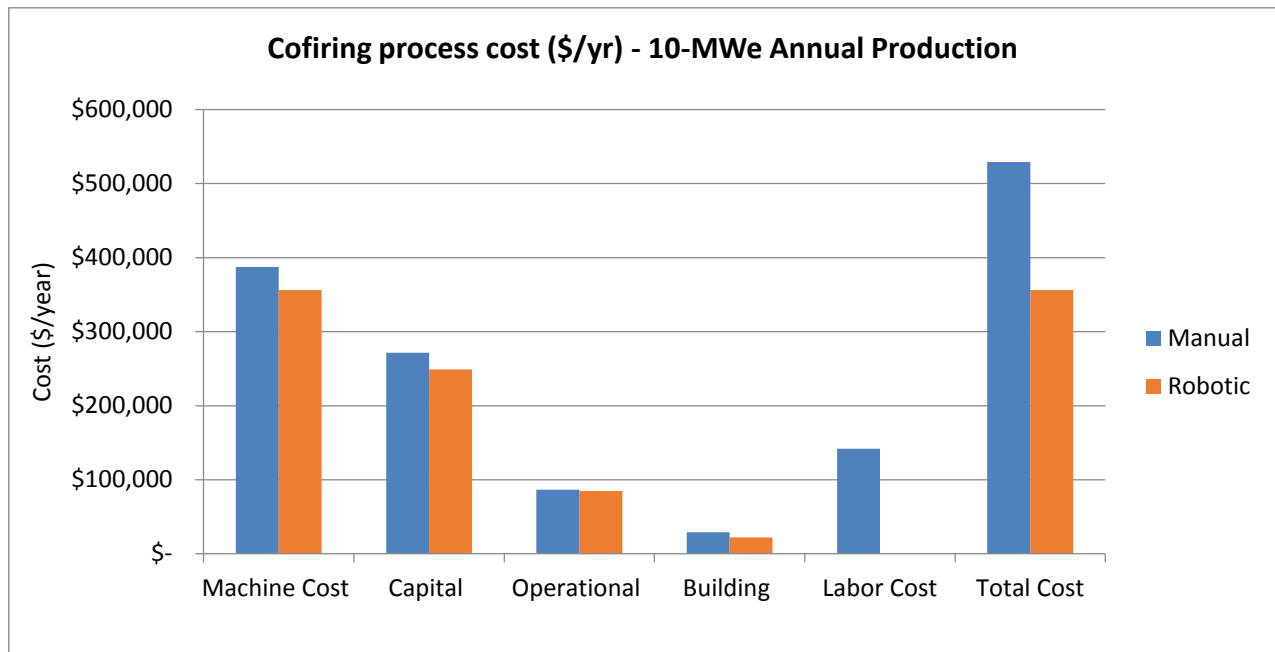


Figure 4.14. Co-firing process cost comparison with manual and automatic loading for an equivalent annual production of 10 MWe

The results of this investigation suggest that it is cheaper to use a robotic loading system instead of manual handling for annual production volumes higher than about 5 MW (65,000 EEA cells/year). Figure 4.14 compares manual and automatic kiln costs for an annual global production of 10 MWe. As can be seen, capital and building cost are similar since in case of manual load, two kilns instead of one are needed to guarantee the required weekly production. The capital and building cost of the additional kiln and the high labor cost make the choice of a shuttle kiln more favorable.

Table 4.30 show machine rates and estimated machine rates of co-firing kilns.

Table 4.30. Machine rates for Co-firing kiln (50-kWe systems)

System size (kWe)	50			
	100	1000	10000	50000
Production volume (units/year)	100	1000	10000	50000
type of handling (load/unload)	manual	automatic	automatic	automatic
Type of kiln	envelope	shuttle	shuttle	shuttle
No of furnaces	1	2	7	28
Load capacity (cells/cycle)	2000	4960	4960	4960
Max load/unload time (hours/cycle)	16.70	6.00	6.00	6.00
Cycle time (hours)	40.7	30	30	30
Max # of cycles/ week/machine	4	6	6	6
Cycle needed/week	3	7	41	163
Total No of cycles needed/year	40	143	1419	6972
Max No of cycles/year	192	576	2016	8064
Kiln Utilization (%)	20.83%	24.83%	70.39%	86.46%
Max annual production (pieces/year)	345600	2628403.2	9299404.8	37597593.6
No of workers/kiln	2	0	0	0
Labor time (hours)	601.85	0.00	0.00	0.00
Labor Cost (\$)	35882.41	0.00	0.00	0.00
Annual operating hours	1066.67	3730.43	36619.35	178008.51
Maintenance factor	0.20	0.20	0.20	0.20
Auxiliary Costs Factor	0.00	0.00	0.00	0.00
Consumption/furnace (KW)	240	320	320	320
Machine Footprint (m2)	44	336	1176	4704
Initial Capital (\$)	7.88E+05	3.96E+06	1.39E+07	5.54E+07
Initial System Cost (\$)	8.76E+05	4.40E+06	1.54E+07	6.16E+07
Annual Depreciation (\$/yr)	5.15E+04	2.59E+05	9.06E+05	3.62E+06
Annual Cap Payment (\$/yr)	9.94E+04	4.99E+05	1.75E+06	6.99E+06
Auxiliary Costs (\$/yr)	0.00	0.00	0.00	0.00
Maintenance (\$/yr)	17892.96	89873.33	314556.66	1258226.64
Salvage Value (\$/yr)	301.23	1513.02	5295.57	21182.30
Energy Costs (\$/yr)	31925.70	148870.93	1461373.17	7103807.86
Property Tax (\$/yr)	3263.98	16394.40	57380.40	229521.60
Building Costs (\$/yr)	3703.42	28280.66	98982.31	395929.25
Interest Tax Deduction (\$/yr)	0.00	0.00	0.00	0.00
Machine Rate (\$/h)	146.15	209.41	100.34	89.64
Capital	92.91	133.44	47.58	39.15
Variable	46.70	64.00	48.50	46.98
Building	6.53	11.98	4.27	3.51

Laser Cutting

Following sintering, the final EEA cells are cut to their final dimensions by means of a laser cutter. In this study an Aurel Automation ALS300 laser trimmer was considered. It is a solid-state laser cutter that uses a Nd-YAG lasing medium (a diode-pumped solid-state laser).

Table 4.31 show machine cost and specifications provided by the vendor.

Table 4.31. Laser cutters cost and specifications

Laser Cutter	ALS300G	ALS300GM
Loading/unloading	manual	automatic
Cost (\$)	90000	150000
Cutting speed (mm/sec)	100	100
Average Consumption (KW)	4	4
Tool size (m2)	1.6	2.5

Considering a cutting speed of 100 mm/sec and EEA size of 18.15 cm, a cutting time per piece of about 7 seconds was estimated.

In the manual case, an operator load and unload cycle time (loading, cutting, unloading) of 25 seconds was calculated for the cutting machine. In the automatic configuration loading and unloading with magazines is fast enough to consider a cycle time of about 9-10 seconds and workers are not required.

As for firing kilns, automatic loading was considered in case of automatic unloading of the firing kiln. Considering 15 min of setup time per day the maximum number of cut cells per week was calculated as:

$$\frac{\text{Max \# of cells cut per week}}{\text{machine}} = \frac{\text{Operational hours (including setup)}}{\text{week * machine}} * 3600 \left(\frac{s}{\text{hour}} \right) / \text{Cycle time (s)}$$

The number of cutting machines required was estimated starting from the maximum number of EEA cells cut per week and the number of EEA cells casted per week as follows:

$$\# \text{ of machines required} = \frac{\# \text{ of cells casted per week}}{\frac{\text{Max \# of cells cut per week}}{\text{machine}}}$$

Finally annual operating hours and labor cost were calculated as:

$$\text{Annual Operating hours} \left(\frac{\text{hours}}{\text{year}} \right) = \frac{\# \text{ of cells required}}{\text{year}} / \text{Process Yield} * \text{Cycle time} \left(\frac{\text{hours}}{\text{cycle}} \right)$$

$$\text{Labor cost} \left(\frac{\$}{\text{year}} \right) = \frac{\# \text{ of workers}}{\text{machine}} * \# \text{ of machines} * \text{Ann. op. hours} \left(\frac{\text{hours}}{\text{year}} \right) * \text{Worker rate} \left(\frac{\$}{\text{hour}} \right)$$

Table 4.32. Machine rates for laser cutting system (50-kWe systems)

System size (kWe)	50			
	100	1000	10000	50000
Production volume (units/year)	100	1000	10000	50000
Type of handling (load/unload)	manual	automatic	automatic	automatic
No of laser cutters	1	2	8	29
No of cell casted /week	5500	34700	202080	808350
Max cells cut/week/machine	11340	28350	28350	28350
Max cells cut/year	544320	2721600	10886400	39463200
Machine utilization (%)	11.94%	23.88%	59.71%	82.36%
worker/machine	1	0	0	0
Cycle time (s)	25	10	10	10
Cutting time (s)	7.26	7.26	7.26	7.26
Annual operating hours	502	1963	19415	96041
labor cost (\$)	14964.62	0.00	0.00	0.00
Machine utilization (%)	13.27%	25.96%	64.20%	87.61%
Maintenance factor	0.10	0.10	0.10	0.10
Auxiliary Costs Factor	0.00	0.00	0.00	0.00
Power Consumption (kW)	4	8	32	116
Machine Footprint (m2)	5	7	21	42
Initial Capital (\$)	9.00E+04	3.00E+05	1.20E+06	4.35E+06
Initial System Cost (\$)	9.90E+04	3.30E+05	1.32E+06	4.79E+06
Annual Depreciation (\$/yr)	5.88E+03	1.96E+04	7.84E+04	2.84E+05
Annual Cap Payment (\$/yr)	1.12E+04	3.74E+04	1.50E+05	5.43E+05
Auxiliary Costs (\$/yr)	0.00	0.00	0.00	0.00
Maintenance (\$/yr)	1021.29	3404.29	13617.17	49362.25
Salvage Value (\$/yr)	34.39	114.62	458.49	1662.03
Energy Costs (\$/yr)	250.42	979.22	9684.96	47909.00
Property Tax (\$/yr)	372.60	1242.00	4968.00	18009.00
Building Costs (\$/yr)	420.84	589.18	1767.54	3535.08
Interest Tax Deduction (\$/yr)	0.00	0.00	0.00	0.00
Machine Rate (\$/h)	26.42	22.18	9.24	6.87
Capital	22.31	19.02	7.69	5.64
Variable	2.53	2.23	1.20	1.01
Building	1.58	0.93	0.35	0.22

EEA Final Quality Control Process

Inspection and testing procedures after co-firing process included in this analysis were:

- Infrared Imaging (to detect defects on the surface or close to the surface)
- Ultrasonic Spectroscopy (to detect defects on the surface or under the surface)
- Vacuum leak test (for leaks detection)

Costs, cycle times and laborers required for each testing procedure (see Table 4.33) were obtained from a TIAX study (Carlson, Yang, & Fulton, 2004).

Table 4.33. Cost, cycle time and laborers required for each testing procedure

Infrared inspection	Cost (\$)	Cycle time(s)	No of workers/station
manual	50000	15	1
auto	150000	5	0.5
Ultrasound inspection	Cost (\$)	Cycle time(s)	No of workers/station
manual	20000	15	1
auto	150000	5	0.5
Vacuum leak test	Cost (\$)	Cycle time(s)	No of workers/station
manual	100000	25	1
auto	300000	10	1

The bottle neck process is the vacuum leak test. For this reason, cycle times of 25 seconds and 10 seconds for the manual and automatic case, respectively (same cycle times of laser cutting process) were assumed. The maximum number of EEA cells tested per week, number of testing stations, annual operating hours and labor cost were calculated with the same formulas as those used for the laser cutting process.

Table 4.34. Machine Rates for quality control station (50-kWe systems)

System size (kWe)	50			
	100	1000	10000	50000
Systems/year	100	1000	10000	50000
type of handling and inspection	manual	automatic	automatic	automatic
No of machines	1	2	8	29
Bottle neck time(s)	25	10	10	10
Max cells tested/year	442368	2371776	10338432	38085120
Machine utilization (%)	14.69%	27.41%	62.87%	85.34%
Annual operating hours	502	1963	19415	96041
No of workers/station	3	1	1	1
Labor Cost (\$/year)	44893.86	58517.03	578761.15	2862982.21
Maintenance factor	0.10	0.10	0.10	0.10
Auxiliary Costs Factor	0	0	0	0
Power Consumption/machine (kW)	10	10	10	10
Machine Footprint (m2)	30	80	320	1160
Initial Capital (\$)	1.70E+05	1.20E+06	4.80E+06	1.74E+07
Initial System Cost (\$)	1.87E+05	1.32E+06	5.28E+06	1.91E+07
Annual Depreciation (\$/yr)	1.11E+04	7.84E+04	3.14E+05	1.14E+06
Annual Cap Payment (\$/yr)	2.12E+04	1.50E+05	5.99E+05	2.17E+06
Auxiliary Costs (\$/yr)	0.00	0.00	0.00	0.00
Maintenance (\$/yr)	1929.10	13617.17	54468.69	197448.99
Salvage Value (\$/yr)	64.95	458.49	1833.97	6648.12
Energy Costs (\$/yr)	626.04	2448.05	24212.40	119772.51
Property Tax (\$/yr)	703.80	4968.00	19872.00	72036.00
Building Costs (\$/yr)	2525.06	6733.49	26933.96	97635.62
Interest Tax Deduction (\$/yr)	0.00	0.00	0.00	0.00
Machine Rate (\$/h)	53.66	90.22	37.23	27.62
Capital	42.14	76.07	30.77	22.55
Variable	5.09	8.18	4.05	3.30
Building	6.43	5.96	2.41	1.77

EEA Cost Summary

As expected, EEA manufacturing cost decreases in moving to higher production volumes (see Table 4.35). EEA cost is seen to fall from about \$2,000/kWe at low volume to about \$90/kWe at high volume.

Table 4.35. EEA manufacturing cost in (\$/kWe) at all production volumes

Equivalent production (MW/year)	EEA Cost (\$/kWe)
0.1	2065.34
1	504.68
5	258.36
10	182.27
25	140.20
50	113.66
100	102.22
250	96.36
500	93.10
1000	90.99
2500	89.43
5000	88.57
12500	88.40

Figure 4.15 shows EEA cost variation with respect to the annual equivalent m² of EEA produced. At very low volumes costs are high since the investment cost for equipment is prohibitive and equipment utilization is low. Table 4.36 and Table 4.37 show EEA manufacturing costs breakdown for 10-kWe and 500kWe system sizes, respectively.

These tables and corresponding graphs (Figure 4.16 and Figure 4.17) show that at low volumes of 1MWe (100 systems per year, 10-kWe systems), capital cost constitute the biggest contribution to EEA cost, while at higher volume, material costs dominate. The substantial difference in labor cost between production volumes of 100 systems per year (50 kWe) and 1,000 systems per year (50 kWe) is related to the shift from manual to automatic configuration of EEA manufacturing processes.

Figure 4.18 shows that anode layer direct manufacturing cost contributes 46-72% of the total EEA cost and its impact on total cost increase with production volume. At a volume of 0.1 MWe per year tape casting process was found to be the most expensive EEA manufacturing process while at higher volume the co-firing process dominates followed by quality control, tape casting and screen-printing processes (Figure 4.19).

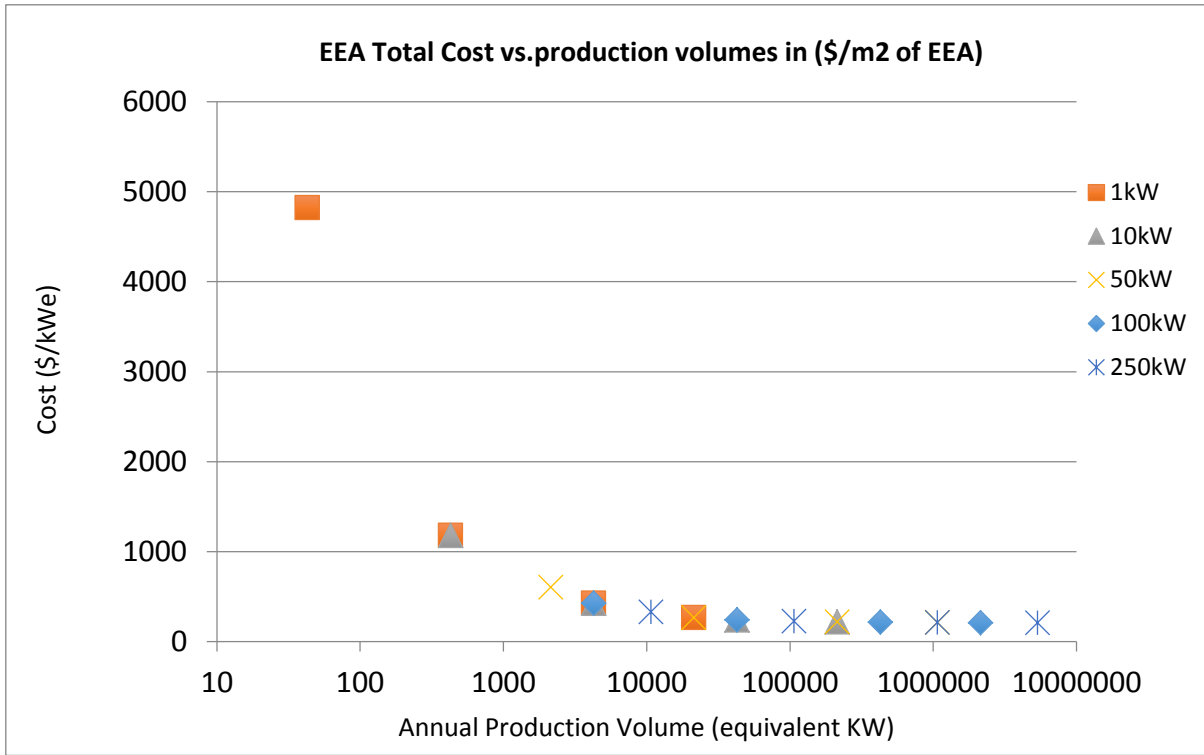


Figure 4.15. EEA Total Cost vs. production volumes in (\$/m2 of EEA)

Table 4.36. EEA manufacturing costs for 10-kWe systems

System Size (kWe)	10			
Production Volume (Units/yr)	100	1000	10000	50000
Direct Material (\$/kWe)	100.62	73.64	69.57	69.13
Labor (\$/kWe)	93.47	29.54	9.54	5.54
Process: Capital (\$/kWe)	186.57	43.72	8.12	5.93
Process: Operational (\$/kWe)	35.51	12.95	5.79	5.23
Process: Building (\$/kWe)	27.95	6.02	1.02	0.76
Scrap (\$/kWe)	60.56	16.40	8.18	6.52
Total (\$/kWe)	504.68	182.27	102.22	93.10

Table 4.37. EEA manufacturing costs for 50-kWe systems

System Size (kWe)	50			
Production Volume (Units/yr)	100	1000	10000	50000
Direct Material (\$/kWe)	80.35	69.79	69.13	69.12
Labor (\$/kWe)	93.32	9.54	5.54	4.98
Process: Capital (\$/kWe)	38.16	16.23	5.93	4.47
Process: Operational (\$/kWe)	14.98	6.95	5.23	4.89
Process: Building (\$/kWe)	5.72	2.05	0.76	0.61
Scrap (\$/kWe)	25.84	9.09	6.52	5.37
Total (\$/kWe)	258.36	113.66	93.10	89.43

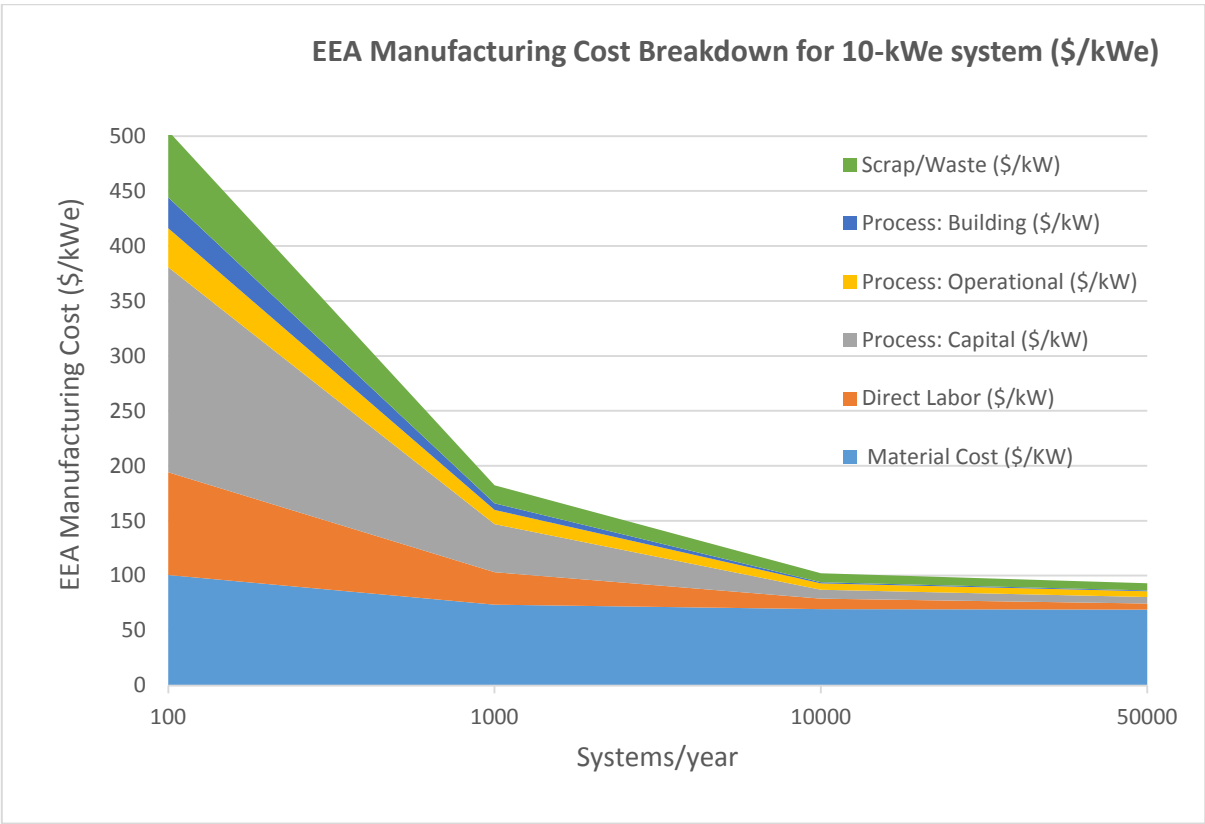


Figure 4.16. Fraction of EEA costs as a function of annual production volume for 10-kWe system

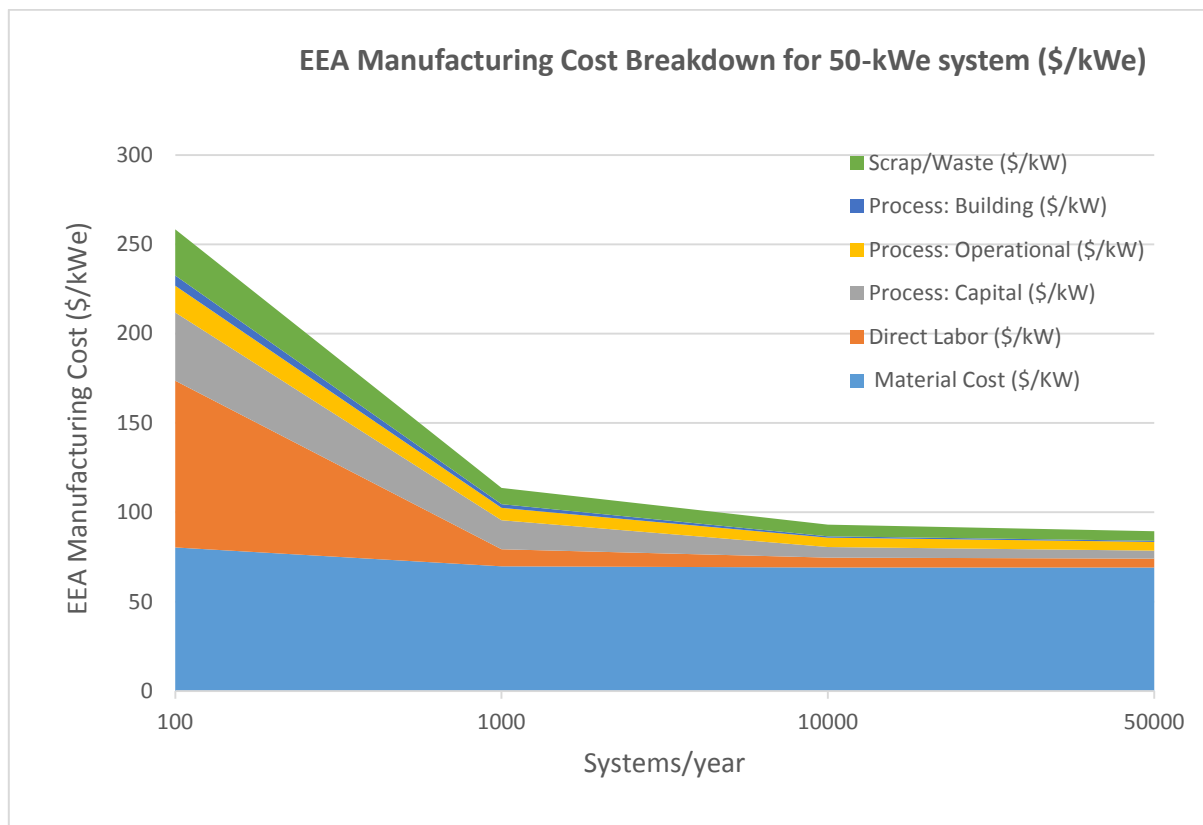


Figure 4.17. Fraction of EEA costs as a function of annual production volume for 50-kWe system

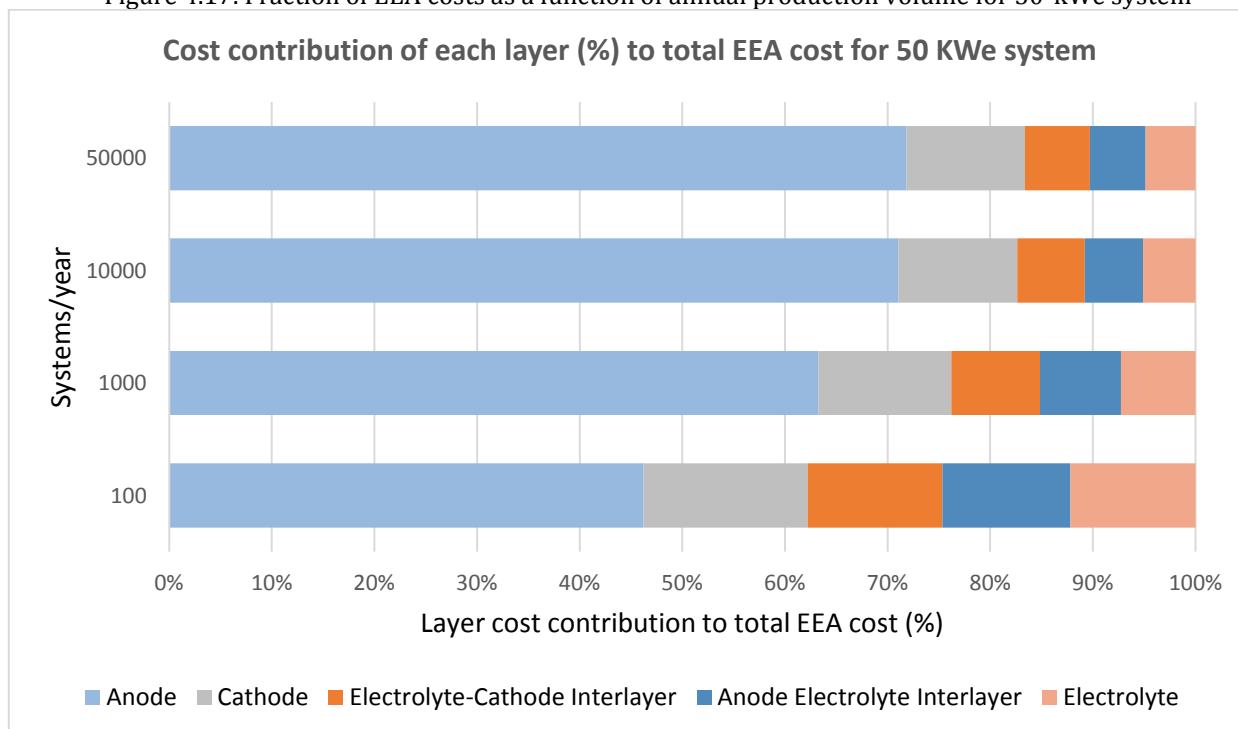


Figure 4.18. Relative percentage of each layer cost to total EEA cost for 50-kWe system

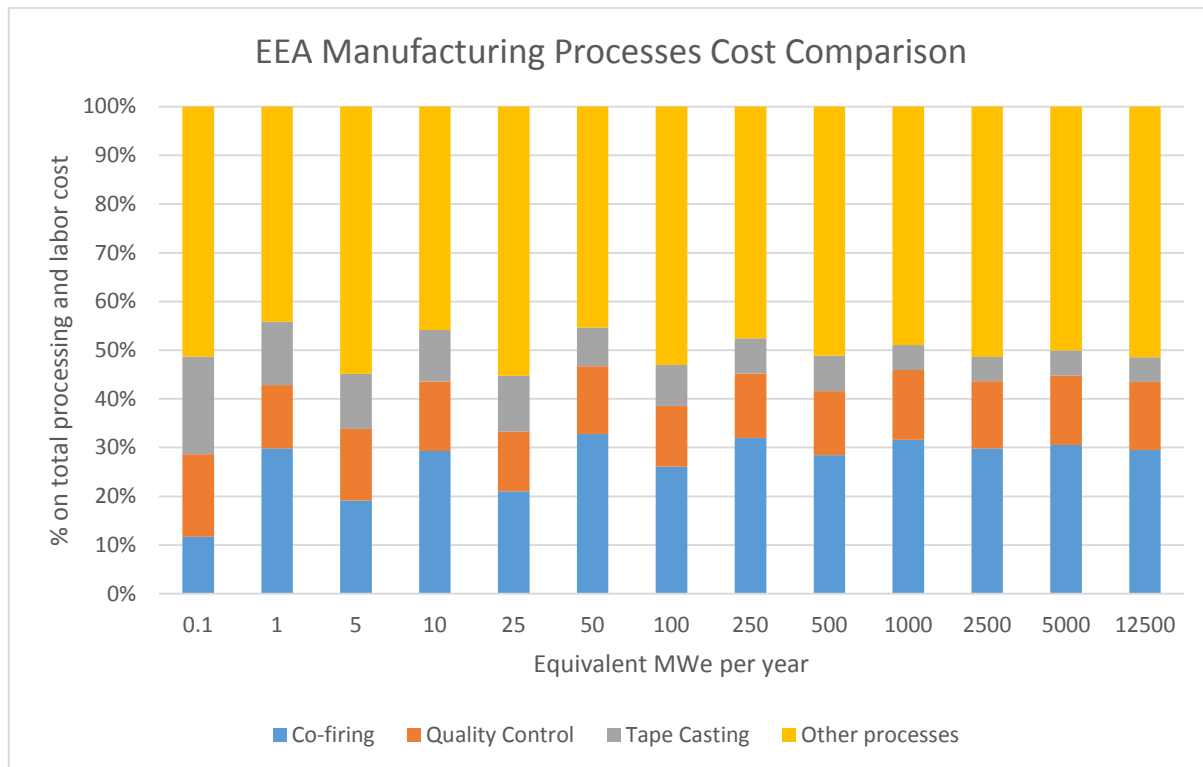
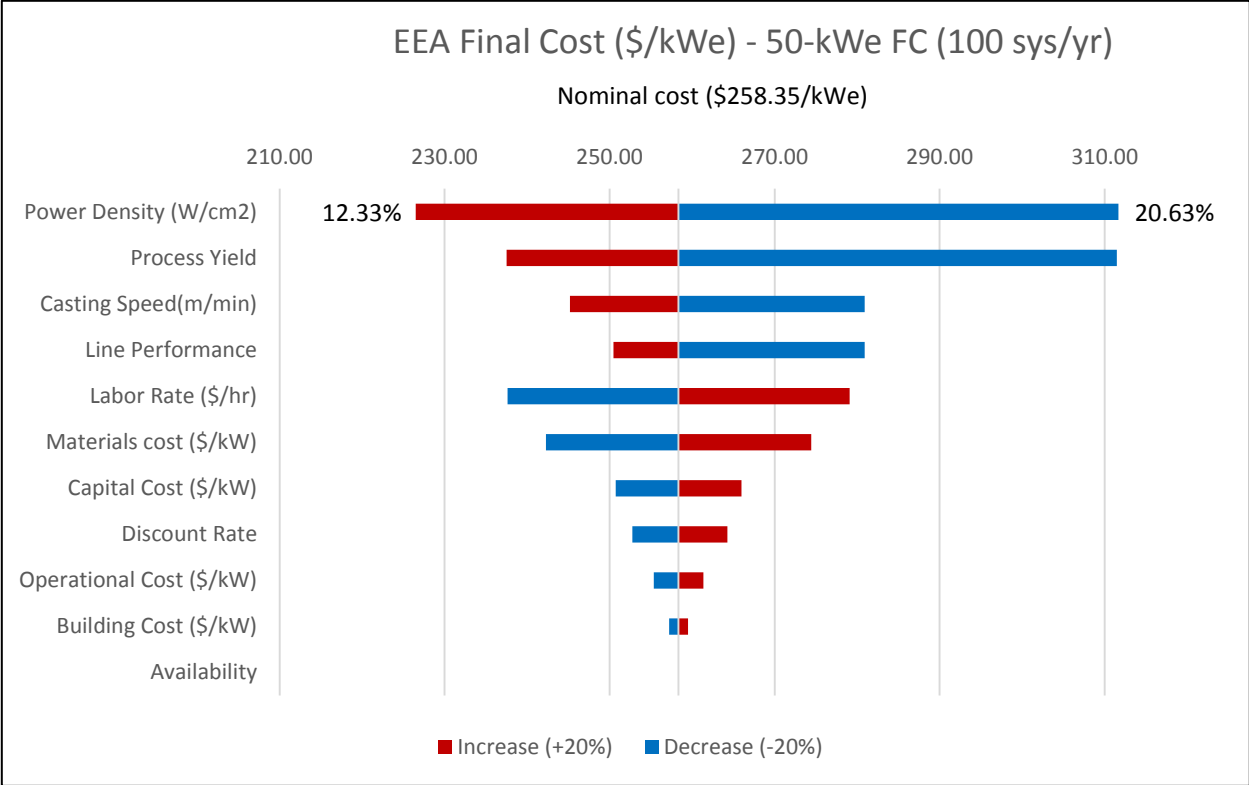


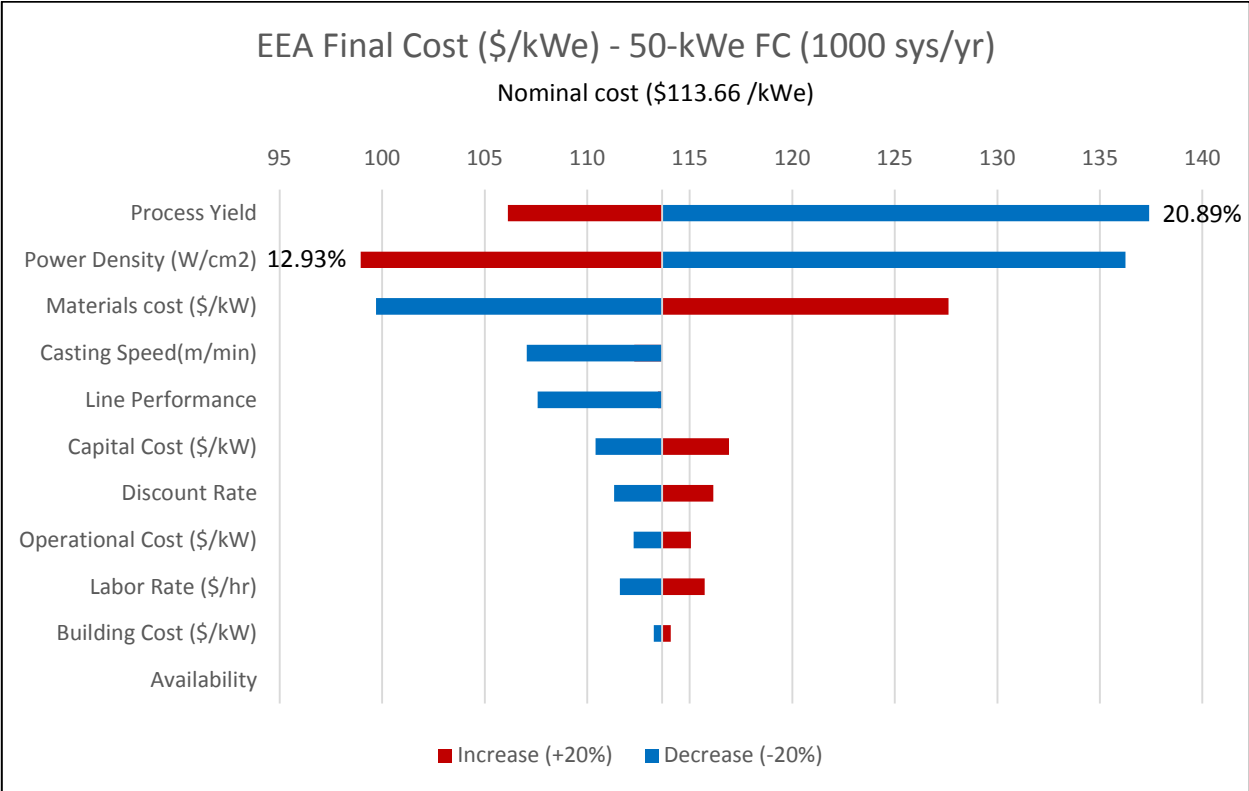
Figure 4.19. EEA manufacturing processes cost contribution to EEA labor and processing costs

Sensitivity Analysis for EEA Functional Cell

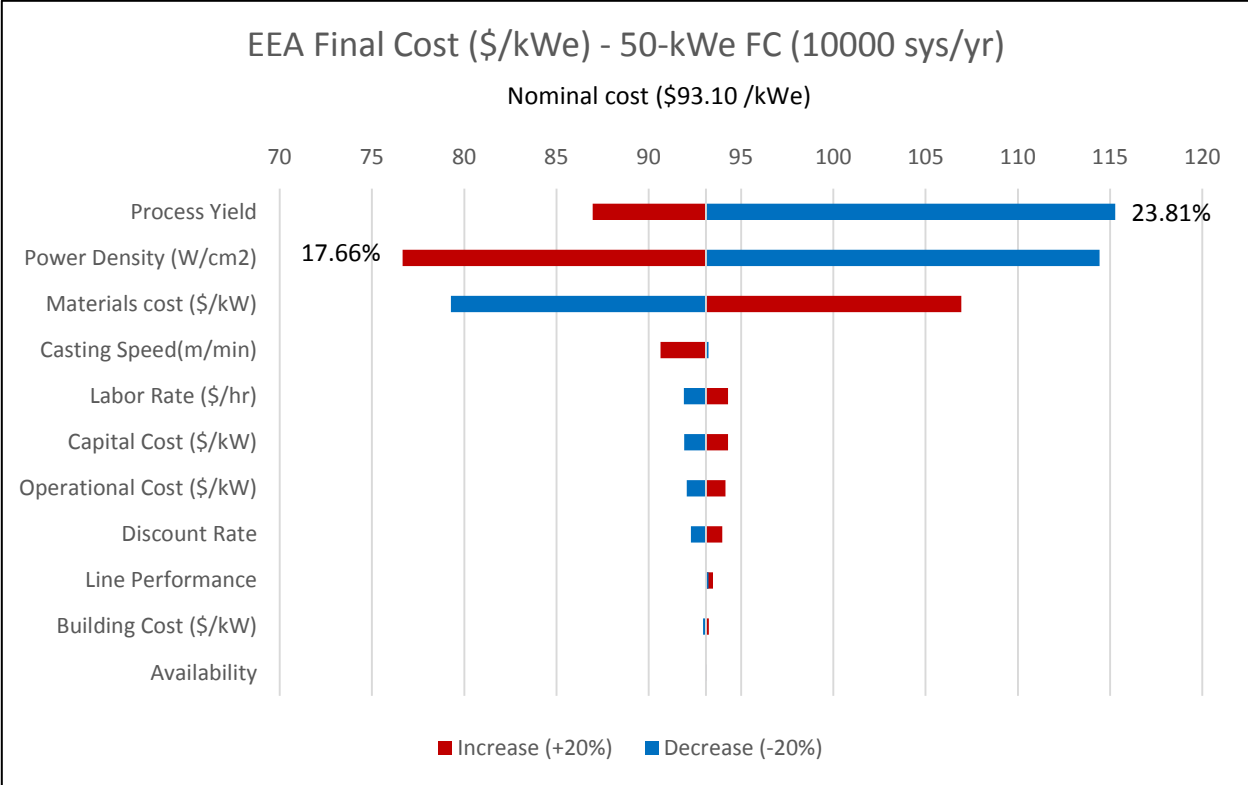
Sensitivity analysis at EEA level was done for 50-kW systems and different production volumes (as shown in Figure 4.20). The impact to the EEA cost in \$/kWe is calculated for a $\pm 20\%$ change in the sensitivity parameter being varied.



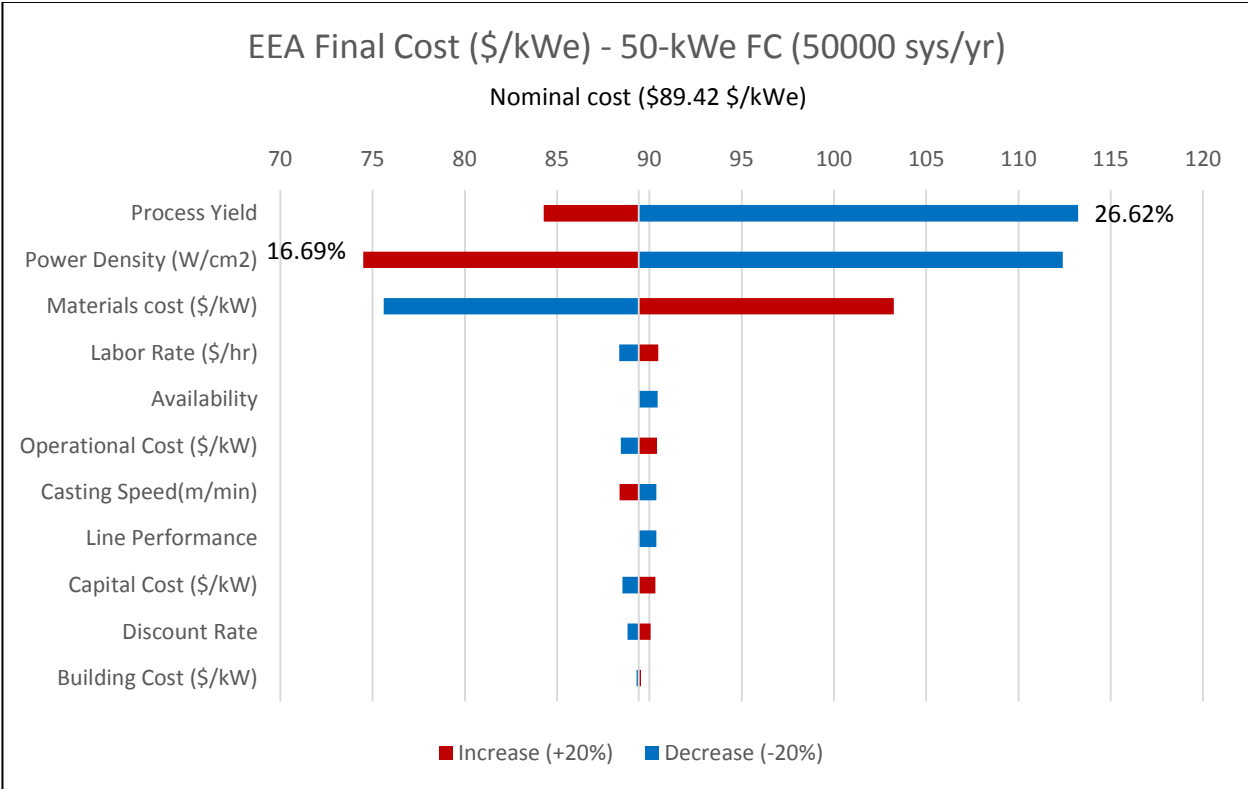
(a)



(b)



(c)



(d)

Figure 4.20. EEA sensitivity analysis for 50-kWe system expressed in (\$/kWe) at different annual production rates

We see from these plots that process yield and power density dominate the cost sensitivity at all production levels since a variation of one of these parameters causes a variation of EEA annual production volume. However, material cost is another important factor and its sensitivity increases with annual production volume.

4.2. Interconnect Manufacturing Cost Analysis

Interconnect Design

Typically, there are two options for SOFC interconnects: metal or ceramic. For SOFC systems, interconnects are usually made from metal material since they need to withstand temperatures up to 1,000°C and usually have a lower manufacturing cost than ceramics. Other properties of the plate include good thermal conductivity, material strength and good electrical conductivity.

In order to maintain good physical properties at elevated SOFC operating temperatures, chrome based alloys have been selected for the primary material. These materials are suitable for temperatures up to 1000 °C, which makes them good materials for the SOFC application (Hsu, Lee, Lee, Shong, & Chen, 2011). The materials modeled in this study are 441 Stainless Steel (chosen as a base case) and Crofer 22 APU.

Two different designs were considered for interconnect manufacturing depending on primary material: Crofer interconnect with a thickness of 315 μm (GhezelAyagh, 2014) and a mass of 123 g and SS441 Interconnect with a thickness of 630 μm (GhezelAyagh, 2014) and a mass of 247 g. The interconnect area is 540 cm^2 and there are four manifolds, each one having dimensions of 3cm (L) x 2.5cm (H).

A 2013 report by Pacific Northwest National Laboratory suggests that photochemical etching should be used to create flow fields (Weimar, Chick, & Whyatt, 2013). This is a good option at low production volumes because the tooling cost is negligible, various flow designs can be created without realizing a production shutdown for tooling changes, and interconnects can be made within a day or two after a design is completed. Ultimately, this process was not modeled due to higher cycle times compared to stamping.

Instead, a stamping process is selected here to form the flow fields. A dual die stamper uses two strokes to create the final interconnect. The first stroke punches out the manifolds and creates the perimeter. The second stroke forms the flow fields. A fully stamped bipolar plate (interconnect) is described in the patent literature (Rock, 2003).

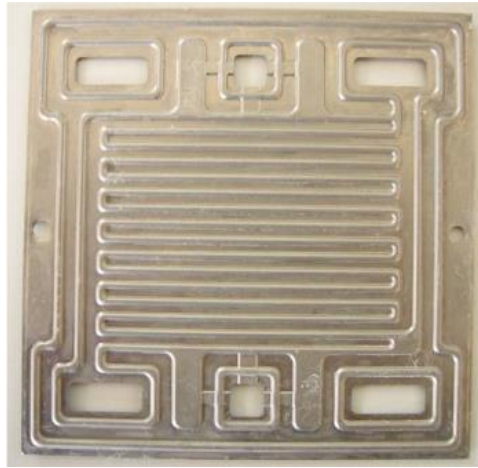


Figure 4.21 Stamped Bipolar Plate (Peng, Liu, Hu, Lai, & Ni, 2010)

Figure 4.21 shows a bipolar plate that has been formed through stamping. This same process is used to create the SOFC interconnect. Notice that on one side of the interconnect, flow fields are continuous from inlet manifold to exit manifold, but on the reverse side, a continuous flow cannot be realized. This is because stamping is a process where features on one side material directly affect the features on the other side.

This non-continuous flow field is called an interdigitated flow field. The reactant gas flows to dead end where it experiences a pressure build up and is forced (rather than diffused) into the electrode. Non-reacted gas flows through the electrode to the lower pressure outlet where it then continues to flow to the outlet manifold. Figure 4.22 shows the difference between the conventional and interdigitated flow designs.

In intermediate temperature solid oxide fuel cells (SOFCs), the use of chromium alloy interconnects such as ferritic stainless steels or Crofer 22 APU can lead to severe degradation in cell performance due to chromium migration into the cells at the cathode side. To protect cells from chromium poisoning and improve their performance, a manganese cobalt spinel oxide (MCO) barrier layer is applied. This material has been cited for high performance and durability (Magdefrau, 2013); (Akanda, 2011); (Kidner, Seabaugh, Chenault, Ibanez, & Thrun, 2011).

Thermal and electrical testing reported in the literature confirm the effectiveness of the spinel protection layer as a means of stopping chromium migration and decreasing oxidation, while promoting electrical contact and minimizing cathode/interconnect interfacial resistance. The thermally grown spinel protection layer bonds well to the SS441 or Crofer22 APU substrate and demonstrates stable performance under thermal cycling (Yang, Xia, & Stevenson, 2005); (Menzler, Tietz, Uhlenbruck, Buchkremer, & Stöver, 2010).

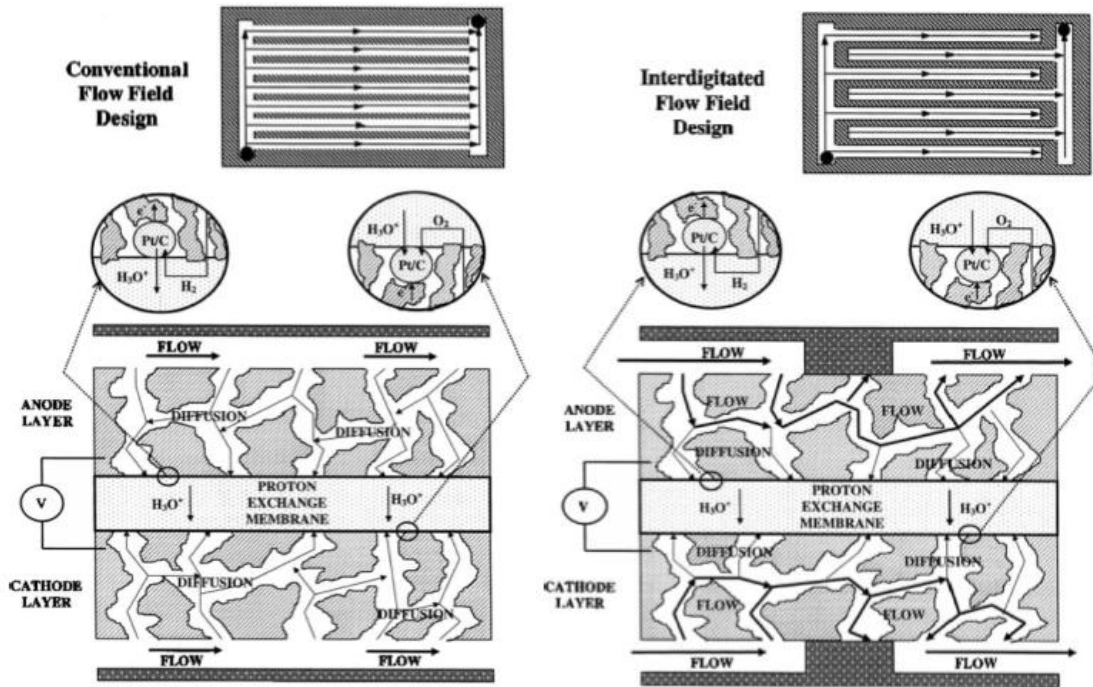


Figure 4.22 Flow field designs on fuel cell stack interconnect (Li & Imran, 2005)

Numerous protective coating technologies have been proposed including magnetron sputtering, PVD, CVD and ASD. The PVD process was selected for good throughput, high purity, uniformity, and defect control. In particular, cathodic-arc deposition has been shown to have relatively high throughputs and capability of processing large batches (Wang & Weng, 2001). However, the major drawback is the relatively high capital expenditure. For both interconnect designs, a 15 μm thick manganese cobalt spinel oxide (MCO) coating was chosen.

Process Flow Description

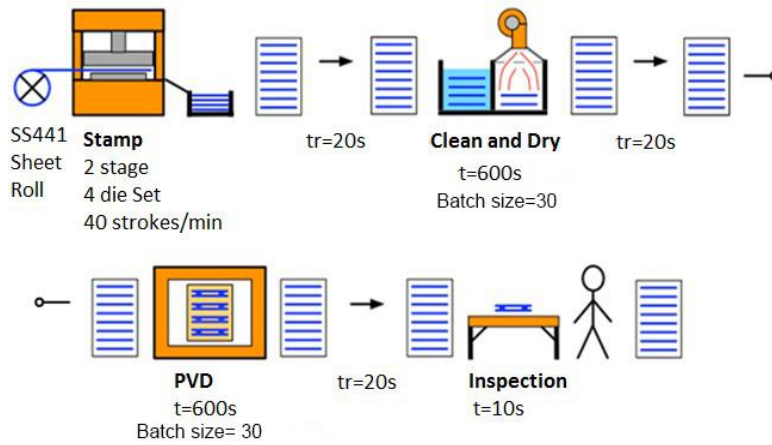
The process flow consists of the following modules:

1. stamping of a sheet roll of stainless steel
2. cleaning and drying
3. physical vapor deposition (PVD) of the coating
4. final inspection

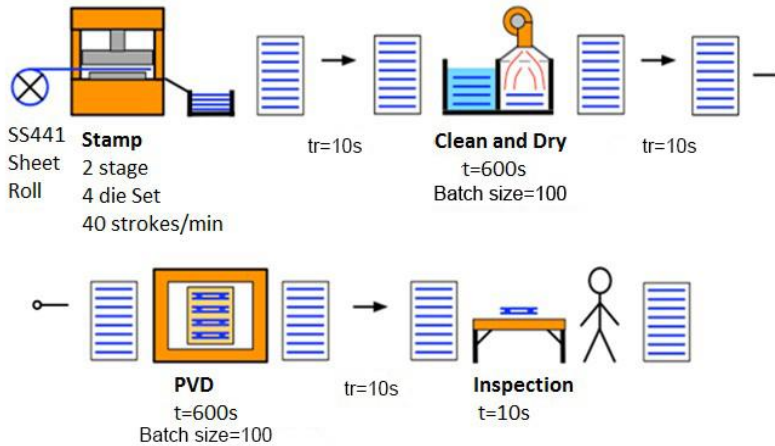
The coating step is expected to be the key cost limiter for metal plates, followed by the stamping and cleaning steps that are more standard process modules. Three different manufacturing lines were considered:

- Manual Line for production volume lower than 25 MWe per year
- Semi-automatic Line for production volume between 25 and 250 MWe per year
- Automatic Line for production volume higher than 250 MWe per year

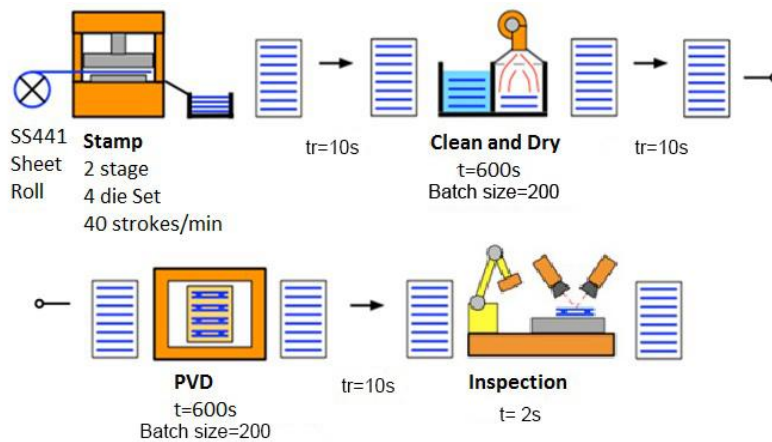
The interconnect process flow for each line configuration is shown in Figure 4.23.



(a) Manual Line



(b) Semi-automatic Line



(c) Automatic Line

Figure 4.23 Interconnect Process Flow (a) Manual Line (b) Semi-automatic Line (c) Automatic Line

The process parameters are shown in Table 4.38.

Table 4.38. Manufacturing parameters as a function of system size and annual volume for manufacturing line of interconnect.

Power (kW)	Systems/year	Line	Process Yield	Line Availability	Line Performance	Setup time (min)	Workers/line
1	100	Manual	85%	80%	89%	60.00	4
	1,000	Manual	85%	80%	89%	60.00	4
	10,000	Manual	85.8%	80.8%	89%	52.08	4
	50,000	Semi	90.6%	85.8%	95%	21.85	1.5
10	100	Manual	85%	80%	89%	60.00	4
	1,000	Manual	85.8%	80.8%	89%	52.08	4
	10,000	Semi	92.8%	88%	95%	15.03	1.5
	50,000	Auto	98%	93.5%	95%	6.31	0.5
50	100	Manual	85%	80%	89%	60.00	4
	1,000	Semi	90.6%	85.8%	95%	21.85	1.5
	10,000	Auto	98%	93.5%	95%	6.31	0.5
	50,000	Auto	99.5%	95%	95%	5.00	0.5
100	100	Manual	85.8%	80.8%	89%	52.08	4
	1,000	Semi	92.8%	88%	95%	15.03	1.5
	10,000	Auto	99.5%	95%	95%	5.00	0.5
	50,000	Auto	99.5%	95%	95%	5.00	0.5
250	100	Semi	88.5%	83.6%	89%	31.76	4
	1,000	Semi	95.8%	91.1%	95%	9.17	1.5
	10,000	Auto	99.5%	95%	95%	5.00	0.5
	50,000	Auto	99.5%	95%	95%	5.00	0.5

Process yield, setup time, line availability are all functions of interconnect annual production volume while line performance is assumed to be 89% for manual configuration and 95% for semi-automatic and automatic configurations. At low volumes (< 100,000 interconnects/year) setup time is assumed to be 60 minutes, line availability to be 80% and process yield to be 85%. At high volumes (>10,000,000 interconnects/year), setup time is estimated to be 5 minutes, line availability to be 95%, and process yield to be 99.5%. For volumes between 100,000 and 10,000,000 interconnects/year, the process parameters were found through exponential interpolation.

Interconnect Manufacturing Process Cost Analysis

For each line configuration, the process bottleneck is the physical vapor deposition step. Considering a loading time per piece (equal to unloading time) of 2 seconds using robots and 4 seconds in the manual loading case, bottleneck time was evaluated as:

$$\text{Bottle neck time (s)} = \frac{\text{PVD cycle time (s)} + \text{Batch size} \left(\frac{\text{Pieces}}{\text{Cycle}} \right) * \frac{\text{Load} + \text{Unload time (s)}}{\text{Piece}}}{\text{Batch size} \left(\frac{\text{Pieces}}{\text{Cycle}} \right)}$$

Table 4.39 shows cost, consumption, footprint and cycle time of each interconnect manufacturing line.

Table 4.39. Interconnect Manufacturing Line Cost, Consumption, Footprint and Cycle time

Equipment	Manual Line		Semi-Automatic Line		Automatic Line	
	Cost (\$)	Consumption (kW)	Cost (\$)	Consumption (kW)	Cost (\$)	Consumption (kW)
Dual Die Stamper	50000	7.5	480000	17	480000	17
Pick & Place Robot	0	0	165000	2	165000	2
Cleaner/Dryer 1	200000	5	500000	10	750000	10
Pick & Place Robot	0	0	165000	2	165000	2
PVD	500000	140	1920000	504	2875000	756
Pick & Place Robot	0	0	0	0	165000	2
Inspection	0	0	0	10	250000	10
<i>Total</i>	750000	152.5	3230000	545	4850000	799
<i>Bottle Neck Time (s)</i>	28		10		7	
<i>Line Footprint (m2)</i>	70		263		353	

Costs and consumptions of semi-automatic and automatic line machines were obtained from LBNL report (Wei, Lipman, Mayyas, Chien, & Chan, 2014) while those of manual line from information available online (e.g., www.alibaba.com).

A summary of the bill of materials for metal interconnects is listed in Table 4.40 with SS441 material chosen as the base case. Table 4.41 show specifications for the MCO powder.

Table 4.40. Interconnect Bill of Materials

Component	Material	Cost (\$/kg)
Sheet Metal	SS 441 (Tianjin Brilliant Import & Export Co.,Ltd.)	2.3-1.5
Sheet Metal	Crofer 22 APU (Elcogen)	25-10.0
Coating powder	MCO (Qingdao Terio Corporation)	300-250

Table 4.41. Manganese Cobalt Oxide powder specifications (Qingdao Terio Corporation)

• Grades & Specifications	
Grades	MCO
Specific Surface Area (m ² /g) :	5-10
Particle Size (D ₅₀ , μm) :	0.4-0.6
Feature	Spinel phase black powder

Assuming that a 1 cm margin on each side of the interconnect is needed, and that manifold areas are punched out during stamping process, a material scrap of 20% was estimated. In addition, the number of defective interconnects is inversely proportional to process yield, and contribute to increase scrap cost. We assume that waste is recyclable and sold at a price equal to 40% of the primary material purchase price.

The formulae below were used to estimate maximum annual production of each line, number of lines needed for each production volume and corresponding line utilization (%). Operating hours per day are assumed to be 16 hours (two 8-hour shifts).

$$\frac{\text{Max \# of Interconnects}}{\text{line * year}} = \frac{\left[\frac{\text{op. hours}}{\text{day}} - \frac{\text{setup time}}{\text{day}} \right] * 3600 \left(\frac{s}{hr} \right) * \text{Ann. op. days} * \text{line availability}}{\frac{\text{cycle time (s)}}{\text{Line performance}}}$$

$$\# \text{ of lines} = \frac{\frac{\frac{\text{Interconnects required}}{\text{year}}}{\text{Process Yield}}}{\frac{\text{Max \# of Interconnects}}{\text{line * year}}}$$

$$\text{Line utilization (\%)} = \frac{\frac{\frac{\text{Interconnects required}}{\text{year}}}{\text{Process Yield}}}{\frac{\text{Max \# of Interconnects}}{\text{line * year}} * \# \text{ of lines}}$$

In addition using cycle time, process yield and line performance values it was possible to evaluate annual operating hours and corresponding labor cost as:

$$\text{Annual operating hours} = \frac{\frac{\text{Interconnects required}}{\text{year}}}{\text{Process Yield}} * \frac{\text{cycle time (s)}}{\text{Line performance}}$$

$$\text{Labor cost} \left(\frac{\$}{\text{year}} \right) = \left[(\text{Annual op. hours} \left(\frac{hr}{yr} \right) + \text{setup} \left(\frac{hr}{yr} \right)) \right] * \frac{\# \text{ of workers}}{\text{line}} * \text{labor rate} \left(\frac{\$}{hr} \right)$$

Table 4.42 show the obtained results in case of 50-kWe systems at all production volumes.

Table 4.42. Machine rate for interconnect manufacturing process (50-kWe systems)

System Size (kW)	50			
	100	1000	10000	50000
Annual Quantity	100	1000	10000	50000
# of Lines	1	1	4	19
Line	Manual	Semi-Auto	Auto	Auto
Cycle Time (s)	28.00	10.00	7.00	7.00
Interconnects/year	65.000	650.000	6.500.000	32.500.000
Line Utilization	23.20%	65.15%	95.12%	96.96%
Annual operating hours (h)	668	2097	13569	66855
# of Workers	4	2	2	10
Production capacity (pieces/line/yr)	329554	1100987	1742360	1773025
Footprint (m2)	70	263	1412	6707
Labor Cost (\$/year)	84694.06	127908.63	203587.24	1054380.87
Initial Capital (\$)	7.50E+05	3.23E+06	2.72E+07	1.29E+08
Initial System Cost (\$)	1.12E+06	4.84E+06	2.91E+07	1.38E+08
Annual Depreciation (\$/yr)	4.90E+04	2.11E+05	1.77E+06	8.43E+06
Annual Cap Payment (\$/yr)	1.28E+05	5.50E+05	3.30E+06	1.57E+07
Auxiliary Costs (\$/yr)	0.00E+00	0.00E+00	0.00E+00	0.00E+00
Maintenance (\$/yr)	8.51E+03	3.67E+04	3.08E+05	1.46E+06
Salvage Value (\$/yr)	3.07E+02	1.32E+03	1.11E+04	5.28E+04
Energy Costs (\$/yr)	1.27E+04	1.43E+05	1.35E+06	6.66E+06
Property Tax (\$/yr)	3.12E+03	1.34E+04	1.13E+05	5.37E+05
Building Costs (\$/yr)	5.89E+03	2.21E+04	1.19E+05	5.65E+05
Interest Tax Deduction (\$/yr)	0.00	0.00	0.00	0.00
Machine Rate (\$/h)	235.73	363.81	381.88	371.75
Capital	190.49	261.41	242.44	233.73
Variable	31.75	85.44	122.36	121.54
Building	13.49	16.96	17.08	16.47

Interconnect Cost Summary

Table 4.43 display the final results for SS441 interconnect costs in (\$/kWe) and (\$/part) for all system sizes and production volumes. As with EEA cells, interconnect costs decrease with annual production volume and are constant for each cumulative global produced power (MW/year).

Table 4.43. SS441 Interconnect manufacturing cost in (\$/kW) and (\$/part) at all production volumes

Equivalent production (MWe/year)	Interconnects/year	Cost (\$/kWe)	Cost (\$/Interconnect)
0.1	1300	1481.13	113.93
1	13000	177.6	13.66
5	65000	61.41	4.72
10	130000	44.49	3.42
25	325000	39.82	3.06
50	650000	27.43	2.11
100	1300000	26.49	2.04
250	3250000	21.56	1.66
500	6500000	19.44	1.5
1000	13000000	19.29	1.48
2500	32500000	18.96	1.46
5000	65000000	18.78	1.44
12500	162500000	18.81	1.45

As expected, at low volumes the high price is due to the high equipment cost and low utilization rate. At the highest volumes, the cost per plate converges to \$1.45/Plate. A cost summary for 10-kWe and 50-kWe systems is shown in Table 4.44 and Table 4.45 respectively.

Table 4.44. SS441 Interconnect manufacturing cost breakdown in (\$/kWe) for 10-kWe systems

System Size (kWe)	10			
	100	1,000	10,000	50,000
Production Volume (Units/yr)				
Direct Material (\$/kWe)	12.62	10.28	9.33	8.56
Scrap (\$/kWe)	0.73	0.57	0.67	0.71
Labor (\$/kWe)	17.01	16.65	1.86	0.41
Process: Capital (\$/kWe)	127.18	12.72	10.97	6.60
Process: Operational (\$/kWe)	11.05	3.37	2.95	2.77
Process: Building (\$/kWe)	9.01	0.90	0.71	0.40
Total (\$/kWe)	177.60	44.49	26.49	19.44

Table 4.45. SS441 Interconnect manufacturing cost breakdown in (\$/kWe) for 50-kWe systems

System Size (kWe)	50			
	100	1,000	10,000	50,000
Production Volume (Units/yr)	100	1,000	10,000	50,000
Direct Material (\$/kWe)	12.26	9.55	8.56	8.44
Scrap (\$/kWe)	0.73	0.64	0.71	0.72
Labor (\$/kWe)	16.94	2.56	0.41	0.42
Process: Capital (\$/kWe)	25.44	10.95	6.60	6.27
Process: Operational (\$/kWe)	4.24	3.02	2.77	2.73
Process: Building (\$/kWe)	1.80	0.71	0.40	0.38
Total (\$/kWe)	61.41	27.43	19.44	18.96

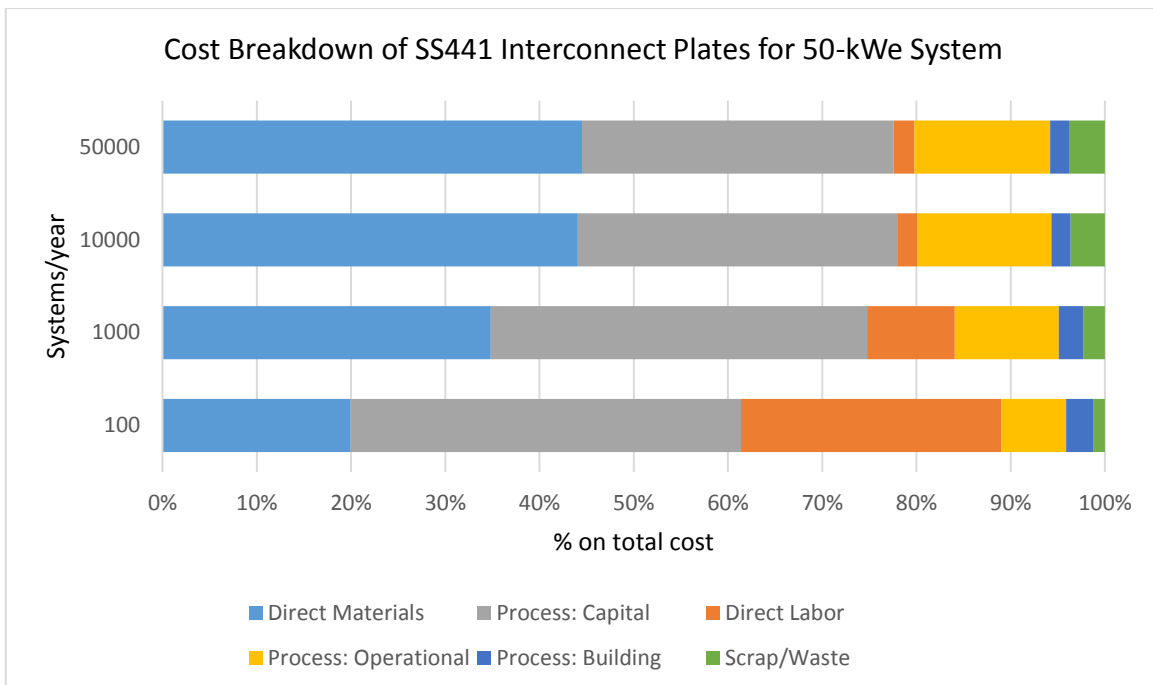


Figure 4.24. Fraction of plate costs for 50-kWe system as a function of annual production volume

Figure 4.24 above shows that capital costs dominate for the 50-kWe system at 100 and 1,000 systems per year and material costs make up 40-45% of the total plate cost at volumes above 1,000 systems per year. Labor costs decrease with annual production volume since the level of automation increases with volume (manual at 100 systems/year; semi-automatic at 100 systems/year; and automatic at 1000 systems/year). The fraction of direct material costs increases with annual production volume. MCO coating powder constitutes about 60% of the total material cost in all cases (see Figure 4.28).

Figure 4.26 shows the impact of MCO coating thickness on interconnect manufacturing cost for a ± 5 -10 μm variation of thickness with respect to the chosen value of 15 μm . It is important to note that varying the coating thickness would impact the amount of material needed and cycle time and thus the processing costs.

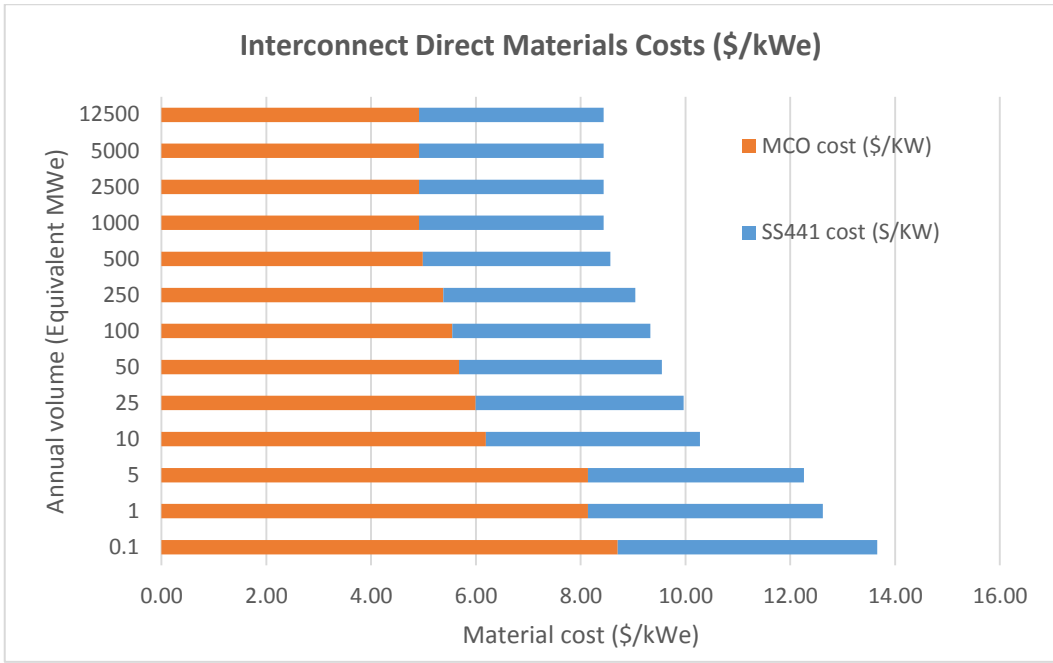


Figure 4.25. Direct material cost variation with annual production volume (\$/kWe)

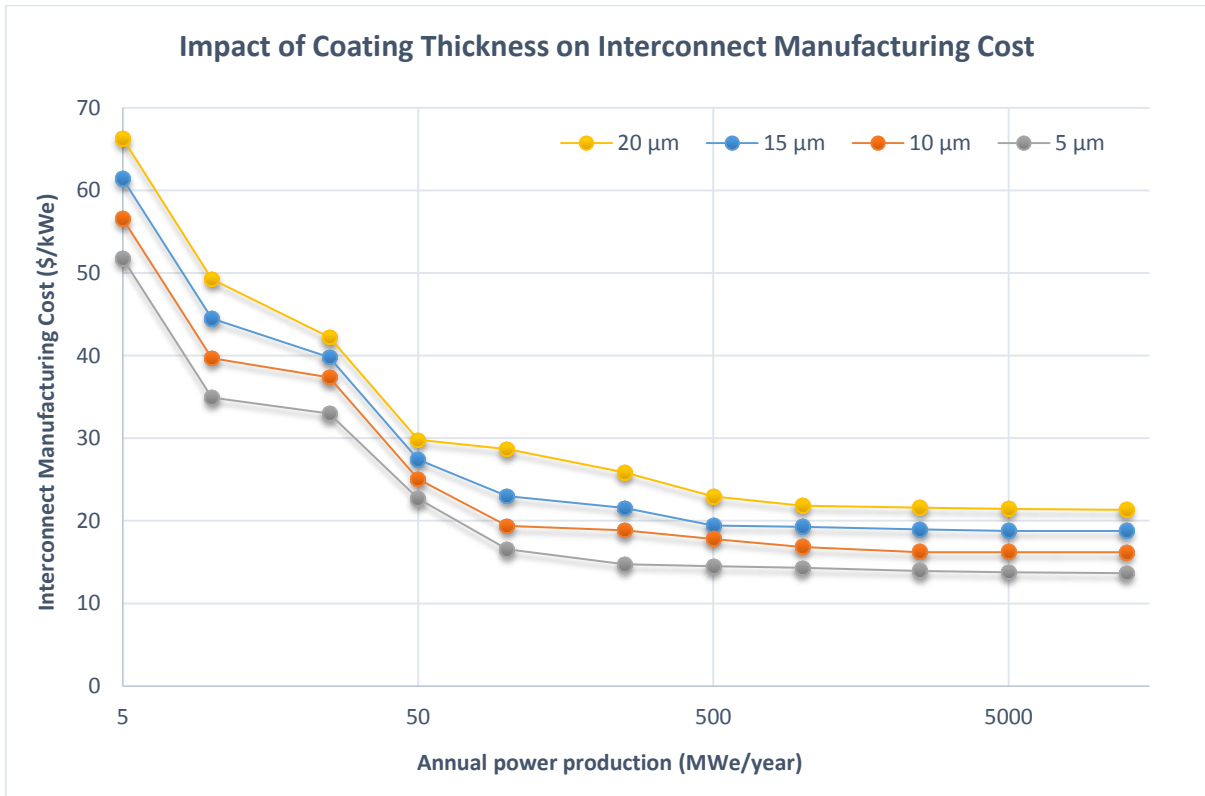


Figure 4.26. Impact of coating thickness on interconnect manufacturing cost for 5-12500 MW annual production

SS441 vs. Crofer 22 APU Interconnect Cost

A side-by-side cost comparison shows the cost relation between SS441 and Crofer 22 APU interconnects. The only difference between the two options is in material cost and scrap cost. Figure 4.27 shows that SS441 plates have a lower cost at all production volumes. The high cost at low volumes for both options is driven by the PVD tooling cost.

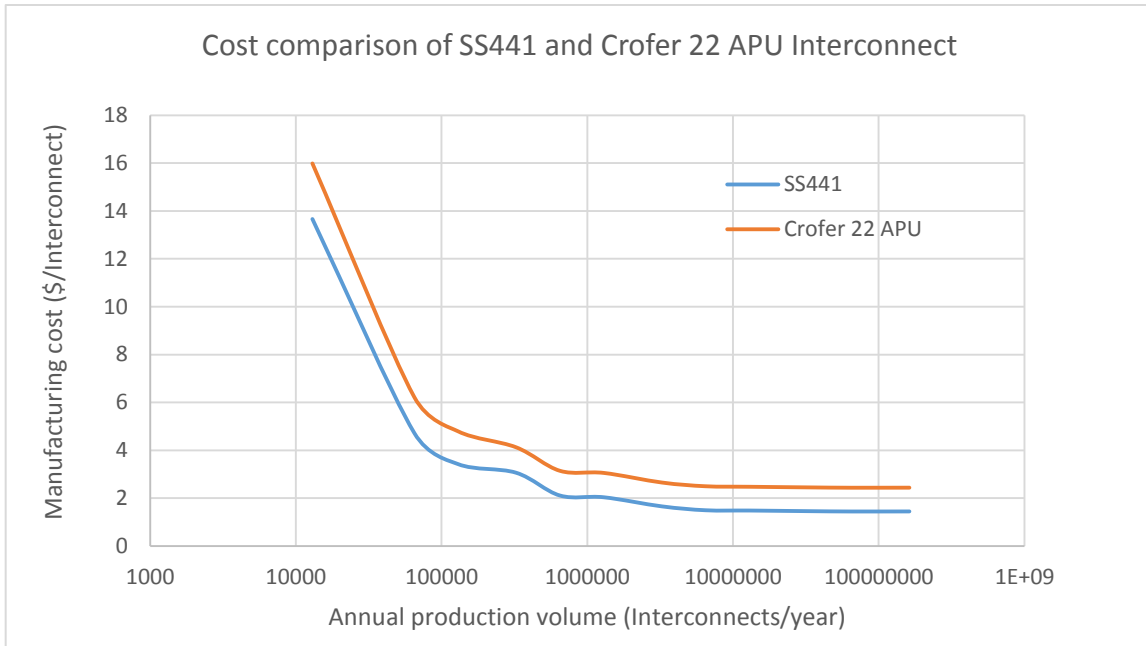


Figure 4.27. Cost Comparison of SS441 and Crofer 22 APU Interconnect as a function of plates/yr.

Figure 4.28 compares SS441 and Crofer 22 APU Interconnect cost as a function of systems/year for a 50 kW_e fuel cell system. Crofer plates are more expensive than SS441 plates because of the higher material cost as shown in Figure 4.29.

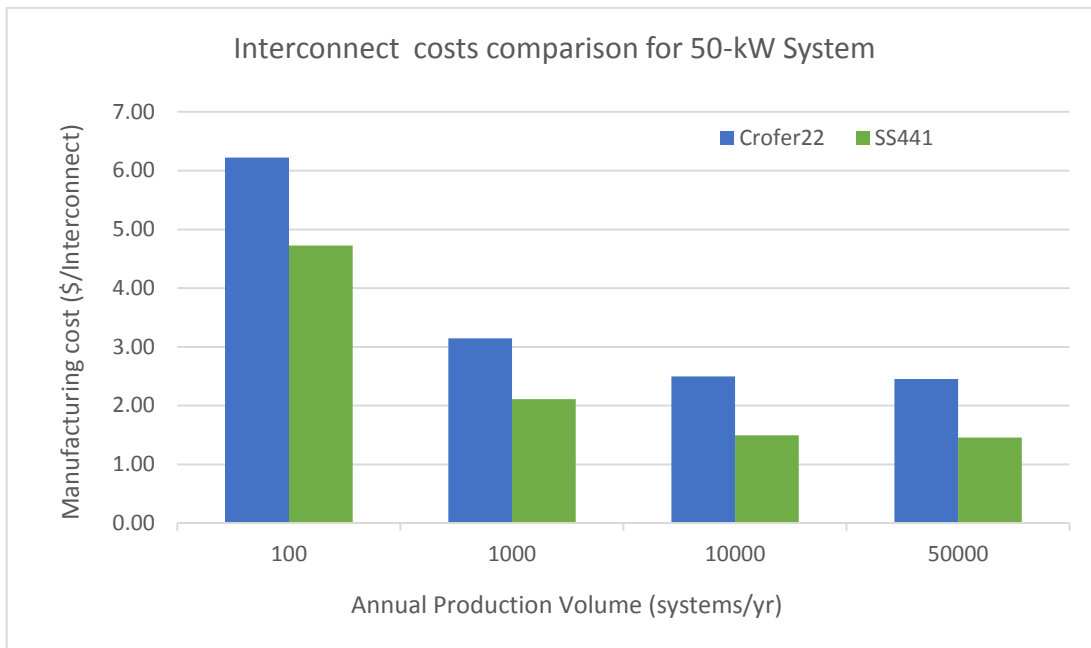


Figure 4.28. Cost Comparison of SS441 and Crofer 22 APU Interconnect for 50-kWe System

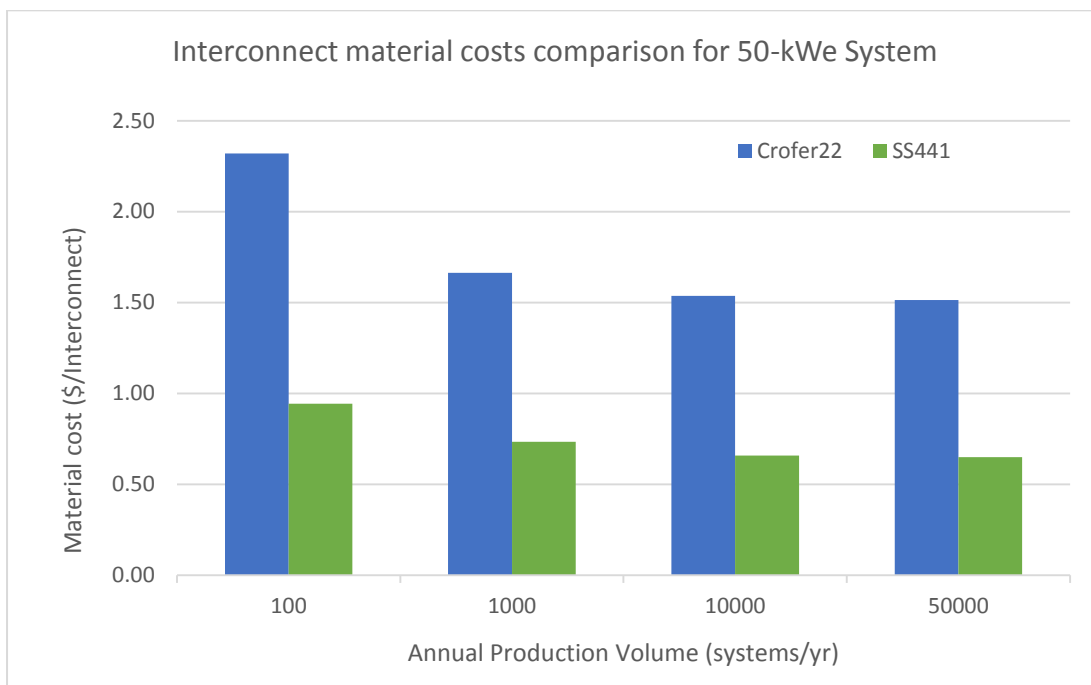


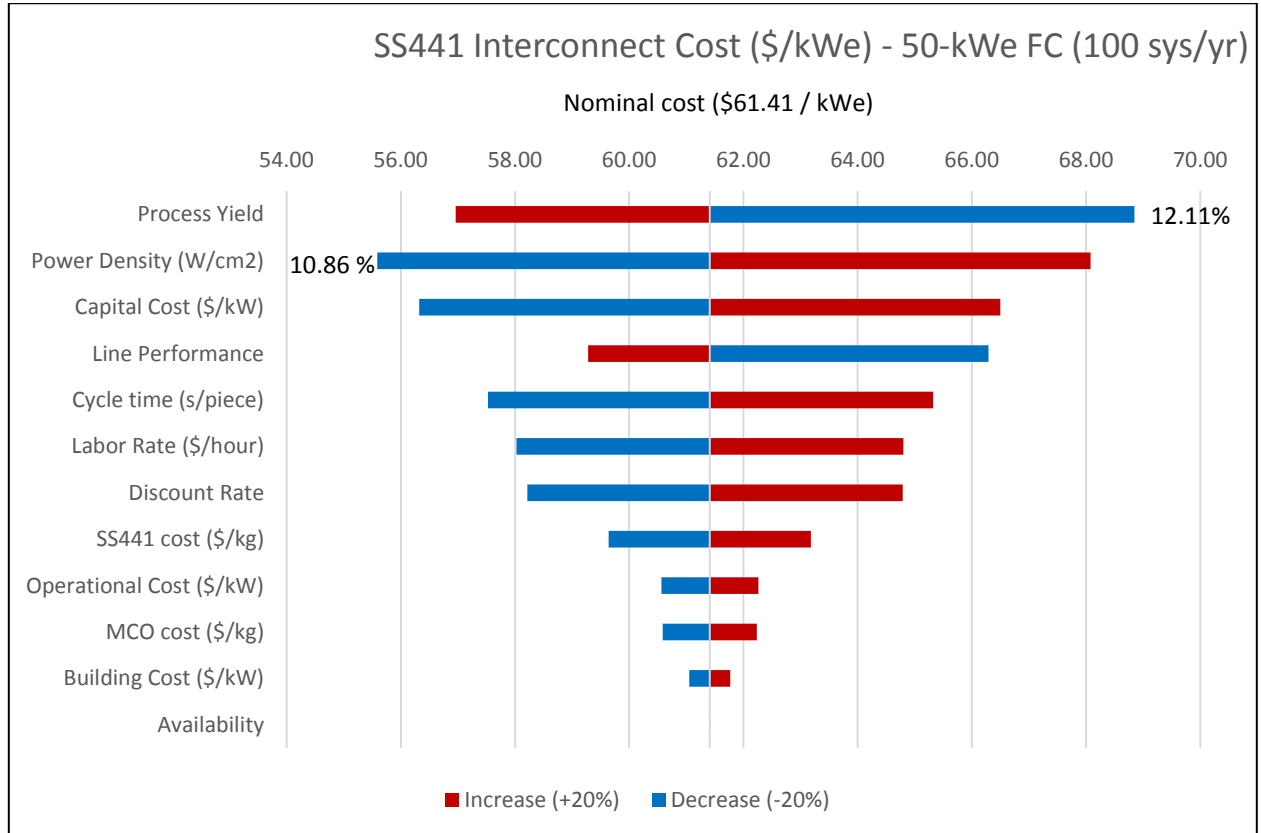
Figure 4.29. Cost Comparison of SS441 and Crofer 22 APU materials in \$/interconnect as a function of systems/year

Interconnect Cost Sensitivity Analysis

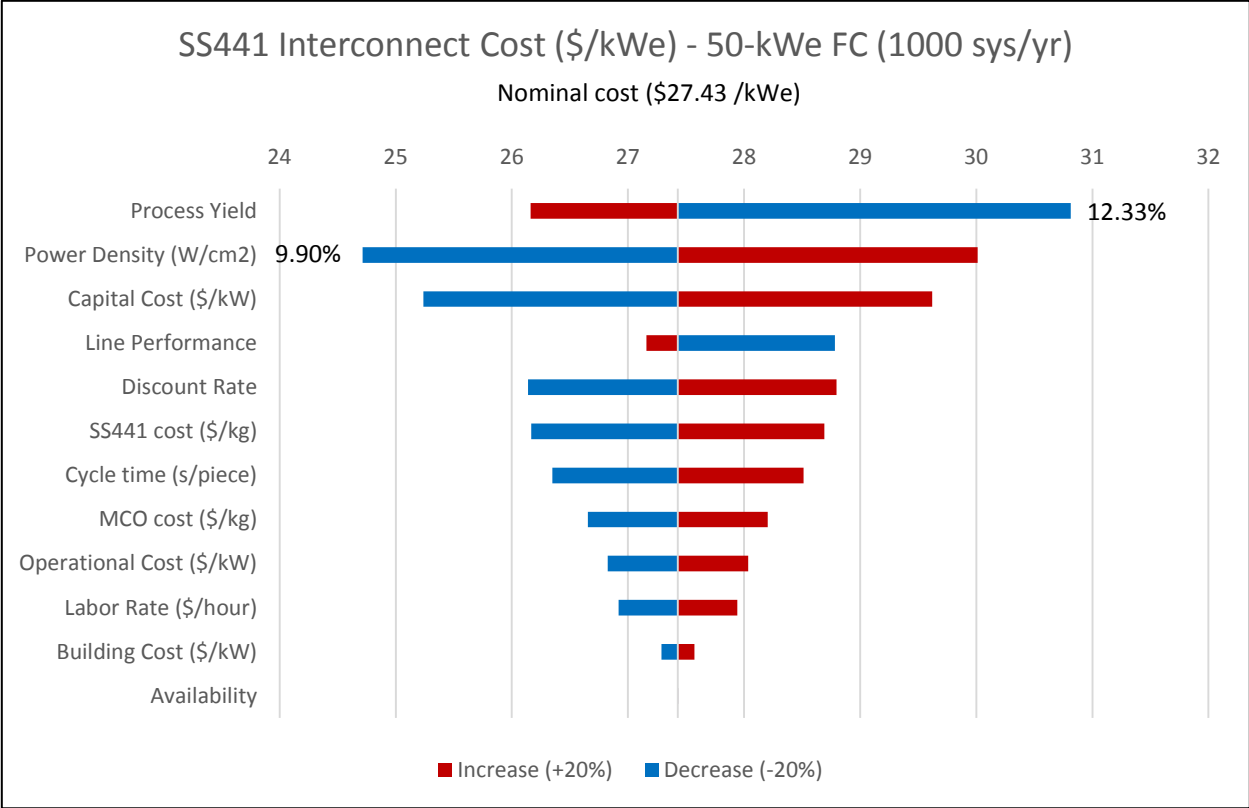
Interconnect cost sensitivity analysis was done for 50-kWe systems at different production volumes (as shown in Figure 4.30). The impact to the cost in \$/kWe is calculated for a \pm -20% change in the sensitivity parameter being varied.

Process yield and power density dominate at all volumes. The third important factor affecting the interconnect cost sensitivity is the capital cost at low volumes (100 and 1,000 systems/year) and line performance reduction at higher volumes (>1,000 systems/year). The labor rate is less important with higher production volume since the level of automation increases with volume.

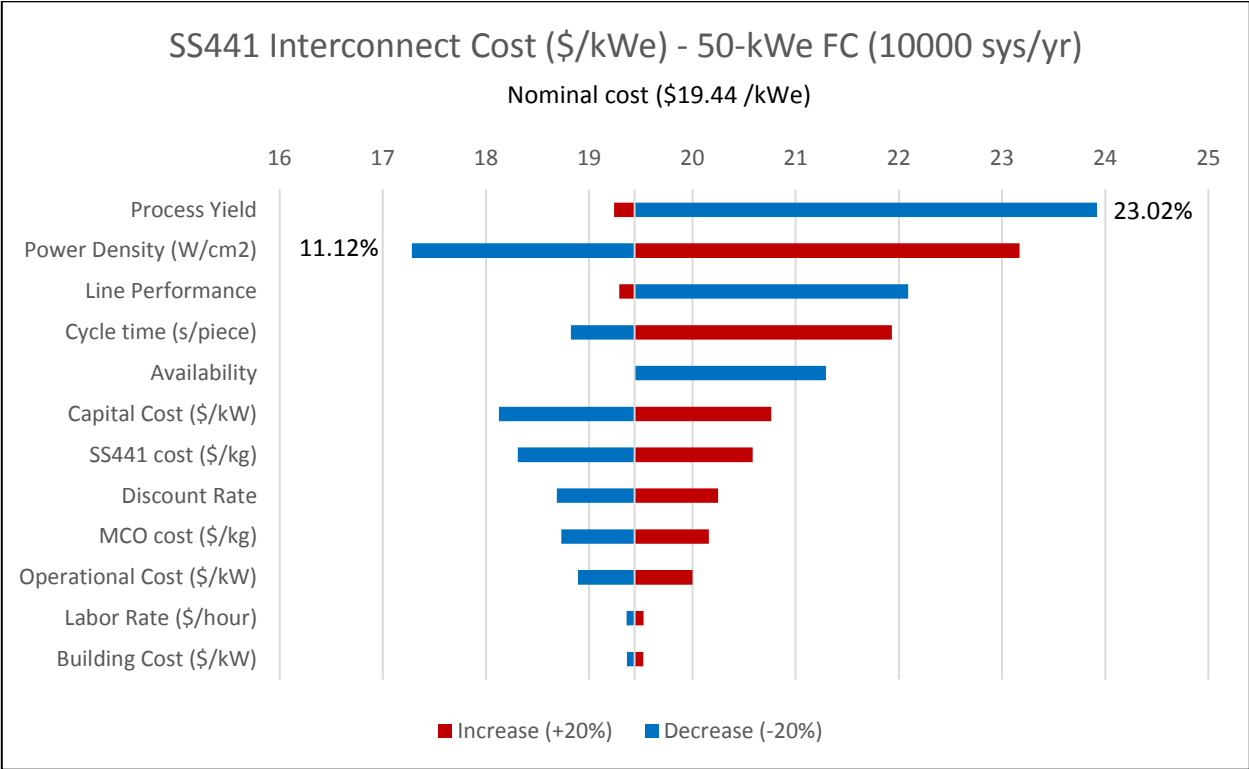
Interconnect cost sensitivity in case of line performance variation is not symmetric because a +20% increase of this parameter is not applicable. Nominal values are equal to 89% and 95% in manual and automatic configurations respectively.



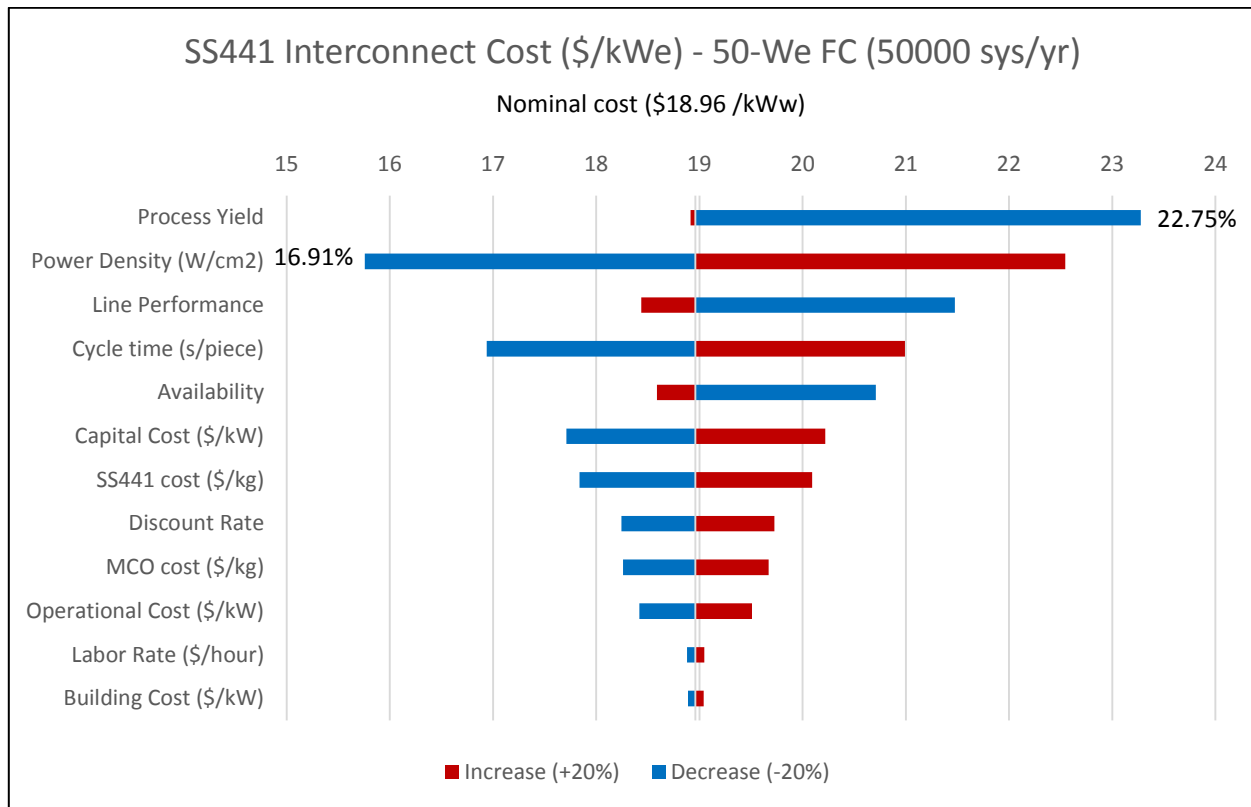
(a)



(b)



(c)



(d)

Figure 4.30. Interconnect cost sensitivity analysis for 50 kWe system expressed in (\$/kWe) at different annual production rates: a) 100 units/yr; b) 1,000 units/yr; c) 10,000 units/yr; and d) 50,000 units/yr.

4.3. Frame Manufacturing Cost Analysis

The purpose of the frame is to provide a place for the cell to be secured within the stack, to provide rigid support and to facilitate connection to the interconnects. The frame is a piece of sheet metal that has a cell size slot punched out. The cell frame is made from SS441 or Crofer 22 APU and has a manganese cobalt oxide coating, similar as the interconnect (Weimar, Chick, & Whyatt, 2013).

Frames can be made of the same metal as the interconnects and also manufactured in the same way. This means the same machines and manufacturing line can be used. Therefore, at low production, there is no capital cost and building cost associated with the frames since the process uses the same machines. If production volume is high enough that the interconnect line has a high tool utilization and additional lines are needed for manufacturing of the frame a similar line is added. Additional lines are needed in case of annual production volume higher than 130000 frames per year (10 MWe per year) since interconnect line utilization was higher than 50%.

However, a single die stamper can replace the dual die stamper since no bending is required for the frame (i.e., the manifolds and cell slot can be punched in one stroke). The cost of the single die stamper is assumed to be \$320,000 (Weimar, Chick, & Whyatt, 2013).

Additional manufacturing lines for frame production were either manual or automatic lines as in Figure 4.23 above.

Table 4.46 show cost, consumption, footprint and cycle time for both additional frame-manufacturing lines.

Table 4.46. Interconnect Manufacturing Line Cost, Consumption, Footprint and Cycle time

Equipment	Manual Line		Automatic Line	
	Cost (\$)	Consumption (kW)	Cost (\$)	Consumption (kW)
Die Stamper	50000	7.5	320000	15
Pick & Place Robots	0	0	165000	2
Cleaner/Dryer 1	200000	5	750000	10
Pick & Place Robots	0	0	165000	2
PVD	500000	140	2875000	756
Pick & Place Robots	0	0	165000	2
Inspection	0	0	250000	10
<i>Total</i>	750000	152.5	4850000	797
<i>Bottle Neck Time (s)</i>	28		7	
<i>Line Floorspace (m2)</i>	70		353	

Including a 1 cm margin on each side of the frame and that cell size slot and manifolds slots are punched out during stamping process a material scrap of 72% was estimated. At the same time, in order to reduce scrap cost, we assume that waste is recyclable and sold at a price equal to 40% of the primary material purchase price.

As with interconnect manufacturing, two different designs were considered for frames manufacturing depending on primary material: Crofer frame with a thickness of 315 μm (GhezelAyagh, 2014) and a mass of 44 g and SS441 frame with a thickness of 630 μm (GhezelAyagh, 2014) and a mass of 88 g. Knowing the maximum annual production and interconnect production volume required for interconnect manufacturing lines, it was possible to estimate the number of frames to produce using additional lines. The number of additional lines, annual operating hours, line utilization and labor cost were evaluated with the same formulae and assumptions used for the interconnect manufacturing analysis.

Table 4.47 summarize additional lines chosen and their relative process parameters for all production volumes.

Table 4.47. Additional lines parameters for all annual production volumes

Power	Systems/yr	Interconnect Line Utilization (%)	# of additional Lines	Additional Line Type	Line max ann. Production (pieces/yr)	Frames to produce with additional lines (pieces/yr)	Additional Line Utilization (%)
1	100	0.39%	0		329554	0	
	1000	3.94%	0		329554	0	
	10000	38.72%	0		335725	0	
	50000	59.04%	1	Manual	368375	199013	54.02%
10	100	3.94%	0		329554	0	
	1000	38.72%	0		335725	0	
	10000	57.12%	1	Manual	380775	323902	85.06%
	50000	93.26%	4	Auto	1742360	6030560	86.53%
50	100	19.72%	0		329554	0	
	1000	59.04%	1	Manual	368375	199013	54.02%
	10000	93.26%	4	Auto	1742360	6030560	86.53%
	50000	96.48%	18	Auto	1773025	31312525	98.11%
100	100	38.72%	0		335725	0	
	1000	57.12%	1	Manual	380775	323902	85.06%
	10000	91.65%	7	Auto	1773025	11815800	95.20%
	50000	99.08%	37	Auto	1773025	64398075	98.16%
250	100	32.68%	0	Manual	355176	0	
	1000	91.42%	2	Auto	1692776	2945171	86.99%
	10000	96.48%	18	Auto	1773025	31312525	98.11%
	50000	98.55%	91	Auto	1773025	160108675	99.23%

Table 4.48 shows the machine rate results in case of 50-kWe systems for all production volumes.

Table 4.48. Machine rate for frame manufacturing process

System Size (kWe)	50			
	100	1.000	10.000	50.000
Systems/year	100	1.000	10.000	50.000
Frames/year	65000	650000	6500000	32500000
Shift Size (hours/day)	16	16	16	16
FRAME ADDITIONAL LINES				
# of Additional Lines	0	1	4	18
Line Type		Manual	Auto	Auto
Cycle Time (s)		28.00	7.00	7.00
Line production capacity (frames/line)	329554	368375	1742360	1773025
Frames to produce with additional lines	0.00	199013	6030560	31312525
Additional Line Utilization (%)	0.00	0.54	0.87	0.98
Annual Operating Hours	0.00	1919.22	12589.41	64412.02
# of Workers	4.00	4.00	2.00	9.00
Labor Cost (\$/year)	0.00	234059.27	188878.42	965061.84
Energy Cost (\$/year)	0.00	36500.18	1251307.45	6402148.24
INTERCONNECT LINE				
Interconnect # of lines	1.00	1.00	4.00	19.00
Line Type	Manual	Semi-Auto	Auto	Auto
Cycle time (s)	28.00	10.00	7.00	7.00
Lines Utilization (%)	0.20	0.59	0.93	0.96
Max annual production (frames/year)	329554	1100987	6969440	33687475
Annual Production Capacity (frames/year)	264554	450987	469440	1187475
Annual Operating Hours	668.28	1553.28	980.00	2442.72
# of Workers	4.00	2.00	2.00	9.00
Labor Cost (\$/year)	84694.06	94734.48	14704.12	34672.50
Energy Cost (\$/year)	12709.55	105958.81	97650.60	243400.00
TOTAL				
Auxiliary Costs Factor	0.00E+00	0.00E+00	0.00E+00	0.00E+00
Initial Capital (\$)	0.00E+00	7.50E+05	1.94E+07	8.73E+07
Initial System Cost (\$)	0.00E+00	1.12E+06	2.91E+07	1.31E+08
Annual Depreciation (\$/yr)	0.00E+00	4.90E+04	1.27E+06	5.70E+06
Annual Cap Payment (\$/yr)	0.00E+00	1.28E+05	3.30E+06	1.49E+07
Auxiliary Costs (\$/yr)	8.00E+00	9.00E+00	1.00E+01	1.10E+01
Maintenance (\$/yr)	0.00E+00	8.51E+03	2.20E+05	9.91E+05
Salvage Value (\$/yr)	0.00E+00	3.07E+02	7.94E+03	3.57E+04
Energy Costs (\$/yr)	1.27E+04	1.42E+05	1.35E+06	6.65E+06
Property Tax (\$/yr)	0.00E+00	3.12E+03	8.07E+04	3.63E+05
Building Costs (\$/yr)	0.00E+00	5.89E+03	1.19E+05	5.35E+05
Interest Tax Deduction (\$/yr)	0.00E+00	0.00E+00	0.00E+00	0.00E+00
Machine Rate (\$/h)	19.02	114.50	393.05	358.21
Capital	0.00	66.33	261.56	230.05
Variable	19.02	43.48	115.64	114.22
Building	0.00	4.70	15.85	13.94

Frame Cost Summary

Table 4.49 displays the final results for SS441 frame costs in (\$/kWe) and (\$/part) for all system sizes and production volumes.

Table 4.49. SS441 Frame manufacturing cost in (\$/kWe) and (\$/part) at all production volumes

Equivalent Power (MWe/year)	Frames /year	Frame Cost (\$/kWe)	Frame Cost (\$/Frame)
0.1	1,300	29.01	2.23
1	13,000	28.23	2.17
5	65,000	28.04	2.16
10	130,000	26.02	2
25	325,000	15.44	1.19
50	650,000	18.58	1.51
100	1,300,000	15.63	1.24
250	3,250,000	16.54	1.47
500	6,500,000	15.97	1.43
1,000	13,000,000	15.01	1.33
2,500	32,500,000	15.14	1.35
5,000	65,000,000	15.33	1.36
12,500	162,500,000	15.21	1.35

For annual production lower than 50,000 kWe, the frame cost decrease with production volume since no additional line are required (see Figure 4.31). The peak observed at 50,000 kWe is due to the shift from zero to one additional line required while the peak at 250,000 kWe is also related to the shift from manual to automatic configuration and thus higher capital and building costs.

Table 4.50 and Table 4.51 show cost breakdown in \$/kWe for 10- and 50-kWe systems respectively. It can be seen that in some cases there is no capital cost and building cost associated with the frames since only interconnect manufacturing equipment is used. Material, scrap and labor costs always decrease always with annual production volume since material cost (\$/kg) decreases and the degree of automation increases with volume.

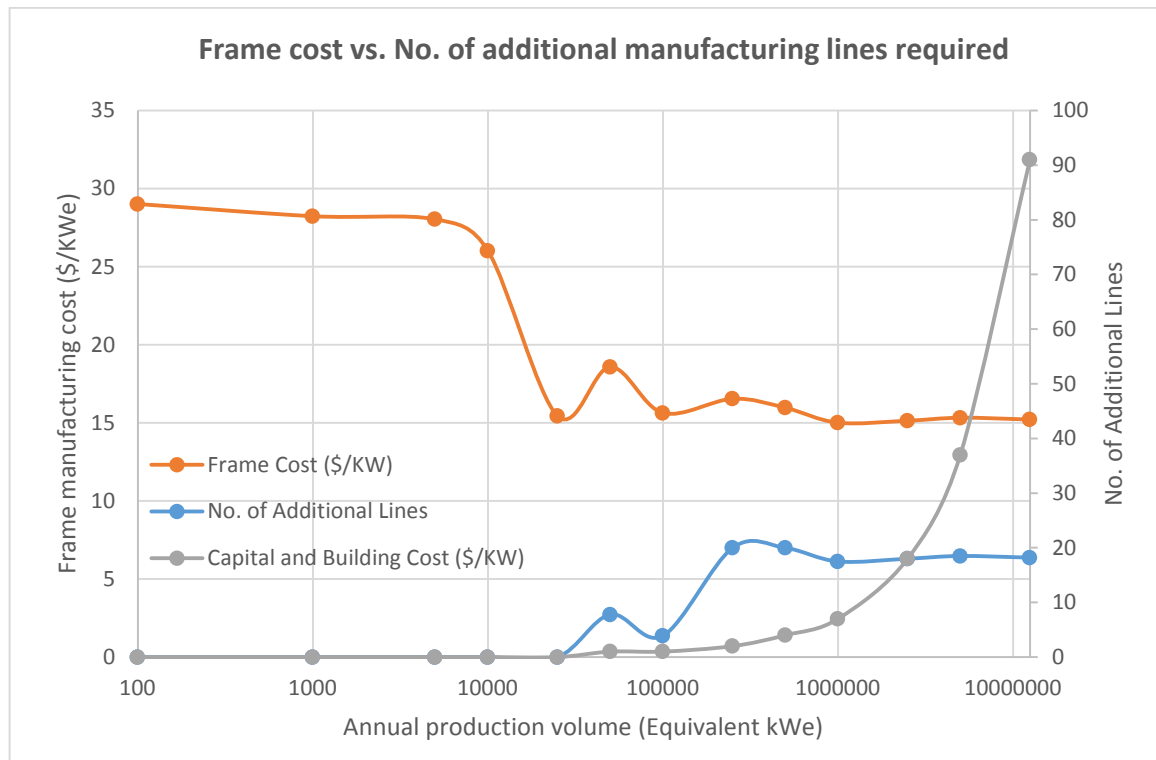


Figure 4.31. Relation between frame cost in (\$/kWe) and number of additional manufacturing lines required

Table 4.50. Frame manufacturing cost breakdown in (\$/kWe) for 10-kWe systems

System Size (kWe)	10			
Production Volume (Units/yr)	100	1,000	10,000	50,000
Direct Material (\$/kWe)	4.48	3.64	3.31	3.04
Scrap (\$/kWe)	4.21	3.21	2.93	2.67
Labor (\$/kWe)	17.01	16.65	5.19	0.41
Process: Capital (\$/kWe)	0.00	0.00	1.27	6.60
Process: Operational (\$/kWe)	2.54	2.52	2.85	2.86
Process: Building (\$/kWe)	0.00	0.00	0.09	0.40
Total (\$/kWe)	28.23	26.02	15.63	15.97

Table 4.51. Frame manufacturing cost breakdown in (\$/kWe) for 50-kWe systems

System Size (kWe)	50			
Production Volume (Units/yr)	100	1,000	10,000	50,000
Direct Material (\$/kWe)	4.35	3.39	3.04	2.99
Scrap (\$/kWe)	4.21	2.98	2.67	2.64
Labor (\$/kWe)	16.94	6.58	0.41	0.40
Process: Capital (\$/kWe)	0.00	2.54	6.60	5.94
Process: Operational (\$/kWe)	2.54	2.91	2.86	2.80
Process: Building (\$/kWe)	0.00	0.18	0.40	0.36
Total (\$/kWe)	28.04	18.58	15.97	15.14

Cost comparison between SS441 and Crofer 22 APU Frame Cost

As with interconnects, the difference between Crofer 22 APU and SS441 frame costs are only related to material and scrap cost and Crofer frames have 30-40% higher cost than SS441 cost depending on production volume.

Figure 4.32 shows the cost difference in \$/kWe between Crofer 22 APU and SS441 frames cost for 50-kWe systems while Figure 4.33 compares Crofer 22 APU and SS441 material cost for 50-kWe systems where material cost is the sum of direct material and indirect material (scrap).

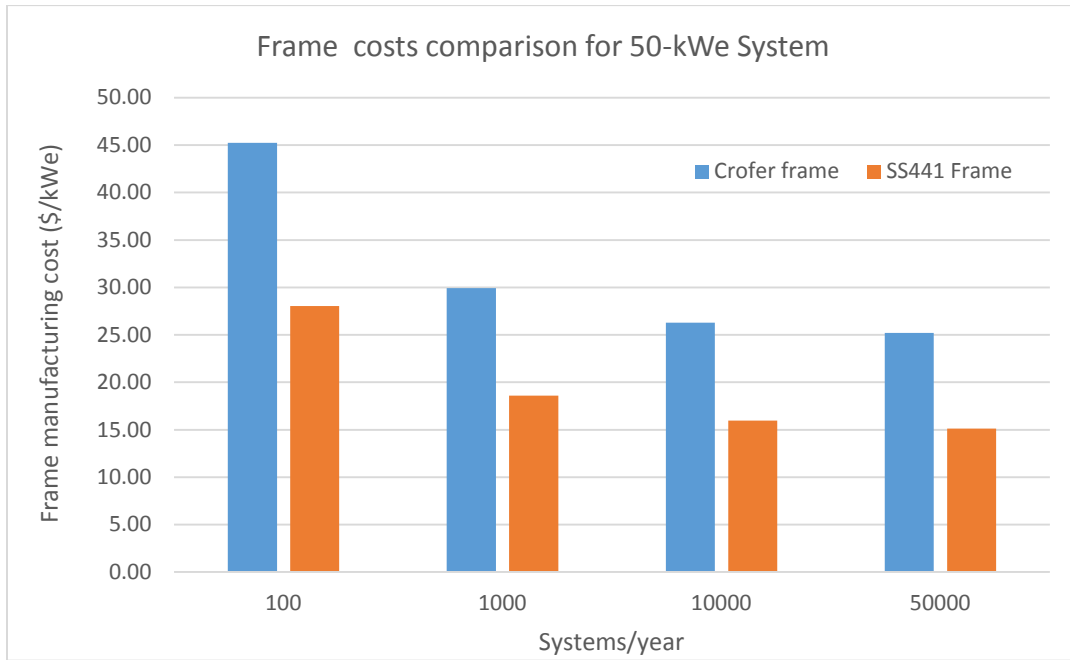


Figure 4.32. Crofer vs. SS441 frame cost for 50-kWe systems at all production volume

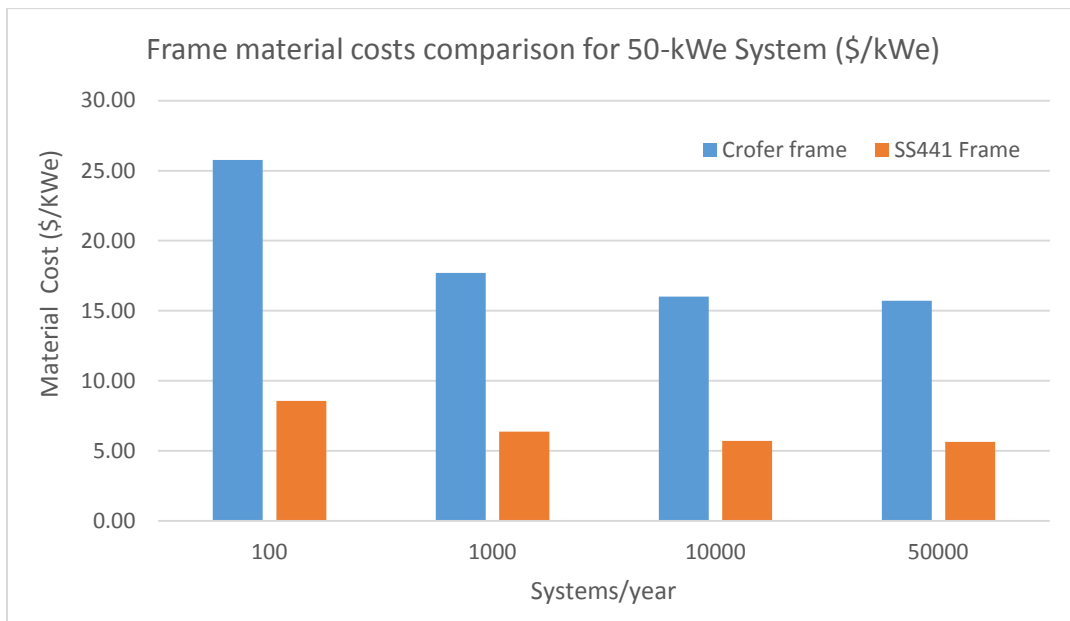
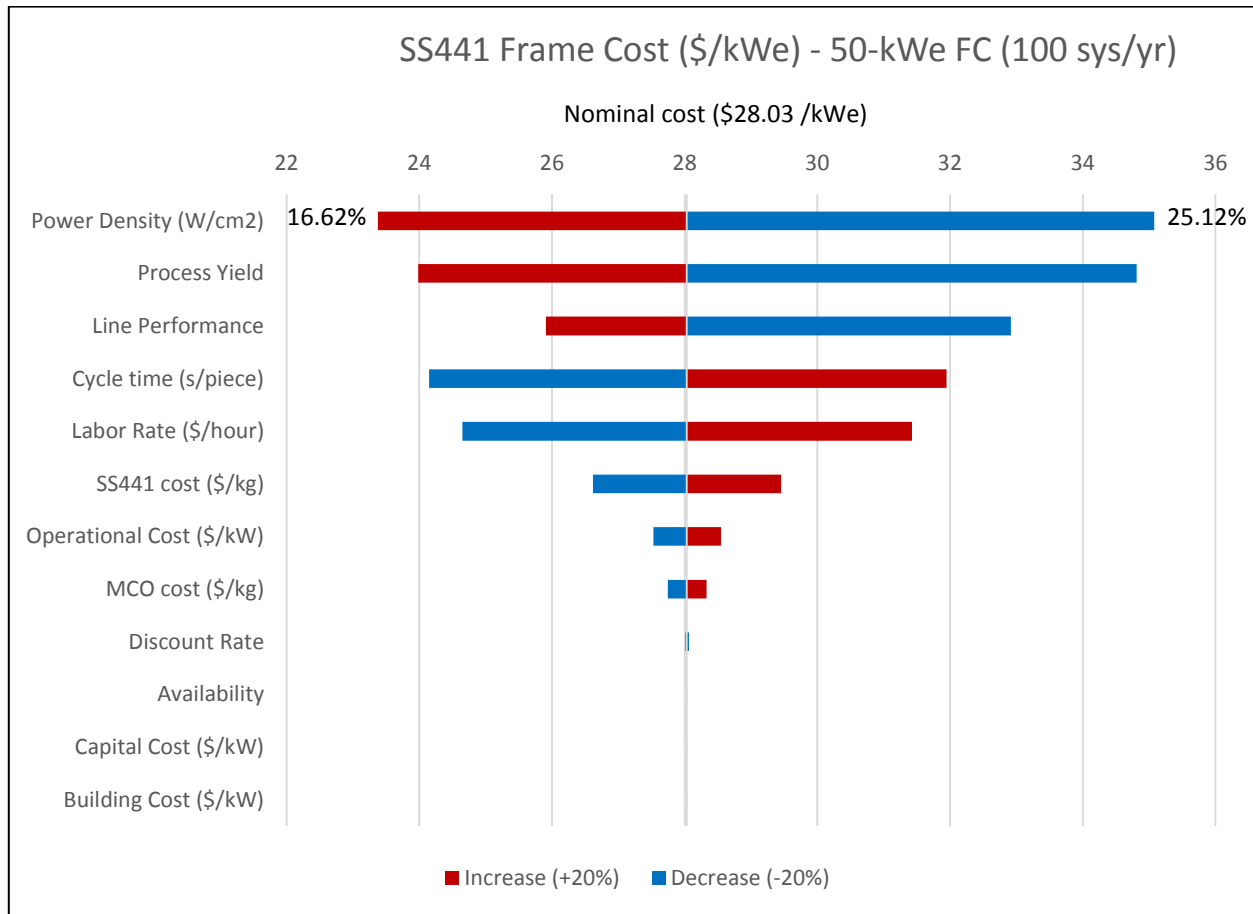


Figure 4.33. Crofer vs. SS441 material cost for 50-kWe systems at all production volume

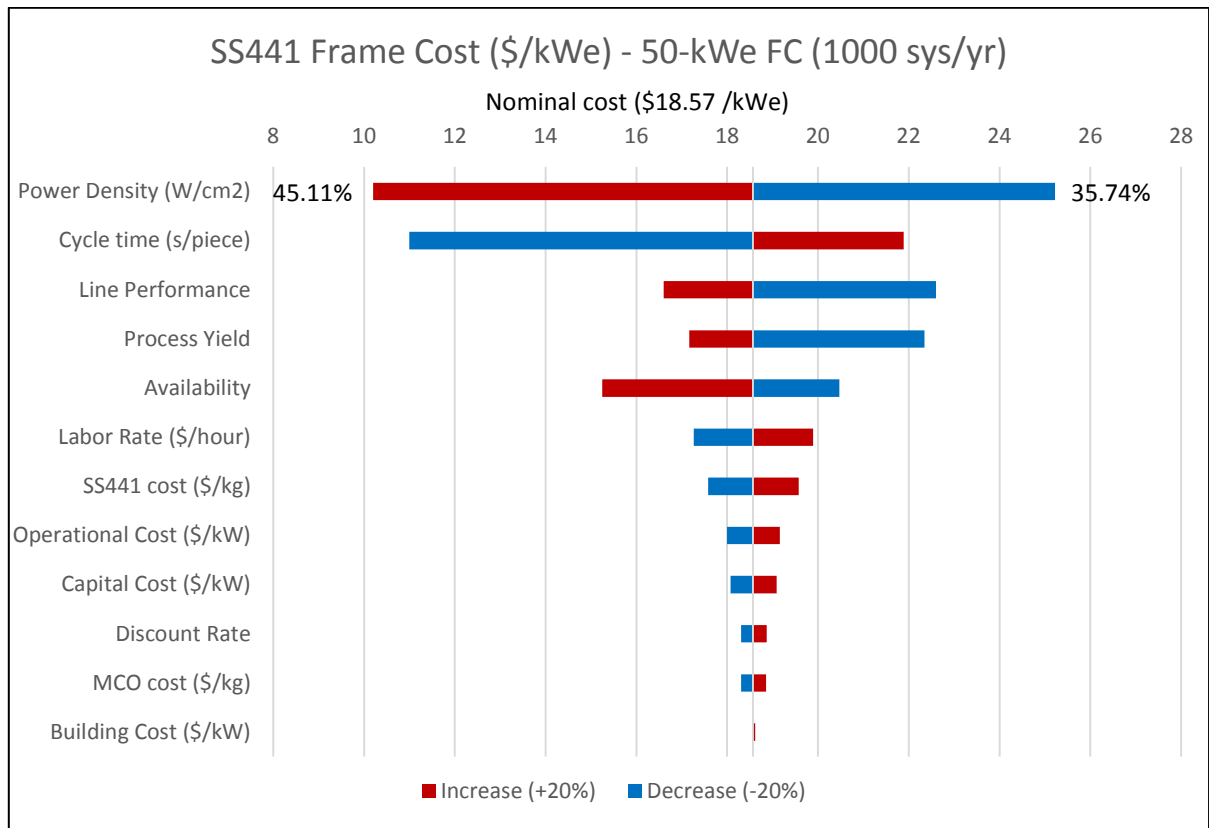
Frame Cost Sensitivity Analysis

Frame cost sensitivity analysis was performed for 50-kWe systems at different production volumes (as shown in Figure 4.34). As before, the impact to the cost in \$/kWe was calculated for a $\pm 20\%$ change in the sensitivity parameter being varied. The difference is that in this case most process parameters and costs were varied in frame and interconnect manufacturing lines at the same time since both are used for frame manufacturing.

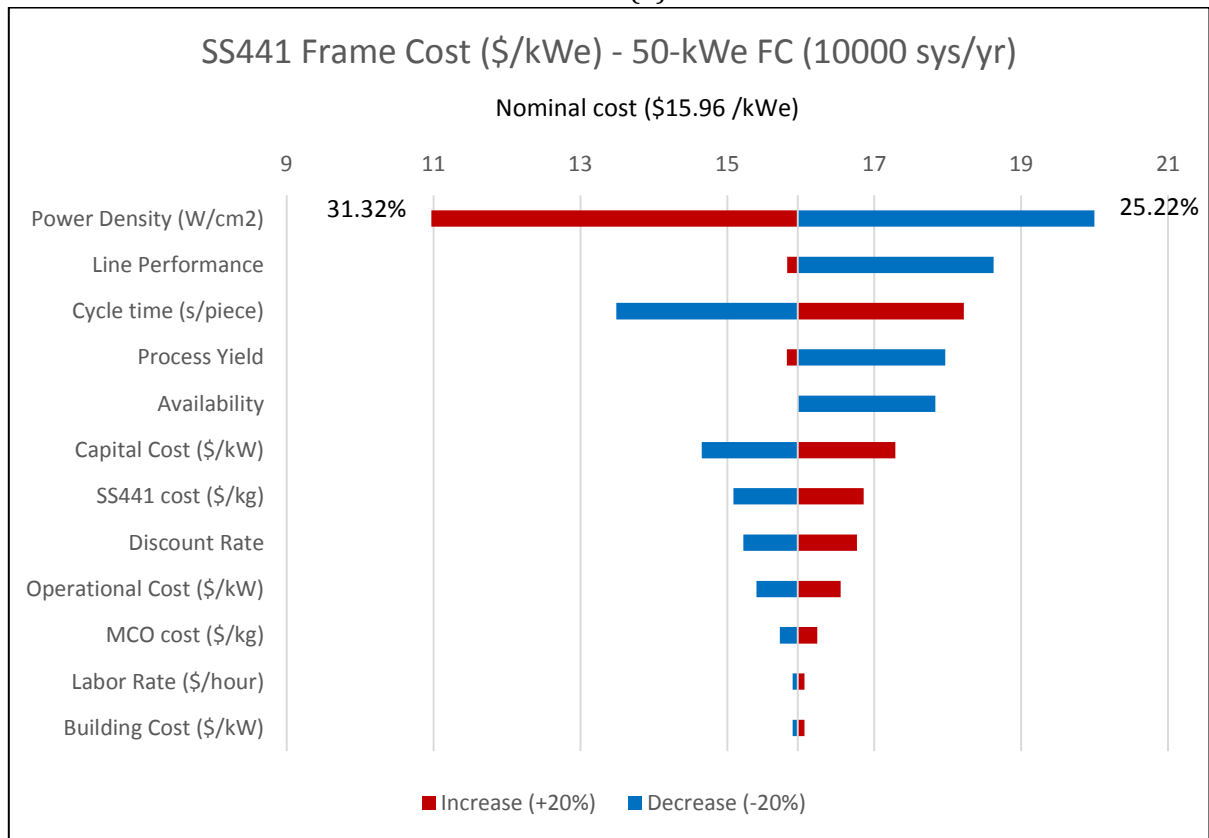
In Figure 4.34 it can be seen that power density dominates at all volumes. Other important factors affecting frame cost sensitivity are line performance and cycle time. Process yield and labor rate are less important with increasing production volume since the level of automation increases with volume while capital cost gains importance as the number of additional lines required increases. Availability is negligible only in the case of 100 systems/year where utilization is low and no additional lines are needed.



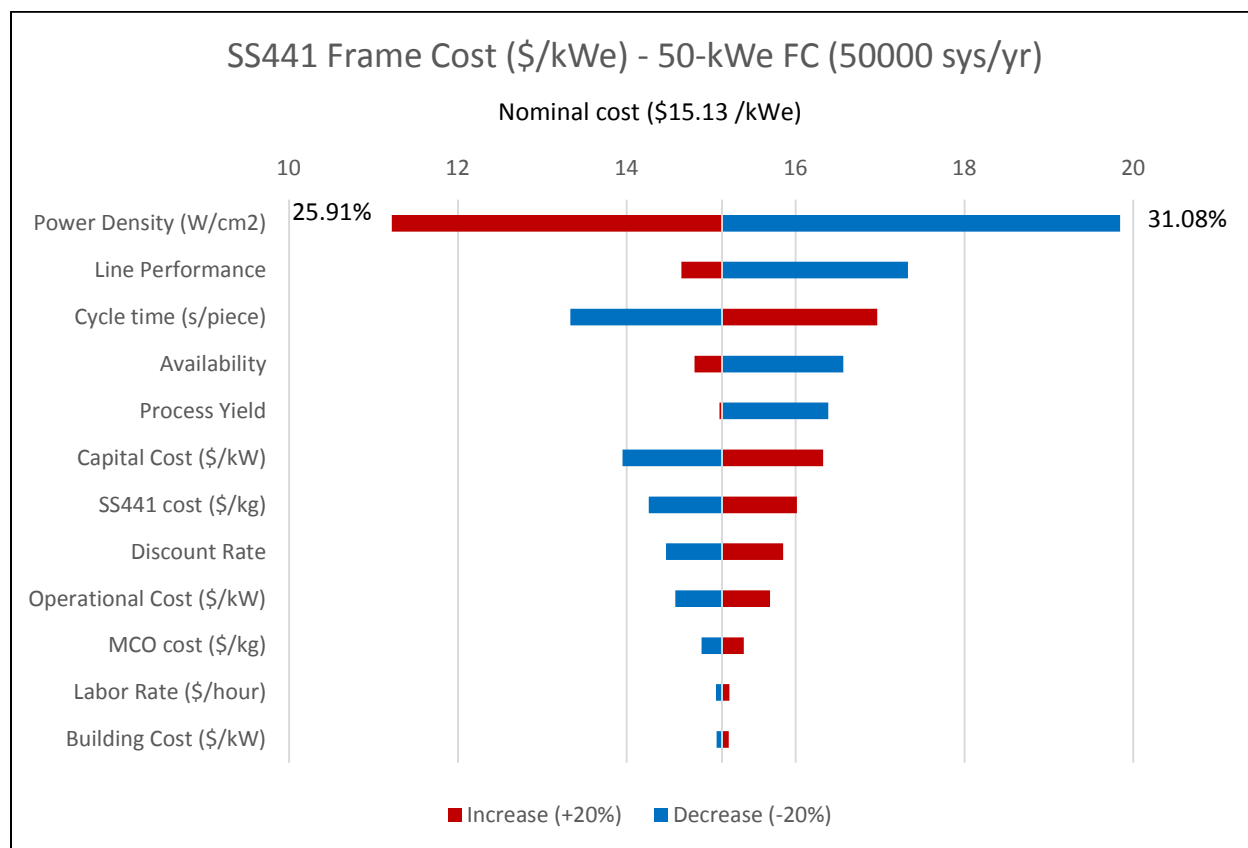
(a)



(b)



(c)



(d)

Figure 4.34. Frame cost sensitivity analysis for 50 kWe system expressed in (\$/kWe) at different annual production rates: a) 100 units/yr; b) 1,000 units/yr; c) 10,000 units/yr; and d) 50,000 units/yr.

4.4. EEA Cell-to-Frame Seal Cost Analysis

Seals provide several critical functions for an SOFC stack: prevention of mixing of fuel and oxidant within the stack and leaking of fuel and oxidant from the stack, electrical isolation of cells in the stack, and providing mechanical bonding of components (Stevenson, 2003). In the window frame cell design (Figure 4.35) the EEA cell is smaller than the interconnect plates, contains no holes and is joined to the metallic window frame which incorporates gas manifolds.

There are two glass sealing steps. In this embodiment, one seal is assumed to be applied during the frame process to seal each cell into its frame in order to form a repeat unit, which can be done piece-by-piece; and one seal sealing step that is assumed to be done during stack assembly to seal all of the repeat units together to form the stack (Weimar, Chick, & Whyatt, 2013).

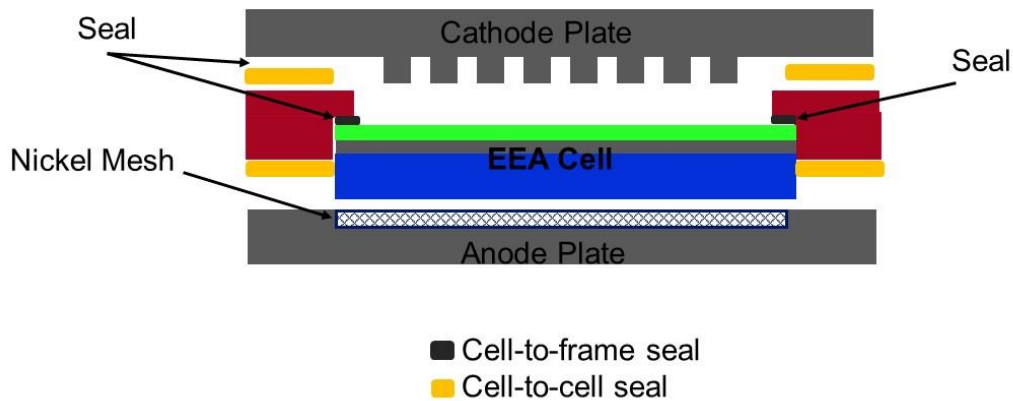


Figure 4.35. Overview of SOFC Seals

SOFC seals can be classified into several types as rigid bonded seals (e.g. glass, glass-ceramics seals and brazes), compressive seals (e.g. metal gasket and mica-based seals) and compliant bonded seals. Each of these seals offers advantages and limitations.

Glass seals are the one most employed in joining planar SOFC since they are stable in the reducing and oxidizing atmosphere, electrically insulating, characterized by a good wetting behavior on YSZ and stainless steel surfaces, and are scalable to low cost, high rate stack production, (Weil S. K., 2006). Among glass seals, alkaline earth aluminosilicate glasses (as barium-calcium-aluminosilicate BCAS based glass) appear to be the best candidates because of their high electrical resistivity, high thermal expansion and rapid crystallization kinetics (Jung, 2013). The disadvantage is their tendency to react chemically with chromia forming alloys and for this reason these seals are effective for short and moderate-term operation.

A promising alternative to glass seals is Ag-CuO braze filler metals with alloying agents added such as TiO₂, aluminum or palladium (Menzler, Tietz, Uhlenbruck, Buchkremer, & Stöver, 2010). Unfortunately, metal brazes are expensive and electrically conductive.

In the case of compressive seals, sealing is obtained when the entire stack is compressively loaded. The load frame required introduces several complexities in the stack design since all stack components must be able to withstand the sealing load. The high cost limits their use.

In this analysis a BCAS glass seal was chosen as a base case since it is the one usually applied for joining steels and mid-temperature SOFC. In addition, an Ag-CuO-Ti metal cell-to-frame seal was also studied and compared to cell-to-frame glass seal cost.

In this chapter cell-to-frame seals costs are analyzed. For cell-to-cell seals cost see chapter 4.5.

Cell-to-Frame Glass Seal

The method of creating a glass seal considered in this study is the one used by PNNL (Weimar, Chick, & Whyatt, 2013):

- 1) Make glass paste using a ball mill (paste composition in Table 4.52)
- 2) Dispense paste onto surface by means of a dispensing robot
- 3) Heat fuel cell components in furnace under a static load (100 to 500 lbs) according to the schedule shown in Table 4.53

Table 4.52. Components of glass seal paste

Components	% in wet paste
Glass powder (VIOX #1716)	69.00%
N-butyl alcohol	18.95%
Polyvinyl Butyral (Butvar B-79)	6.09%
Benzyl n-butyl phthalate	5.28%
Phospholan PS-236 surfactant	0.68%

Table 4.53. Heating schedule for sealing cells into frames

Segment	Rate/Time	Temperature
Ramp	3°C/min	600°C
Ramp	5°C/min	750°C
Hold	1 hour	750°C
Ramp	15°C/min	50°C

Table 4.54 below shows prices of glass seal paste components. Costs vary with order quantity (kg/order). Ceradine VIOX #1716 is now the intellectual property of Battelle. The supplier (3M Advanced Materials Division - Specialty Glass Platform) kindly provided a rough order of magnitude (ROM) estimate (not an official quotation) but did not give the permission to publish prices (similar ROM estimates were found for Akzo Nobel, Univar USA and Dowd & Guild, Inc.).

Table 4.52. Cost of glass seal paste components depending on order quantity

Vendor/Country	Material	Order quantity (kg)	Price (\$/kg)	Comments
Ceradyne Viox, Inc. (Seattle WA)	Glass n° 1716 (B203- BaO-CaO-SiO ₂ - Al ₂ O ₃)	1-4000		
Akzo Nobel Surface Chemistry LLC (Chicago, IL)	Phospholan™ PS-236	1-1000		
Dowd & Guild, Inc. (CA)	Butvar-B79	1-10000		
Fine and Prime Distributors (FIBRID) PTY LTD (South Africa)	N-Butyl Alcohol (purity 99.5%)	1-1000	4-1.8	CIF price
Univar USA	Santicizer 160 (Benzyl n-butyl phthalate)	63.5-5000		

Manual and automatic configurations were included in the analysis for the dispensing process. In the manual dispensing line:

- A worker dispenses the paste on the EEA cell perimeter using a desktop dispensing robot and then places the cell onto the frame
- A worker places a weighted plate onto the cell and load the piece in the furnace

- A worker unloads the furnace

In contrast, the automatic dispensing line includes the following steps:

- Paste is dispensed on the EEA cell perimeter by means of an in-line dispensing robot
- A robot places the cell onto the frame and a weighted plate onto the cell
- A robot loads the piece in the furnace
- A robot unloads the furnace

Table 4.55 show dispensing line costs, consumption and footprint of manual and automatic dispensing lines.

Table 4.53. Costs, consumption and footprint of manual and automatic dispensing lines.

Dispensing line	Manual	Automatic
Dispenser	desktop	in-line
Cost (\$)	3,000	14,000
Consumption (kW)	0.5	2.4
Footprint (m ²)	1	2
Weighted plate positioning onto the cell	manual	in-line
Cost (\$)	0	30,000
Consumption (KW)	0	1.00
Footprint (m ²)	1	1.00

A manual line is chosen for annual production volume $\leq 13,000$ pieces/year and three workers per line are needed. An automatic line needs only a worker in the dispensing line and another worker every four furnaces is needed to check that the module is operating correctly.

The bottleneck here is represented by the furnace cycle time which depends by the heating schedule of the furnace and the residence time of a piece in the furnace. For the heating schedule, an approximate drying time of 330 minutes was estimated.

Maximum conveyor speed and cycle time per part were estimated as:

$$\text{Conveyor speed } \left(\frac{m}{s}\right) = \frac{\text{Furnace length}(m)}{\text{Drying time}(s)}$$

$$\text{Cycle time}(s) = \frac{\text{Piece width}(m)}{\text{Conveyor speed} \left(\frac{m}{s}\right) * \# \text{ of pieces per row}}$$

Four different annealing furnaces were considered (Abbott Furnace). The vendor provided approximate costs (including installation), average consumption and furnace sizes (see Table 4.56).

Table 4.54. Annealing furnaces costs and process parameters

ABBOTT ANNEALING FURNACE	A	B	C	D
Type of load	manual	robotic	robotic	robotic
Conveyor speed (m/min)	0.05	0.09	0.09	0.09
Furnace width (m)	0.32	0.32	0.64	0.92
Furnace length (m)	15	30	30	30
Drying time (min)	330	330	330	330
Piece width (m)	0.28	0.28	0.28	0.28
Piece length (m)	0.28	0.28	0.28	0.28
Cycle time per row (s)	369.6	184.8	184.8	184.8
Pieces per row	1	1	2	3
Cycle time/part (s)	369.60	184.80	92.40	61.60
Furnace consumption (kW)	35	35	67	100
Furnace Cost (\$)	600,000	1,100,000	1,200,000	1,350,000
Furnace Footprint (m2)	27	54	108	150

From the table above it can be observed that furnace sizes vary in length and width allowing different conveyor speeds and numbers of pieces fitting in each row. Piece width and length include approximately 4 cm margin.

As mentioned above, furnace loading can be manual or automatic. In the case of manual loading, two workers are needed. Otherwise it is sufficient to use a robot at both ends of the furnace. The furnace cost includes price of robots and installation. Manual loading was considered only for the small furnace (configuration A) while in the other cases automatic loading was adopted since with high manual cycle time, robot cost and consumption resulted in cheaper parts.

Availability of the line is assumed to be 100% aside from regularly schedule maintenance since the furnace needs to stay on and run 24 hours per day and setup time is 10 minutes per day. Turning it on and off would could cause more problems and cost more to maintain. For this reason, three shifts per day were considered.

Line performance is 99% since the conveyor speed is assumed to be low enough that the effective speed during manufacturing operation is more or less equal to designed speed. The vendor suggested a high value (99.5%) for process yield since paste is dispensed using robot and defective pieces obtained using this kind of furnace process is typically very low.

Furnace configurations were chosen depending on annual production volume as:

- Configuration A for production volumes \leq 13000 pieces/year
- Configuration B for production volumes equal to 65000 pieces/year
- Configuration C for production volumes equal to 130000 pieces/year

- Configuration D for production volumes higher than 130000 pieces/year

Ball mills were sized based on paste quantity to mill per day (kg/day) which depends on the furnace daily production rate. The same ball mill sizes, costs, assumptions and calculations as those used for EEA manufacturing were considered.

The seal dimensions are 5 mm width and 0.2 mm thick. Approximate cell to frame seal mass per piece was estimated as:

$$\text{Seal mass (kg)} = [(EEA \text{ size})^2 - (EEA \text{ size} - \text{seal width} * 2)^2] * \text{seal thickness} * \text{paste density}$$

where glass paste equivalent density is 2.98 kg/cm³.

Under these assumptions, it was possible to evaluate the following:

$$\frac{\text{Max \# of sealed pieces}}{\text{line} * \text{year}} = \frac{\left[\frac{\text{op. hours}}{\text{day}} - \frac{\text{setup time}}{\text{day}} \right] * 3600 \left(\frac{s}{\text{day}} \right) * \text{Ann. op. days} * \text{line availability}}{\frac{\text{cycle time (s)}}{\text{Line performance}}}$$

$$\# \text{ of lines} = \frac{\frac{\text{EEA required}}{\text{year}}}{\frac{\text{Process Yield}}{\frac{\text{Max \# of sealed pieces}}{\text{line} * \text{year}}}}$$

$$\text{Line utilization (\%)} = \frac{\frac{\text{EEA required}}{\text{year}}}{\frac{\text{Process Yield}}{\frac{\text{max \# of sealed pieces}}{\text{line} * \text{year}}}} * \# \text{ of lines}$$

$$\text{Annual operating hours} = \frac{\text{EEA required}}{\text{year}} * \frac{\text{cycle time (s)}}{\text{Line performance}}$$

$$\text{Labor cost} \left(\frac{\$}{\text{year}} \right) = \left[(\text{Annual op. hours} \left(\frac{\text{hr}}{\text{yr}} \right) + \text{setup} \left(\frac{\text{hr}}{\text{yr}} \right)) \right] * \frac{\# \text{ of workers}}{\text{line}} * \text{labor rate} \left(\frac{\$}{\text{hr}} \right)$$

Table 4.57 show machine rate results in case of 50-kWe systems for all production volumes.

Table 4.55. Machine rate for cell-to-frame sealing process

System Size (kWe)	50			
Systems/year	100	1000	10000	50000
EEA cells/year	65000	650000	6500000	32500000
Shift Size (hours)	24	24	24	24
# of Lines	1	2	20	99
Line Configuration	B	D	D	D
Cycle Time (s)	184.80	61.60	61.60	61.60
Line Utilization (%)	58.92%	98.20%	98.20%	99.19%
Annual operating hours (h)	3387	11291	112910	564551
Setup time (hours/year)	24	79	789	3946
# of Workers	2	3	25	124
Line production capacity (pieces/year/line)	110871	332614	332614	332614
Total Consumption (kW)	39.20	207.60	2073.00	10248.60
Total Footprint (m2)	66.00	315.00	3086.00	15191.00
Operating Labor Cost (\$/year)	2.03E+05	5.08E+05	4.24E+06	2.12E+07
Auxiliary Costs Factor	0	0	0	0
Initial Capital (\$)	1.15E+06	2.79E+06	2.79E+07	1.38E+08
Annual Depreciation (\$/yr)	7.48E+04	1.82E+05	1.82E+06	9.02E+06
Annual Cap Payment (\$/yr)	1.30E+05	3.17E+05	3.16E+06	1.57E+07
Auxiliary Costs (\$/yr)	8.00E+00	9.00E+00	1.00E+01	1.10E+01
Maintenance (\$/yr)	1.30E+04	3.17E+04	3.16E+05	1.57E+06
Salvage Value (\$/yr)	4.38E+02	1.07E+03	1.07E+04	5.27E+04
Energy Costs (\$/yr)	1.66E+04	1.46E+05	1.46E+06	7.29E+06
Property Tax (\$/yr)	4.77E+03	1.16E+04	1.16E+05	5.74E+05
Building Costs (\$/yr)	9.67E+03	4.61E+04	4.52E+05	2.23E+06
Interest Tax Deduction (\$/yr)	0.00E+00	0.00E+00	0.00E+00	0.00E+00
Machine Rate (\$/h)	51.23	48.80	48.69	48.29
Capital	38.25	27.94	27.93	27.65
Variable	8.73	15.75	15.73	15.68
Building	4.26	5.11	5.03	4.96

Cell-to-Frame glass seal cost results

Table 4.58 display the final results for glass cell-to-frame costs in (\$/kWe) and (\$/part) for all system sizes and production volumes.

Table 4.56. Cell-to-frame sealing process cost in (\$/kWe) and (\$/part) at all production volumes

Equivalent Power (MWe/year)	EEA cells/year	Cost (\$/kWe)	Cost (\$/seal)
0.1	1,300	969.82	74.60
1	13,000	217.22	16.71
5	65,000	78.87	6.07
10	130,000	44.13	3.39
25	325,000	27.25	2.10
50	650,000	23.24	1.79
100	1,300,000	21.3	1.64
250	3,250,000	21.58	1.66
500	6,500,000	21.23	1.63
1,000	13,000,000	21.23	1.63
2,500	32,500,000	21.16	1.63
5,000	65,000,000	21.13	1.63
12,500	162,500,000	21.09	1.62

It can be observed that cost decreases with annual production volume and is constant for each cumulative global produced power (MWe/year). At low volumes the high price is due to the high equipment cost and low utilization rate. At the highest volumes, the cost converges to \$1.62/seal. A cost summary related to 10-kWe and 50-kWe systems is shown in Table 4.59 and Table 4.60, respectively.

Table 4.57. Cell-to-frame sealing process cost breakdown in (\$/kWe) for 10-kWe systems

System Size (kWe)	10			
	100	1,000	10,000	50,000
Production Volume (Units/yr)	100	1,000	10,000	50,000
Direct Material (\$/kWe)	5.73	3.00	1.80	1.76
Labor (\$/kWe)	122.02	20.34	8.47	8.47
Process: Capital (\$/kWe)	68.37	14.09	6.31	6.31
Process: Operational (\$/kWe)	12.99	4.42	3.56	3.55
Process: Building (\$/kWe)	8.08	2.28	1.15	1.14
Scrap (\$/kWe)	0.03	0.02	0.01	0.01
Total (\$/kWe)	217.22	44.13	21.30	21.23

Table 4.58. Cell-to-frame sealing process cost breakdown in (\$/kWe) for 50-kWe systems

System Size (kWe)	50			
Production Volume (Units/yr)	100	1,000	10,000	50,000
Direct Material (\$/kWe)	3.47	2.04	1.76	1.75
Labor (\$/kWe)	40.67	10.17	8.47	8.49
Process: Capital (\$/kWe)	25.91	6.31	6.31	6.24
Process: Operational (\$/kWe)	5.91	3.56	3.55	3.54
Scrap (\$/kWe)	2.89	1.16	1.14	1.12
Process: Building (\$/kWe)	0.02	0.01	0.01	0.01
Total (\$/kWe)	78.87	23.24	21.23	21.16

Labor cost dominates at all volumes above 1300 EEA cells/year, followed by capital cost, operational cost, material cost, building cost and scrap cost (Figure 4.36). The relative percentage of labor cost to total cost varies from 40 to 56% above 1300 EEA cells/year. This is related to:

- high cycle time (and thus a high number of annual operating hours required to guarantee the annual production rate)
- a production shift of 24 hours a day (instead of 16 hours a day) which allows a reduction in the number of furnaces required and the required capital cost.

Material costs constitute only 3-9% of the total cost at these production volumes.

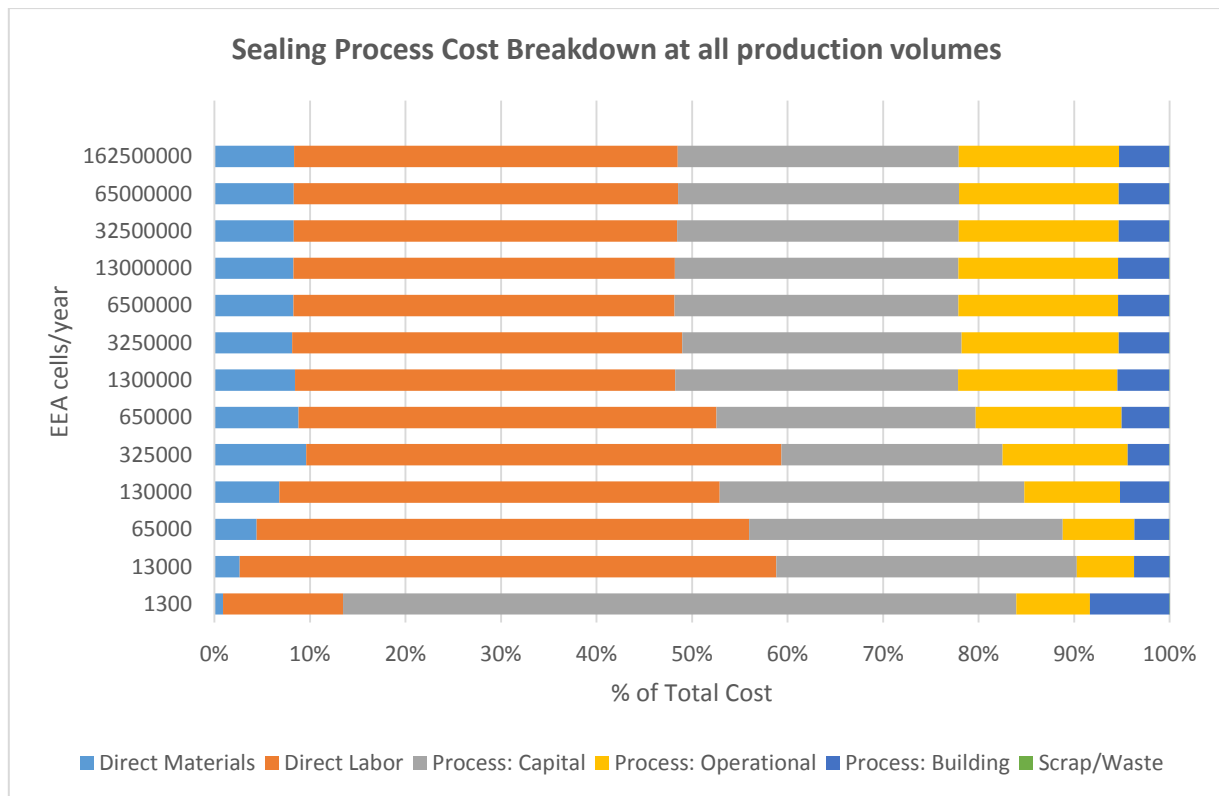


Figure 4.36. Sealing process cost breakdown at all production volumes

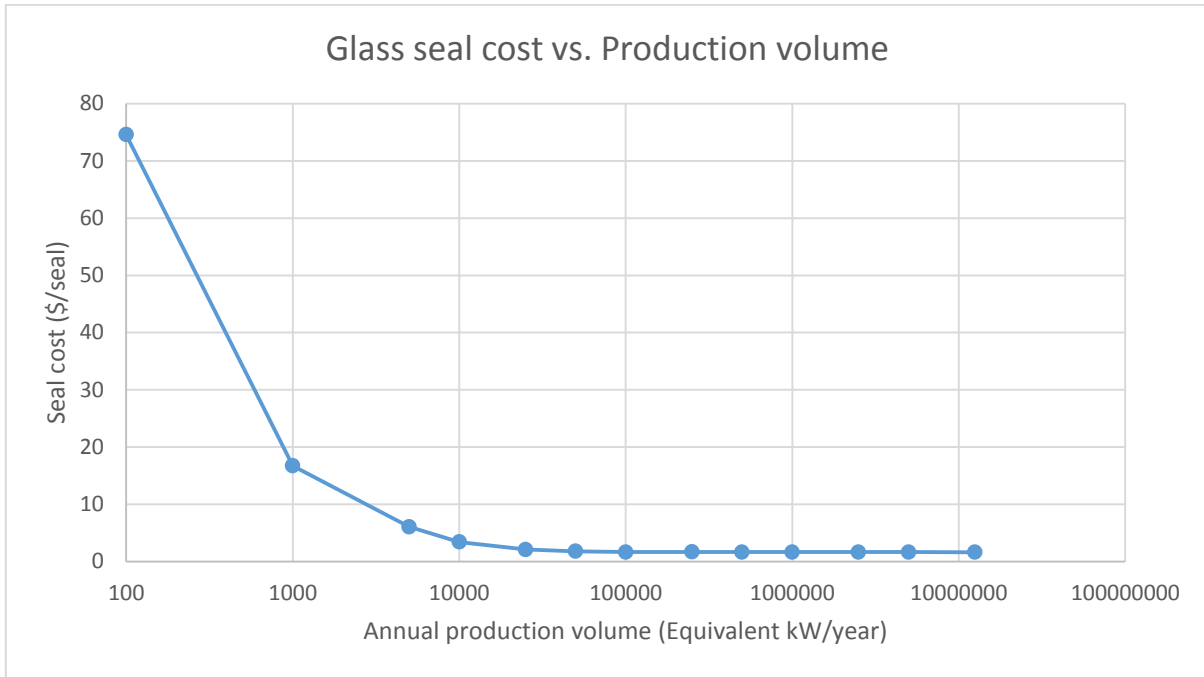


Figure 4.37. Glass seal cost in (\$/seal) with respect to annual equivalent production volume

It is also interesting to notice that for value of annual production volume higher than 50 MWe the seal manufacturing cost tends to remain constant around \$1.63/seal (see Figure 4.37). This is because same manufacturing equipment is used and material cost does not vary since material prices (\$/kg) reach the lowest values provided by suppliers.

Cell-to-Frame Metal Seal

The method of creating a metal seal chosen as reference is the one used by (Weil, Coyle, Darsell, Xia, & Hardy, 2005) and (Yong, Hardy, & Weil, 2005).

The metal seal is 95.5% by mol Ag, 4% by mol Cu, and 0.5% by mol TiH₂. It is formed via air brazing. The complete process of forming the metal seal is outlined below:

- 1) Ball Mill Cu, Ag, and Titanium Hydride into Powder
- 2) Mix powder with B75717 Ferro Corp at 1:1 weight ratio to form paste
- 3) Dispense paste onto surface by means of a dispensing robot
- 4) Heat fuel cell components in furnace under a static load (100 g) according to the schedule shown in Table 4.61

Table 4.59. Heating schedule for sealing cells into frames

Segment	Rate/Time	Temperature
Ramp	10°C/min	1000°C
Hold	15 min	1000°C
Ramp	15°C/min	15°C

Table 4.62 shows prices of metal seal paste components. CIF costs (insurance and freight costs) vary with order quantity (kg/order).

Table 4.60. Cost of metal seal paste components depending on order quantity

Vendor/Country	Material	Order quantity (kg)	Price (\$/kg)	Comments
Luoyang Tongrun info technology Co.,Ltd (China)	Ag nano powder (purity 99.9%,particle size 100 nm)	10	775	CIF price
		100	765	CIF price
		1000	752	CIF price
		10000	745	CIF price
CNPC Powder Group Co.,Ltd (China)	Cu powder (purity 99.5%,300 mesh)	100	13	CIF price
		1000	10.7	CIF price
		10000	9.8	CIF price
Guangzhou Jiechuang Trading Co., Ltd. (China)	TiH2 powder (purity 99.5%,particle size 1-3 um)	1	350	CIF price
		10	300	CIF price
		100	250	CIF price
		1000	200	CIF price
Ferro Corporation (Ohio)	Polymer binder (B75717)	Contact Ferro Corp. for a current price quote		

The seal dimensions are the same of glass seal. Metal paste equivalent density is 1.72 kg/cm³. The same configurations as glass seal paste were used for paste dispensing lines, ball mills and furnaces. The only difference is in the cycle time since approximate total brazing time is about 312 minutes.

Table 4.61 summarizes cycle time and furnace parameters for each configuration while Table 4.62 shows estimated machine rates in the case of 50-kWe systems for all production volumes.

Table 4.61. Brazing furnaces costs and process parameters

Abbott Furnace	A	B	C	D
Type of load	manual	robotic	robotic	robotic
Conveyor speed (m/min)	0.05	0.10	0.10	0.10
Furnace width (m)	0.32	0.32	0.64	0.92
Furnace length (m)	15	30	30	30
Drying time (min)	315	315	315	315
Piece width (m)	0.28	0.28	0.28	0.28
Piece length (m)	0.28	0.28	0.28	0.28
Cycle time per row (s)	352.8	176.4	176.4	176.4
Pieces per row	1	1	2	3
Cycle time/part (s)	352.80	176.40	88.20	58.80
Furnace consumption (KW)	35	35	67	100
Furnace Cost (\$)	600,000	1,100,000	1,200,000	1,350,000
Furnace Footprint (m2)	27	54	108	150

Table 4.62. Machine rate for cell-to-frame brazing process

System Size (kWe)	50			
	100	1,000	10,000	50,000
Systems/year	100	1,000	10,000	50,000
Cells/year	65,000	650,000	6,500,000	32,500,000
Shift Size	24	24	24	24
# of Lines	1	2	19	95
Line	B	D	D	D
Cycle Time (s)	176.40	58.80	58.80	58.80
Line Utilization (%)	56.53%	94.21%	99.17%	99.17%
Annual operating hours (h)	3,233	10,778	107,778	538,890
Setup time (hours/year)	23	75	753	3767
# of Workers	3	3	24	119
Operating Labor Cost	0.00	0.00	0.00	0.00
Production Capacity (pieces/year/line)	115,567	346,702	346,702	346,702
Total Consumption	37.30	207.60	1,967.30	9,830.50
Total Footprint	65.00	315.00	2,928.00	14,567.00
Auxiliary Costs Factor	0	0	0	0
Initial Capital (\$)	1.13E+06	2.79E+06	2.65E+07	1.32E+08
Annual Depreciation (\$/yr)	7.41E+04	1.82E+05	1.73E+06	8.65E+06
Annual Cap Payment (\$/yr)	1.80E+05	4.43E+05	4.21E+06	2.10E+07
Auxiliary Costs (\$/yr)	8.00E+00	9.00E+00	1.00E+01	1.10E+01
Maintenance (\$/yr)	1.29E+04	3.17E+04	3.01E+05	1.50E+06
Salvage Value (\$/yr)	4.33E+02	1.07E+03	1.01E+04	5.06E+04
Energy Costs (\$/yr)	0.00E+00	0.00E+00	0.00E+00	0.00E+00
Property Tax (\$/yr)	4.72E+03	1.16E+04	1.10E+05	5.51E+05
Building Costs (\$/yr)	0.00E+00	0.00E+00	0.00E+00	0.00E+00
Interest Tax Deduction (\$/yr)	0.00	0.00	0.00	0.00
Machine Rate (\$/h)	61.05	45.03	42.77	42.76
Capital	55.61	41.02	38.95	38.95
Variable	3.98	2.94	2.79	2.79
Building	1.46	1.08	1.02	1.02

Cell-to-Frame metal seal cost results

On the next page Table 4.65 displays the final results for metal cell-to-frame costs in (\$/kWe) and (\$/part) for all system sizes and production volumes. Table 4.66 and Table 4.67 show sealing process cost breakdown for system sizes of 10 and 50 KWe respectively.

Table 4.63. Cell-to-frame sealing process cost in (\$/kWe) and (\$/part) at all production volumes

Equivalent Power (MWe/year)	EEA cells/year	Cost (\$/kWe)	Cost (\$/seal)
0.1	1,300	963.14	74.09
1	13,000	214.02	16.46
5	65,000	100.41	7.72
10	130,000	47.64	3.66
25	325,000	31.2	2.40
50	650,000	28.02	2.16
100	1,300,000	26.37	2.03
250	3,250,000	26.69	2.05
500	6,500,000	26.03	2.00
1,000	13,000,000	26.02	2.00
2,500	32,500,000	25.95	2.00
5,000	65,000,000	25.92	1.99
12,500	162,500,000	25.88	1.99

Table 4.64. Cell-to-frame sealing process cost breakdown in (\$/kWe) for 10-kWe systems

System Size (kWe)	10			
Production Volume (Units/yr)	100	1,000	10,000	50,000
Direct Material (\$/kWe)	8.46	7.80	7.39	7.37
Labor (\$/kWe)	116.47	19.41	8.09	8.17
Process: Capital (\$/kWe)	68.25	13.94	6.30	5.98
Process: Operational (\$/kWe)	12.71	4.20	3.42	3.38
Process: Building (\$/kWe)	8.08	2.26	1.14	1.08
Scrap (\$/kWe)	0.04	0.04	0.04	0.04
Total (\$/kWe)	214.02	47.64	26.37	26.03

Table 4.65. Cell-to-frame sealing process cost breakdown in (\$/kWe) for 50-kWe systems

System Size (kWe)	50			
Production Volume (Units/yr)	100	1,000	10,000	50,000
Direct Material (\$/kWe)	8.08	7.40	7.37	7.37
Labor (\$/kWe)	58.24	9.71	8.17	8.11
Process: Capital (\$/kWe)	25.62	6.30	5.98	5.98
Process: Operational (\$/kWe)	5.58	3.42	3.38	3.38
Scrap (\$/kWe)	2.85	1.16	1.08	1.07
Process: Building (\$/kWe)	0.04	0.04	0.04	0.04
Total (\$/kWe)	100.41	28.02	26.03	25.95

Capital cost is the highest value only for production of 0.1 MWe per year because of the high equipment investment. At higher volumes labor costs always constitute the largest contribution to total cost (see Figure 4.38). Materials costs gain in importance with volume and are the second highest cost element at a production volume equal to 25 MWe. The fraction of total cost due to materials cost increases with volume from 1% to 29%.

As in the case of glass seals, for production higher than 50 MWe the cost tends to remain constant around a value of \$2 per seal. The percentage of material cost to total cost at this production volume is 28.5%, the percentage of labor cost to total cost is equal to 31.5%, and the percentage of capital cost relative to total cost is 23%.

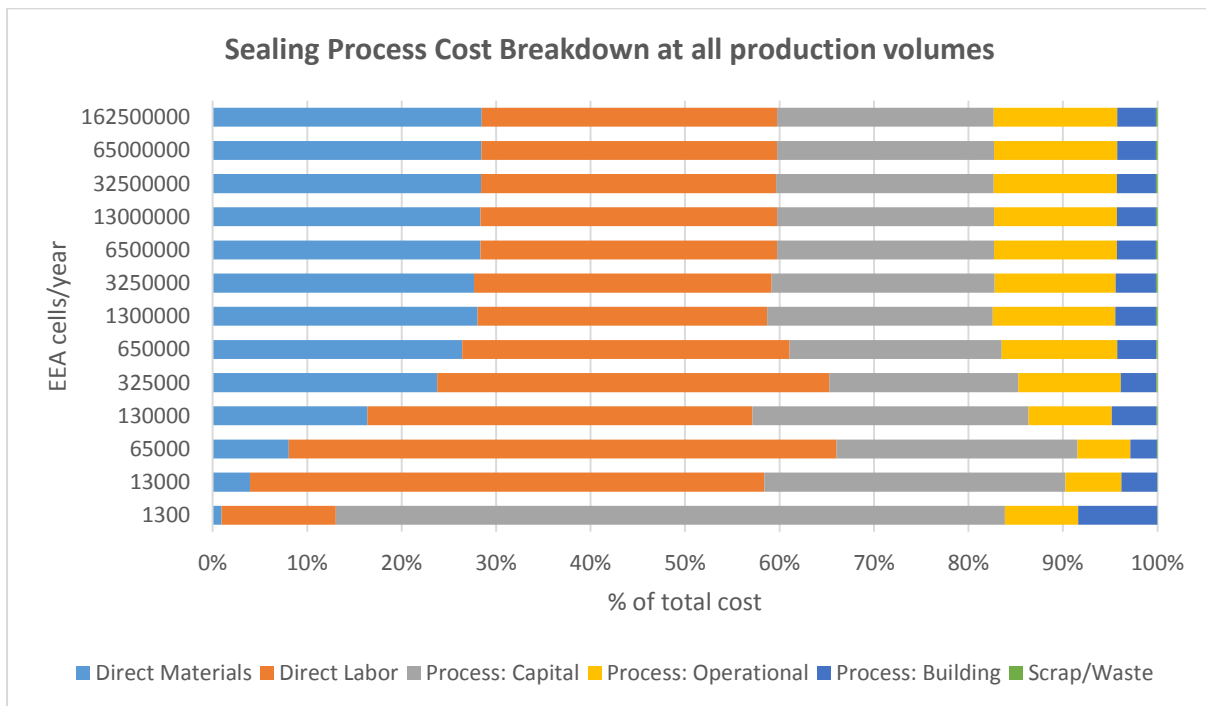


Figure 4.38. Sealing process cost breakdown at all production volumes

Cost comparison between Glass seal and Metal seal

At low volumes (0.1 and 1 MWe/year) the glass seal option was found to be more expensive even though the glass paste cost is cheaper than silver cost. This is related mainly to the higher cycle time and thus a higher labor cost (see Figure 4.39).

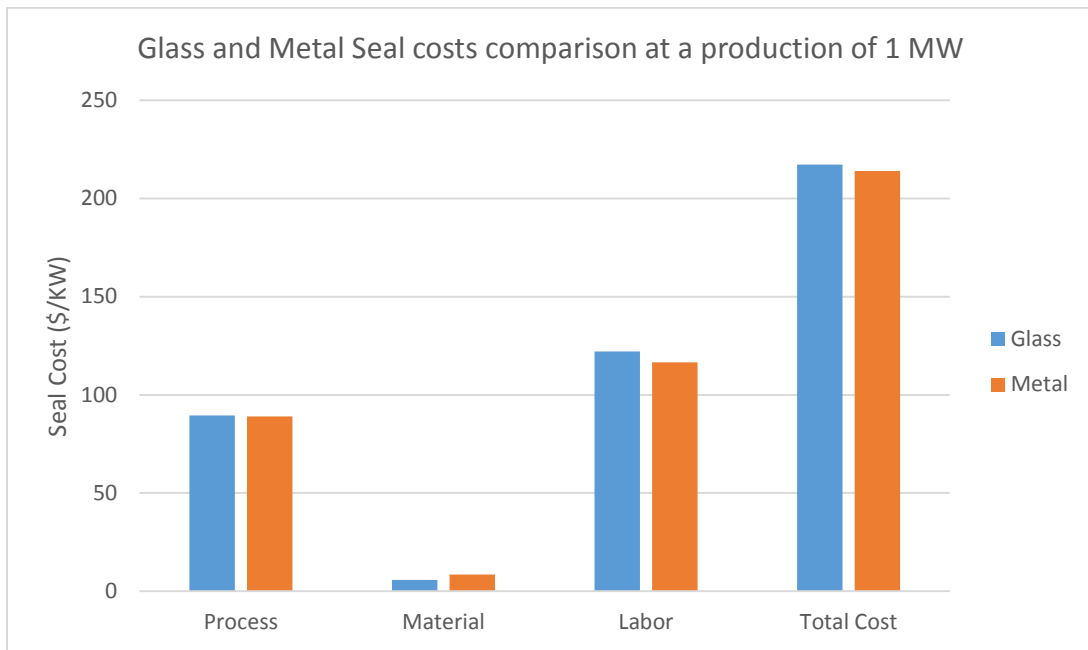


Figure 4.39. Seals cost comparison in (\$/kWe) for an annual equivalent production of 1 MWe

Figure 4.40 compares the two alternatives for production volumes higher than 1 MWe. As shown, the glass seal cost is lower than the metal seal cost. The cost difference between the two alternatives varies from 7% to 19% depending on production volume and furnaces used.

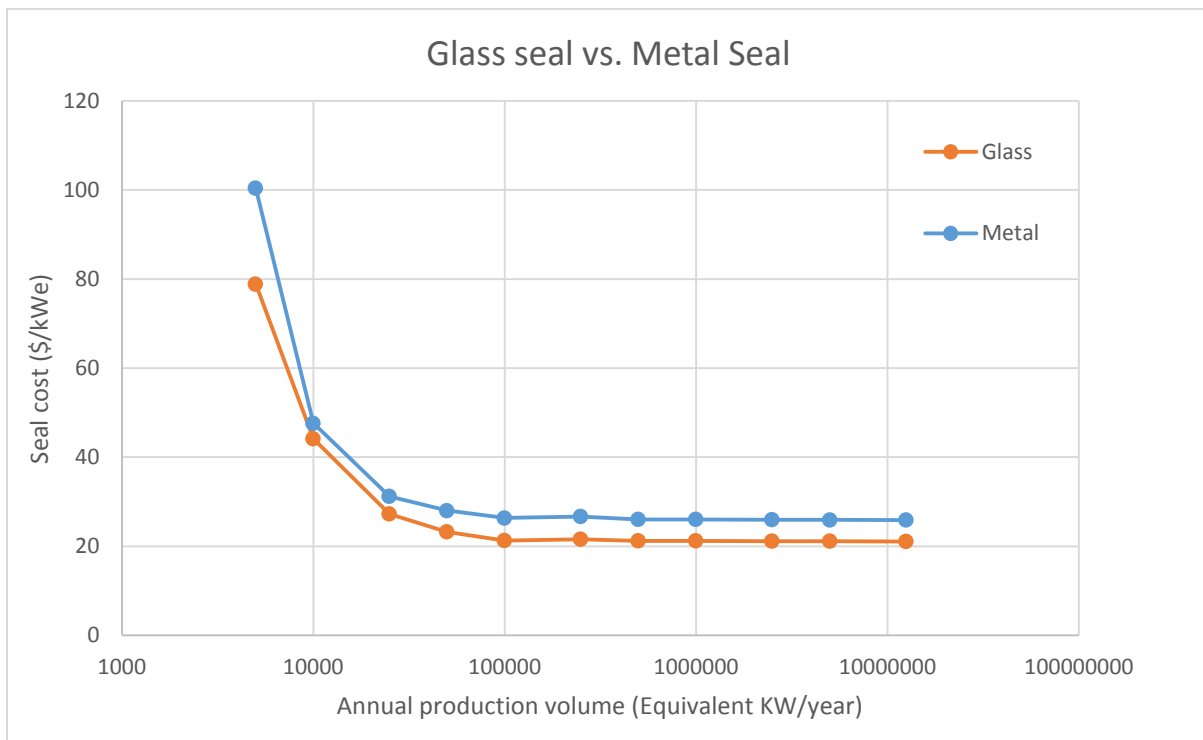


Figure 4.40. Glass seal cost vs. metal seal cost in (\$/kWe) for production volumes greater than 1MWe.

Figure 4.41 shows processing, material and labor costs for both glass and metal seals manufacturing process to better understand the differences in costs. Metal seal processing and labor costs are lower than for the glass seal because the metal brazing process is characterized by a smaller cycle time and thus lower consumption and manual labor.

Material cost is higher in the case of brazed seal because of the high cost of silver powder.

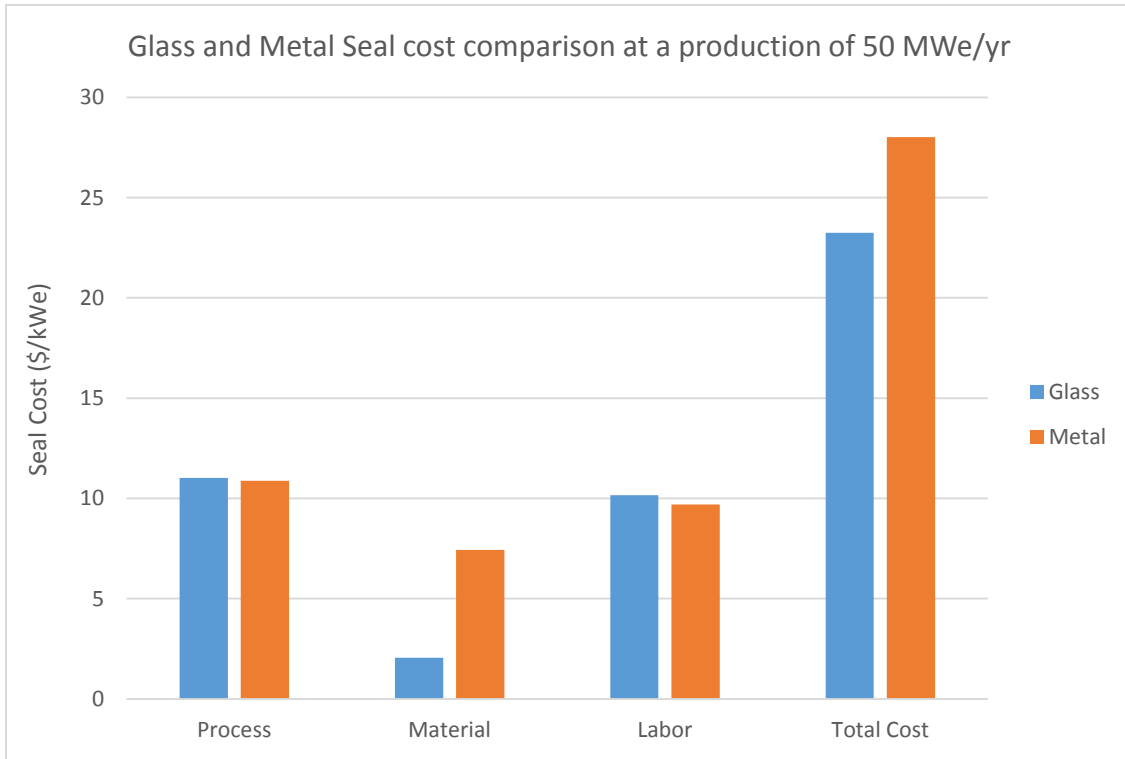
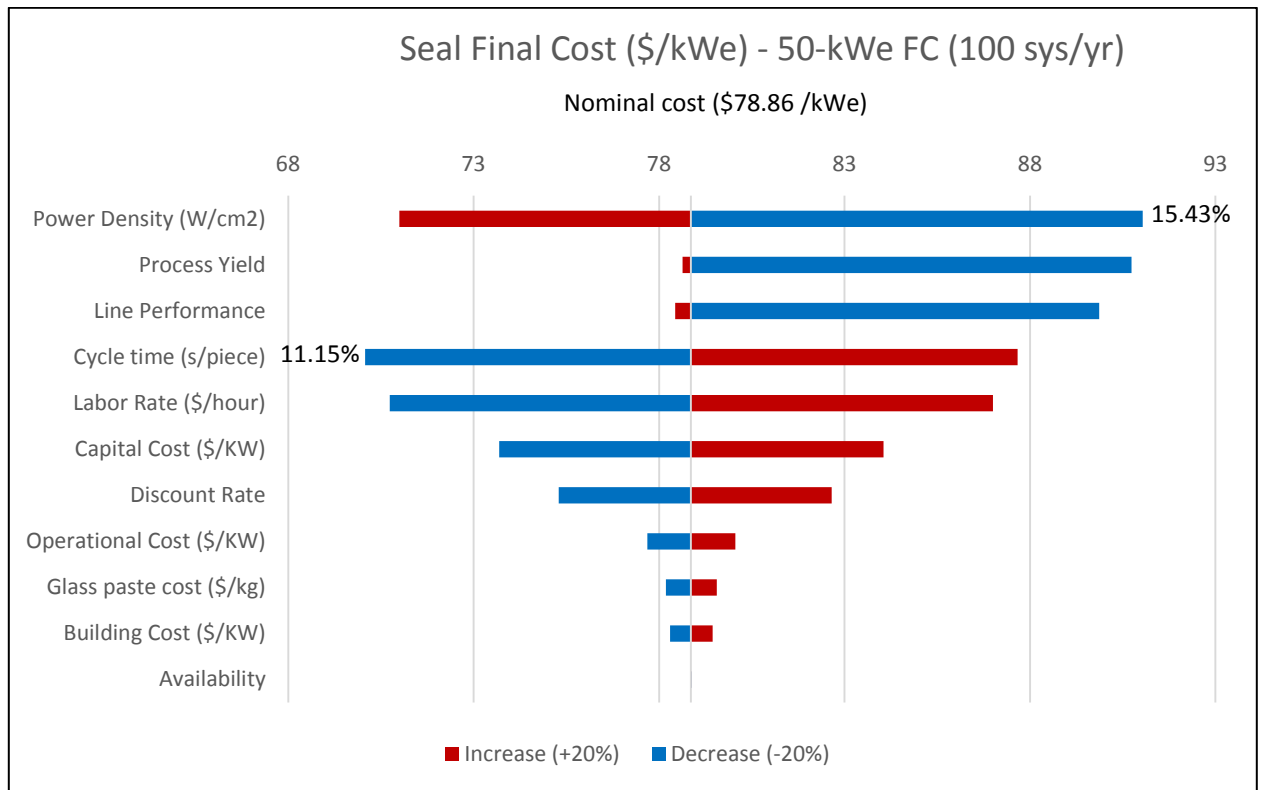


Figure 4.41. Glass and brazed seals cost comparison for an equivalent annual production of 50 MWe

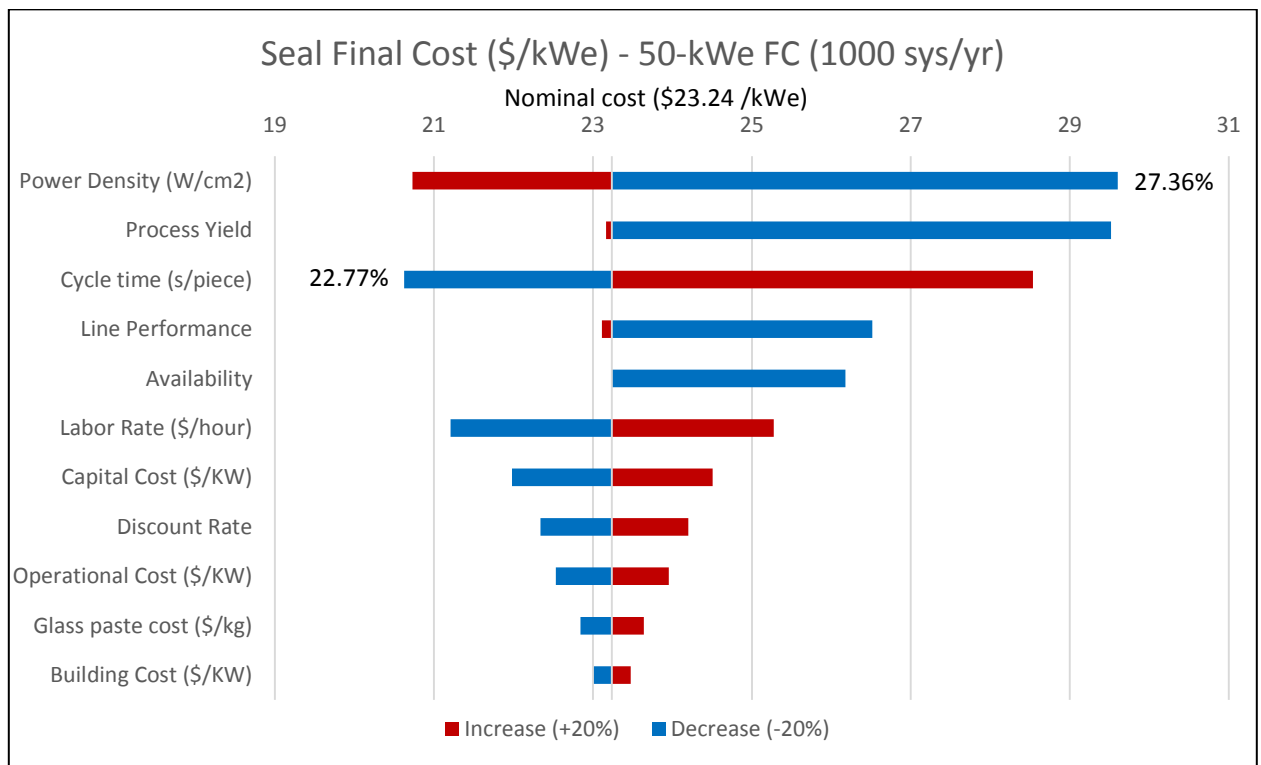
Sensitivity Analysis for Cell-to-frame Glass Seal Cost

Sensitivity analysis was performed for 50-kWe systems at all production volumes (as shown in Figure 4.42). The impact to the cost in \$/kW is calculated for a ±20% change in the sensitivity parameter being varied.

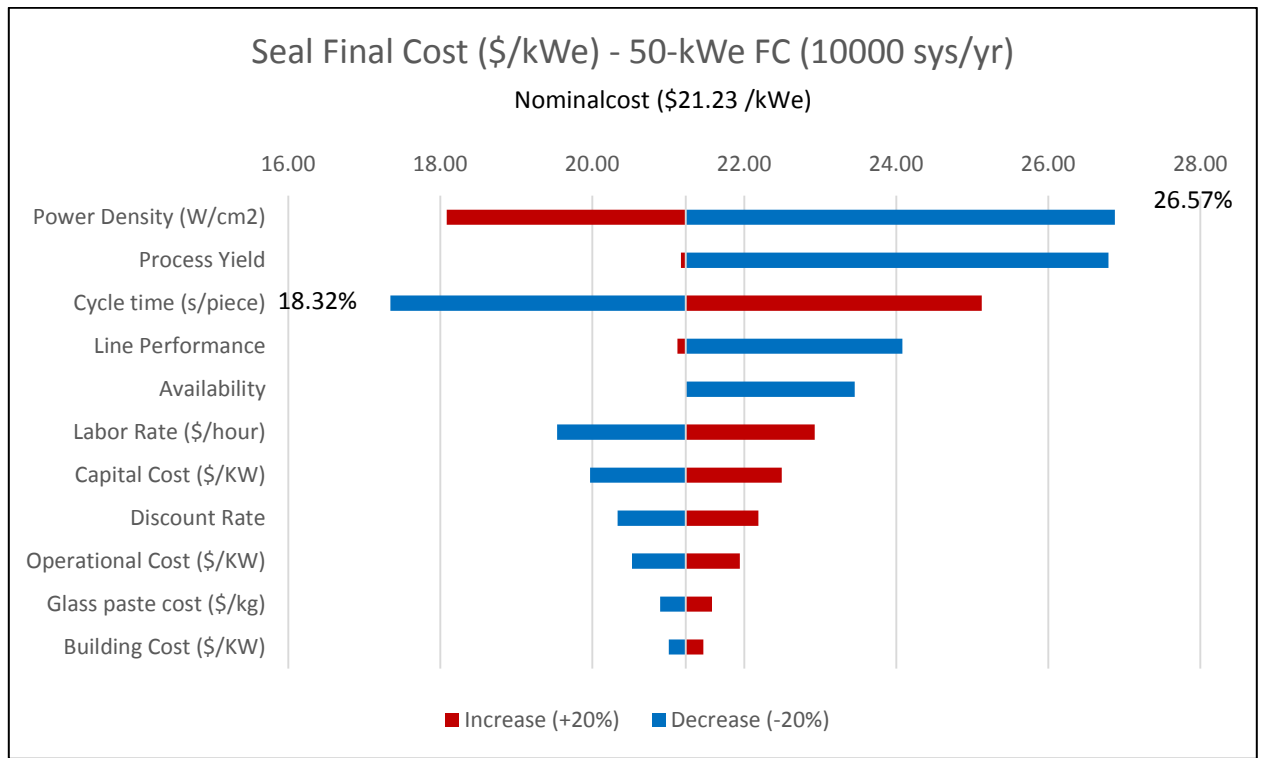
Cycle time is the parameter that causes the largest cost decrease at all volumes, followed by power density and labor rate. This result is expected given the high value of cycle time. The biggest cost increase is caused by a decrease of power density followed by process yield. Other important factors affecting the sensitivity are line performance and labor rate.



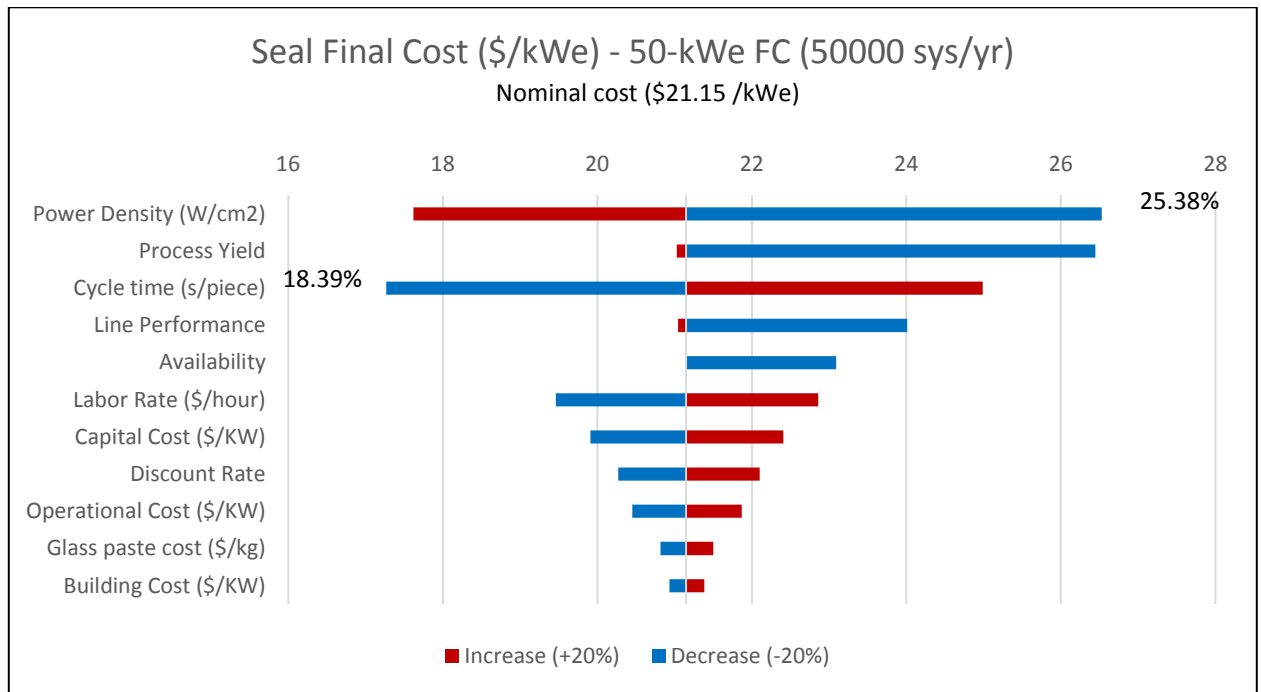
(a)



(b)



(c)



(d)

Figure 4.42. Glass seal cost sensitivity analysis for 50-kWe system expressed in (\$/kWe) at different annual production rates: a) 100 units/yr; b) 1,000 units/yr; c) 10,000 units/yr; and d) 50,000 units/yr.

4.5. Stack Assembly and Testing Analysis

Process Flow and Considerations

The repeat cell units are stacked up on a cast steel manifold in a frame. A current collector or end plate is attached to both ends of each stack (Weimar, Chick, & Whyatt, 2013). Then the stack is pressed, repeats units are bound with metallic compression bands and finally power electronics, sensors and stack housing are added. Following assembly the stack is moved to a condition and testing station. The number of repeat units depends on the electrical and thermal characteristics and electrical power output of the fuel cell stack, which determines the fuel cell system size.

Glass sealing paste is applied between the cells and the interconnect plates during the stack assembly process to form an initial cohesive bond. During the subsequent stack assembly heating and reduction process, the organic components burn out, leaving the electrically conductive materials bonded to the cells and interconnects, thus providing a good electrical connection between the cell and interconnect layer while maintaining a strong adhesive bond. The bonding material further provides the required mechanical strength and integrity for the cells and interconnects at nominal stack operating temperatures (Rehg, Guan, Montgomery, Verma, & Lear, 2007).

Figure 4.43 below shows a simple stack assembly process flow for SOFC using semi-automatic assembly line, while Table 4.68 summarizes the estimated time for each step in this assembly process.

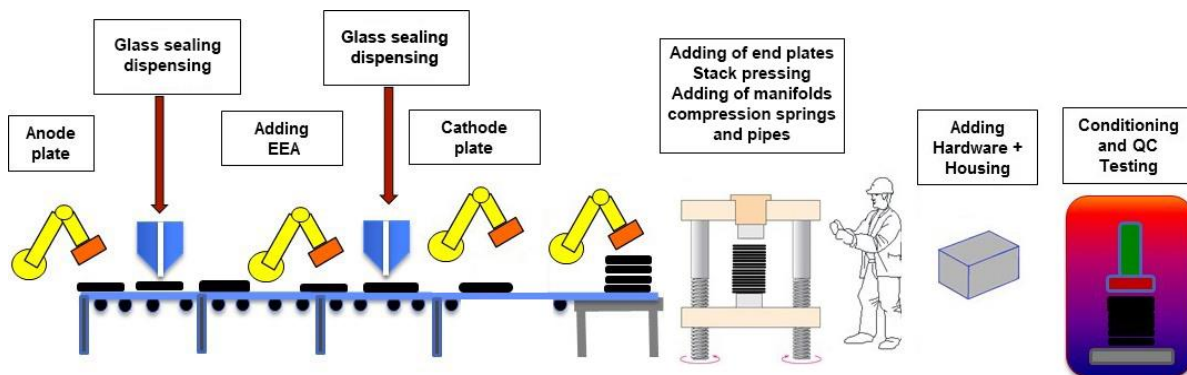


Figure 4.43. Process flow showing the main steps in the SOFC stack assembly process

Table 4.66. Estimated process time for SOFC stack assembly

Operation	Cycle Time (s)	Manual/Automatic
Feeding anode plate into the system	5	Robot
Adding nickel mesh	5	Robot
Glass sealing dispensing	6	Robot
Adding EEA	2	Robot
Glass sealing dispensing	6	Robot
Adding cathode plate	5	Robot
Pressing of the whole stack and adding end plates and compression springs etc.	120	Robot
Add Power Electronics; hosing and sensors	<i>variable</i>	Manual
Adding Stack Housing	20	Manual
Conditioning and Testing	16-24 hours	Automatic

Because of the brittle nature of the EEAs which makes them weak when subjected to tensile loads, springs are often used to apply compressive load on the repeat unit at all times (Norsk, Olsen, Nielsen, & Erikstrup, 2008). This can be achieved by using a load frame with mechanical springs that can provide compression to the stacks during assembly and operation (see Figure 4.44). A stack assembly load frame includes a base plate for supporting the stack, a moveable spring holder above the stack, a retaining plate above the spring holder, and tie rods to maintain the post-sintered spacing. Another advantage of the springs is that they can minimize effect of the coefficient of thermal expansion (CTE) mismatch by reducing the amount of trapped air between repeat units.

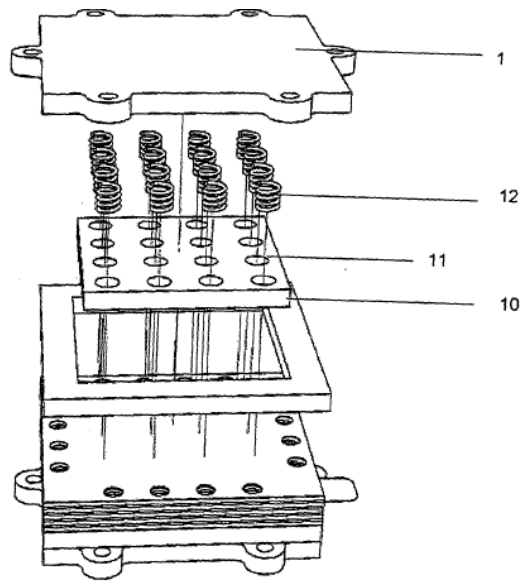


Figure 4.44. Compression assembly for SOFC stack using springs (Norsk et al., 2007)

Three main characteristics should be monitored in the quality checking process (Richards, Tang, & Petri, 2011): 1) physical properties such as dimensions, density or porosity, flatness, uniformity and discontinuity; 2) chemical properties like compositions, phases and impurities; and finally 3) electrochemical properties. A vacuum leak test is performed during this stage. Quality checking is usually performed at both EEA cell level and stack level. Optical and infrared thermography is usually used to measure the thickness of the EEA layers. Leak test, fuel utilization and electrochemical acceptance testing are usually performed at the stack level during stack condition and testing process (see Figure 4.45 for an example of the SOFC testing and conditioning unit).

For example, the anode is supplied with a mixture of 50% H₂ and 50% N₂ (or mixture of reformat fuel) and an I-V curve and a fuel utilization curve are taken. Some SOFC manufacturers also perform other electrochemical analyses in some units in order to see the effect of thermal cycling on the durability and voltage degradation of the systems (Borglum B. , 2009). In this test the stack is heated up to 750°C and then cooled down to <150°C. Figure 4.45 below shows an example of the block diagram of a SOFC power-conditioning system (PCS) as described in (Mazumder, Acharya, & Haynes, 2004).

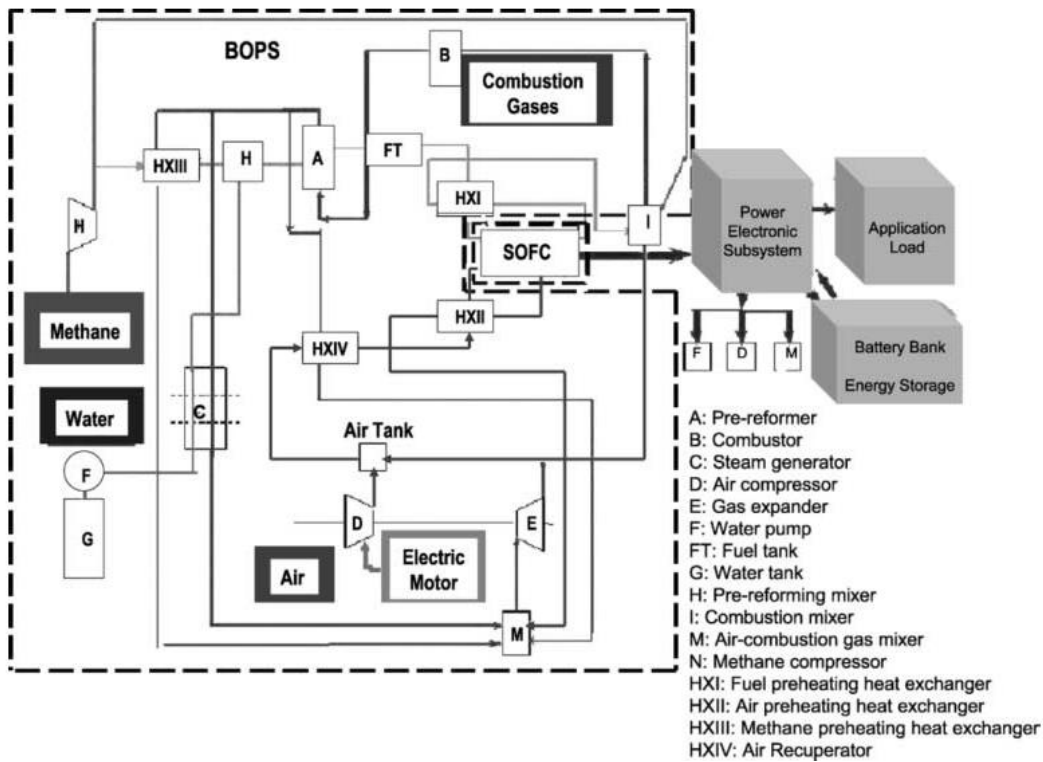


Figure 4.45. Block diagram of a SOFC power-conditioning system (PCS). It shows the solid-oxide fuel cell (SOFC) stack, the power-electronics subsystem (PES) and application load (AL), and the balance of plant subsystem (BOP)(Mazumder, Acharya, & Haynes, 2004)

Stack Assembly Lines Process Parameters

Stack assembly costs were based on the amortized workstation costs and the estimated times to perform the required assembly process. Three designs of stack assembly were analyzed: manual, semi-automated and fully automated.

The selection of assembly line type is based on the number of EEAs assembled annually. In this study the following design options were chosen: if the number of EEAs per year is less than 100k units then manual assembly is utilized; when the number of EEAs falls between 100k and 600k units a semi-automated line is utilized; and when there are more than 600k EEAs then an automated assembly line is installed (Wei, Lipman, Mayyas, Chien, & Chan, 2014).

The level of automation was chosen based on industry inputs and the judgment of the research team for manual and semi-automated assembly lines. Manual assembly consists of workers using their hands to individually acquire and place each element of the stack (cell registration). An entire stack is assembled at a single workstation. The worker sequentially builds the stack (vertically) and then binds the cells with metallic compression bands or tie rods. The finished stacks are removed from the workstation by conveyor belt (James, Spisak, & Colella, 2012).

At higher production levels (100-600k EEA's), stack assembly is semi-automatic, requiring less time and labor and ensuring superior quality control. This is termed "semi-automatic" because the end components (end plates, current conductors, and initial cells) are assembled manually.

A fully automated assembly line is strongly indicated for very high production volumes which exceed 600,000 EEAs per annum in order to reduce assembly time and to have better quality fuel cell stacks (Wei, Lipman, Mayyas, Chien, & Chan, 2014). Table 4.69 below summarizes the proposed selection of assembly line, which is based on industry assessment and engineering estimates.

Table 4.67. Estimated capital cost estimates for several assembly lines.

No. of EEA cells	Assembly line type	Initial capital cost estimate (\$)	No. of workers per line
<100k	Manual	20,000	2
100k-600k	Semi-automatic	400,000	2
>600k	Automatic	850,000	1

Other processing notes:

- Machine footprint is a function of the line width (1.67m) and machines size
- 6-axis RX160 robots from Staubli are used

Index time (or the required time to assemble all the stacks included in one fuel cell system) is estimated based on the type of assembly line and the number of stacks per system while availability is assumed to increase with annual production volume from 0.8 to 0.95.

Process performance and setup time depends on grade of automation of assembly process while process yield is constant at a value of 99.5% since it is assumed that at this very close to final product step, defective parts are detected by EEA quality control systems and not built into stacks.

Table 4.68 displays the process parameters used in the analysis for the assembly line while Table 4.69 shows the estimated cost for metal end-plates and compression springs relative to the fuel cell size and the annual production volume.

Table 4.68. Assembly process line parameters

Power	Systems/year	Process Yield	Availability	Line Performance	Index time (min/system)	Setup time (min/day)
1 kWe	10	0.995	0.80	0.89	60	20
	100	0.995	0.80	0.89	60	20
	1,000	0.995	0.81	0.95	15	10
	50,000	0.995	0.86	0.98	12	5
10 kWe	10	0.995	0.80	0.89	120	20
	100	0.995	0.81	0.95	24	10
	1,000	0.995	0.88	0.98	18	5
	50,000	0.995	0.93	0.98	18	5
50 kWe	10	0.995	0.80	0.89	600	20
	100	0.995	0.86	0.98	90	5
	1,000	0.995	0.93	0.98	90	5
	50,000	0.995	0.95	0.98	90	5
100 kWe	10	0.995	0.81	0.95	240	10
	100	0.995	0.88	0.98	180	5
	1,000	0.995	0.95	0.98	180	5
	50,000	0.995	0.95	0.98	180	5
250 kWe	10	0.995	0.84	0.95	600	10
	100	0.995	0.91	0.98	450	5
	1,000	0.995	0.95	0.98	450	5
	50,000	0.995	0.95	0.98	450	5

Table 4.69. Estimated cost for end-plates and compression springs

Power	Annual Production volume (sys/yr)	Estimated cost of end plates (\$/system)	Estimated cost of compression springs (\$/system)
1 kWe	100	60	10
	1,000	48	10
	10,000	38.4	10
	50,000	34.56	10
10 kWe	100	100	20
	1,000	80	20
	10,000	64	20
	50,000	57.6	20
50 kWe	100	400	35
	1,000	320	35
	10,000	256	35
	50,000	230	35
100 kWe	100	600	65
	1,000	480	65
	10,000	384	65
	50,000	346	65
250 kWe	100	800	165
	1,000	640	165
	10,000	512	165
	50,000	461	165

In addition, a nickel mesh was included at the anode side to improve the electrical contact between the anode and interconnect. The supplier, Anping County Bolin Metal Wire Mesh Co., provided varying costs depending on annual order quantity.

Table 4.70. Pure Nickel wire mesh cost

Order quantity (m2)	50	1000	10000	50000
Mesh count	80	80	80	80
Wire diameter (mm)	0.13	0.13	0.13	0.13
Material	Pure Nickel	Pure Nickel	Pure Nickel	Pure Nickel
Price (\$/m2)	49.1	32.7	25.1	24.1

The number of assembly lines were estimated as follows:

$$\# \text{ of assembly lines} = \text{roundup} \left[\frac{\frac{\text{systems required}}{\text{year}} * \frac{\text{index time} \left(\frac{\text{hours}}{\text{system}} \right)}{\text{Performance} * \text{Process Yield}}}{\left(\frac{\text{op. hours}}{\text{day}} - \text{setup time} \left(\frac{\text{hours}}{\text{day}} \right) \right) * \frac{\text{op. days}}{\text{year} * \text{line}} * \text{Availability}} \right]$$

which corresponds to a number of annual operating hours per line, line utilization and labor cost equal to:

$$\frac{\text{Annual operating hours}}{\text{line}} = \text{roundup} \left[\frac{\frac{\text{systems required}}{\text{year}} * \frac{\text{index time} \left(\frac{\text{hours}}{\text{system}} \right)}{\text{Performance} * \text{Process Yield}}}{\# \text{ of assembly lines}} \right]$$

$$\text{Line Utilization (\%)} = \frac{\frac{\text{Annual operating hours}}{\text{line}}}{\left(\frac{\text{op. hours}}{\text{day}} - \text{setup time} \left(\frac{\text{hours}}{\text{day}} \right) \right) * \frac{\text{op. days}}{\text{year} * \text{line}} * \text{Availability}}$$

$$\text{Labor cost} \left(\frac{\$}{\text{year}} \right) = \# \text{ of lines} * \frac{\text{Annual operating hours}}{\text{year}} * \frac{\# \text{ of workers}}{\text{line}} * \text{labor rate} \left(\frac{\$}{\text{hr}} \right)$$

The seal dimensions are 5 mm width and 0.2 mm thick and seal paste and assumed to be the same as that used for cell-to-frame joining. Figure 4.46 indicates where cell-to-cell seals are positioned (S2 and S3).

On the upper side a seal (S2) is dispensed along the edge of the interconnect while on the lower side seal paste is dispensed along the edge of the interconnect and also along the perimeter of gas manifolds (S3). Each repeat unit has an estimated a mass of 2.03 g.

This serves the purpose of keeping the anode and cathode reactants in their respective flow fields while also preventing leakage to the outside environment.



Figure 4.46. Cell-to-cell seal

Regarding sealing paste preparation, similar ball mills as that used for anode slurry milling were used and machines were sized depending on quantity of paste to mill per day.

Table 4.74 and Table 4.73 show estimated machine rates and costs for ball mills and stack assembly lines, respectively.

Table 4.71. Machine rates for paste milling process (50-kWe systems)

System size (kWe)	50			
	100	1000	10000	50000
Systems/year	100	1000	10000	50000
Material handling (load/unload)	manual	manual	automatic	automatic
No of ball mills	1	1	1	1
Workers/machine	1	1	0	0
Quantity of paste/repeat unit (g)	2.030	2.030	2.030	2.030
Quantity of slurry to mill/day (kg)	1.32	11.88	63.34	303.51
Max load capacity (kg)	5	50	300	1000
Max # of cycles/year/machine	240.00	240.00	240.00	240.00
# of cycles required/year/machine	101	112	210	219
Machine utilization (%)	22.21%	22.17%	36.95%	55.39%
Labor time (hours)	50.75	56.28	0.00	0.00
Annual operating hours (hours)	2385.43	2645.23	4959.80	5172.36
Labor cost(\$)	1512.97	1677.75	0.00	0.00
Power Consumption/machine (KW)	0.4	1.7	5	12
Machine Footprint (m2)	6	16	26	44
Maintenance factor	0.10	0.10	0.10	0.10
Auxiliary Costs Factor	0.00	0.00	0.00	0.00
Initial Capital (\$)	733	3274	7175	15692
Initial System Cost (\$)	7.33E+01	3.27E+02	7.18E+02	1.57E+03
Annual Depreciation (\$/yr)	4.79E+01	2.14E+02	4.69E+02	1.03E+03
Annual Cap Payment (\$/yr)	6.66E+00	2.98E+01	6.53E+01	1.43E+02
Auxiliary Costs (\$/yr)	0.00	0.00	0.00	0.00
Maintenance (\$/yr)	8.32	37.15	81.42	178.07
Salvage Value (\$/yr)	0.28	1.25	2.74	6.00
Energy Costs (\$/yr)	118.99	560.81	3092.68	7740.53
Property Tax (\$/yr)	145.08	648.02	1420.15	3105.92
Building Costs (\$/yr)	503.01	1344.70	2186.38	3701.42
Interest Tax Deduction (\$/yr)	0.00	0.00	0.00	0.00
Machine Rate (\$/h)	0.33	0.99	1.38	2.87
Capital	0.003	0.011	0.013	0.026
Variable	0.05	0.23	0.64	1.53
Building	0.27	0.75	0.73	1.32

Table 4.72. Machine rates for stack assembly lines (50-kWe systems)

System size (kWe)	50			
	100	1000	10000	50000
Systems/Year	100	1000	10000	50000
No of stacks per system	5	5	5	5
Stacks/year	500	5000	50000	250000
EEA cells per stack	130	130	130	130
Type of assembly line	Manual	Fully-Automated	Fully-Automated	Fully-Automated
Lines	1	1	5	24
Scrap (%)	0.50%	0.50%	0.50%	0.50%
Process Yield (%)	99.5%	99.5%	99.5%	99.5%
Line Availability (%)	80.0%	85.8%	93.5%	95.0%
Line Performance (%)	89.0%	98.0%	98.0%	98.0%
Setup time (min)	20.0	5.0	5.0	5.0
Index Time (min)	600.00	100.00	100.00	100.00
Line Utilization (%)	37.54%	52.16%	95.72%	98.12%
Annual Operating Hours/line	1129.24	1709.23	3418.45	3560.89
Workers	2.00	1.00	1.00	1.00
Labor Cost (\$)	6.73E+04	5.10E+04	5.10E+05	2.55E+06
Power Consumption (KW)	5	20	100	480
Assembly line Footprint (m2)	67	168	840	4032
Maintenance factor	0.10	0.10	0.10	0.10
Auxiliary Costs Factor	0.00	0.00	0.00	0.00
Initial Capital (\$)	2.00E+04	8.50E+05	4.25E+06	2.04E+07
Initial System Cost (\$)	2.20E+04	9.35E+05	4.68E+06	2.24E+07
Annual Depreciation (\$/yr)	1.31E+03	5.55E+04	2.78E+05	1.33E+06
Annual Cap Payment (\$/yr)	2.50E+03	1.06E+05	5.31E+05	2.55E+06
Auxiliary Costs (\$/yr)	0.00E+00	0.00E+00	0.00E+00	0.00E+00
Maintenance (\$/yr)	2.27E+02	9.65E+03	4.82E+04	2.31E+05
Salvage Value (\$/yr)	7.64E+00	3.25E+02	1.62E+03	7.79E+03
Energy Costs (\$/yr)	7.04E+02	4.26E+03	4.26E+04	2.13E+05
Property Tax (\$/yr)	8.28E+01	3.52E+03	1.76E+04	8.45E+04
Building Costs (\$/yr)	5.66E+03	1.41E+04	7.07E+04	3.39E+05
Interest Tax Deduction (\$/yr)	0.00E+00	0.00E+00	0.00E+00	0.00E+00
Machine Rate (\$/h)	8.11	80.35	41.42	39.87
Capital	2.20	61.89	30.94	29.70
Variable	0.82	8.14	5.32	5.20
Building	5.08	10.33	5.17	4.96

Conditioning and Testing Stations

After the assembly process stacks are moved to the conditioning and testing station. During the testing process a load is applied to the top of the stack and then the stack is heated to an approximate temperature of 850° C. Next the furnace temperature is lowered to 750°C and reducing gas is flowed through the anode cavities to reduce NiO to Ni. Then electrochemical acceptance tests are performed. The anode is supplied with a mixture of 50% H₂ and 50% N₂ (or mixture of reformat fuel) and an I-V curve and a fuel utilization curve are taken. Finally, the furnace is cooled down to ambient temperature.

The entire loading, heating, reducing, testing and cooling procedure is estimated to require 24 hours. For this analysis, Fuelcon’s sintering and testing stations were included. The loading process of carts (placing and fixing the stacks) is done outside the station in a separate area. Once the stacks are mounted, the shuttle cars can be moved to the station and placed within one of cart slots. Figure 4.47 show drawings with details of 16-fold sintering stations.

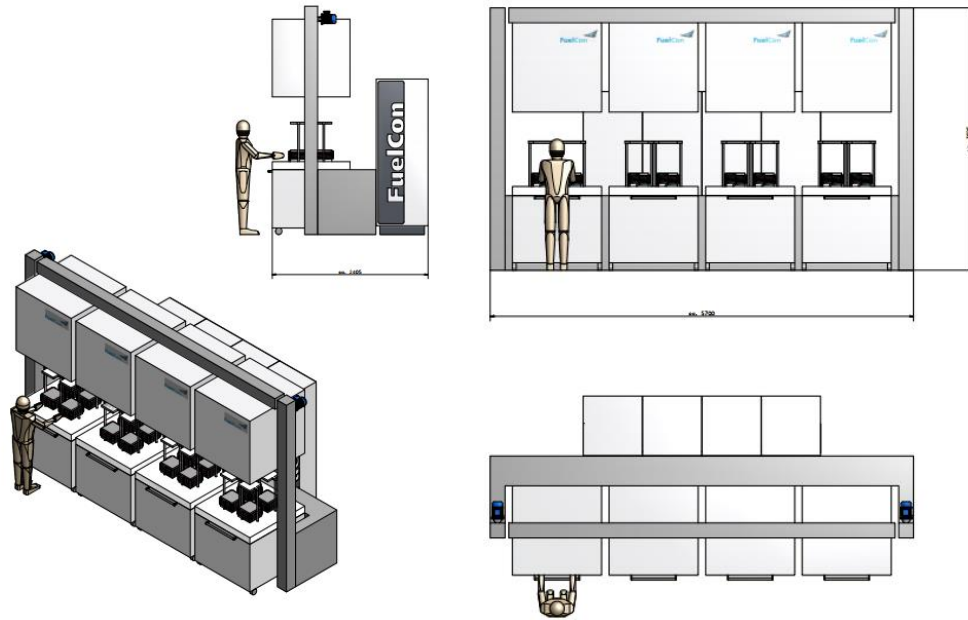


Figure 4.47. FuelCon 16-fold sintering stations drawings

Three different station configurations were considered as shown on Table 4.73.

Table 4.73. Stack sintering and testing stations specifications

Stack sintering and testing station	4-fold sintering and reduction station with 1 cart	8-fold sintering and reduction station with 2 carts	16-fold sintering and reduction station with 4 carts
Stacks tested/cycle	4	8	16
Cost (\$)	400,000	700,000	1,300,000
Worker/station	1	1	1
Cycle time (h)	16-24	16-24	16-24
Toolsize (m2)	4.32	7.44	13.68
Average power consumption (kW)	15	30	60

The number of testing stations was evaluated starting from the number of cycles required per year as follows:

$$\frac{\text{Cycles required}}{\text{year}} = \frac{\frac{\text{stacks required}}{\text{year}}}{\frac{\text{stacks tested}}{\text{cycle}}}$$

$$\# \text{ of testing stations} = \frac{\frac{\text{cycles required}}{\text{year}}}{\frac{\text{cycles}}{\text{day}} * \text{annual op. days} \left(\frac{\text{days}}{\text{year}}\right)}$$

Considering a number of maximum cycles per station equal to 240 (operational days per year) it was possible to estimate also station utilization and annual operating hours as:

$$\text{Station utilization (\%)} = \frac{\frac{\text{cycles required}}{\text{year}}}{\frac{\text{Max \# of cycles}}{\text{year} * \text{station}} * \# \text{ of stations}}$$

$$\text{Annual operating hours} = \frac{\frac{\text{cycles required}}{\text{year}} * \text{cycle time} \left(\frac{\text{hours}}{\text{cycle}}\right)}{\# \text{ of stations} * \text{Overall yield}}$$

Finally labor hours and labor cost were evaluated as:

$$\text{Annual labor hours} = \frac{\text{load and unload time}}{\text{cycle}} * \frac{\text{cycles required}}{\text{year}}$$

$$\text{Labor cost} \left(\frac{\$}{\text{year}}\right) = \text{Annual labor hours} * \text{labor rate} \left(\frac{\$}{\text{hr}}\right)$$

The time required for a worker to load and unload a station is 20 minutes for a 4-fold station, 40 minutes for an 8-fold station and 60 minutes for 16-fold station per the vendor. Reformate fuel cost for conditioning and testing station was calculated considering data shown on Table 4.74.

Table 4.74. Stack fuel utilization for conditioning cycle

H ₂ for conditioning
H₂ density at RT=0.089 g/L
price=4-5 \$/kg*
Testing and conditioning time 16-24 hrs.
Fuel Utilization
1-kWe system: 0.80 SLPM
10-kWe system: 0.91 SLPM
50-kWe system: 4.54 SLPM
100-kWe system: 9.08 SLPM
250-kWe system: 22.7 SLPM

* <http://www.h2carblogger.com/?p=461>

Table 4.75 shows estimated machine rate processing costs for stack conditioning and testing process.

Table 4.75. Machine rates for stack conditioning and testing process (50-kWe systems)

System size (kWe)	50			
	100	1000	10000	50000
Sistems/year	100	1000	10000	50000
Stacks/year	500	5000	50000	250000
# of stations	1	2	14	66
Type of station	4-fold station	16-fold station	16-fold station	16-fold station
Stacks tested/station	4	16	16	16
Cycles required/year	125	313	3125	15625
Max No. of cycles/year	240	480	3360	15840
Station utilization (%)	52%	65%	93%	99%
Annual operating hours/station	3015	3769	5384	5710
Power Consumption (KW)	15	120	840	3960
Conditioning Time/cycle (hours)	24	24	24	24
Workers/station	1	1	1	1
Labor hours	42	313	3125	15625
Labor Cost for loading unloading (\$/year)	1242	9316	93156	465781
Machine Footprint (m2)	13	78	546	2574
Maintenance factor	0.10	0.10	0.10	0.10
Auxiliary Costs Factor	0.00	0.00	0.00	0.00
Initial Capital (\$)	4.00E+05	2.60E+06	1.82E+07	8.58E+07
Initial System Cost (\$)	4.40E+05	2.86E+06	2.00E+07	9.44E+07
Annual Depreciation (\$/yr)	2.61E+04	1.70E+05	1.19E+06	5.61E+06
Annual Cap Payment (\$/yr)	4.99E+04	3.25E+05	2.27E+06	1.07E+07
Auxiliary Costs (\$/yr)	0.00E+00	0.00E+00	0.00E+00	0.00E+00
Maintenance (\$/yr)	4.54E+03	2.95E+04	2.07E+05	9.74E+05
Salvage Value (\$/yr)	1.53E+02	9.93E+02	6.95E+03	3.28E+04
Energy Costs (\$/yr)	5.64E+03	5.64E+04	5.64E+05	2.82E+06
Property Tax (\$/yr)	1.66E+03	1.08E+04	7.53E+04	3.55E+05
Building Costs (\$/yr)	1.09E+03	6.57E+03	4.60E+04	2.17E+05
Machine Rate (\$/h)	20.80	56.62	41.88	39.91
Capital	16.51	42.92	30.05	28.33
Variable	3.38	11.40	10.22	10.07
Building	0.91	2.30	1.61	1.52

Stack Assembly and Conditioning Cost Summary

Assembly and conditioning costs are lumped together and summarized in Table 4.78 for all system sizes. Cost ranges between \$822 per kWe at low production volume (e.g. 1kWe FC and 100 systems/year) to less than \$13 per kWe at the highest production volumes.

High costs are expected at low production volume due to several factors such as high initial cost for the assembly line and testing stations, high floor space cost relative to the production rate, and high prices of some components like end-plates and compression bands when purchased in small volume.

Cost values show a decreasing trend with increasing both production volume and system size as shown clearly in Figure 4.48. In addition, it is important to mention that at the same cumulative global produced capacity, assembly and conditioning cost decrease with larger SOFC system size. For

example, for an annual production of 10 MWe per year (see Figure 4.49), the stack assembly and testing cost difference between 1 kWe and 10 kWe stacks is substantial since they are constituted by a different number of repeat units (13 cells per stack and 130 cells per stack respectively).

This means that 1,000 stacks of 1 kWe power or 100 stacks of 10 kWe power must be assembled and tested per year for an equivalent capacity of 10 MWe. Stack assembly time increases with stack size but the effect of the decreasing number of stacks to test per year on total cost is always bigger. This explains the lower assembly cost of the 10 kWe stack.

Table 4.76. Stack assembly and conditioning process cost in (\$/kWe) and (\$/part) at all production volumes

Equivalent Power (MWe/yr)	System Power (kWe)	Systems/yr	Stack blocks/yr	Stack Blocks/Sys	Repeat Units/Stack Block	Cost (\$/kWe)
0.1	1	100	100	1	13	821.91
1	1	1,000	1,000	1	13	255.14
10	1	10,000	10,000	1	13	143.97
50	1	50,000	50,000	1	13	128.96
1	10	100	100	1	130	98.95
10	10	1,000	1,000	1	130	34.92
100	10	10,000	10,000	1	130	20.83
500	10	50,000	50,000	1	130	18.42
5	50	100	500	5	130	40.65
50	50	1,000	5,000	5	130	21.70
500	50	10,000	50,000	5	130	16.51
2,500	50	50,000	250,000	5	130	15.64
10	100	100	1,000	10	130	31.64
100	100	1,000	10,000	10	130	18.55
1,000	100	10,000	100,000	10	130	15.02
5,000	100	50,000	500,000	10	130	14.44
25	250	100	2,500	25	130	21.48
250	250	1,000	25,000	25	130	14.33
2,500	250	10,000	250,000	25	130	13.19
12,500	250	50,000	1,250,000	25	130	12.90

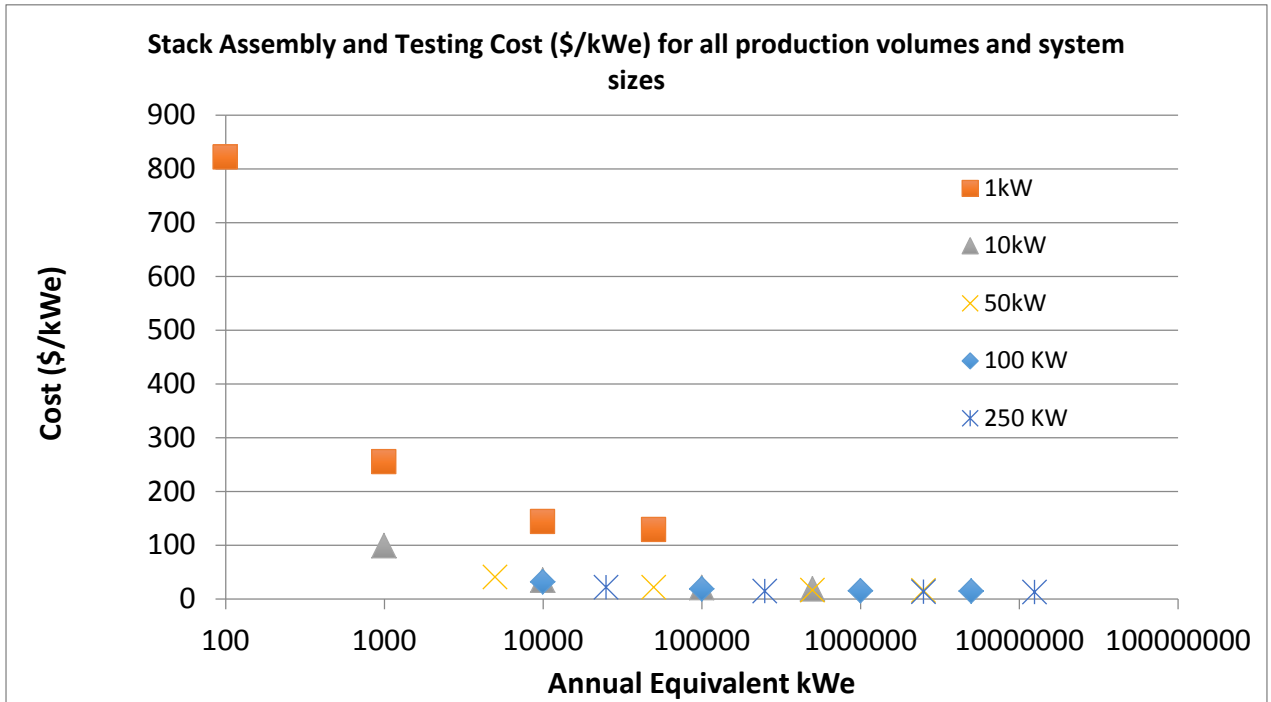


Figure 4.48. Stack assembly and testing cost in (\$/kWe) for all system sizes and production volumes

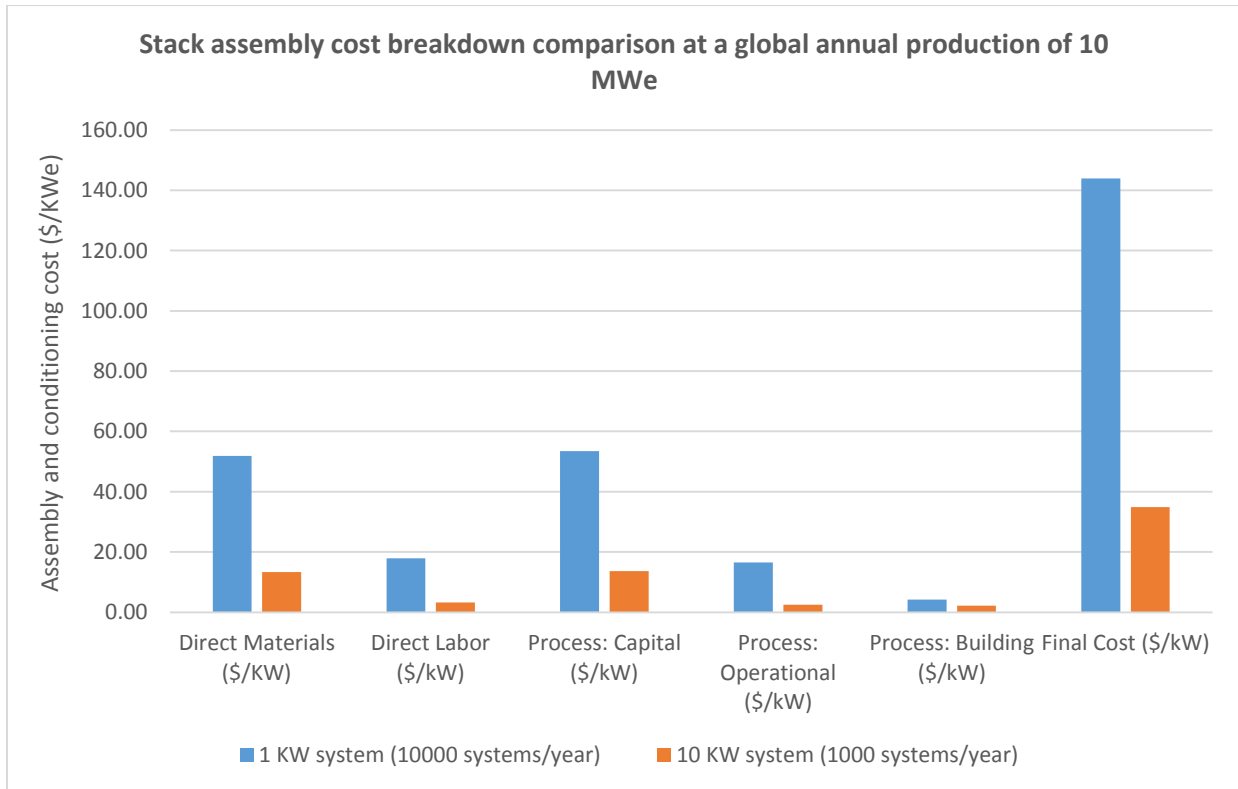


Figure 4.49. Comparison of assembly and conditioning cost for different system size in (\$/kWe) at a global annual production of 10 MWe

Table 4.79 and Table 4.80 show cost breakdowns that cover materials, labor, capital, operational and building costs. At low volumes (100 systems/year) labor cost, together with capital and material costs, constitute the largest contributions to the total cost because of the high manual labor required in the manual assembly line. At higher volumes direct materials and capital costs dominate. Direct materials include glass sealing paste, end plates, compression bands, and reformat fuel for leak testing.

Table 4.77. Stack Assembly and Testing Costs for 10-kWe system

System Size (kWe)	10			
Production Volume (Units/yr)	100	1,000	10,000	50,000
Material (\$/kWe)	17.57	13.38	10.15	9.47
Labor (\$/kWe)	13.91	3.24	1.21	1.21
Process: Capital (\$/kWe)	52.27	13.69	6.97	5.59
Process: Operational (\$/kWe)	6.06	2.45	1.86	1.73
Process: Building (\$/kWe)	9.14	2.17	0.64	0.43
Total (\$/kWe)	98.95	34.92	20.83	18.42

Table 4.78. Stack Assembly and Testing Costs for 50-kWe system

System Size (kWe)	50			
Production Volume (Units/yr)	100	1,000	10,000	50,000
Material (\$/kWe)	12.11	9.12	7.56	7.05
Labor (\$/kWe)	14.02	1.24	1.21	1.21
Process: Capital (\$/kWe)	10.45	8.59	5.59	5.29
Process: Operational (\$/kWe)	2.25	2.01	1.73	1.70
Process: Building (\$/kWe)	1.83	0.74	0.43	0.40
Total (\$/kWe)	40.65	21.70	16.51	15.64

In comparing the different processes involved, at high volumes, conditioning and testing process constitute the biggest contribution to the total cost (see Figure 4.50). On the contrary, at low volume (100 systems/year) the assembly process has a bigger impact on total cost since assembly is performed by manual labor. Assembly time, number of workers and labor costs for a manual assembly line are much higher than for a fully-automatic assembly line.

For material costs, Figure 4.51 shows that end plates cost constitutes more than the half of the total material cost followed by glass sealing paste, compression bands and reformat fuel cost.

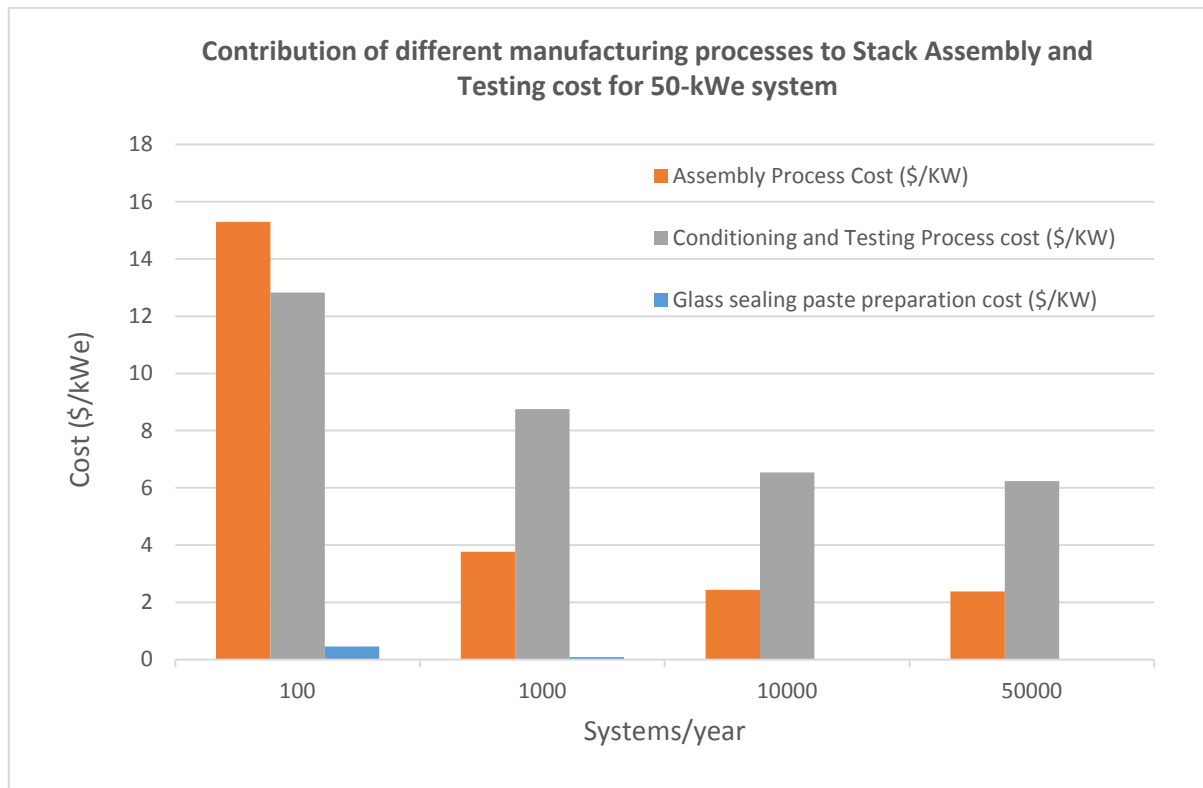


Figure 4.50. Contribution of different manufacturing processes to stack assembly and testing cost for 50-kWe system

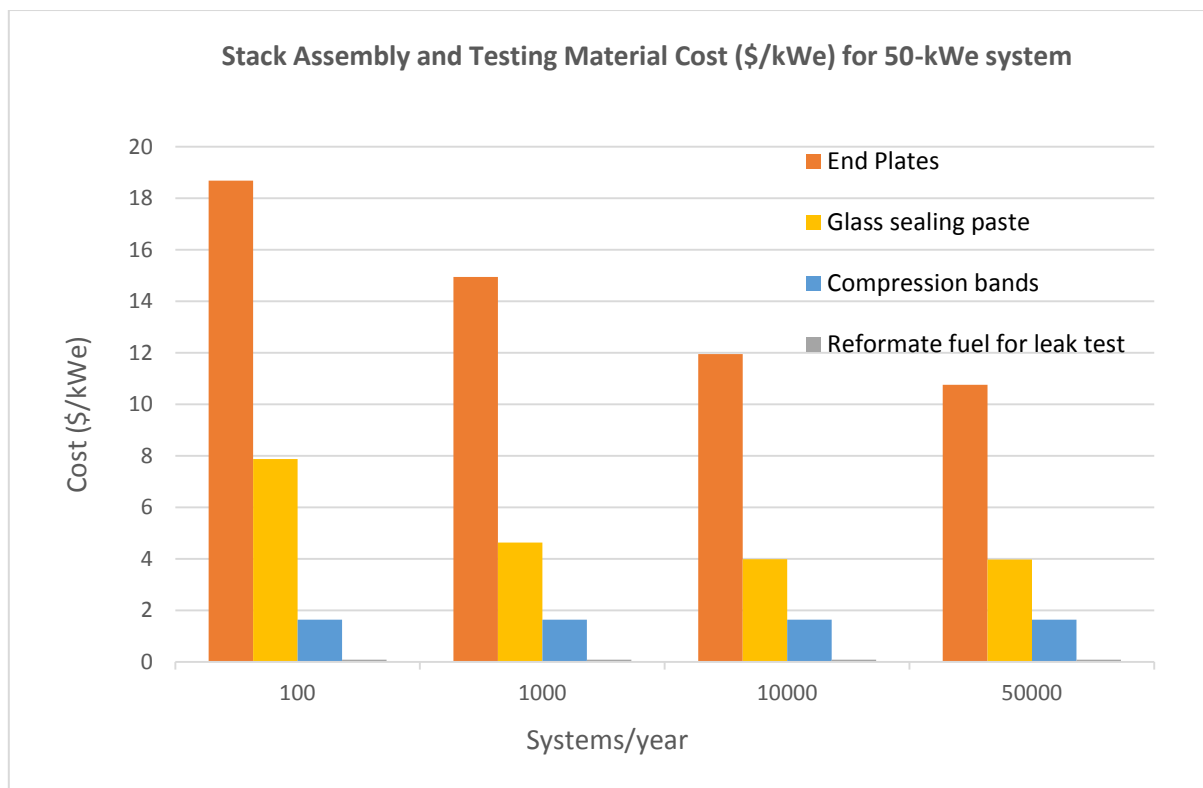


Figure 4.51. Stack Assembly and Testing Material Cost (\$/kWe) for 50-kWe system at all production volumes

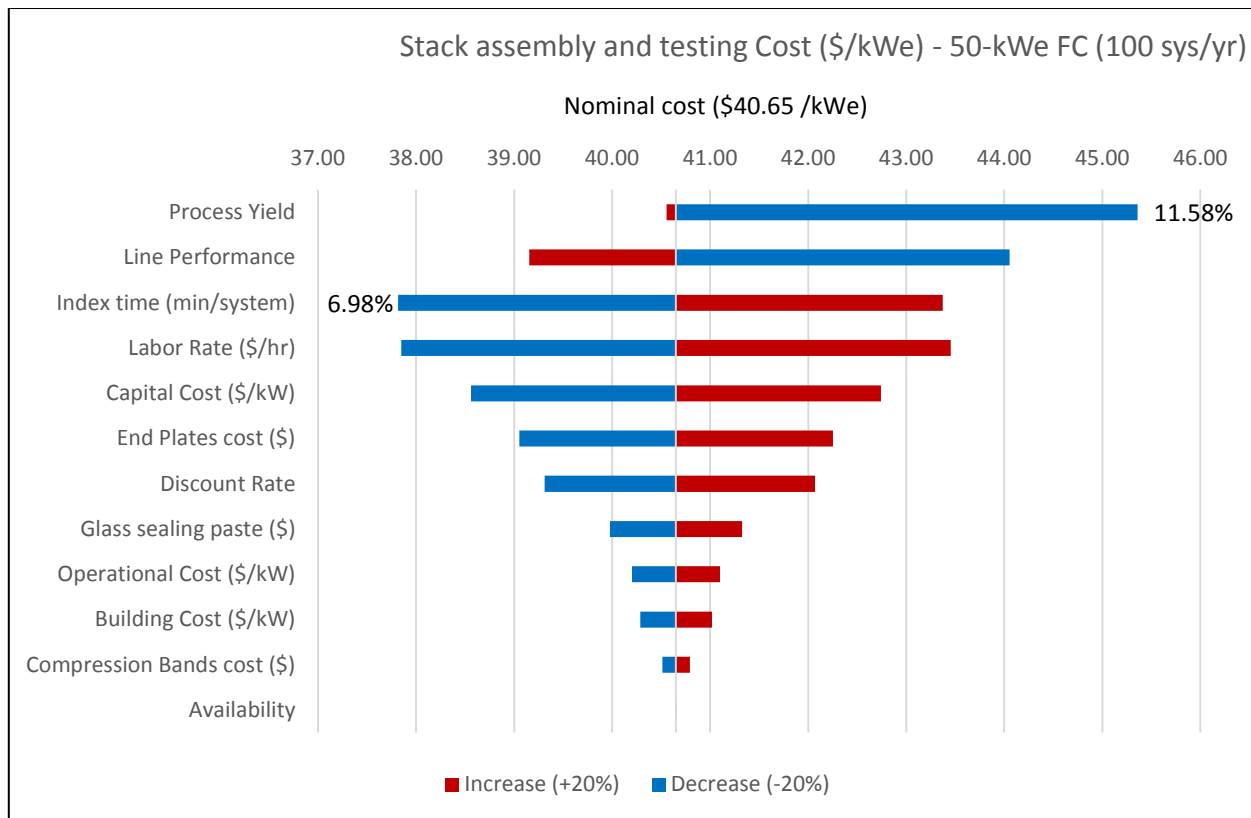
Sensitivity Analysis for Stack Assembly and Testing Process

Sensitivity analysis for stack assembly and testing level was done for 50-kWe systems at different production volumes (as shown in Figure 4.52). The impact to the cost in \$/kWe is calculated for a ±20% change in the sensitivity parameter being varied.

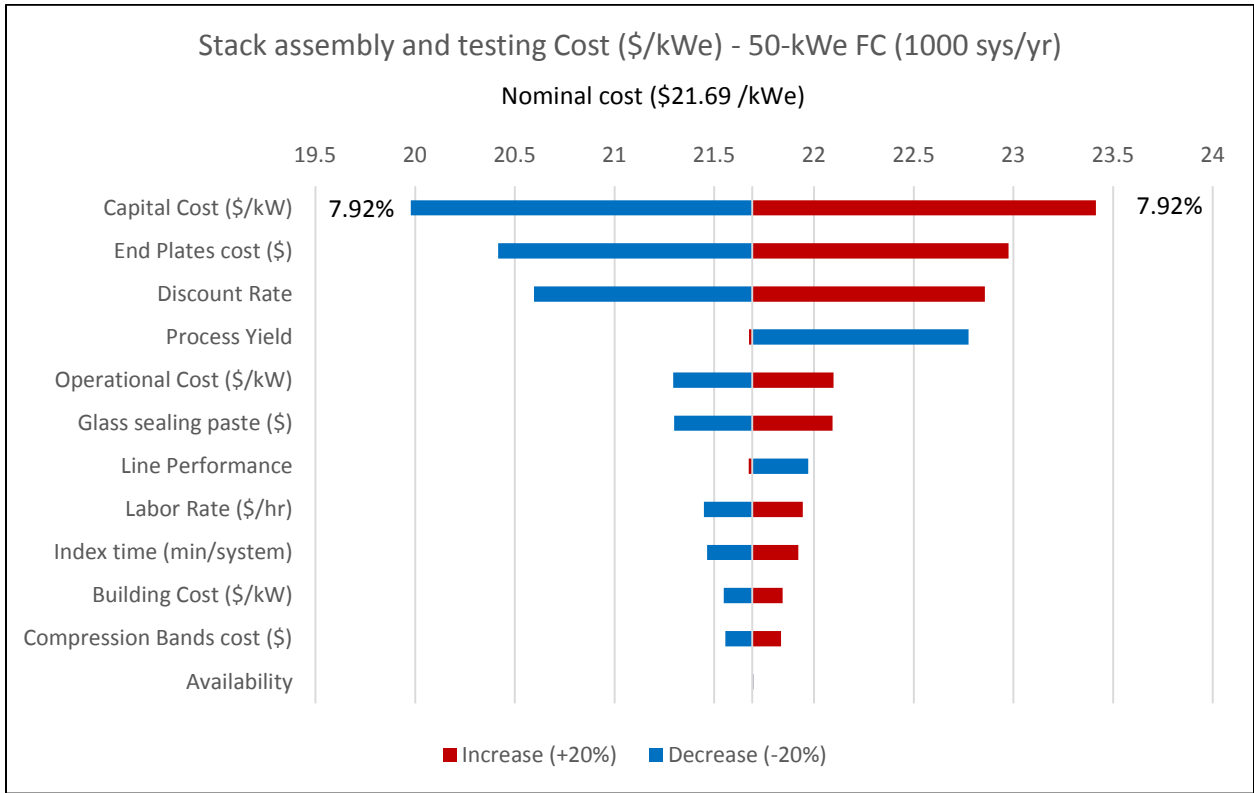
It can be seen from these plots (Figure 4.52) that for annual production volume higher than 100 systems per year, process yield, capital cost, end plate cost, and discount rate dominate the assembly and testing cost. For a production of 100 systems per year process yield, assembly line performance and index time variation are the most important factors that affect the assembly and testing cost.

A decrease in availability causes a decrease of maximum annual operating hours and so an increase of assembly line annual utilization. For this reason a decrease of availability in case of low production volume causes only an increase of line utilization and sensitivity is negligible while in case of high production volume (>1000 systems/year) it causes an increase of assembly lines needed (and so capital costs) in order to guarantee the annual production.

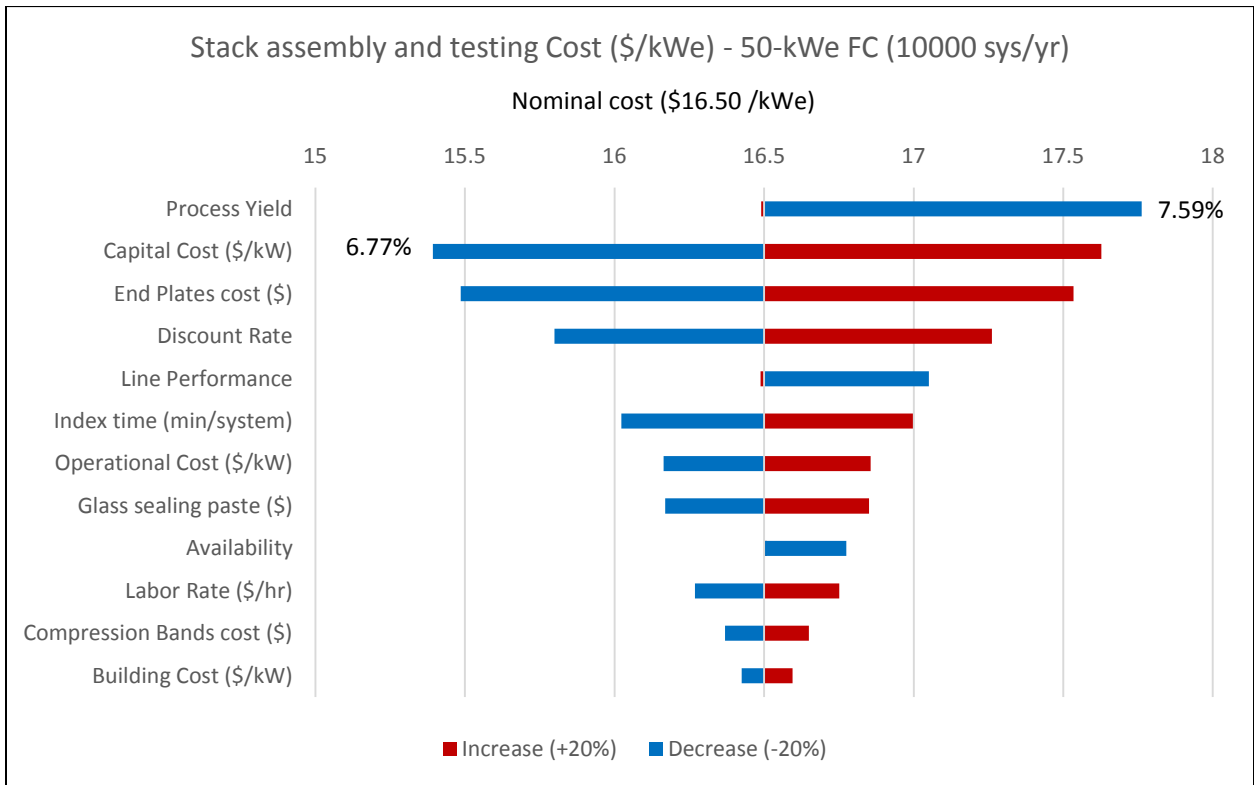
Line performance and index time sensitivities have similar behavior since they both represent variations (by a different amount) of the system assembly time but for production volume higher than 100 systems/year, a line performance increase does not play as an importance role as index time increase since there is a shift from manual to automatic assembly configuration and a shift of line performance from 89% to 98%.



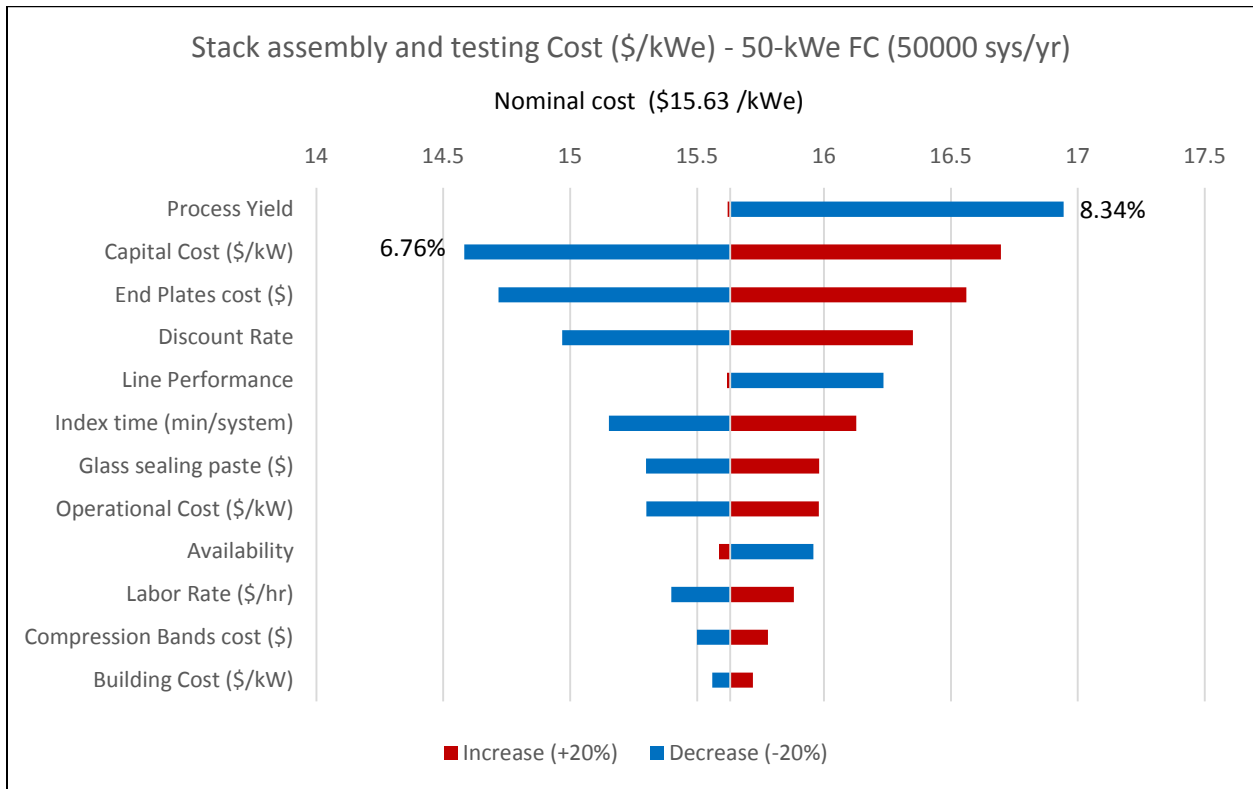
(a)



(b)



(c)



(d)

Figure 4.52. Stack assembly and testing cost sensitivity analysis for 50 kWe system expressed in (\$/kWe) at different annual production rates: a) 100 systems/yr; b) 1,000 systems/yr; c) 10,000 systems/yr; and d) 50,000 systems/yr.

4.6. FC Stack Manufacturing Cost Results

SOFC Stack Cost Summary

Table 4.81 displays the direct cost results for the SOFC stack broken down by systems size and annual manufacturing volume.

Table 4.79. Direct Cost results for SOFC Stack (\$/kWe)

	1kWe	10kWe	50 kWe	100 kWe	250 kWe
100 systems/year	5386.89	1039.32	477.59	339.06	249.12
1,000 systems/year	1195.51	342.34	214.77	194.38	180.52
10,000 systems/year	451.38	196.66	176.42	170.86	167.25
50,000 systems/year	322.04	178.33	169.71	167.24	165.88

Stack cost per unit of electric power (\$/kWe) is seen to decrease both with increasing system size (Figure 4.53) and increasing annual production rate (Figure 4.54). As system size or system manufacturing rate increase, stack cost decrease. In comparing the two effects, cost seems to be slightly more sensitive to system size than to production rate.

Considering the same cumulative global produced capacity, stack cost decreases with larger SOFC system size. This cost reduction is only related to stack assembly and testing cost reduction with system size. For a clearer explanation, see chapter 4.5.4.

Detailed stack costing results are shown below for 10 kWe and 50 kWe stacks. These represent a synthesis of system designs, functional specifications, and DFMA costing analysis for FC stack components. Three sets of plots are shown:

1. Overall stack costs per kWe as function of production volume (100, 1,000, 10,000, and 50,000 systems per year) (Figure 4.55 and Figure 4.56)
2. Breakdown of the stack cost in a stack components level (Figure 4.57 and Figure 4.58)
3. Disaggregation of stack cost by relative percentage of stack components costs to overall stack cost (Figure 4.59 and Figure 4.60)

Figure 4.55 and Figure 4.56 show that material costs dominate at high volumes. As mentioned in chapter 4.1.3.2, material cost tends to be constant at high volume since material prices were collected mostly for order quantity varying between 1 and 50,000 kilograms. At low volumes, capital and labor costs also have a strong impact on overall stack cost since a higher degree of manual labor and lower machine utilization are present.

Figure 4.59 and Figure 4.60 show that EEA cell cost constitutes more than the half of the stack cost above an annual production of 1MWe (100 systems of 10 KWe power). Both interconnect and cell-to-frame seal constitute the second big contributions to the stack cost (each about 10-20 % of stack cost). Frame cost contribution to stack cost varied differently with production volume since in some cases, additional lines were added and capital and building cost increased substantially.

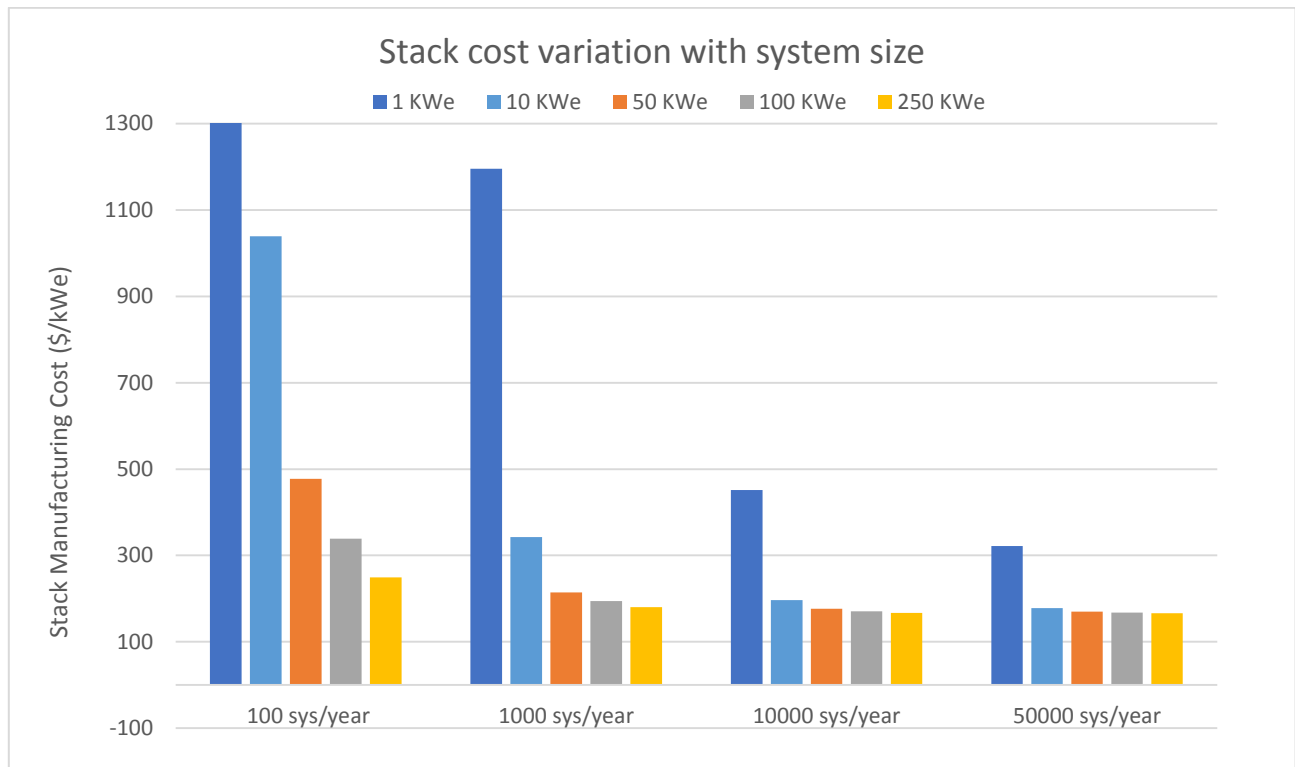


Figure 4.53. Stack manufacturing cost variation with system size in (\$/kWe)

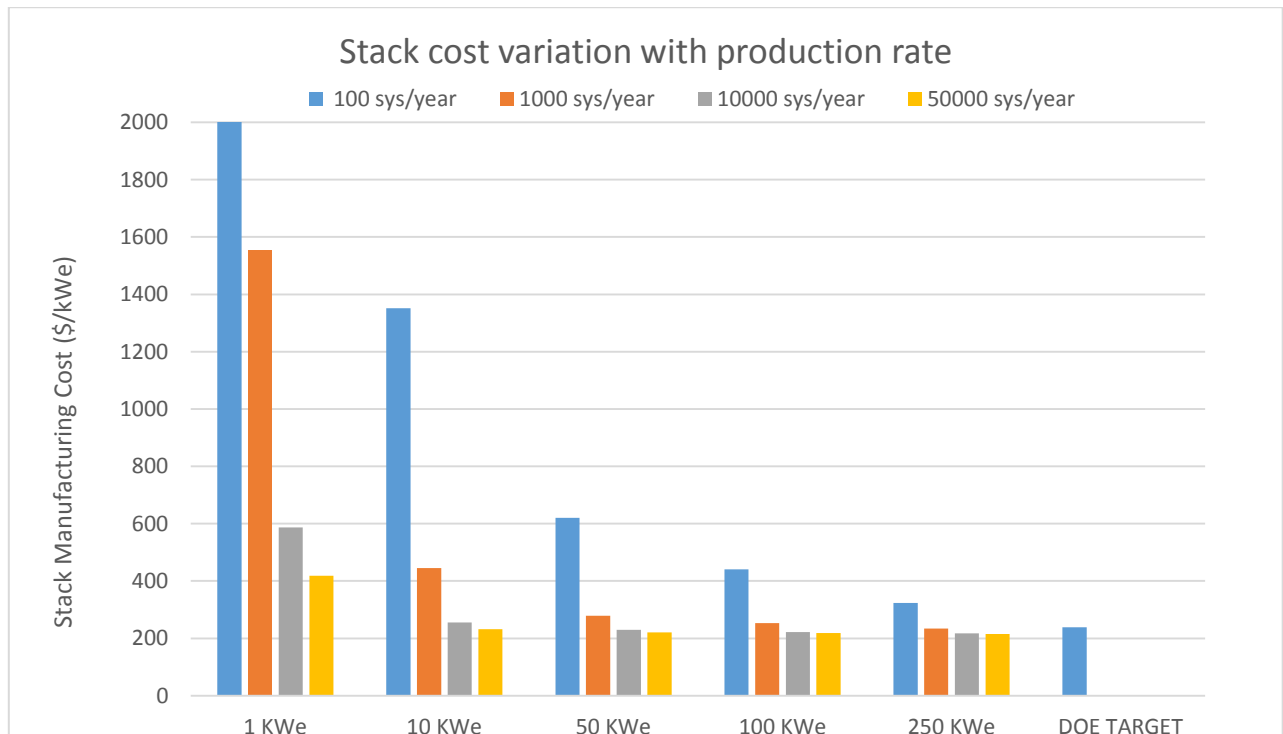


Figure 4.54 Stack manufacturing cost variation with annual production rate in (\$/kWe)

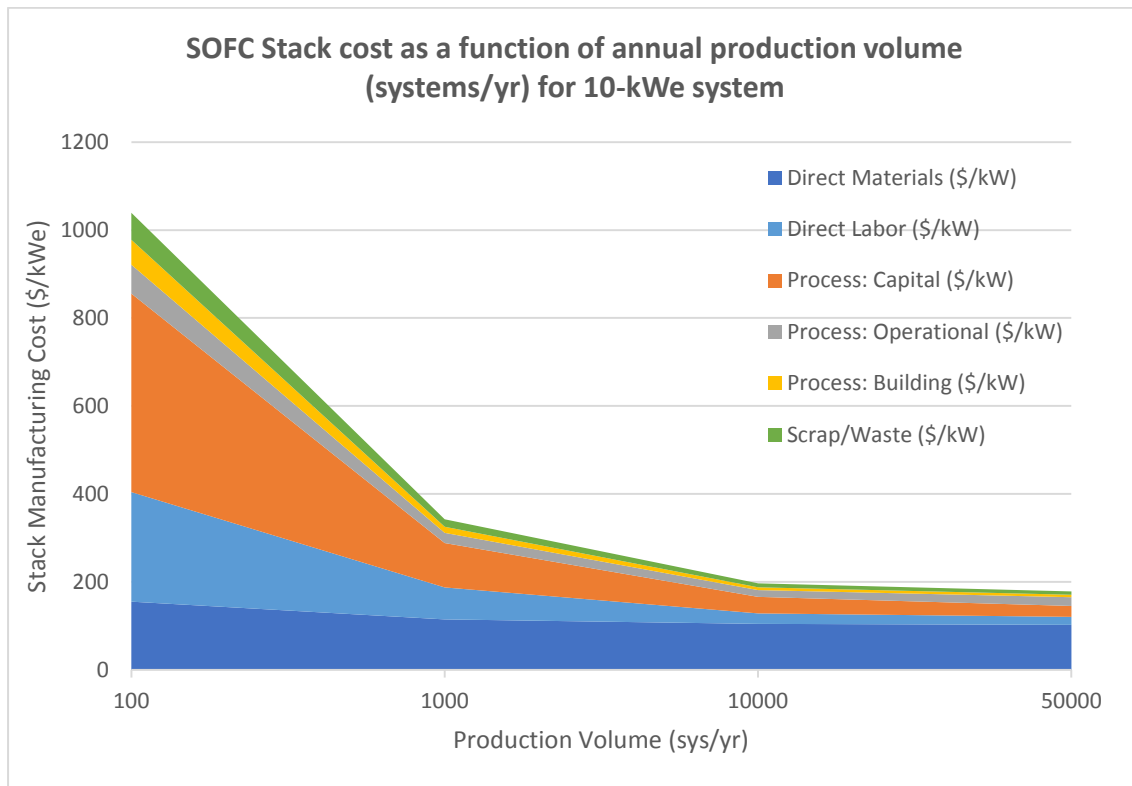


Figure 4.55. SOFC Stack cost as a function of annual production volume (systems/yr) for 10-kWe system

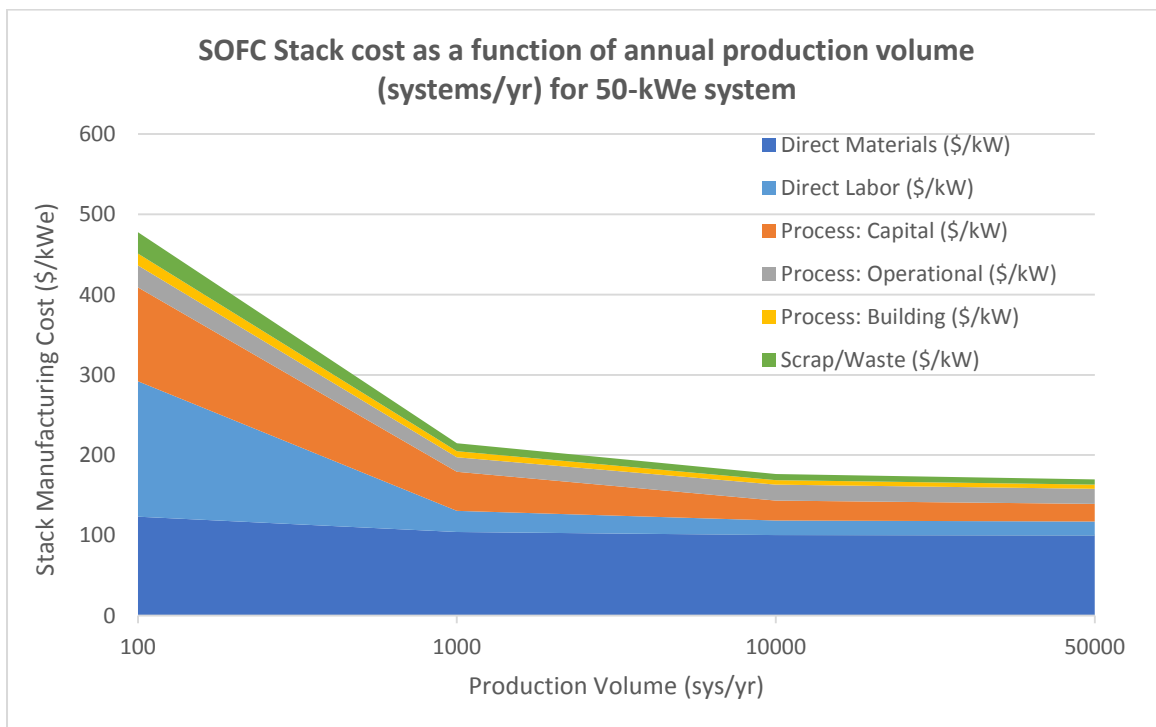


Figure 4.56. SOFC Stack cost as a function of annual production volume (systems/yr) for 50-kWe system

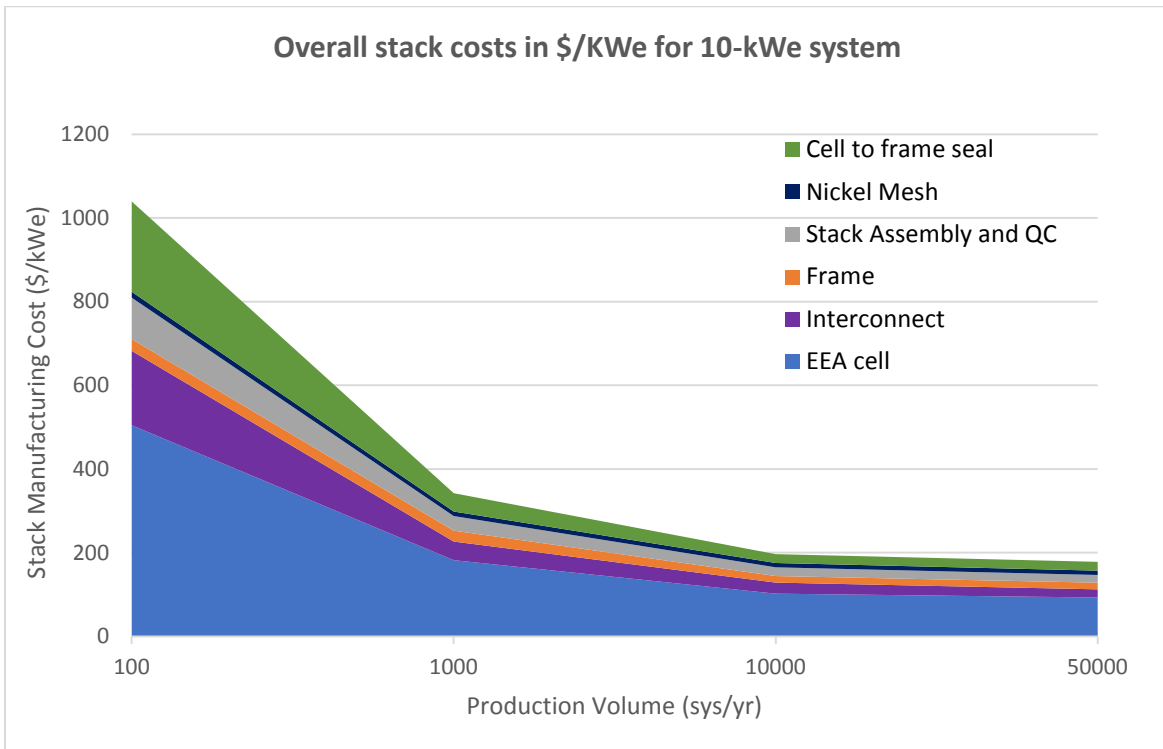


Figure 4.57. Breakdown of the stack cost in a stack components level for 10-kWe system

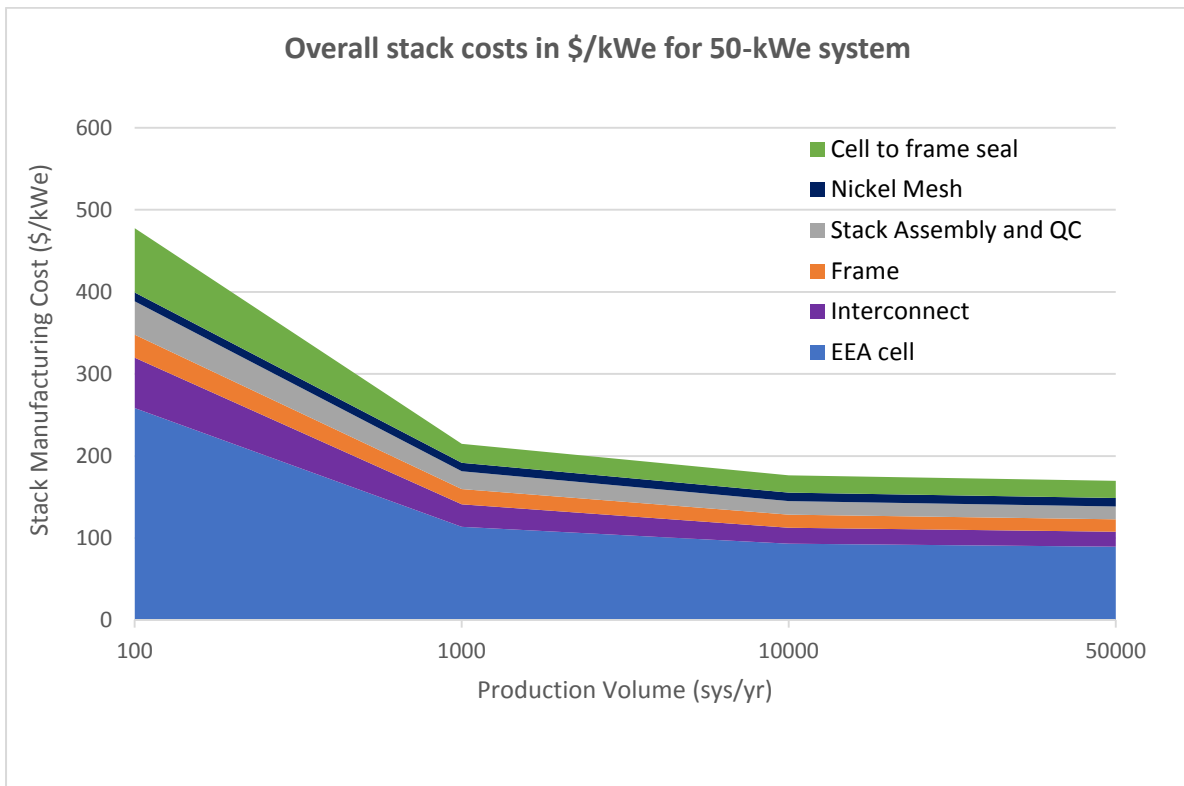


Figure 4.58. Breakdown of the stack cost in a stack components level for 50-kWe system

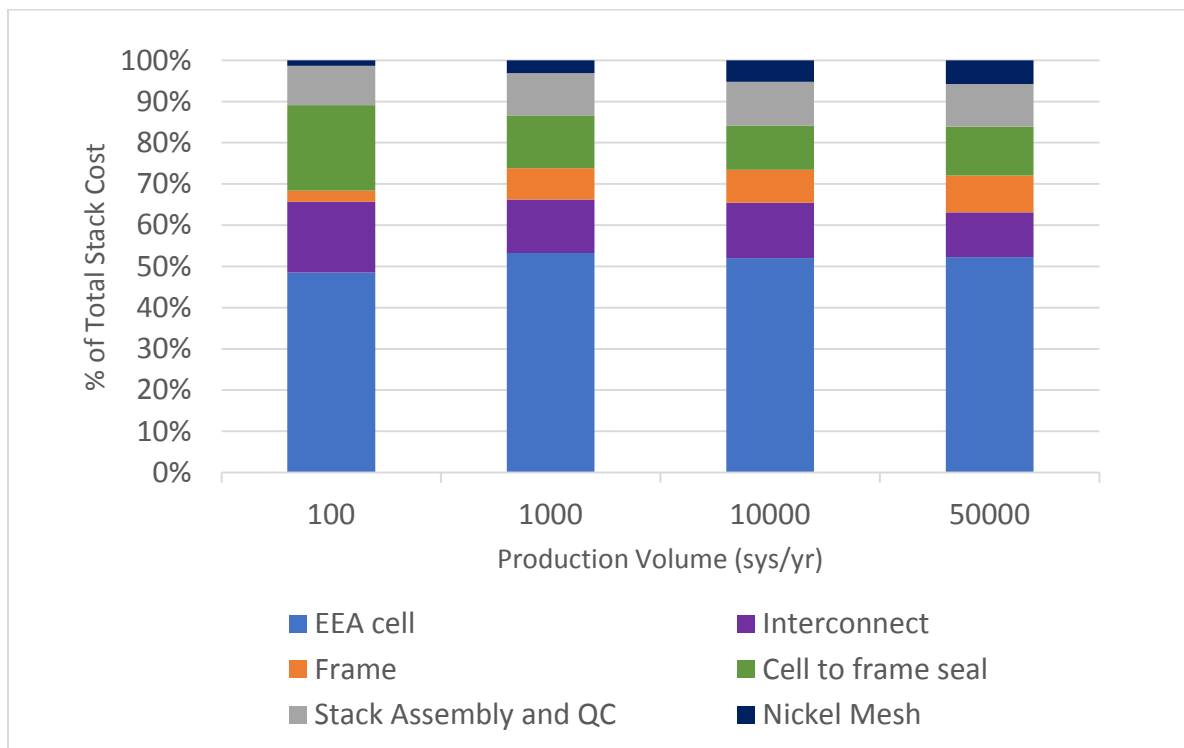


Figure 4.59. Disaggregation of stack cost by relative percentage of stack components cost to overall stack cost for 10-kWe system

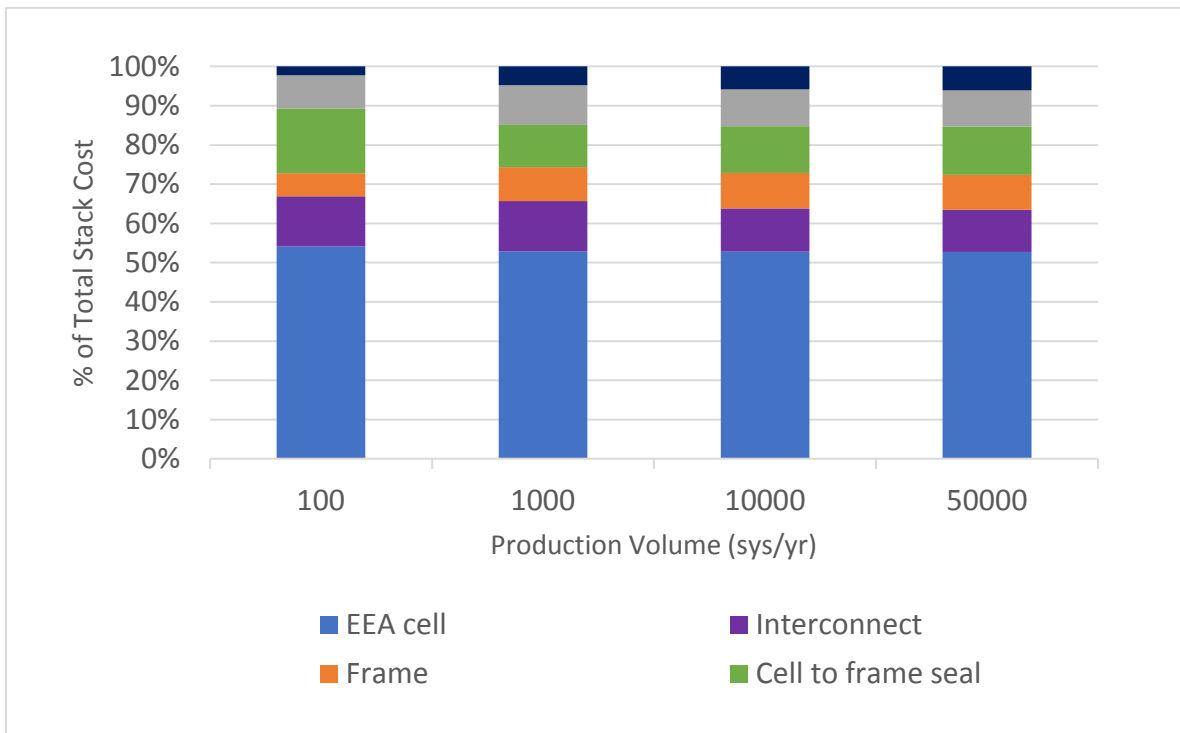


Figure 4.60. Disaggregation of stack cost by relative percentage of stack components cost to overall stack cost for 50-kWe system

Cost Comparison (Base design vs. alternative design)

In this section, the base case stack design chosen (SS441 interconnect, SS441 frame and cell-to-frame glass seals) is compared with an alternative and more expensive design (Crofer 22 APU Interconnect, Crofer 22 APU frame and metal seals). Table 4.82 show both costs of stack base design and stack alternative design at all production volume. As shown, the choice of the alternative design would increase the stack manufacturing cost by 1-20%. This cost difference increases with both system size and production volume.

Table 4.80. Stack Base design vs. Alternative Design cost comparison in (\$/kWe) at all production volume

Equivalent Power (MWe/year)	System Power (kWe)	Systems/year	Base Case Cost (\$/kWe)	Alternative Case Cost (\$/kWe)	Cost increase (%)
0.1	1	100	5386.89	5458.25	1.32%
1	1	1,000	1195.51	1252.33	4.75%
10	1	10,000	451.38	491.14	8.81%
50	1	50,000	322.04	355.12	10.27%
1	10	100	1039.32	1096.14	5.47%
10	10	1,000	342.34	382.10	11.61%
100	10	10,000	196.66	229.51	16.71%
500	10	50,000	178.33	209.83	17.67%
5	50	100	477.59	538.39	12.73%
50	50	1,000	214.77	247.85	15.40%
500	50	10,000	176.42	207.92	17.86%
2,500	50	50,000	169.71	201.06	18.47%
10	100	100	339.06	378.82	11.73%
100	100	1,000	194.38	227.23	16.90%
1,000	100	10,000	170.86	201.94	18.19%
5,000	100	50,000	167.24	199.34	18.81%
25	250	100	249.12	281.59	13.03%
250	250	1,000	180.52	212.10	17.49%
2,500	250	10,000	167.25	198.61	18.74%
12,500	250	50,000	165.88	198.02	19.38%

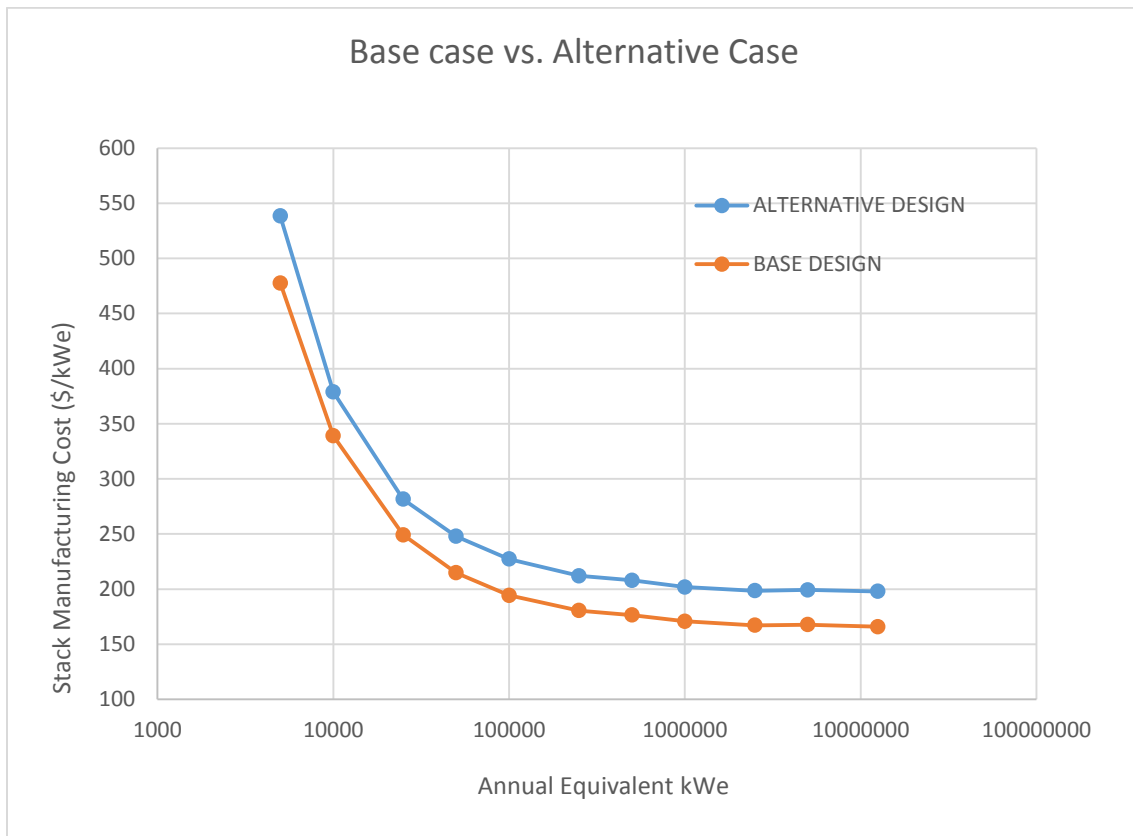


Figure 4.61. Stack Base design vs. Alternative Design cost comparison in (\$/kWe) at all production volume

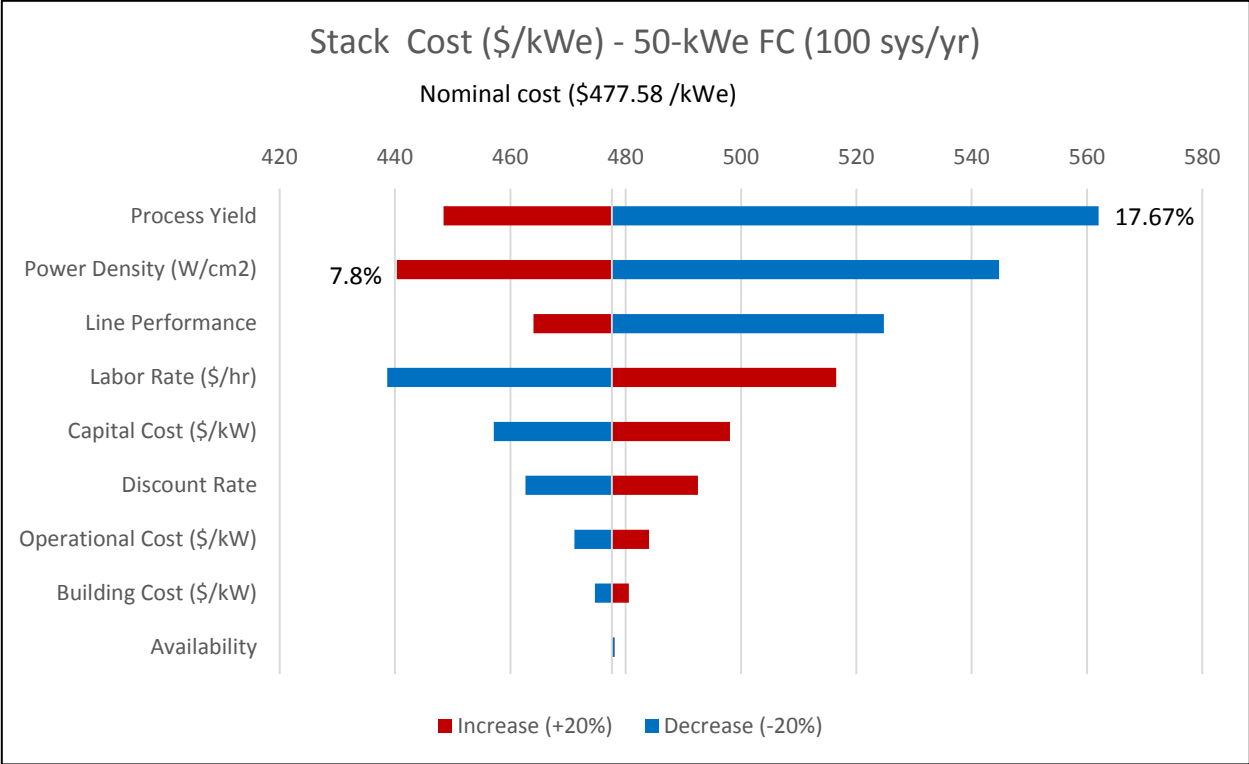
Sensitivity Analysis for Stack Manufacturing Cost

Sensitivity analysis results for the 50-kWe system case at all production volumes are shown in Figure 4.62. Global sensitivity of different parameters on stack manufacturing cost was obtained summing the effects of these parameters on the manufacturing cost of each stack component.

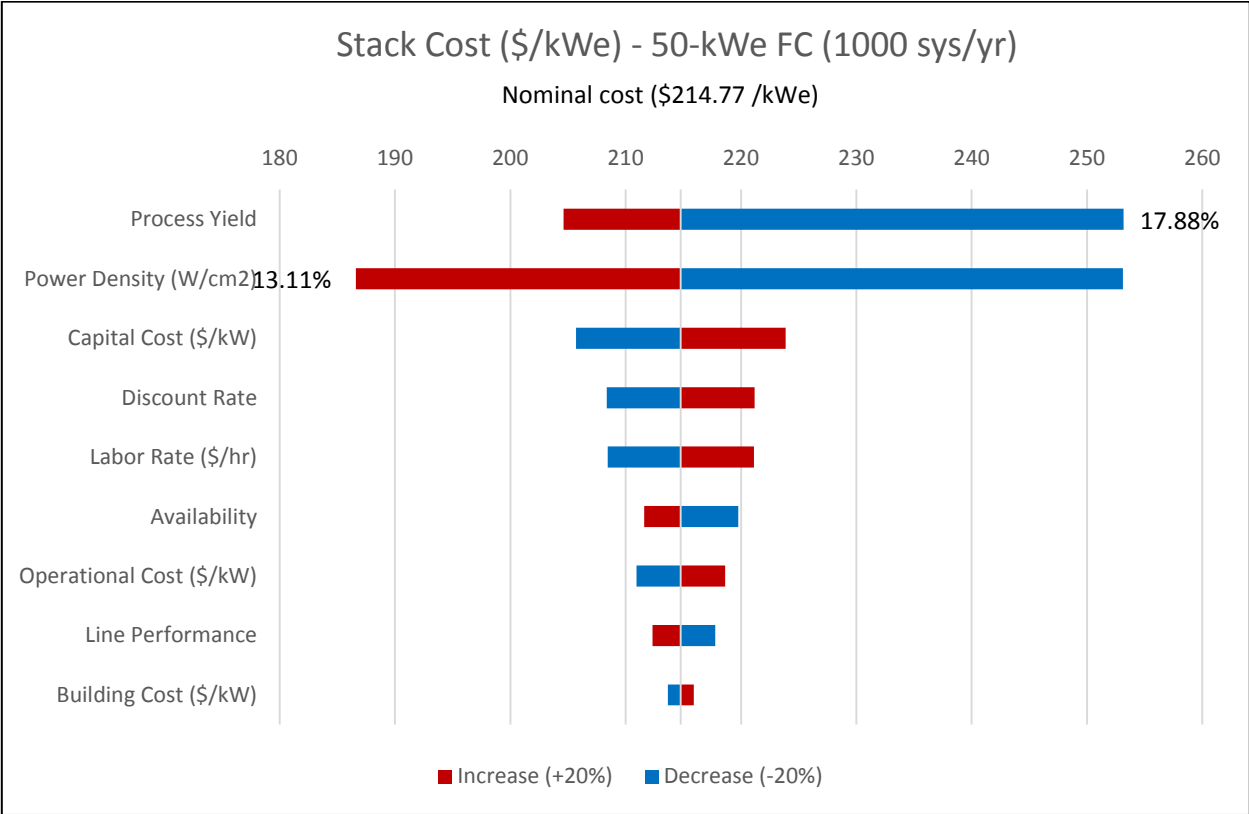
As expected, power density and process yield are the parameters that most affect the stack manufacturing cost. For example in the case of 50 kWe stack (at 10,000 units per year), a 20% decrease of power density or process yield both shift the stack manufacturing cost from \$176.42/kWe to about \$212/kWe. A 20% increase of power density or process yield shifts stack cost from \$176.42/kWe to \$149.83/kWe and from \$176.42/kWe to \$169.98/kWe respectively.

In addition, the sensitivity of these parameters increases with the production volume. In the case of 50 kWe stacks, a 20% decrease of process yield causes increases of EEA cell cost of 17.67% (100 units/year), 17.88% (1,000 units/year), 20.19% (10,000 units/year) and 21.74% (50,000 units/year). Line performance also has a great impact on stack manufacturing cost. The reason is that labor and operational costs increase with lower line speed since annual operating hours increase.

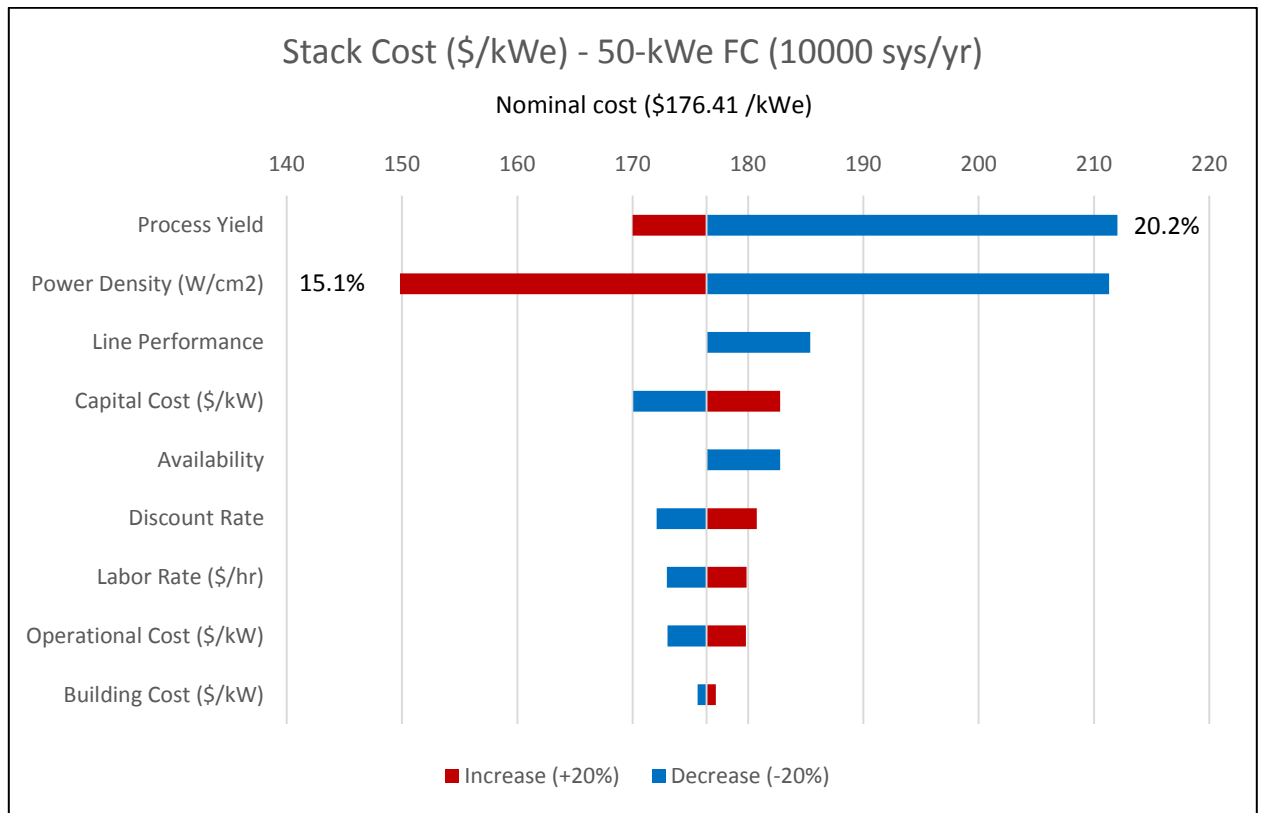
Availability has negligible impact at the low volume of 100 systems per year since in that case its variation causes only an increase of line utilization rate but not an increase of machines needed. Labor rate is less important with higher production volume since the level of automation increases with volume. In all cases, operating costs and building costs have the least effect on stack manufacturing cost.



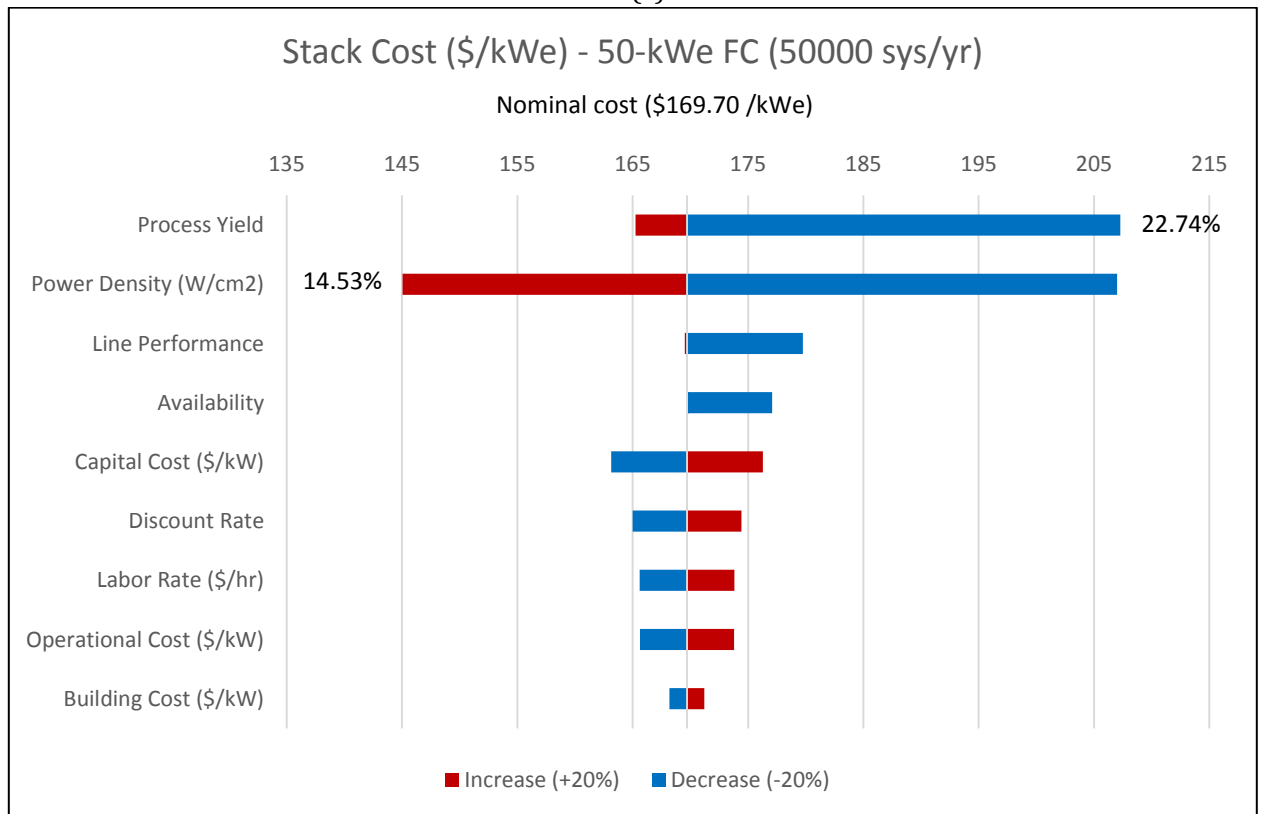
(a)



(b)



(c)



(d)

Figure 4.62. Stack cost sensitivity analysis for 50 kWe system expressed in (\$/kWe) at different annual production rates: a) 100 units/yr; b) 1,000 units/yr; c) 10,000 units/yr; and d) 50,000 units/yr.

Stack Manufacturing Cost Results vs. DOE Cost Target

The SOFC stack cost target assuming mass-manufacturing related cost advantages along with learning from repetition and increased capacity, is \$225/kWe in 2011 dollars (NETL, 2013), which corresponds to a stack cost target of \$238.38/kWe in 2015 dollars.

Prior to comparing the modeled results with the DOE target of \$238 per kWe, a cost contingency (cost margin) should be added in order to cover minor pieces of equipment or parts replacement that were not explicitly examined (for example slurry container, slurry sieves, conveyor belts, doctor blade substitution, screens and squeegees substitution). Similar assumptions were made in other manufacturing cost studies ((James, Spisak, & Colella, 2012),(Weimar, Chick, & Whyatt, 2013)).

Considering a cost margin of 20 %, it would be necessary to produce the following volumes to reach this target (see Figure 4.63):

- at least 10000 units of 10 kWe power (annual equivalent power of 100 MWe)
- at least 10000 units of 50 kWe power (annual equivalent power of 500 MWe)
- at least 1000 units of 100 kWe power (annual equivalent power of 100 MWe)
- at least 1000 units of 250 kWe power (annual equivalent power of 250 MWe)

Figure 4.64 compares results obtained adding different values of cost contingency for a 100-kWe system

As a reference, FuelCell Energy Inc. (GhezalAyagh, 2014), has estimated a minimum annual production of 250 MWe (considering different stack power) in order to be below DOE target cost (see Figure 4.65). Fuel Cell Energy Inc. stack factory costs in (\$/kW_{dc gross}) are in 2011\$ and it is not known if non-recurring expenses (as for example R&D and engineering costs) are also included.

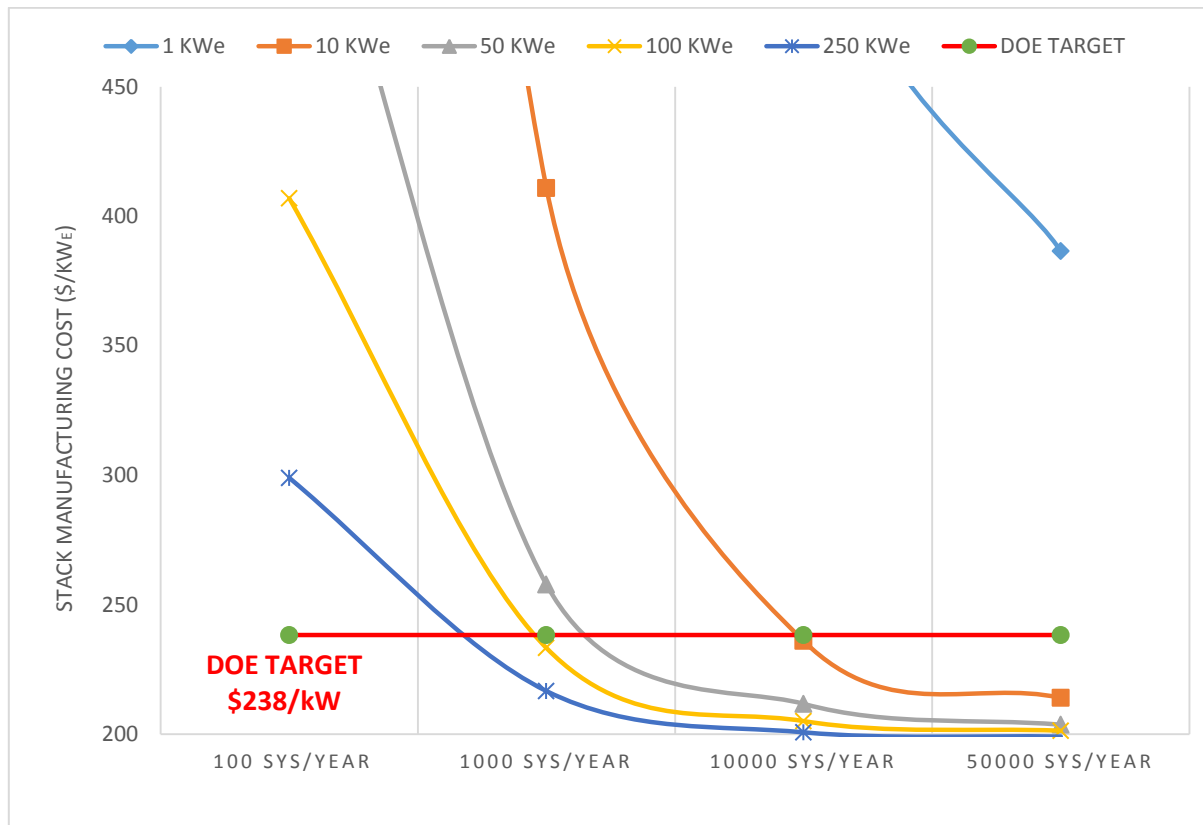


Figure 4.63. Modeled stack manufacturing costs with an additional 20% cost vs. DOE target at all analyzed volumes (in 2015\$)

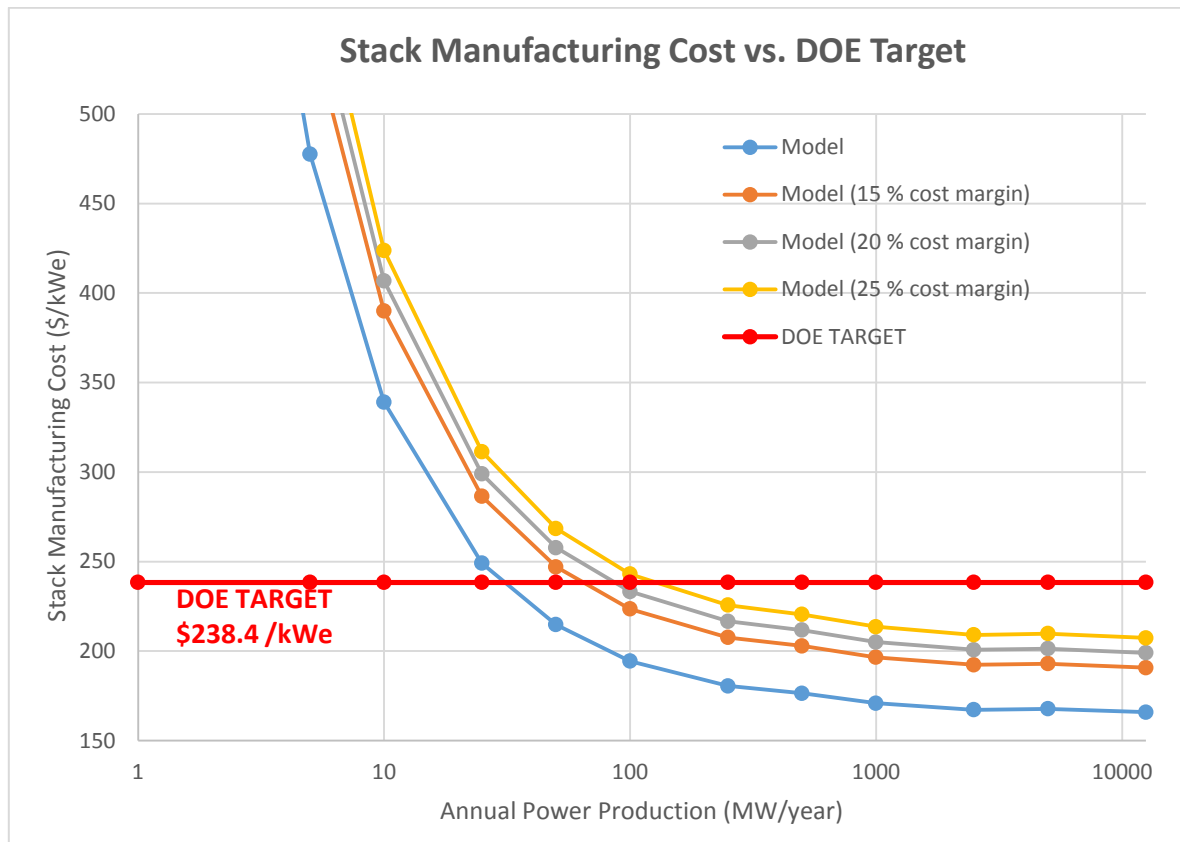


Figure 4.64. Stack manufacturing cost for 100-kWe system vs. DOE target considering different values of cost contingency

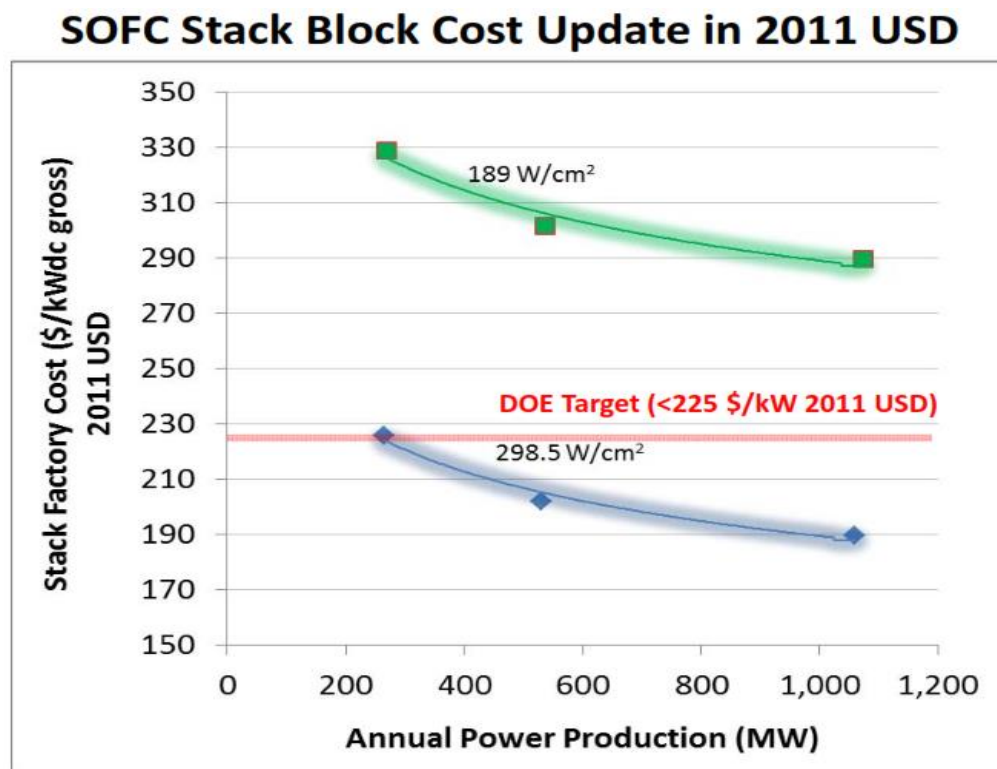


Figure 4.65. Fuel Cell Energy Inc. Stack Factory cost vs. DOE target(GhezelAyagh, 2014)

Comparison of modeled values with Strategic Analysis results

As one point of reference, the cost modeling results of this work are compared here with the cost estimates by Strategic Analysis (James, Spisak, & Colella, 2012). The present work is based on a cell-to-window frame geometry, a co-firing process of all layers of the cell in a single sintering step and a PVD coating of interconnect.

Stack design chosen by Strategic Analysis has a similar power density (291 W/cm²) but is based on a cell-to-edge geometry of the cells (i.e., the NexTech Flexcell design). Some of the different manufacturing technologies involved are:

- Stamping and MCO coating of cathode
- Stamping and wash coating of anode
- Tape casting of electrolyte and anode substrate
- Spraying and annealing of anode-electrolyte interlayer
- Screen printing and annealing of electrolyte-cathode interlayer
- Stamping and MCO spray coating of interconnect (thickness 200 μm)
- Isostatic pressing of electrolyte and support layer
- Sintering of electrolyte and support layer
- Tape casting of cell-to-cell ceramic seals

It is expected that a simpler stack design with fewer annealing processes and parts handling steps would further reduce manufacturing cost of the SOFC stack. For this reason, it is interesting to compare the estimated manufacturing cost of the two different designs.

Figure 4.66 compares both stack costs considering a power of 100 kWe per stack and production volumes of 100, 1,000, 10,000, 50,000 stacks per year. These cost differences are related mainly to:

1. Lower cost of co-firing process in this work compared to multi-step firing and annealing processes (see Figure 4.67)
2. Higher manufacturing cost of modeled interconnect here because of the higher thickness (625 μm) and the more expensive PVD coating process if compared to spray coating (see Figure 4.68)
3. Lower cost of modeled cell-to-cell sealing process since sealing paste dispensing here is much cheaper than seals tape casting process (see Figure 4.69)
4. Modeled frame and cell-to-frame seals manufacturing cost repeat unit cost are somewhat lower at higher volume than cell-to-window frame geometry (see Figure 4.71)

In case of low production volume (100 units per year) modeled stack costs were found to be higher than those evaluated by SA. This is because at low volume, the high capital investment and labor cost, makes the impact of higher frame cost, cell-to-frame seals cost and interconnect cost more dominant than the cost reduction from the co-firing process. On the contrary, in case of production volume higher than 100 units, the modeled values are significantly lower than SA values since co-firing process has a greater impact on reducing stack cost and this impact increases with production volume.

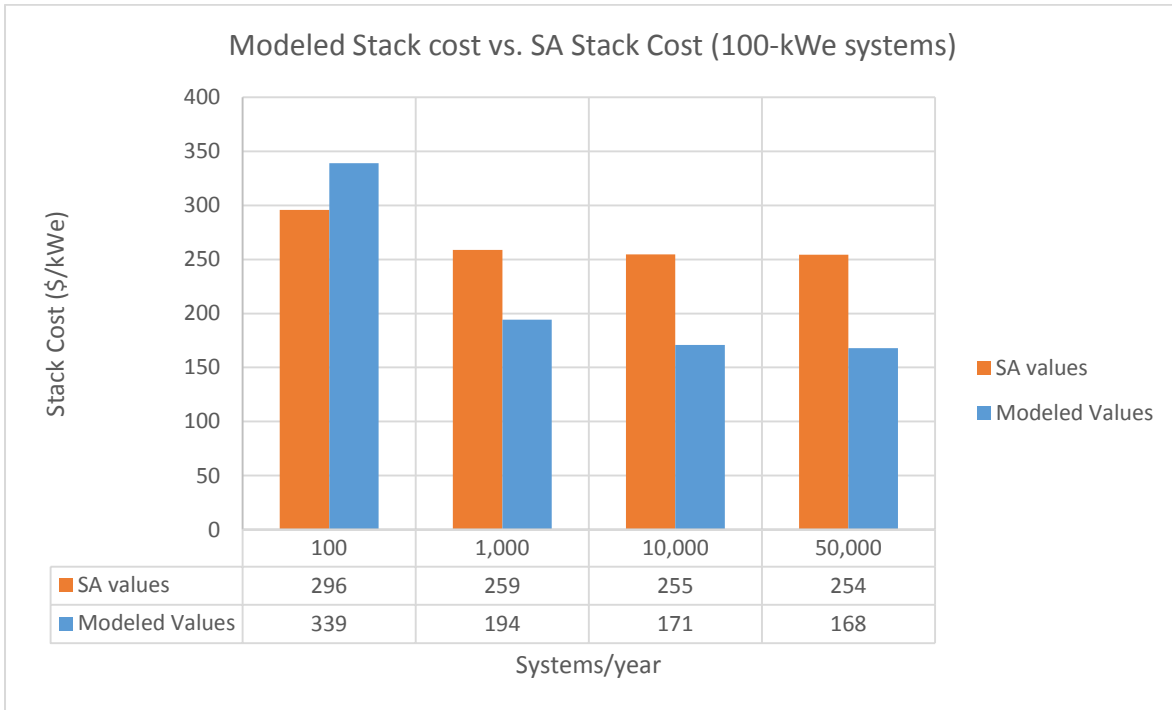


Figure 4.66. Modeled Stack cost vs. SA Stack Cost for a stack power of 100 kWe

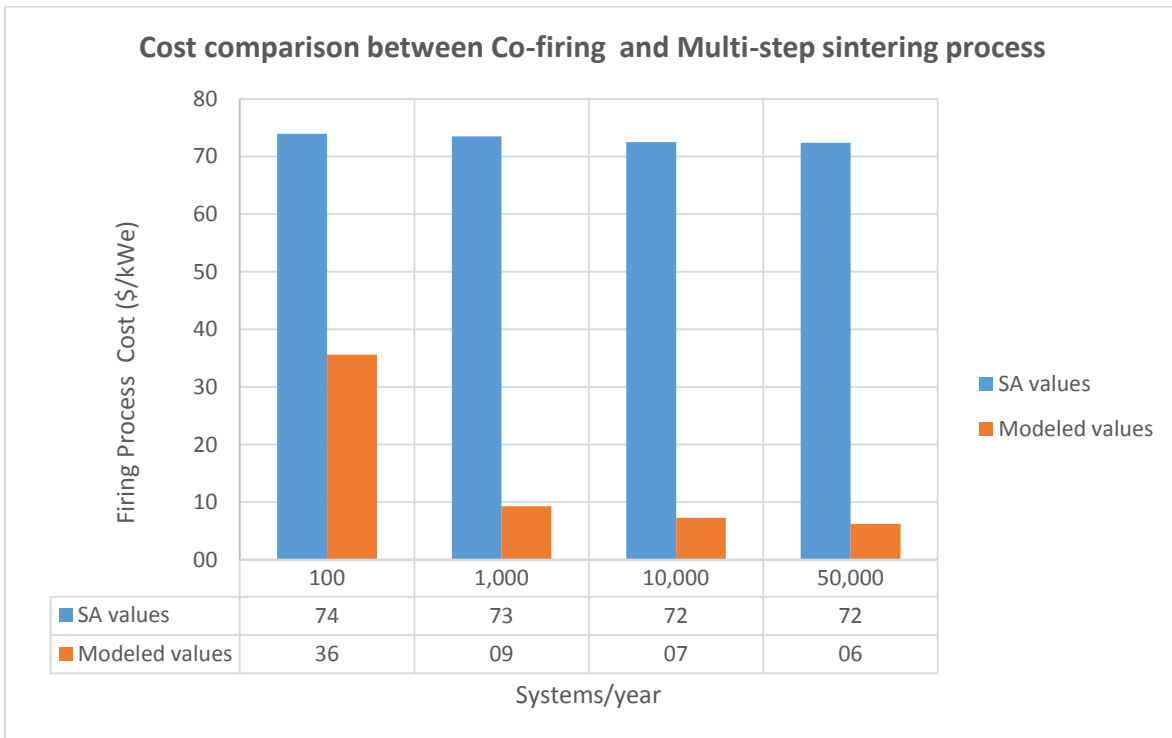


Figure 4.67. Cell Co-firing and Multi-step sintering cost comparison for a 100-kWe stack

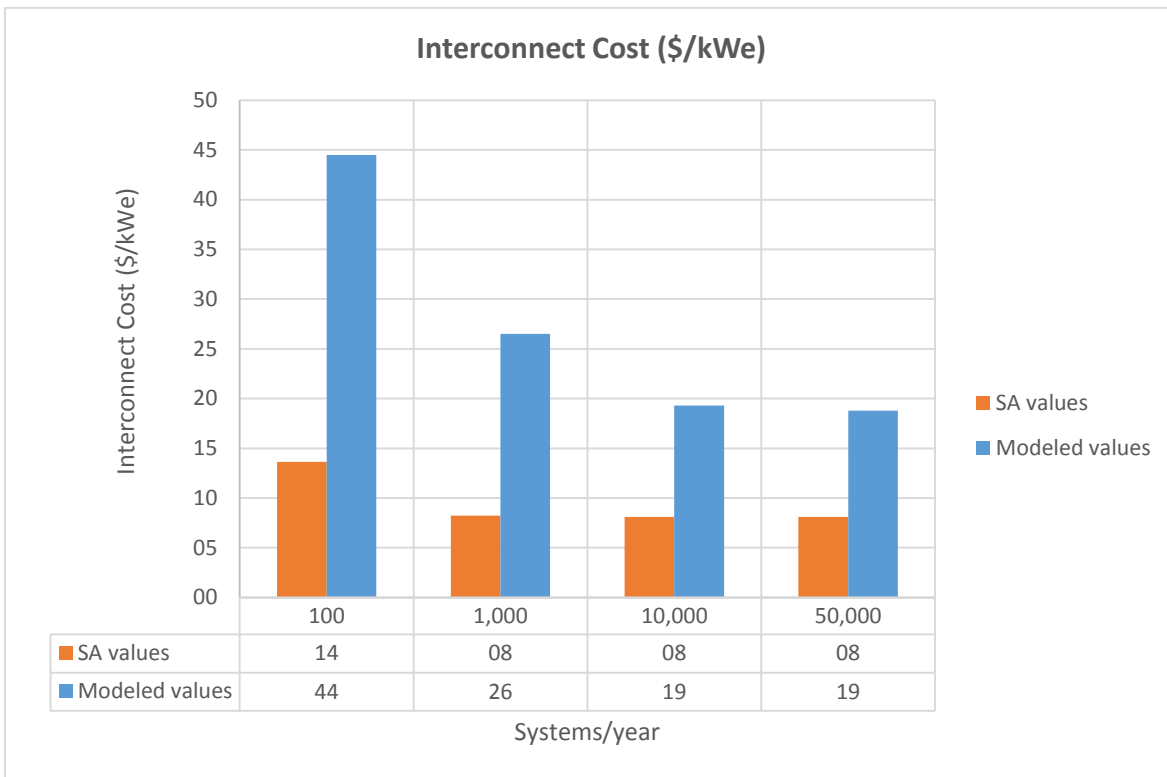


Figure 4.68. Interconnect cost comparison for a 100-kWe stack at all production volumes

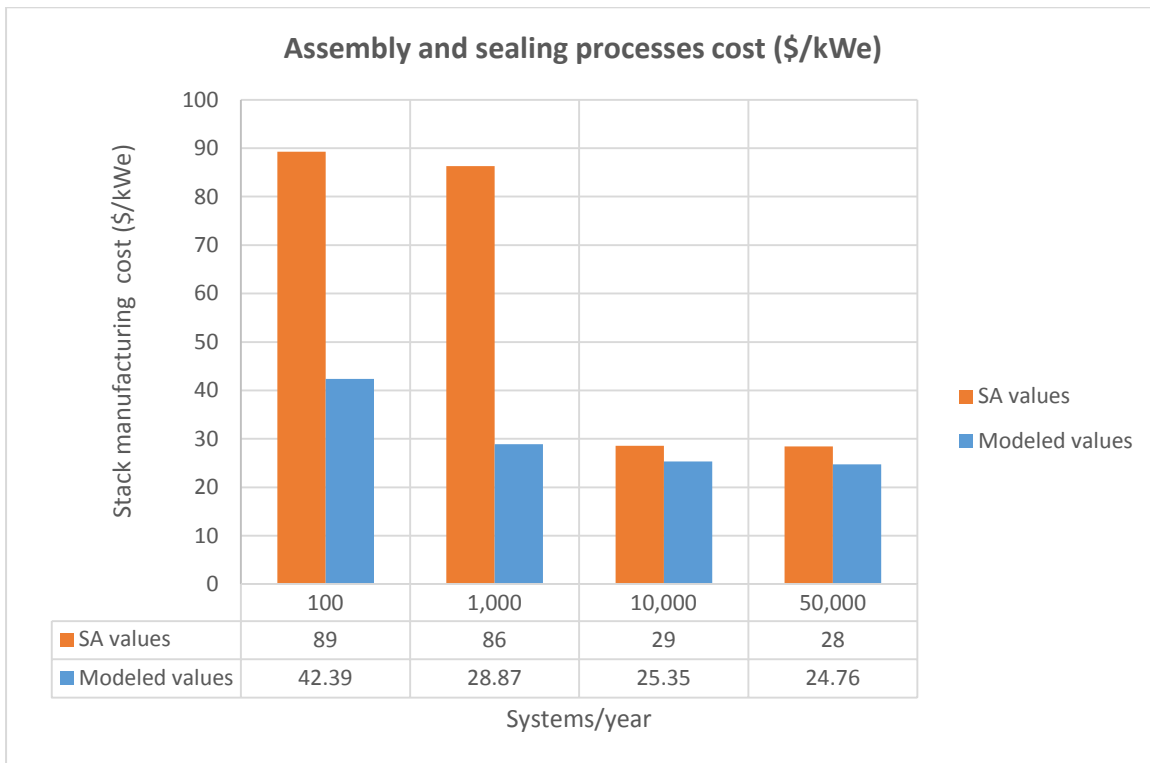


Figure 4.69. Cost comparison of assembly and sealing processes for a 100kWe stack

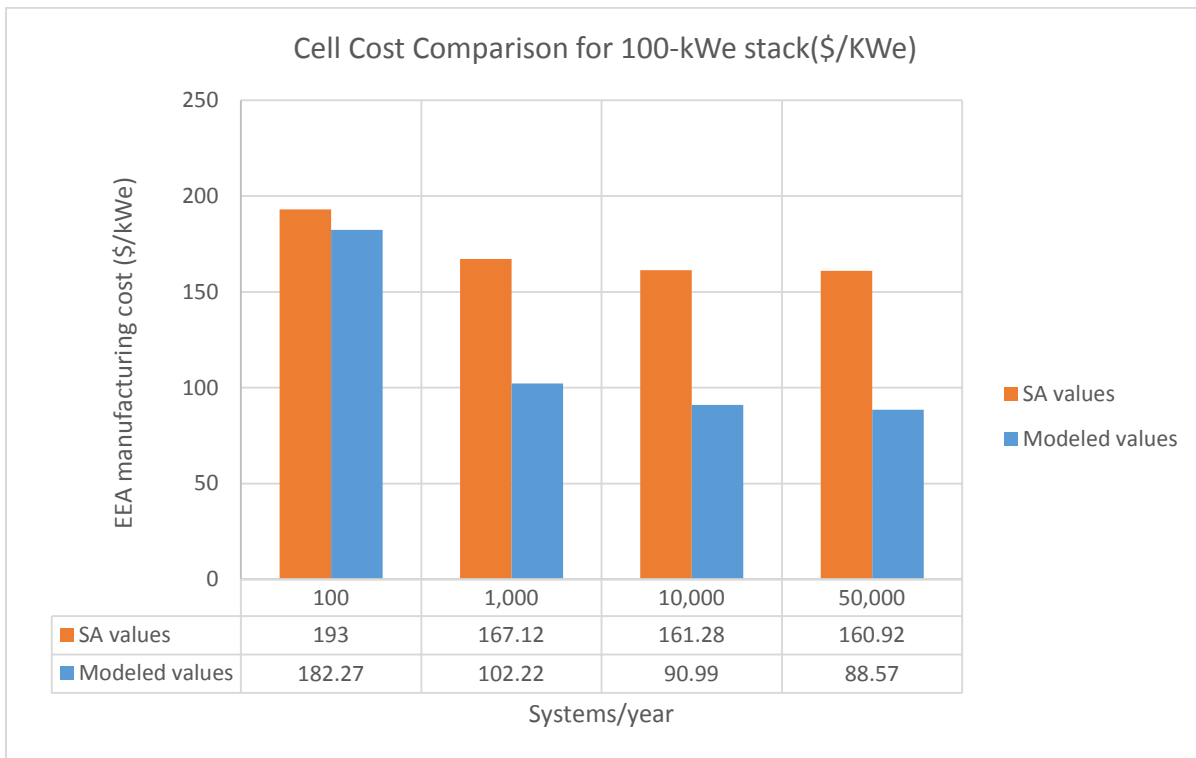


Figure 4.70. Cell cost comparison for a 100-kWe stack at all production volumes

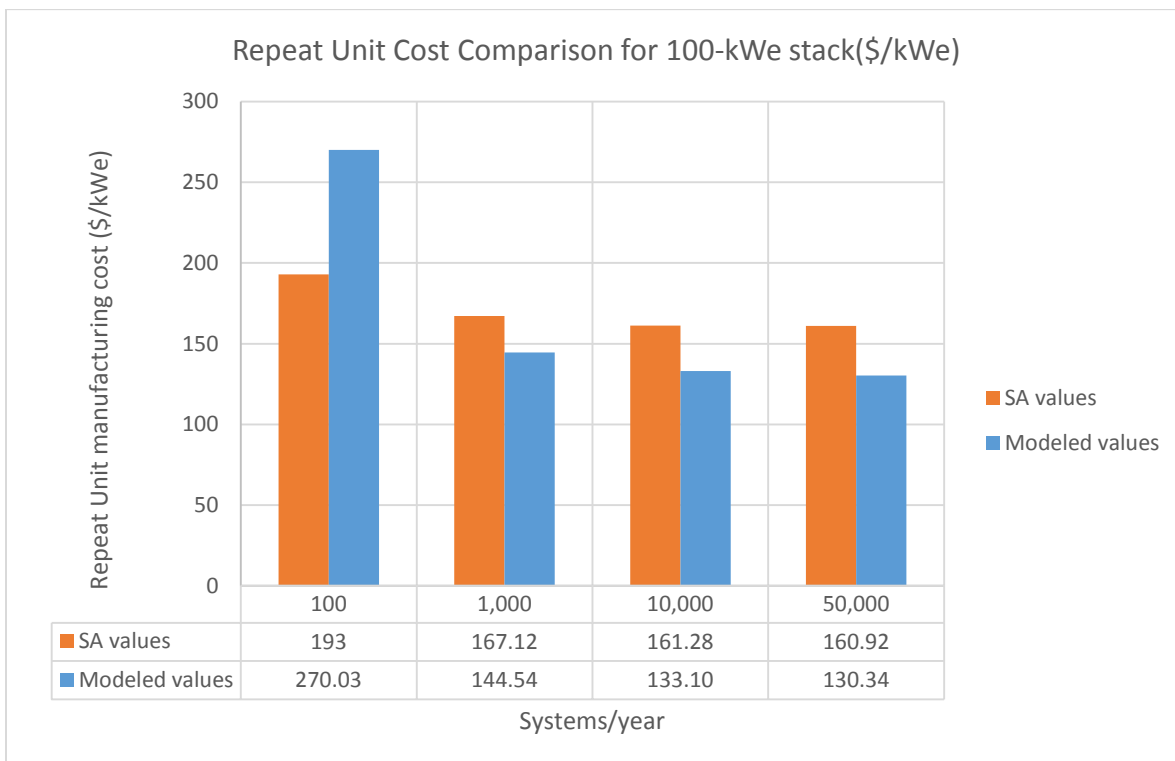


Figure 4.71. Repeat Unit cost comparison for a 100-kWe stack

Stack Costing Summary and Directions for Future Work

Based on the present analysis, it was found that stack cost per unit of electric power (\$/kWe) decreases both with increasing system size and increasing annual production rate. As system size or system manufacturing rate increase, stack cost decrease. In comparing the two key cost drivers, cost seems to be more sensitive to system size than to production rate.

Considering the same cumulative global produced capacity, stack costs decrease with larger SOFC system size. This cost reduction is only related to stack assembly and conditioning cost. Based on the stack assembly and conditioning process cost results, it is more cost effective to assemble and test fewer large stacks as compared to a large number of lower power stacks.

This work finds that the greatest contributor to the stack manufacturing cost is the electrode-electrolyte assembly unit (EEA), representing about 40-55% of the stack cost. Anode manufacturing costs accounts for 45-70% of total costs. The one-step co-firing process represents the most expensive manufacturing process followed by quality control, tape casting, and screen printing processes.

Both interconnect and cell-to-frame seal manufacturing costs constitute the next largest contributions to the stack manufacturing cost (each about 10-20 % of stack cost). The frame manufacturing cost contribution (0.5 to 9% of the stack cost) varies with annual power production since at low production volumes interconnect manufacturing lines can be utilized and thus there is no capital cost and building cost associated with the frames manufacturing process, but additional capital and building costs are required at higher volume.

At low annual power production (<10 MWe/year) capital and labor costs most affect the stack cost since the investment cost for equipment is prohibitive, equipment utilization is low and manual manufacturing processes are involved. By contrast, at the highest volumes material cost dominate (about 60% of stack cost) with capital, operational and labor costs constituting each about 10-12% of stack cost. Scrap costs constitute 3-6% of stack cost and decrease with production volume since it is assumed that an increasing level of automation is employed, quality control and inspection systems are more efficacious, and manufacturing process yield increases.

In analyzing material costs, it was found that off-shore supplier quotes (mainly from China and Japan) are competitive with U.S. distributors. Regarding material cost escalation, for production volumes varying from 0.1 MW to 50 MW per year, prices in (\$/kg) decrease dramatically with the opportunity for reduction of cost by 60%.

Labor cost decreases substantially with both production volume and level of automation ranging from a maximum of \$312/kWe to a minimum constant value of about \$18-20/kWe for annual power productions higher than 100 MWe where all manufacturing processes are fully automatic. This demonstrates that an increase of automation can reduce labor cost but at the same time, a high market demand is required in order to make the investment in capital equipment economically viable.

In comparing the two cell-to-frame seal options analyzed (barium-calcium-aluminosilicate based glass and Ag-CuO-TiO₂ braze), brazed seals are cheaper only when annual production volumes are lower than 5 MWe per year because the effect of a smaller brazing time in decreasing cost is greater than the countervailing increase in silver price. By contrast, at higher volumes glass seals are more affordable and the cost difference between the two alternatives varies from 7% to 19% depending on production volume and furnaces capacity (cycle time).

For interconnects and metal frame, the most common Fe-Cr alloys (e.g., stainless steel 441) for intermediate temperature SOFC are more cost effective than the use of Crofer 22 APU. Based on the modeled values, the use of Crofer 22 APU can increase the cost of metal parts by 15-40% and the cost difference between the two designs rises with production volumes for all stack size. In addition, a reduction of interconnect MCO coating thickness has a great impact on decreasing interconnect manufacturing costs. For example, a reduction of thickness from 15 to 5 μm can reduce the cost of interconnects by 15-28%.

Cathodic arc plasma spray deposition provides a high ionization rate and short cycle times compared to the other physical vapor deposition technologies, and coating thickness of 15-20 μm are required in order to obtain good performance as corrosion resistance and lifetime stability. Therefore, a key opportunity for interconnect manufacturing cost reduction would be to demonstrate that lower coating thicknesses are feasible for this kind of application.

In comparing the stack design chosen as a base case (SS441 interconnect, SS441 frame and cell-to-frame glass seals) with the alternative and more expensive design analyzed (Crofer 22 APU interconnect, Crofer 22 APU frame and metal seals), we found that the choice of the alternative design would increase the stack manufacturing cost by 1-20%. The cost rise is driven by both increasing system size and increasing production volume.

Prior to evaluating the modeled stack manufacturing cost against the DOE SOFC stack cost target of \$238/kWe in 2015 dollars (NETL, 2013), a cost margin was added in order to cover minor pieces of equipment or parts replacement that were not explicitly costed. It was found that with a cost contingency of 10-20%, an annual power production of at least 100 MWe (10,000 units of 10 kWe) would be needed in order to meet the \$238 target. This result is somewhat consistent with the estimation of one industry report (GhezelAyagh, 2014) of at least 250 MWe annual but indicates that this work may underestimate overall stack costs. Furthermore, based on this study, the use of more expensive components as Crofer 22 APU interconnects or brazed seals precludes meeting the DOE cost target in all cases analyzed.

A comparison of modeled values with Strategic Analysis stack manufacturing cost estimation (James, Spisak, & Colella, 2012) indicates clearly that the adoption of a single step co-firing process is much cheaper than multiple firing steps of the cell and the corresponding cost saving increase with production volume. This result confirms that co-firing process can be a critical module for the scale-up, mass production and successful commercialization of the SOFC technology.

Moreover, assembly and sealing cost comparison demonstrates that glass sealing paste applied using dispensing robot during stack assembly is always cheaper compared to a tape casted rigid seal. The latter is always more expensive since it is formed separately through tape casting, sintering and laser cutting processes.

Finally, sensitivity analysis demonstrates that power density and process yield are the parameters that most affect the stack manufacturing cost. For example in the case of 50 kWe stack (10,000 units per year), with a 20% decrease of power density or process yield both shift the stack manufacturing cost from \$176.42/kWe to about \$212/kWe, whereas with a 20% increase of power density or process yield shifts the stack cost from \$176.42/kWe to \$149.83/kWe and from \$176.42/kWe to \$169.98/kWe respectively.

In addition, the sensitivity of these parameters increases with the production volume. In the case of 50 kWe stacks, a 20% decrease of process yield causes increases of EEA cell cost of 17.67% (100 units/year), 17.88% (1,000 units/year), 20.19% (10,000 units/year) and 21.74% (50,000 units/year).

Based on these results, the recommendations are:

- increased power density should be one of the first objectives of manufacturing R&D;
- scale-up to high volume production requires quality control and measurement technologies consistent with high-volume manufacturing processes; and
- accurate in-line inspection and final quality testing of EEAs and sub-assemblies prior to stack assembly are essential for fuel cell mass production.

Sensitivity analysis also indicates that EEA is highly cost sensitive to material cost and casting speed. This is because:

- anode manufacturing cost constitutes 45-70% of EEA manufacturing cost;
- anode material cost accounts for 75-85% of EEA total material cost ; and
- anode material cost constitutes 35-40% of the stack manufacturing cost at high volume (>50 MW per year).

R&D is needed to demonstrating the feasibility for reducing the anode thickness. Progress in this field would allow increasing the casting speed (and so EEA manufacturing throughput) and reducing EEA material contribution to stack cost. These observations are consistent with FuelCell Energy Inc.'s efforts to reduce the anode thickness to 600 μm (GhezelAyagh, 2014).

Line performance, which accounts for speed losses, is another important factor affecting the cost. A decrease causes an increase of annual operating hours and increase in labor and operational costs. Line availability, which accounts for losses due to malfunctions and unplanned maintenance, has a great impact on manufacturing cost only at high production volume where machine utilizations are high. At high volumes, a decrease of annual operating hours due to downtime losses can causes an increase of manufacturing lines needed (and so capital costs) to guarantee the required annual power production. To minimize these losses, accurate in-line speed controllers and process control tools should be implemented to check if equipment is running at its maximum designed speed and detect malfunctioning or technical imperfections.

5. Balance of Plant Costs

5.1. Overview

In this chapter, balance of plant costing for two different types of SOFC stationary fuel cell systems, namely 1) SOFC CHP and 2) SOFC power-only, are considered. The key differences in system design and configuration between these two will be discussed. For both applications, we examined the following:

- System operating on natural gas reformat
- System capacities of 1, 10, 50, 100, 250kWe
- System annual production volumes of 100, 1,000, 100,00 and 50,000 units

5.2. Costing Approach

The general approach used here is a bottom-up costing analysis based on the system designs described above. Key data and design information was gathered by examining existing fuel cell systems, consulting industry advisors, and examining various FCS specification sheets for data sources. Methods of determining the representative components found in this model range from inspection of existing stationary FCS, information gathered through surveys of industry partners, discussions and price quotes with vendors, and utilization of components used for common but similar functions in other applications. Thus, the system represented here reflects the authors' best assessment of existing or planned systems but does not necessarily capture all system components with exact fidelity to existing physical systems, nor does there exist a physical system that is exactly the same as that described here

The BOP is divided into six subsystems or subareas listed below:

1. Fuel Processing Subsystem
2. Air Subsystem
3. Heat Management Subsystem
4. Power Subsystem
5. Controls & Meters Subsystem
6. Miscellaneous Subsystem

For the CHP systems with reformat fuel, fuel processor costs were adopted from earlier work by Strategic Analysis (James et al., 2012). All other subsystem components were estimated using bottom-up costing analysis and vendor quotes. We did not consider the case of BOP components built in-house (i.e., "make" versus "buy") because the components are largely commodity parts (e.g. tanks, motors, cabinets, variable frequency drives, tubing, piping, inverters, valves, heat exchangers, switches). Our research team also deemed it unlikely that a FC manufacturer would embark upon a program of producing BOP commodity parts in-house, with infrequent exceptions still being investigated.

Thus, the BOP is largely assumed to be comprised of purchased components that are either assembled or integrated by a fuel cell system manufacturer. In some cases, customized designs are required for FC system applications since CHP systems are not being produced in high volume. However, they are still assumed to be comprised of commodity products that could be produced in larger volume in the future, and perhaps as more integrated sub-assemblies. In such cases, it is possible that a FCS manufacturer would work closely with a contract manufacturer or parts vendor to prototype and develop such subassemblies. This type of parts integration and subassembly design were not explicitly considered in this work, but may represent further cost-reduction opportunities.

5.3. System Terminology

The FCS consists primarily of the fuel cell stack and the balance of plant (BOP) components. The BOP includes items such as valves, compressors, pumps, inverters, wiring, piping, meters, controls, and all other components that are associated with the complete operation of the fuel cell system.

Six major areas make up the BOP for SOFC CHP system, shown in Figure 5.1:

1. Fuel Subsystem
2. Air Subsystem
3. Heat Management Subsystem
4. Power Subsystem
5. Controls & Meters Subsystem
6. Miscellaneous Subsystem

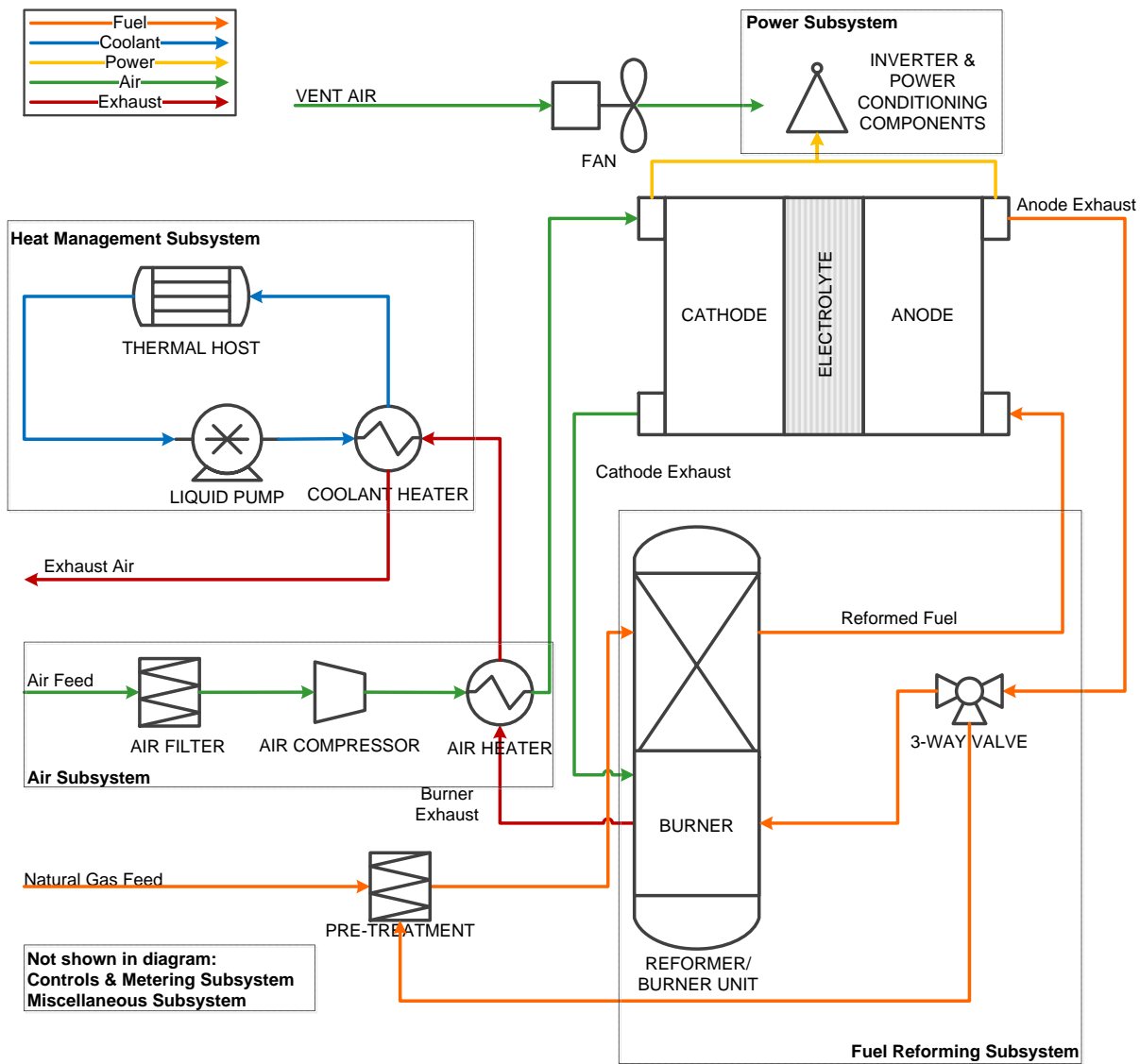


Figure 5.1. System Schematic of SOFC CHP system

Each subsystem is described below:

1. Fuel Processing Subsystem

The Fuel Processing Subsystem consists of a fuel processor for producing hydrogen fuel from natural gas. Pre-treated natural gas enters the burner and is reformed to hydrogen-rich gas in the fuel reforming unit. The reformed fuel enters the fuel cell stack and is re-circulated to the burner/reformer system through the 3-way valve. The fuel processing subsystem is comprised of components associated with the operation of the fuel reformer, which includes parts such as sensors, controls, filters, pumps, and valves.

2. Air Subsystem

The Air Subsystem consists of components associated with oxidant delivery to the fuel cell stack. Atmospheric air undergoes cleanup, compression, and heat treatment before entering the fuel cell stack. Additional components such as piping, manifolds and valves are employed for air delivery into the fuel cell stack. Gas sensors are also used to monitor oxidant levels throughout the system.

3. Heat Management Subsystem

The Heat Management Subsystem consists of liquid-liquid and liquid-gas heat exchangers associated with heat management in the FCS. For CHP operation, the exhaust heat from the burner unit and the fuel cell stack can be utilized to provide both water and space heating (thermal host) through the use of a liquid-liquid and gas-liquid heat exchangers. In order to obtain the costs of the heat exchangers, the maximum heat from the fuel cell was calculated using the thermal and electrical efficiencies from the functional specs found in the previous chapter. Using the value, the required heat exchange area was evaluated using the log mean temperature difference method (Incropera et al., 2007), where the required temperatures were obtained from our design specifications. Using the computed areas, the costs of the heat exchangers were computed for both brazed plate and bolted heat exchangers with cost functions available from an online database (Rafferty, 1998)

4. Power Subsystem

The Power Subsystem includes equipment for power inversion (from direct current (DC) to alternating current (AC) and power regulation. In order for fuel cells to deliver power at the required voltage, a DC-DC converter is used to regulate fluctuating DC fuel cell voltage input to a specified voltage output, particularly for direct DC backup power applications. For most stationary FC applications, the fuel cell will be connected to the electricity grid where AC power is required for residential or utility power. An inverter is necessary for converting the DC power provided by a fuel cell to AC power and an additional DC-DC converter may or may not be needed depending on system design and the characteristics of the inverter. A transistor and a transformer were included in this section to account for voltage fluctuations in the cell for the purposes of voltage and current conversions (step-up/down) to help meet the fluctuating electrical demands from the facility. A fan is included in this subsystem to provide air cooling of electronic components due to the potential of overheating. Additional components for the working operation of the power subsystem include relays, switches, fuses, resistors, and cables.

5. Controls & Meters Subsystem

The Controls and Meters Subsystem contains system controls-related components for system operation and equipment monitoring. During a fuel cell system's operation, variables such as flow rates, power output, temperature and cooling needs to be controlled. Sensors, meters and pressure gauges are used for system monitoring of these variables. A variable frequency drive (VFD) is used to control the system's actuation units, which include regulation of valves, pumps,

switches etc. A central processing unit (CPU) acts as the primary controller of the system, keeping the fuel cell system operating at the specified condition by monitoring the interaction between the monitoring sensors and actuating parts.

6. Miscellaneous Subsystem

The miscellaneous subsystem comprises external items outside of the stack that provides support, structure, and protection for the FCS. These items include: tubing, enclosure, fasteners, fire/safety panels, and labor.

Figure 5.2 shows the system design for SOFC electricity only case. Most BOP components remain similar to the CHP design. The most notable change is the absence of the heat management system. Heat from the burner is used for heating of the incoming air stream and directed out of the system without heat exchanger applications.

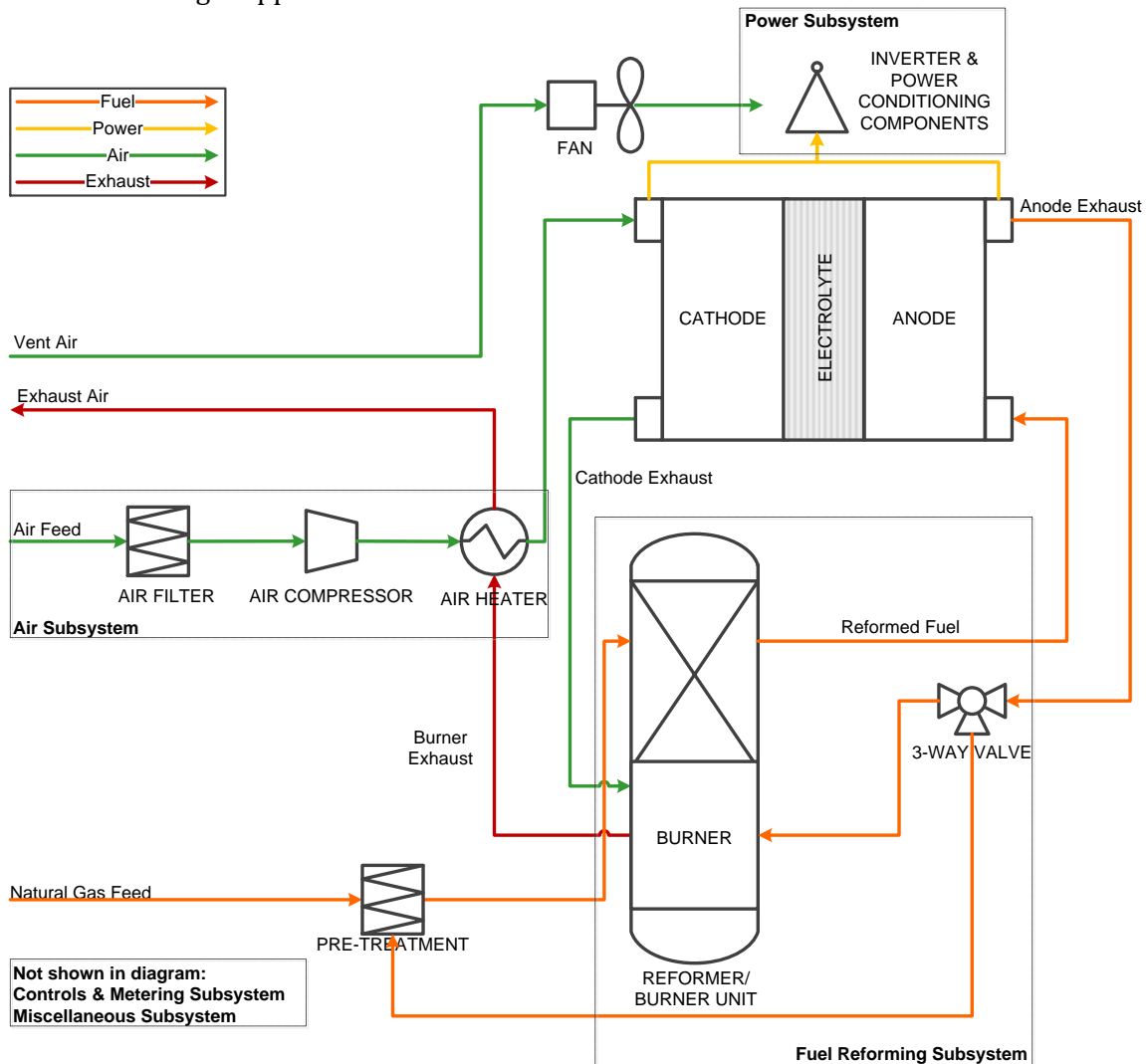


Figure 5.2. System schematic of SOFC electricity only system

5.4. Balance of Plant Cost Results

5.4.1. CHP System with Reformate fuel

In the CHP system with reformate fuel, the stationary fuel reactor is designed to carry out external natural gas steam reforming processes, which include fuel/air preheating, steam reforming, and water gas shift (WGS) reaction. In this report, the fuel processor costs were adopted from SA's previous work on fuel processors for their SOFC systems. The results from their DFMA analysis were scaled to higher power levels and adopted as a representation of cost for the Fuel Processing Subsystem.

Figure 5.3 displays the component breakdown of BOP subsystem costs for the 100-kWe CHP system with reformate fuel at production volumes of 100 and 1000 systems per year. For the 100-kWe CHP system, the Power Subsystem accounts for approximately 40% of the BOP costs at both volumes. The cost of the Power Subsystem is dominated by the power inverter, which accounts for approximately 85% of the subsystem cost. The second highest costing subsystem is the Controls/Metering Subsystem, where various flow and temperature sensors contribute to the subsystem's costs. All other subsystems contain fairly balanced costs among each component.

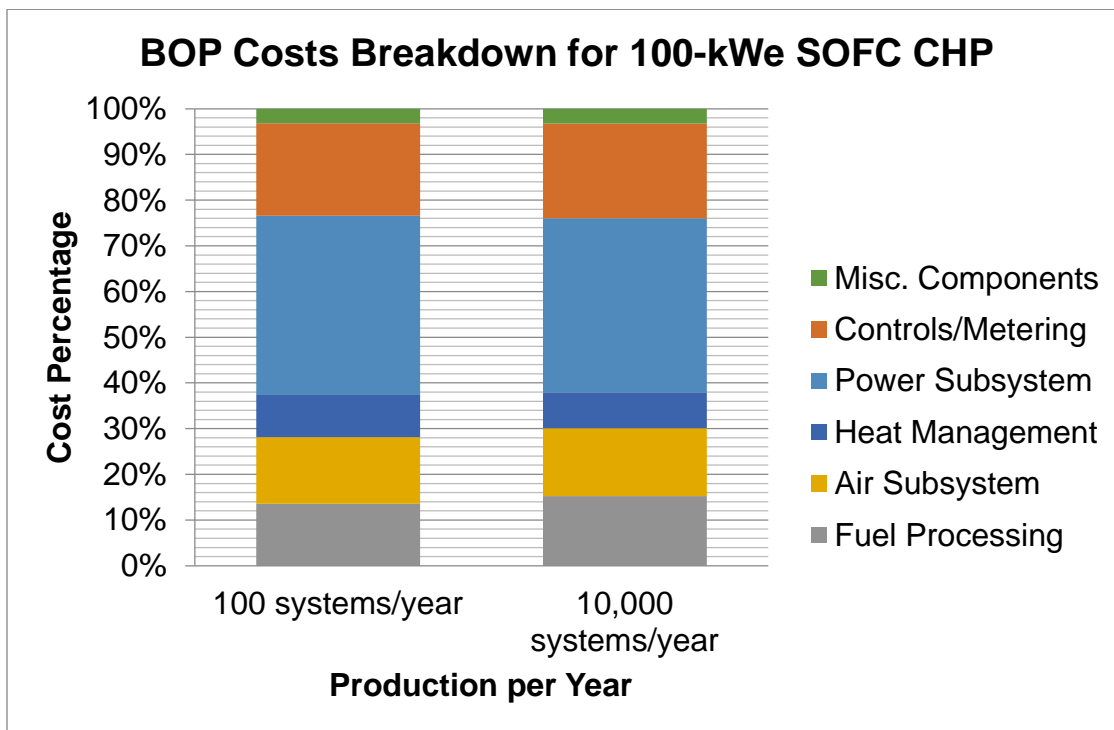


Figure 5.3. BOP cost breakdown for 100-kWe SOFC CHP, at 100 & 1000 systems/year

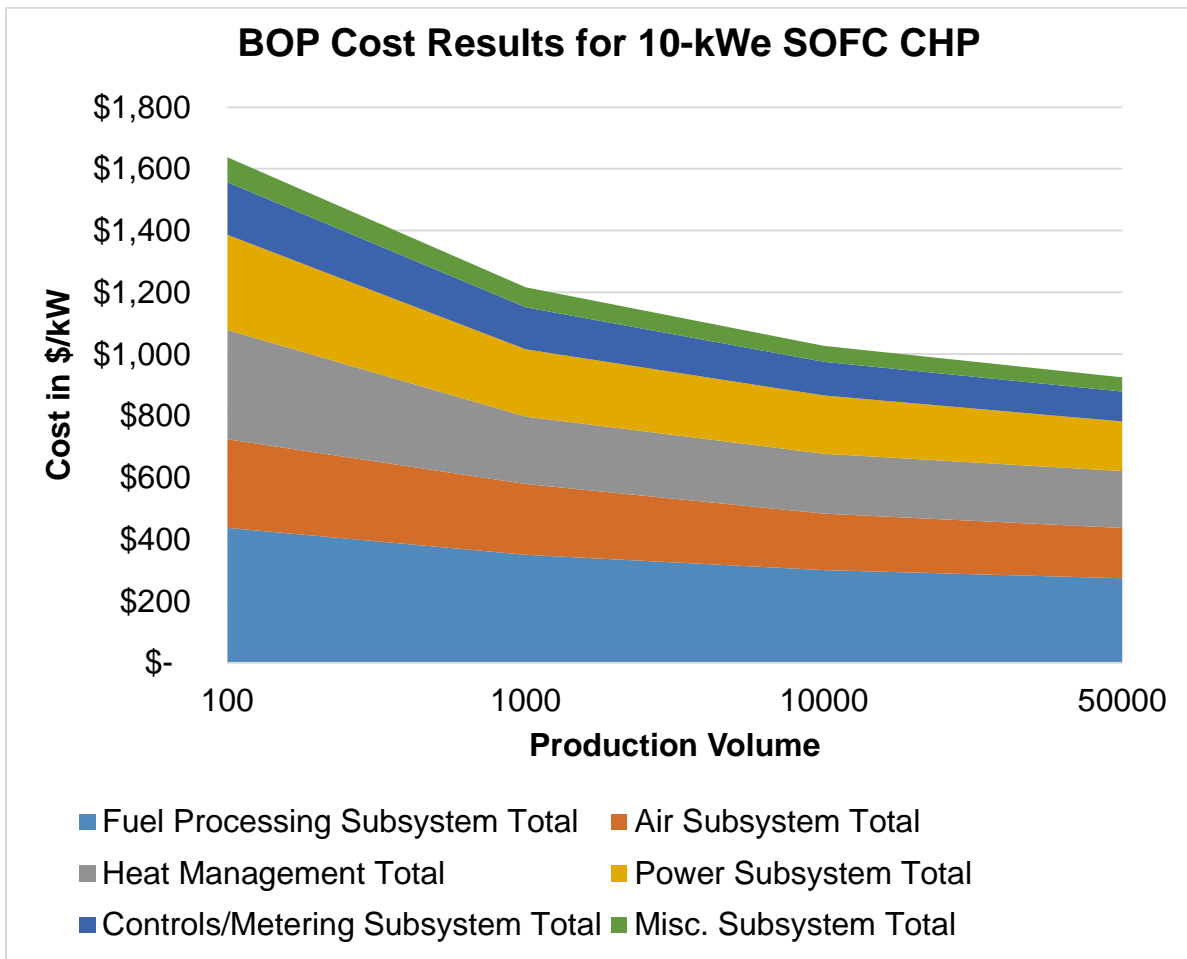


Figure 5.4. BOP costs as a function of manufacturing volume for 10-kWe SOFC CHP with reformate fuel

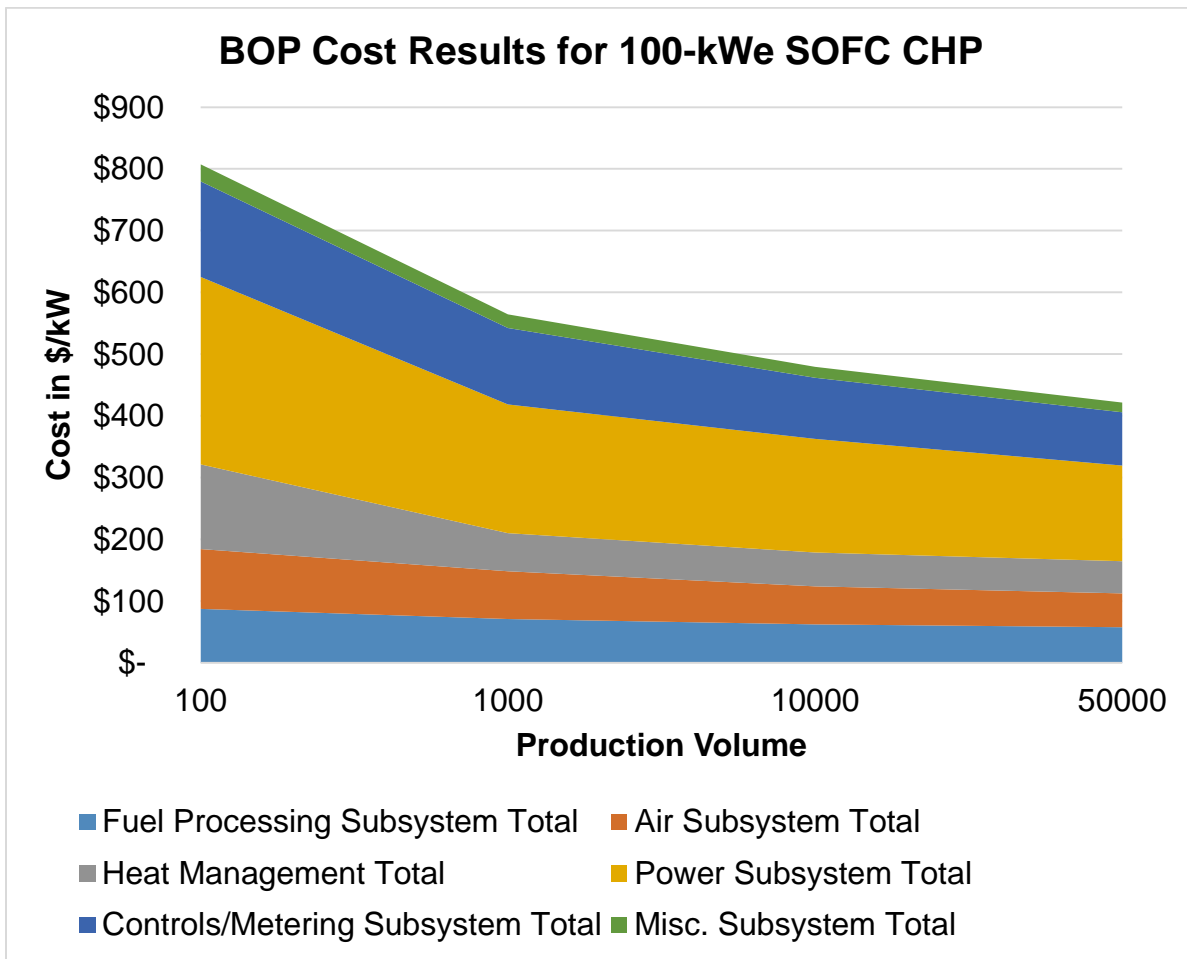


Figure 5.5. BOP costs as a function of manufacturing volume for 100-kWe SOFC CHP with reformate fuel

Figures 5.4 and 5.5 displays the BOP costs as a function of manufacturing volume for the 10-kWe and 100-kWe CHP system with reformate fuel. The cost per unit of electric output decreases with increasing manufacturing volume. Table 4.1 summarizes BOP cost results in dollars per kilowatt for all system sizes and at all production volumes. There is a general trend of cost reduction across increasing volume production and increasing system capacity. While both of these factors affect cost, increasing system capacity is seen to have a greater impact on driving cost per kilowatt down. For example, increasing production from 10,000 to 50,000 units/year for a 10-kWe CHP reformate system decreases BOP costs by an estimated 10%. Comparing this with the 50-kWe CHP reformate system at production of 10,000 units (i.e., equivalent to 10-kWe and 50,000 units per year or 500-MW net power annually), a cost reduction of 34% is achieved.

Table 5.1. Summary of BOP costs in \$/kWe for SOFC CHP

System Size	100 units/year	1000 units/year	10000 units/year	50000 units/year
250-kWe	\$ 693	\$ 488	\$ 419	\$ 365
100-kWe	\$ 807	\$ 564	\$ 479	\$ 422
50-kWe	\$ 1,002	\$ 721	\$ 611	\$ 537
10-kWe	\$ 1,638	\$ 1,217	\$ 1,027	\$ 925
1-kWe	\$ 9,295	\$ 7,117	\$ 6,045	\$ 5,428

Table 5.2 shows the volume reduction trend for 100-kWe SOFC CHP system with reformat fuel. The data shows that cost reduction is seen to be generally 20% per ten-fold increase in annual volume⁸, with the exception of the Heat Management and Controls Subsystem, where 55% and 31% are seen in the first ten-fold volume increase. In general, the highest cost reduction occurs in the first ten-fold increase in volume (e.g. increasing production from 100 to 1,000 systems/year), and decreases with the next volume increase.

Table 5.2. Volume reduction trend for 100-kWe SOFC CHP with reformat fuel

Cost Reduction from:	100-1,000 systems/yr	1,000-10,000 systems/yr	10,000-50,000 systems/yr
Fuel Processing Subsystem	19%	12%	7%
Air Subsystem	20%	20%	11%
Heat Management Subsystem	55%	11%	5%
Power Subsystem	31%	12%	16%
Controls/Metering Subsystem	20%	20%	13%
Misc. Components Subsystem	20%	20%	11%

5.4.2 Electricity Only System with Reformate fuel

This section presents results for SOFC with electrical power production only. The overall system design shares similarities with the CHP case, with the exception of the Thermal Management Subsystem. For the electricity only case, the burner exhaust is directed out of the system without space or water heating applications. Therefore, no space or water heating exchangers are needed for this design.

Figure 5.6 shows the BOP volume results for a 10kWe SOFC electricity only system. Note that the Heat Management is absent in this case and there are only 5 subsystems for the case of electricity only systems. Cost per kilowatt is driven by increase in production volume. For the electricity-only case, BOP costs exhibit a similar decreasing cost trend as the CHP case with increasing production volume. BOP costs are lower in comparison with CHP cases due to removal of both space and water heating heat exchangers. Similar trends are also seen across all system size for electricity-only cases.

⁸ Note that the last column of Table 5.2 represents a factor of 5 increase in production volume, so extrapolating to 100,000 systems gives reductions of 11%, 19%, 8%, 19%, 17%, and 19% from 10,000 to 100,000 systems per year (10X increase) for the respective subsystems.

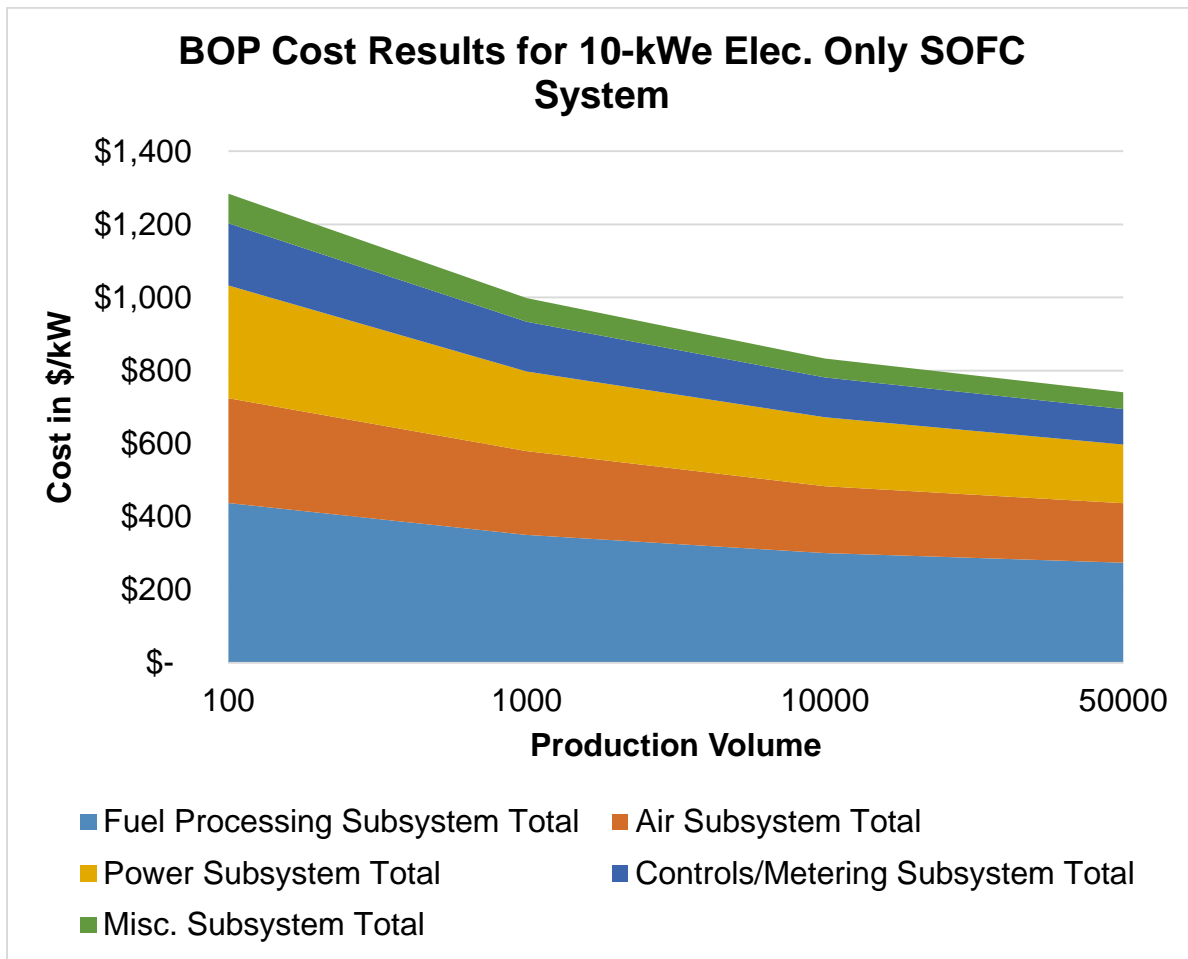


Figure 5.6. BOP costs as a function of manufacturing volume for 10-kWe SOFC electricity-only with reformat fuel

5.5. Conclusions

This part of the study presents a detailed balance of plant cost analysis for stationary fuel cell systems including the cost dependencies of increasing system size and increasing manufacturing volumes. The balance of plant encompasses components and structures outside of the fuel cell stack associated with the operation of the complete fuel cell system.

Based on the analysis, system costs (\$/kWe) decrease with both increasing system size and manufacturing volume. Volume reduction has a more significant effect in the initial volume scale-up, i.e. the greatest cost reduction occurs in the first ten-fold volume increase in production, from 100 systems/year to 1,000 systems/year. While production volumes affects costs, increasing system capacity also drives down BOP system cost per kilowatt.

For the CHP reformat system, the Power Subsystem represents the largest subsystem cost for the 100-kWe system, representing approximately 40% of the total BOP. In particular, the power inverter is a dominant cost driver, representing approximately 80% of the cost in the power subsystem. At about 23% of overall system cost, the power inverter is nearly as expensive as the stack at the 100-kWe system size. The second biggest subsystem is the Controls and Metering Subsystem, representing about 21% of the system.

For electricity-only systems where waste heat is not utilized, total BOP costs per kilowatt are reduced by 15-20% compared with CHP systems. This number accounts for the absence of heat exchangers needed for space and water heating applications.

The BOP analysis in this report provides greater detail in component requirements than previous fuel cell system cost studies that primarily focus on the cost of the stack. Our study uses a bottom-up analysis to account for the inclusion of the interconnected subsystems outside of the stack. We will see in the next chapter that the BOP can actually be the dominant cost driver in FCS assuming that fuel cell stack manufacturing adopts more fully automated processing with much higher production volumes than today. Most research to date has focused on cost reduction in the stack and overlooks the BOP. Our studies indicated that there is a need to assess BOP in greater detail. With increased manufacturing volume of fuel cell systems, there will be greater potential for fuel cell companies to standardize an increase in the number of BOP parts for specific fuel cell systems. Commoditization of BOP components for FCS may in turn significantly impact system cost which in turn can increase the market adoption of emerging fuel cell systems.

6. Total System Costs

Direct costs for SOFC CHP system as a function of system size and manufacturing volume are shown in Figure 6.1. In general, increasing system size has a larger impact than increasing manufacturing volume for the same annual cumulative production increase in MWe (e.g. moving from 10kWe, 100 systems per year (1MWe/yr) to 1,000 systems per year (10MWe/yr) compared to moving to 100kWe, 100 systems per year). This is driven by the BOP costs per kWe being more favorable in moving to a higher system power vs. a higher volume at the same system power, whereas the reduction in stack costs are comparable in moving to either higher power or higher volume.

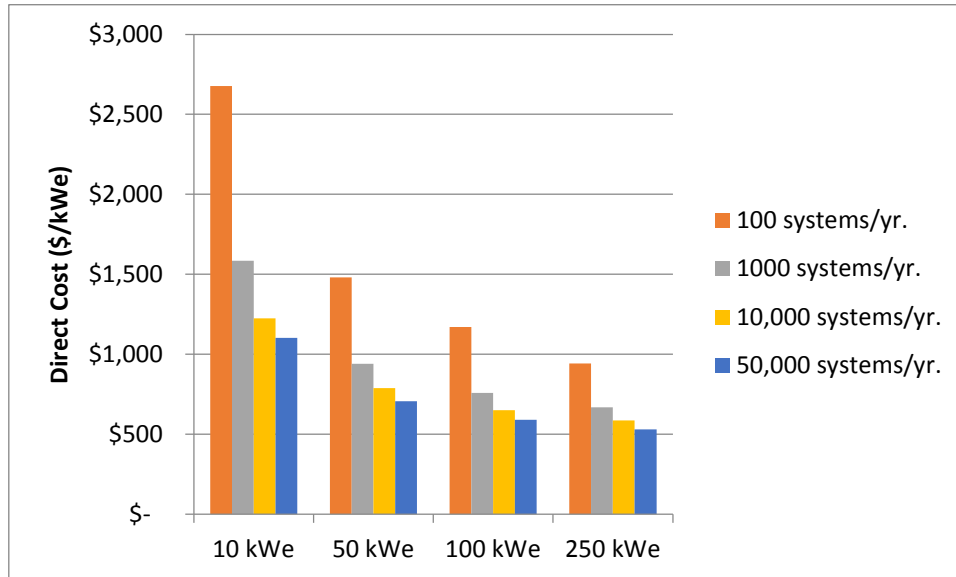


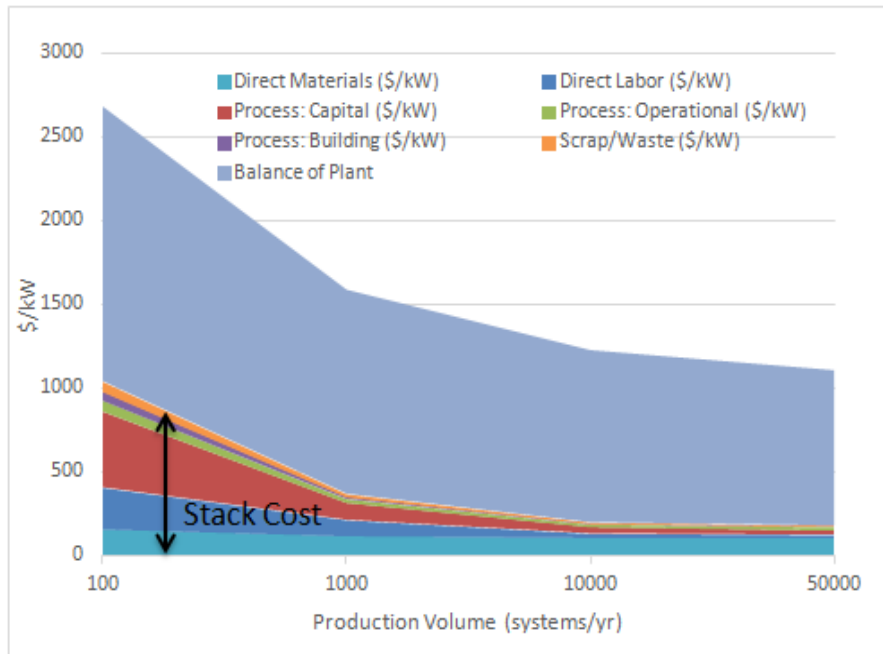
Figure 6.1 Direct costs for SOFC CHP systems as a function of system size and manufacturing volume.

Figure 6.2 shows the dependence of direct cost components as a function of annual manufacturing volume for 10-kWe, 50-kWe, and 100-kWe system sizes.

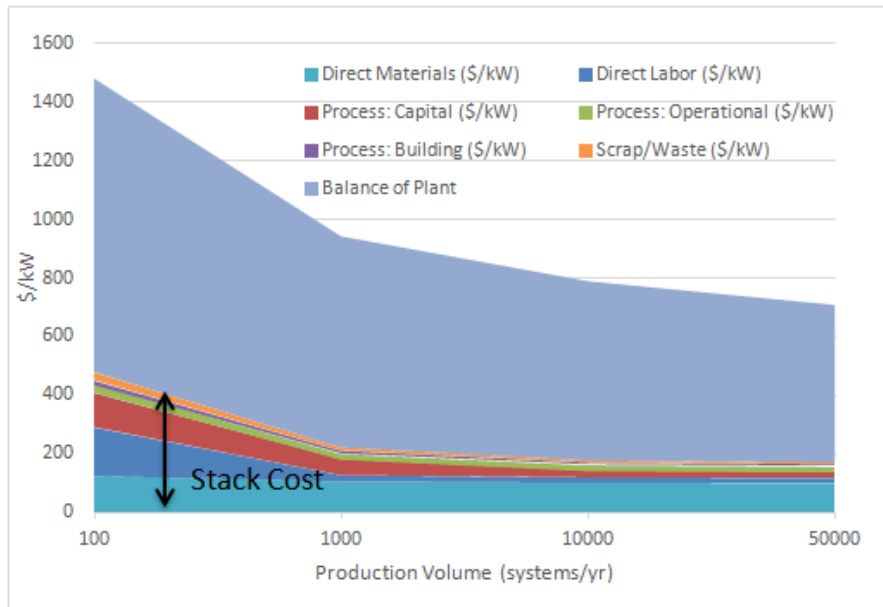
Table 6.1 has a summary of stack, BOP and total costs as a function of system size and annual manufacturing volume. Total direct costs and estimated price is also given assuming a corporate markup of 50% and an installed cost adder of 33%, following the earlier TCO report by Wei et al. (2014). The lower part of the table has cost declinations for the stack and BOP as a function of manufacturing volume or as a function of system size.

From the table, it can be seen that the BOP cost fraction of the overall direct system cost is in all cases greater than 60% of the system cost. In general at the lower system sizes, the BOP becomes a greater proportion of overall cost as manufacturing volume increases due to large reduction in stack cost which far outstrip reductions in BOP cost. At the higher system sizes (100kWe and 250kWe), the BOP fraction is roughly stable at 70% of overall costs since reductions in BOP cost as a function of volume are similar to reductions in the stack cost.

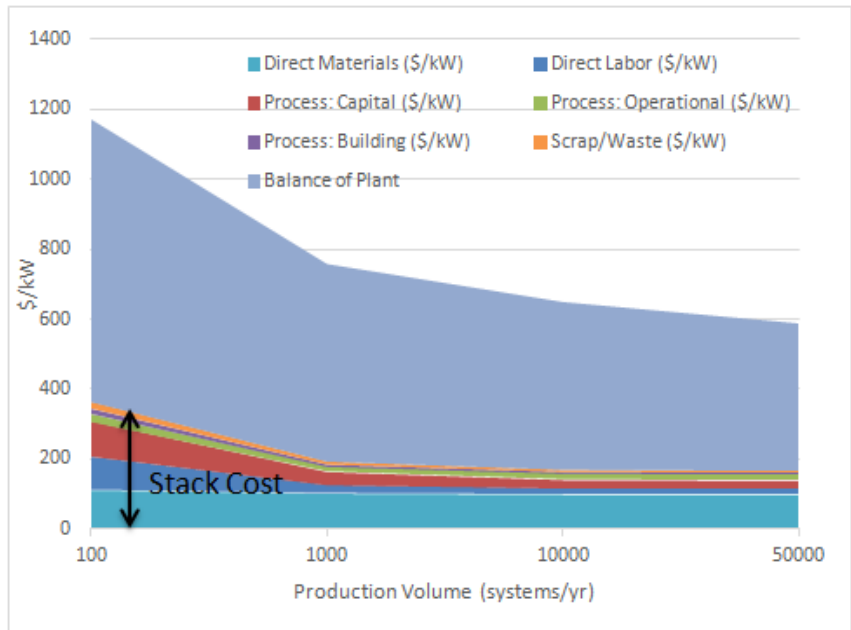
The largest stack cost reduction is observed at lower stack size and lower annual volumes, due large increases in tool utilization as volume is increased. Note that the stack cost is leveling off once a certain level of annual volume has been reached, e.g., the stack reduction in cost is very small in moving from 100kWe, 10,000 systems per year to 50,000 systems per year, or from 1GWe to 5GWe.



(a)



(b)



(c)

Figure 6.2. CHP direct system costs for 10, 50, and 100-kWe SOFC systems.

Table 6.1 . Summary of stack, BOP, total direct costs, and installed system costs with cost declination percentages as a function of annual manufacturing volume and system size.

System size	Stack Cost				BOP Cost				Total Direct Cost			
	Annual Manufacturing Volume				Annual Manufacturing Volume				Annual Manufacturing Volume			
	100	1000	10000	50000	100	1000	10000	50000	100	1000	10000	50000
1 kWe	\$ 5,387	\$ 1,196	\$ 459	\$ 322	\$ 9,295	\$ 7,117	\$ 6,045	\$ 5,428	\$ 14,681	\$ 8,313	\$ 6,504	\$ 5,750
10 kWe	\$ 1,039	\$ 367	\$ 197	\$ 178	\$ 1,638	\$ 1,217	\$ 1,027	\$ 925	\$ 2,677	\$ 1,584	\$ 1,224	\$ 1,103
50 kWe	\$ 478	\$ 220	\$ 176	\$ 170	\$ 1,002	\$ 721	\$ 611	\$ 537	\$ 1,480	\$ 941	\$ 788	\$ 707
100 kWe	\$ 364	\$ 194	\$ 171	\$ 168	\$ 807	\$ 564	\$ 479	\$ 422	\$ 1,171	\$ 759	\$ 650	\$ 589
250 kWe	\$ 249	\$ 181	\$ 167	\$ 166	\$ 693	\$ 488	\$ 419	\$ 365	\$ 942	\$ 669	\$ 587	\$ 530
	Stack Cost Fraction				BOP Cost Fraction				Price with corporate markup and installation cost			
1 kWe	37%	14%	7%	6%	63%	86%	93%	94%	\$ 29,290	\$ 16,584	\$ 12,976	\$ 11,471
10 kWe	39%	23%	16%	16%	61%	77%	84%	84%	\$ 5,341	\$ 3,160	\$ 2,441	\$ 2,201
50 kWe	32%	23%	22%	24%	68%	77%	78%	76%	\$ 2,952	\$ 1,877	\$ 1,572	\$ 1,410
100 kWe	31%	26%	26%	28%	69%	74%	74%	72%	\$ 2,337	\$ 1,514	\$ 1,297	\$ 1,176
250 kWe	26%	27%	29%	31%	74%	73%	71%	69%	\$ 1,879	\$ 1,334	\$ 1,170	\$ 1,058
	Stack Cost Pct Reduction fr. Previous Volume				BOP Cost Pct Reduction fr. Previous Volume				Total Cost Pct Reduction fr. Previous Volume			
1 kWe	-	78%	62%	30%	-	23%	15%	10%	-	43%	22%	12%
10 kWe	-	65%	46%	9%	-	26%	16%	10%	-	41%	23%	10%
50 kWe	-	54%	20%	4%	-	28%	15%	12%	-	36%	16%	10%
100 kWe	-	47%	12%	2%	-	30%	15%	12%	-	35%	14%	9%
250 kWe	-	28%	7%	1%	-	30%	14%	13%	-	29%	12%	10%
	Stack Cost Pct Reduction fr. 100 system/yr				BOP Cost Pct Reduction fr. 100 system/yr				Total Cost Pct Reduction fr. 100 system/yr			
1 kWe	-	78%	91%	94%	-	23%	35%	42%	-	43%	56%	61%
10 kWe	-	65%	81%	83%	-	26%	37%	44%	-	41%	54%	59%
50 kWe	-	54%	63%	64%	-	28%	39%	46%	-	36%	47%	52%
100 kWe	-	47%	53%	54%	-	30%	41%	48%	-	35%	44%	50%
250 kWe	-	28%	33%	33%	-	30%	39%	47%	-	29%	38%	44%
	Stack cost reduction fr. previous power level				BOP cost reduction fr. previous power level				Total cost reduction fr. previous power level			
1 kWe	-	-	-	-	-	-	-	-	-	-	-	-
10 kWe	81%	69%	57%	45%	82%	83%	83%	83%	82%	81%	81%	81%
100 kWe	65%	47%	13%	6%	51%	54%	53%	54%	56%	52%	47%	47%
50kWe	-	-	-	-	-	-	-	-	-	-	-	-
250kWe	48%	18%	5%	2%	31%	32%	31%	32%	36%	29%	26%	25%

A summary of direct system cost and prices with corporate markup and prices for installed systems is shown in Table 6.2. Comparing the equipment costs only with the DOE targets (reproduced below from Table 1.2) and assuming a 50% corporate markup, the 10-kWe system is meeting the 2015, and 2020 targets at 10,000 systems per year and 50,000 systems per year, respectively. The 250-kWe system meets the 2015 target at a volume of 100 systems per year, and meets the 2020 target at a volume of 10,000 units per year.

Table 6.2. Summary of total direct costs, price with corporate markup, and installed system costs for SOFC CHP systems. A corporate markup of 50% and installation factor of 1.33 is assumed.

System size (kWe)	Total Direct Cost			
	Annual Manufacturing Volume			
	100	1000	10000	50000
1 kWe	\$ 14,681	\$ 8,313	\$ 6,504	\$ 5,750
10 kWe	\$ 2,677	\$ 1,584	\$ 1,224	\$ 1,103
50 kWe	\$ 1,480	\$ 941	\$ 788	\$ 707
100 kWe	\$ 1,171	\$ 759	\$ 650	\$ 589
250 kWe	\$ 942	\$ 669	\$ 587	\$ 530
	Price with corporate markup			
1 kWe	\$ 22,022	\$ 12,470	\$ 9,756	\$ 8,625
10 kWe	\$ 4,016	\$ 2,376	\$ 1,836	\$ 1,655
50 kWe	\$ 2,220	\$ 1,412	\$ 1,182	\$ 1,061
100 kWe	\$ 1,757	\$ 1,139	\$ 975	\$ 884
250 kWe	\$ 1,413	\$ 1,004	\$ 881	\$ 795
	Price with corporate markup and installation cost			
1 kWe	\$ 29,290	\$ 16,584	\$ 12,976	\$ 11,471
10 kWe	\$ 5,341	\$ 3,160	\$ 2,441	\$ 2,201
50 kWe	\$ 2,952	\$ 1,877	\$ 1,572	\$ 1,410
100 kWe	\$ 2,337	\$ 1,514	\$ 1,297	\$ 1,176
250 kWe	\$ 1,879	\$ 1,334	\$ 1,170	\$ 1,058

Table 1.2. DOE Multiyear plan system equipment cost targets for 10-kWe and 100-250-kWe system sizes for 2015 and 2020, and NETL stack cost target.

System Type	2015 Target	2020 Target
10-kWe CHP System	\$1,900/kWe	\$1,700/kWe
100-250-kWe, CHP System	\$2,300/kWe	\$1,000/kWe
Stack Cost at high production volume (NETL 2013)⁹	\$238/kWe	

⁹ Stack Cost target is quoted for “Nth of a kind DG SOFC unit (1 GW cumulative installed capacity)” assumed to be achieved in 2030 (NETL 2013). The target in US2011\$ is \$225/kWe, or \$238/kWe in US2015\$.

7 Life Cycle Assessment (LCA) Model

Modeling the “total cost of ownership” (TCO) of fuel cell systems involves considering capital costs, fuel costs, operating costs, maintenance costs, “end of life” valuation of recoverable components and/or materials, valuation of externalities and comparisons with a baseline or other comparison scenarios. When externalities are included in TCO analysis, both “private” and “total social” costs can be considered to examine the extent to which they diverge and there are un-priced impacts of project implementation. These divergences can create market imperfections that lead to sub-optimal social outcomes, but in ways that are potentially correctible with appropriate public policies (e.g., applying prices to air and water discharges that create pollution).

TCO analysis also critically depends on the assumed duty cycle of operation of the equipment, resulting in the system “capacity factor” or utilization factor.¹⁰ For grid-connected CHP systems this is far less clear. The optimal (most economic) duty cycle for any given CHP installation depends on several complex factors, including site variables, prevailing utility rates and “standby charges,”¹¹ and site requirements. Various types of tools and analyses can help to address these key TCO considerations. In this chapter, we present the key components of the TCO model including life cycle cost modeling (LCC) and life cycle impact assessment modeling (LCIA), taking as an input the installed system costs presented in the previous chapter.

A rolled up summary of the model is described in the final section on “TCO Modeling” for several commercial building types in six different cities including Phoenix, Minneapolis, Chicago, New York City, Houston, and San Diego. These cities were chosen to represent several climate zones within the United States and to sample regions of the U.S. with differing mixes of grid-supplied electricity. Comparisons for FC CHP systems are to a “baseline” case of grid based electricity and conventional fuel-based heating systems (e.g. gas-fired water heaters and boiler systems). An LCC, LCIA, or TCO comparison with other technologies such as fossil fuel-fired or biomass-based CHP systems was not in the scope of this work but could be explored in future work.

7.1 Life Cycle Assessment (LCA) Model

According to the Environment Protection Agency (EPA, 2014a), life cycle assessment (LCA) can be defined as a technique to assess the environmental aspects and potential impacts associated with a product, process, or service, by studying and analyzing the following:

- Inventory of relevant energy and material inputs and environmental releases
- Potential environmental impacts associated with identified inputs and releases

The LCA101 document published by EPA, entitled "Life Cycle Assessment: Principles and Practice," provides an introductory overview of Life Cycle Assessment and describes the general uses and major components of LCA.

¹⁰ In this report, system availability is the percentage of hours in the year that the FCS is available for operation. For example, the system may not be available some hours due to scheduled maintenance. The system utilization is then defined as the percentage of kWh produced by the fuel cell system out of the total kWh of potential output at the nameplate power rating of the system and for the available hours of operation.

¹¹ Standby rates are charges levied by utilities when a distributed generation system, such as an on-site CHP system, experiences a scheduled or emergency outage, and then must rely on power purchased from the grid. These charges are generally composed of two elements: energy charges, in \$/kWh, which reflect the actual energy provided to the CHP system; and demand charges, in \$/kW, which attempt to recover the costs to the utility of providing capacity to meet the peak demand of the facility using the CHP system. Source: ACEEE, <http://www.aceee.org/topics/standby-rates>, accessed 5/29/14.

A typical LCA is made up from four stages including (Rooijen, 2006; Baratto, and Diwekar, 2005):

- Goal and scope definition
- Inventory analysis
- Impact assessment
- Interpretation

In this chapter an LCA model is developed to analyze energy, greenhouse gas emissions (GHG) and the costs associated with adoption of fuel cell systems in some commercial buildings within United States. LCA contains detailed analysis starting from pre-manufacturing and going to manufacturing, use and maintenance, and end-of-life phases (Figure 7.1). LCA also can include another phase that accounts for the impacts associated with fuel extraction and processing.

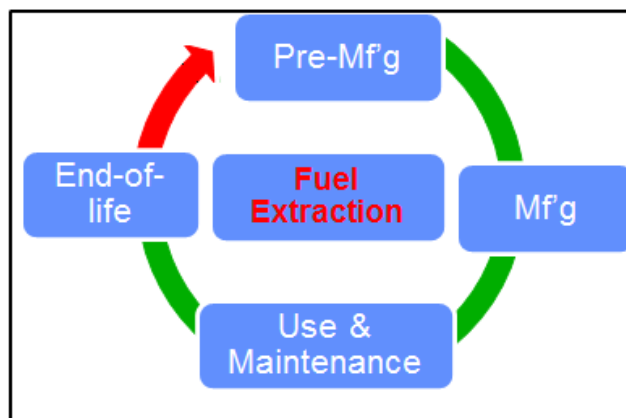


Figure 7.1. Life cycle assessment loop showing different lifetime phases

The objectives of this model are: (1) to provide a LCA model for a representative LT PEM fuel cell system, and (2) to provide a use-phase model of life-cycle costs of ownership including environmental assessments. Section 7.1.1 below discusses the use-phase model since it is the dominant phase for a FCS.

7.1.1 Use-phase Model

Use-phase is defined as the operational phase of the fuel cell system when it is functioning in the field as a backup, stationary power, or CHP system. The use-phase is the most demanding phase among LCA phases in terms of energy and cost and has the greatest GHG impact among all phases. Figure 7.2 below shows the sequence of steps in developing the use-phase model. The current use-phase model is developed for a CHP system operating on reformat fuel produced from natural gas input fuel, with the reforming process is assumed to be onsite. GHG emission analysis is based on the emissions associated with the reforming process and does not include fuel extraction and transportation.

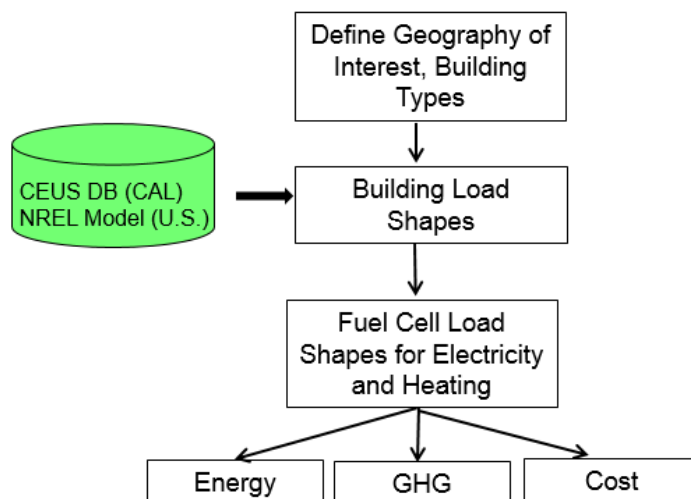


Figure 7.2. Flow chart showing methodology used in developing the use-phase model.

Inventory tables for the use-phase model include the following information:

- Prices of electricity and natural gas (NG). Electricity prices for peak/off-peak and demand charges as well as NG prices for several locations in U.S. have been compiled and stored in the model based on 2009-2013 EIA data and a national database of utility rates¹².
- Natural gas input required for both fuel cell and any NG required for boilers (if required).
- The emissions produced in the reforming process.
- Non-cooling electricity, electricity powered-cooling, water heating and space heating load shapes for several locations and commercial building types in U.S. have been collected using modeled data from National Renewable Energy Lab (Deru et. al, 2011) and stored in the model as a basis for electrical and heating demand calculations.
- The maintenance and replacement schedule for system components and parts that need to be replaced/refurbished during the system's lifetime (e.g. reformer, startup/battery and air compressor). Operation and maintenance (O&M) costs for fuel cell systems are usually correlated to the generated power by fuel system and expressed in (\$/kWh). This value is calculated from the expected costs associated with replacing/refurbishing some fuel cell parts/subsystems.¹³
- Displaced boiler, water heating, or space heating equipment is not included, under the assumption that the FCS does not have 100% availability. For example, especially in the near-term, planned or unplanned outages may reduce FCS availability to 90-95% and a conventional heating system is assumed to still be required for those times when the FCS is unavailable. System designs with redundant FC modules could improve overall system availability with a higher capital cost penalty, but were not included in this analysis. Higher expected FCS availability in the future should make these redundant expenditures unnecessary when 98-99%+ system availabilities are more fully proven.

¹² http://www.eia.gov/dnav/ng/ng_pri_sum_dcu_nus_m.htm and http://en.openei.org/wiki/Utility_Rate_Database, accessed on September 1, 2014.

¹³ Note that this O&M cost is different from the scheduled annual preventive maintenance as the latter is necessary to check if the system is functioning according to expectations and typically determined by the contract between customers and fuel cell vendor (exact value depends on the size of the system).

Table 7.1 below summarizes key parameters used in developing use-phase model and methodology used in collecting data.

Table 7.1. Key parameters used in developing use-phase model for reformat CHP systems.

Parameter	Description
Building Types	Small hotels and hospitals
Locations	Five different locations from different climate zones in the US were chosen for small hotel building type analysis. These locations are: Phoenix (AZ), Chicago (IL), Minneapolis (MN), New York City (NY), and Houston (TX). An additional city, San Diego (CA) was examined for large hospital cases.
Load Shapes	Electricity load, cooling load, space heating load and hot water load derived from NREL database for commercial building types ¹⁴ . Representative samples for 3 different days (weekday, weekend and peak-day) were tabulated for each month and then used to estimate monthly energy usages.
Fuel Cell System Size	Building dependent: <ul style="list-style-type: none"> • 10kWe or 50 kWe FCS for small hotels (non-load following) • 250kWe FCS for large hospitals (non-load following)
Waste Heat Usage	Waste heat can be used for: <ul style="list-style-type: none"> • Space heating and hot water (focus of this report) • Hot water only (future work)
Supplementary Energy sources	Purchased electricity from the grid if total electrical and cooling demand exceeds fuel cell capacity. Fuel-based conventional heating based conventional heating if the total space heating and water heating demand exceeds FC output at any given time.
Electricity Cost	State dependent (See Wei, et al. 2014)
Installed cost	\$2500/kWe for 10-kWe systems, \$1900/kW for 50-kW systems and \$1600/kWe for 250-kWe systems. ¹⁵
O&M cost	\$0.03/kWe
Scheduled maintenance cost	FC system size dependent
Natural gas price	State-specific averages from 2008-2013
FC System availability	96%
Lifetime of System	15 years

Figure 7.3 below shows the logic used in developing the use-phase model for a 50-kWe fuel cell system. This model has four inputs: electricity demand excluding cooling loads, electricity demand solely for space cooling using traditional electrically-driven vapor-compression air conditioners, hot water heating demand, and space heating demand as a function of time, as recorded in daily load curves for

¹⁴ The electricity load here refers to non-cooling load and the cooling load in kWh is split out explicitly. Note that load shapes for hospitals in San Diego were drawn from the California Commercial End Use Survey (CEUS).

¹⁵ There is a small difference in capital costs for each system size depending on whether it is providing water heating only or both water and space heating. However, this cost delta is less than 5% of total installed costs, and the higher cost value was taken for all cases.

three different days per month (weekday, weekend and peak day). These load shapes were collected from an NREL modeling simulation (Deru et al., 2011). Wei et al. (2014) contains some examples of these load shapes. The operating mode of this system will follow the total electricity load (sum of ‘non-cooling electricity load’ and ‘electricity for cooling load’), so that the fuel cell system will cover all of the electrical demand at any time when total electricity demand less than or equal to 50kWe; however, if the total demand exceeds fuel cell capacity (i.e. total electricity loads >50kWe) then the system will cover the 50-kWe maximum level and the remaining will be purchased directly from the grid. Similar logic is used for heating demand.

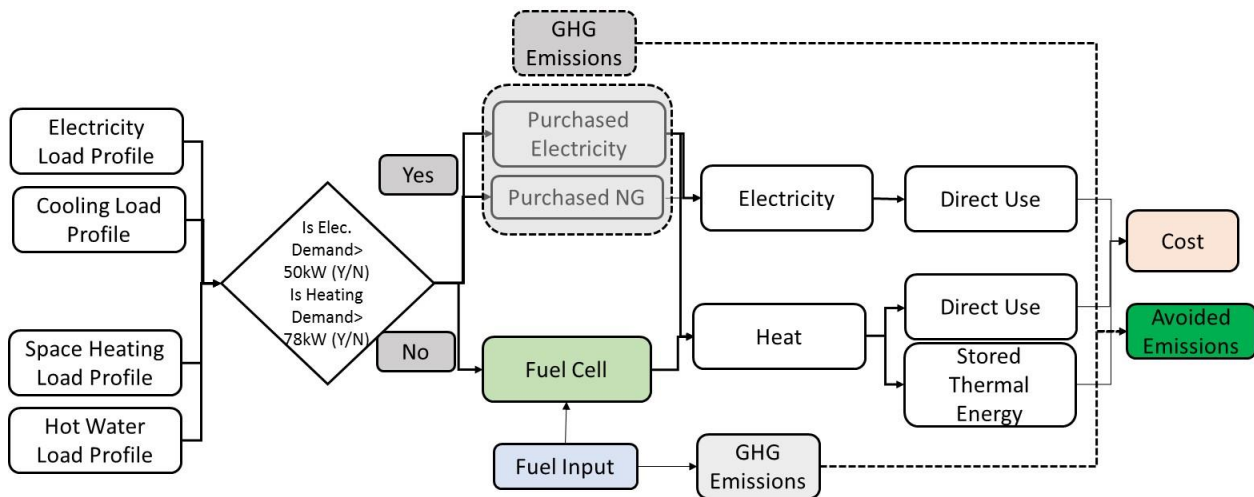


Figure 7.3. Flow chart and logic used to model 50-kWe CHP system with reformat fuel.

Previous studies have analyzed the ability of a stationary SOFC fuel cell system to thermally integrate with buildings based on the heat supply temperature from the fuel cell system, the space heating supply temperature, and the supply temperature for building service water heating systems. For example, space heating supply temperature can be estimated as $\sim 82^{\circ}\text{C}$ for large U.S. office buildings using hydronic fluid loops and as $\sim 23^{\circ}\text{C}$ for small U.S. office buildings using air circulation loops. The supply temperature for building service water heating systems can be estimated as $\sim 60^{\circ}\text{C}$ for both small and large U.S. office buildings using hydronic fluid loops (Colella and Srivastava, 2012). Recent field trials of about a dozen high temperature PEM fuel cell systems installed in commercial buildings showed an average heat supply temperature from the fuel cell system to the building of $\sim 48.4^{\circ}\text{C}$ (Dillon and Colella, 2014). The high temperature operation of SOFC fuel cell systems makes it ideal waste heat capture applications. To evaluate different design options, this analysis considered using the fuel cell systems to supply both space heating and hot water heating.

7.1.2 Results and Discussion

This section presents results for 10-kWe and 50-kWe SOFC FCS in small hotel building type in five different cities: Phoenix, Houston, Minneapolis, Chicago and New York. Six cities were examined (San Diego, California¹⁶ is also included) for 250-kWe SOFC FCS in large hospital buildings. These building types have more relative heating demand than other building types and are thus expected to be more favorable for CHP. Note also that Phoenix and Minneapolis represent two

¹⁶ Buildings in California were taken from a separate database (CEUS) that the non-California cities and did not include the small hotel building type. The California database includes other building types studied here such as hospitals and small offices.

extremes of the electricity grid: in Phoenix there is a relatively low carbon-intensity and Minneapolis there is a relatively high carbon-intensity with more coal power in the grid mix.

Electricity and heat utilization are shown in Tables 7.2-7.4 for 10, 50, and 250kWe. Electricity utilization is defined as the amount of electricity utilized from the fuel cell over the maximum amount of electricity that a fuel cell can generate. Similarly, heat utilization is the heat utilized from the fuel cell over the maximum heat output of a fuel cell. In general, a high utilization of both electrical and heat output of the system means that a CHP system achieves higher efficiency. In commercial buildings, the heating load is typically lower than the electrical load and higher overall system efficiency can be obtained by sizing the system to accommodate the heating load. However, from the previous chapter we have seen that smaller sized systems have higher installed costs in \$/kWe. A range of fuel cell sizes is chosen to explore the tradeoffs between FC capital cost and overall efficiency.

For the small hotel case, as shown in Tables 7.2 and 7.3, the overall heat utilization for space and water heating varies from 90-100% for the 10-kWe case and 45-84% for the 50-kWe case. The highest utilization occurs at the largest fuel cell capacity of 250kWe for space and water heating, which means that all heat from the fuel cell is utilized for space and water heating. In general, high electricity efficiencies are achieved across all system sizes. For 10kWe and 250kWe, maximum electricity utilization is achieved for all cities.

Table 7.2. Summary of FCS utilization factors for 10kWe CHP SOFC

FCS Utilization Factors for 10kW CHP SOFC	Heat Utilization: Space and Water Heating	Heat Utilization: Water Heating Only	Electricity Utilization
AZ	91%	88%	100%
IL	99%	98%	100%
MN	100%	99%	100%
NY	99%	98%	100%
TX	91%	91%	100%

Table 7.3. Summary of FCS utilization factors for 50kWe CHP SOFC

FCS Utilization Factors for 50kW CHP SOFC	Heat Utilization: Space and Water Heating	Heat Utilization: Water Heating Only	Electricity Utilization
AZ	53%	42%	91%
IL	83%	59%	82%
MN	84%	62%	82%
NY	82%	59%	75%
TX	45%	45%	86%

Table 7.4. Summary of FCS utilization factors for 250kWe CHP SOFC

FCS Utilization Factors for 250kW CHP SOFC	Heat Utilization: Space and Water Heating	Heat Utilization: Water Heating Only	Electricity Utilization
AZ	97%	16%	100%
IL	100%	24%	100%
MN	100%	26%	100%
NY	100%	24%	100%
TX	97%	17%	100%

Tables 7.5-7.7 show output results for use-phase models for small hotels (10,50-kWe) and large hospital (250-kWe) with a FCS providing both space and water heating. As shown Table 7.5, slightly lower costs are seen for most cities compared to the conventional alternative for a 10-kWe FCS providing space and water heating, with the exception of Arizona. There is about a 1-16% cost difference, with the highest cost difference occurring in New York. The overall cost of the FCS case in Arizona is within 1% of the No FC case.

For the 50-kWe FCS supplying both water heating and space heating, the overall cost of the FCS case is within 3-15% of the No FC case. However, for the cases of Minneapolis and New York, the cost of the No-FCS case is higher by 9% and 28%, respectively. This indicates that there may be a niche application for FCS for small hotels in both New York and Minneapolis due to a favorable spark spread and sufficient heating demand.¹⁷

For the 250-kWe FCS case supplying both water and space heating to a large hospital, the results vary greatly by geographic location. New York, Texas, and California shows lower costs for the FCS cases versus conventional heating methods, by 4-17%. New York and California exhibited the largest cost improvements, with 13% and 17%, respectively. For other geographic locations such as Arizona, Illinois, and Minneapolis, costs are within 1-5% of the No-FCS Case.

¹⁷ Spark spread is defined as follows: $SS = \text{Price of Electricity} - [(\text{Price of Gas}) * (\text{Heat Rate})] = \$/\text{MWh} - [(\$/\text{MMBtu}) * (\text{MMBtu} / \text{MWh})]$, or equivalently, the theoretical gross margin of a gas-fired power plant from selling a unit of electricity. Heat rate is often taken as 2.0 by convention for gas-fired plants. CHP systems powered by natural gas are more economically favorable in regions with large spark spread.

Table 7.5. Output results for use-phase models for 10-kWe small hotel

10kW FCS/ Space and Water Heating	AZ	IL	MN	NY	TX
Annual electricity demand (kWh)	576,668	424,147	419,590	369,661	497656
Annual heat demand (kWh)	100,261	254,840	301,855	251,944	83071
Annual electricity demand met by FCS (kWh)	84,096	84,096	84,096	84,096	84096
Annual heat demand met by FCS (kWh)	31,282	34,230	34,339	34,212	31390
Capital Cost	\$ 2,409	\$ 2,409	\$ 2,409	\$ 2,409	2409
O&M Cost	\$ 2,523	\$ 2,523	\$ 2,523	\$ 2,523	2523
Scheduled Maintenance	\$ 500	\$ 500	\$ 500	\$ 500	500
Fuel Cost- FC only	\$ 5,052	\$ 4,142	\$ 3,652	\$ 4,697	3727
Fuel Cost- Non FC	\$ 2,413	\$ 6,407	\$ 6,857	\$ 7,171	1325
Electricity Cost	\$40,333	\$25,495	\$35,998	\$46,949	32476
Demand Charge	\$ 3,635	\$ 3,460	\$ 1,937	\$ 8,882	9422
Fixed Monthly Charge	\$ 150	\$ 348	\$ 131	\$ 1,241	\$ 295
Total, FCS	\$57,014	\$45,283	\$54,006	\$74,371	\$52,677
No FCS	AZ	IL	MN	NY	TX
Fuel Cost- Non FC	\$ 3,574	\$ 7,449	\$ 7,779	\$ 8,352	\$ 2,185
Electricity Cost	\$47,305	\$32,104	\$45,374	\$61,530	\$39,414
Demand Charge	\$ 5,445	\$ 6,021	\$ 3,422	\$16,959	\$15,489
Fixed Monthly Charge	\$ 150	\$ 348	\$ 131	\$ 1,241	\$ 295
Total, No FCS	\$56,473	\$45,922	\$56,706	\$88,082	\$57,384
Percent Change with FCS	1.0%	-1.4%	-4.8%	-15.6%	-8.2%

Table

7.6. Output results for use-phase models for 50-kWe small hotel

50kW FCS/ Space and Water Heating	AZ	IL	MN	NY	TX
Annual electricity demand (kWh)	576,668	424,147	419,590	369,661	497,656
Annual heat demand (kWh)	100,261	254,840	301,855	251,944	83,071
Annual electricity demand met by FCS (kWh)	382,253	345,791	345,368	314,930	362,313
Annual heat demand met by FCS (kWh)	90,828	142,764	145,416	142,049	78,340
Capital Cost	\$ 9,153	\$ 9,153	\$ 9,153	\$ 9,153	\$ 9,153
O&M Cost	\$11,468	\$10,374	\$10,361	\$ 9,448	\$10,869
Scheduled Maintenance	\$ 1,000	\$ 1,000	\$ 1,000	\$ 1,000	\$ 1,000
Fuel Cost- FC only	\$25,252	\$20,705	\$18,254	\$23,481	\$18,629
Fuel Cost- Non FC	\$ 201	\$ 3,102	\$ 3,875	\$ 3,447	\$ 39
Electricity Cost	\$15,360	\$ 4,889	\$ 6,679	\$ 6,926	\$ 9,524
Demand Charge	\$ 3,635	\$ 3,460	\$ 1,937	\$ 8,882	\$ 9,422
Fixed Monthly Charge	\$ 150	\$ 348	\$ 131	\$ 1,241	\$ 295
Total, FCS	\$66,219	\$53,030	\$51,390	\$63,577	\$58,931
No FCS	AZ	IL	MN	NY	TX
Fuel Cost- Non FC	\$ 3,574	\$ 7,449	\$ 7,779	\$ 8,352	\$ 2,185
Electricity Cost	\$47,305	\$32,104	\$45,374	\$61,530	\$39,414
Demand Charge	\$ 5,445	\$ 6,021	\$ 3,422	\$16,959	\$15,489
Fixed Monthly Charge	\$ 150	\$ 348	\$ 131	\$ 1,241	\$ 295
Total, No FCS	\$56,473	\$45,922	\$56,706	\$88,082	\$57,384
Percent Change with FCS	17.3%	15.5%	-9.4%	-27.8%	2.7%

Table 7.6. Output results for use-phase models for 250-kWe large hospital

250kW FCS/ Space and Water Heating	AZ	IL	MN	NY	TX	CA
Annual electricity demand (kWh)	9,140,359	7,851,821	7,330,505	7,623,915	9,532,518	2,166,348
Annual heat demand (kWh)	2,828,571	3,682,030	3,862,705	4,311,481	2,962,266	604,357
Annual electricity demand met by FCS (kWh)	2,102,400	2,102,400	2,102,400	2,102,400	2,102,400	1,964,680
Annual heat demand met by FCS (kWh)	837,538	875,103	875,103	875,103	836,451	551,664
Capital Cost	\$ 35,976	\$ 35,976	\$ 35,976	\$ 35,976	\$ 35,976	\$ 35,976
O&M Cost	\$ 63,072	\$ 63,072	\$ 63,072	\$ 63,072	\$ 63,072	\$ 58,940
Scheduled Maintenance	\$ 3,000	\$ 3,000	\$ 3,000	\$ 3,000	\$ 3,000	\$ 3,000
Fuel Cost- FC only	\$ 126,179	\$ 103,456	\$ 91,210	\$ 117,331	\$ 93,086	\$ 90,762
Fuel Cost- Non FC	\$ 70,110	\$ 81,329	\$ 76,358	\$ 113,102	\$ 55,265	\$ 1,031
Electricity Cost	\$ 478,999	\$ 428,409	\$ 315,087	\$ 904,475	\$ 581,527	\$ 10,951
Demand Charge	\$ 52,624	\$ 71,101	\$ 119,111	\$ 210,542	\$ 178,937	\$ 23,511
Fixed Monthly Charge	\$ 6,367	\$ 516	\$ 341	\$ 1,241	\$ 295	\$ 2,794
Total, FCS	\$ 836,328	\$ 786,860	\$ 704,155	\$1,448,739	\$1,011,159	\$ 226,967
No FCS	AZ	IL	MN	NY	TX	CA
Fuel Cost- Non FC	\$ 100,839	\$ 107,626	\$ 99,542	\$ 142,926	\$ 77,908	\$ 16,759
Electricity Cost	\$ 628,966	\$ 593,645	\$ 449,323	\$1,269,001	\$ 754,975	\$ 186,343
Demand Charge	\$ 63,848	\$ 87,490	\$ 147,992	\$ 260,526	\$ 215,513	\$ 67,485
Fixed Monthly Charge	\$ 6,367	\$ 516	\$ 341	\$ 1,241	\$ 295	\$ 2,794
Total, No FCS	\$ 800,020	\$ 789,276	\$ 697,198	\$1,673,693	\$1,048,691	\$ 273,381
Percent Change with FCS	4.5%	-0.3%	1.0%	-13.4%	-3.6%	-17.0%

7.2 Conclusions for Use-Phase Model

Earlier LCA analysis showed that the fuel cell CHP system use-phase has a high environmental impact relative to the other LCA phases and is responsible for 90% of the fuel cell system life cycle's total environmental impact (Wei et al., 2014). This is mainly due to the emissions caused by the steam reforming process with natural gas as a fuel input. Since the 'use and maintenance' phase accounts for a major portion of environmental impact of fuel cell systems, a realistic use-phase model was developed which can analyze energy, and overall costs for several commercial buildings. This model takes modeled load shapes for a given building and calculates generated power (electricity and heat), and FCS capital, operational, and fuel costs.

The use-phase model shows that adopting a SOFC system as an alternative energy system can be a cost competitive power source in some building types and locations with the installed cost assumptions above corresponding to 100MWe of annual production volume. In cities where there is sufficient heat demand from buildings, SOFC offers great potential from both an economic and environmental standpoint due to their ability to produce both electricity and useful heat.

In the next section, the environmental impacts of fuel cell systems in different locations across the U.S. are explored. We will show that adoption of CHP fuel-cell systems in areas of the U.S. with high carbon intensity grid-based electricity (e.g., Chicago) can result in reduced GHG emissions and concomitant health and environmental benefits.

7.3 Life Cycle Impact Assessment (LCIA) Modeling

Similar to the approach we used for PEM fuel cells in Wei et al. (2014), we developed an LCIA model to quantify the environmental and human health damages caused by fuel cell systems in commercial buildings. These fuel cells displace grid-based electricity and some fraction of heating demand fuel, as specified by the user of the model. We calculate an average electricity intensity that is displaced by the FCS and use commercial building surveys to estimate the mix of heating fuel types by region that is displaced by the FCS. Externalities to be valued include morbidity, mortality, impaired visibility, recreational disruptions, material damages, agricultural and timber damages, and global warming. Details for computing average electricity intensity and the mix of heating fuel types by region are described in LT PEM report (Wei et al., 2014).

Direct emission factors reported in recent literature on fuel cells allowed us to determine reasonable estimates for CO₂, CO, NO_x, SO_x, PM₁₀ and VOC (Table 7.8).

Table 7.8. SOFC Fuel cell emission factors in grams per kWh using natural gas as an input fuel.

Pollutant	g/kWh
CO ₂	340
NO _x	Negligible
SO _x	Negligible
PM ₁₀	Negligible
VOC	Negligible
CO	Negligible

Source: NETL (2009) and EPA (2015)

The calculation of offset emissions from the FCS displacing grid based electricity and conventional heating fuels uses the same modeling approach described in Wei et al. (2014) and a detailed description can be found in that reference. One change from the earlier treatment is that the valuation of offset CO₂ is taken at the approximate market price of CO₂ emissions in the California Cap and Trade market, at \$10/tonne rather than the social cost of carbon which is approximately \$44/tonne.

7.4 Total Cost of Ownership Modeling Results

Figure 7.4 outlines the approach for comparing fuel cell total cost of ownership with grid based electricity and conventional heating. A fuel cell CHP system will typically increase the cost of electricity but provide some saving by offsetting heating energy requirements. The cost of fuel cell electricity in this case is taken to be the “levelized cost of electricity” or the levelized cost in \$/kWh for the fuel cell system taking into account capital costs, operations and maintenance (O&M), fuel, and capital replacement costs (inverter, stack replacement, etc.) only. In this work we credit all saving from heating fuel savings, electricity demand charge savings, carbon credits from net system savings of CO₂eq, and net avoided environmental and health externality damages to the fuel cell system cost of electricity and call this quantity “cost of electricity with total cost of ownership savings.” This allows comparison of fuel cell COE with TCO credits or “total cost of electricity” to the reference grid electricity cost (\$/kWh).

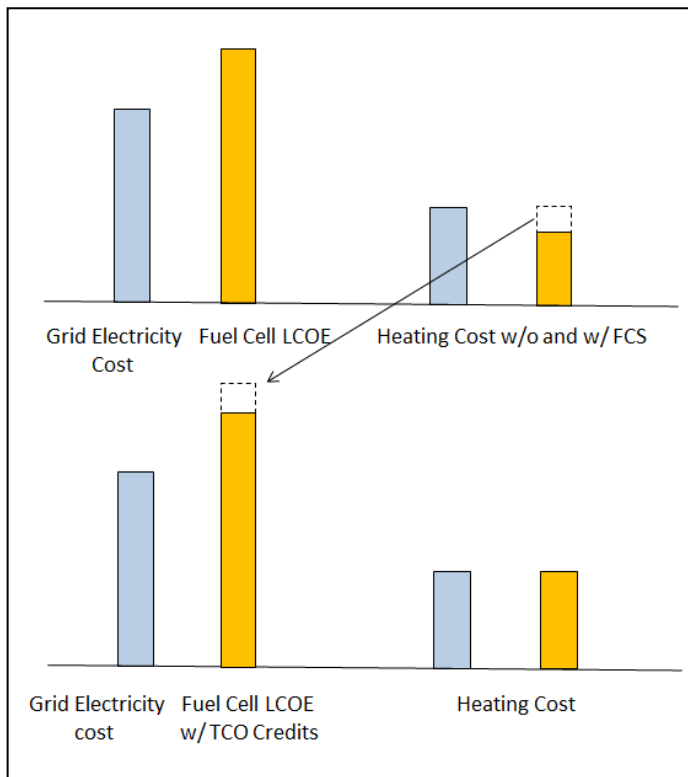


Figure 7.4. Cost of energy service for FC CHP and conventional electricity and heating systems.¹⁸

¹⁸ Note: a fuel cell CHP system will typically increase the levelized cost of electricity (upper left two bars). But if waste heat is utilized, the cost of heating is reduced (upper right two bars). In this treatment, all non-electricity credits (heating, carbon, etc.) are applied to a “total cost of electricity” (lower left two bars).

The LCOE for the FC system follows a standard convention for the levelized cost of electricity:

$$LCOE \text{ [Fuel cell power]} \left(\frac{\$}{kWh} \right) = \frac{\sum_{\text{annual}}(\text{Capital cost, O\&M, Maintenance, Fuel})}{\text{Annual electricity output in kWh}}$$

The LCOE with TCO credits for the FC is then given by the following equation:

$$LCOE \text{ with TCO Credits [Fuel cell power]} \left(\frac{\$}{kWh} \right) = \frac{\sum_{\text{annual}}(\text{Capital cost, O\&M, Maintenance, Fuel}) - (\text{TCO Credits})}{\text{Annual electricity output in kWh}}$$

where

$$TCO \text{ Credits} = \text{Heating Fuel Savings} + CO_2 \text{ Credits} + \text{Health and Environmental Impact Savings}$$

Results for a 50-kWe SOFC FCS in a small hotel are shown in Table 7-9. The total electricity cost is lower in the FCS case for Minneapolis and New York. The levelized cost of electricity from the FCS is reduced by 29% and 36% in Minnesota and Chicago, respectively after taking into account heating credit, GHG credit, and health and environmental impact savings. In particular, Figure 7-5 below shows that for a 50-kWe SOFC FCS in Chicago, the levelized cost of electricity from the fuel cell system is \$0.119/kWhe. Heating savings reduce this by \$0.013/kWhe and health and environmental savings by \$0.028/kWhe. The cost of electricity from the fuel cell with TCO savings is thus 36% from the raw levelized cost, and below the cost of commercial electricity at \$0.091/kWhe.

Table 7.9. Levelized cost of electricity with total cost of ownership savings for a 50-kWe SOFC Fuel cell system with the fuel cell system providing both water and space heating and assuming \$1900/kWe installed cost.

Output results from use-phase model for small hotel (50 kW FC system)										
Output	Phoenix, AZ		Minneapolis, MN		Chicago, IL		NYC, NY		Houston, TX	
	No FCS	Fuel Cell	No FCS	Fuel Cell	No FCS	Fuel Cell	No FCS	Fuel Cell	No FCS	Fuel Cell
FC System Utilization		91.0%		82.0%		82.0%		75.0%		86.0%
Total Electricity Demand (kWh/yr)	576,668	576,668	419,590	419,590	424,147	424,147	369,661	369,661	497,656	497,656
Total Space Heating Demand (kWh/yr)	23,307		174,743		135,869		135,869		0	
Total Water Heating Demand (kWh/yr)	76,954		127,112		118,971		116,075		83,071	
Annual Generated Power by FC (kWh)		382,253		345,368		345,791		314,930		362,313
FC fraction of Electricity Demand		66%		82%		82%		85%		73%
Annual Generated Heat by FC (kWh)		90,829		145,416		142,764		142,049		78,340
Capital Cost (\$/yr)		9,153		9,153		9,153		9,153		9,153
O&M Cost (\$/yr)		11,468		10,361		10,374		9,448		10,869
Scheduled Maintenance (\$/yr)		1000		1000		1000		1,000		1,000
Fuel Cost for Fuel Cell (\$/yr)		25252		18254		20705		23481		18629
Fuel Cost for Conv. Heating (\$/yr)	3574	201	7780	3875	7449	3102	8352	3447	2185	39
Purchased Electricity Energy Cost (\$/yr)	47305	15360	45374	6679	32104	4889	61530	6926	39414	9524
Demand Charge (\$/yr)	5445	3635	3422	1937	6021	3460	16959	8882	15489	9422
Fixed Charge, Electricity (\$/yr)	150	150	131	131	348	348	1241	1241	295	295
Total Electricity Cost (\$/yr)	52899	66018	48927	47515	38473	49929	79730	60130	55198	58892
Total Cost of Electricity (\$/kWh)	0.092	0.114	0.117	0.113	0.091	0.118	0.216	0.163	0.111	0.118
Purchased Electricity Cost (\$/kWh)	0.092	0.098	0.117	0.118	0.091	0.111	0.216	0.311	0.111	0.142
LCOE of FC power (\$/kWh)		0.123		0.112		0.119		0.137		0.109
Fuel savings from conventional heating (\$/yr)		3373		3905		4347		4905		2146
Fuel savings per kWh(\$/kWh)		0.009		0.011		0.013		0.016		0.006
LCOE of FC power with fuel savings (\$/kWh)		0.114		0.101		0.107		0.121		0.104
GHG credit at \$10/ton CO ₂ (\$/kWh)		-0.0003		0.0037		0.003		0.0002		0.0001
Health, Environmental Savings (\$/kWh)		0.0014		0.0180		0.028		0.008		0.0017
LCOE with TCO Savings for Fuel Cell Power (\$/kWh)		0.113		0.079		0.076		0.113		0.102
LCOE with TCO Savings for FC and Purchased Power, (\$/kWh)		0.108		0.086		0.082		0.142		0.113

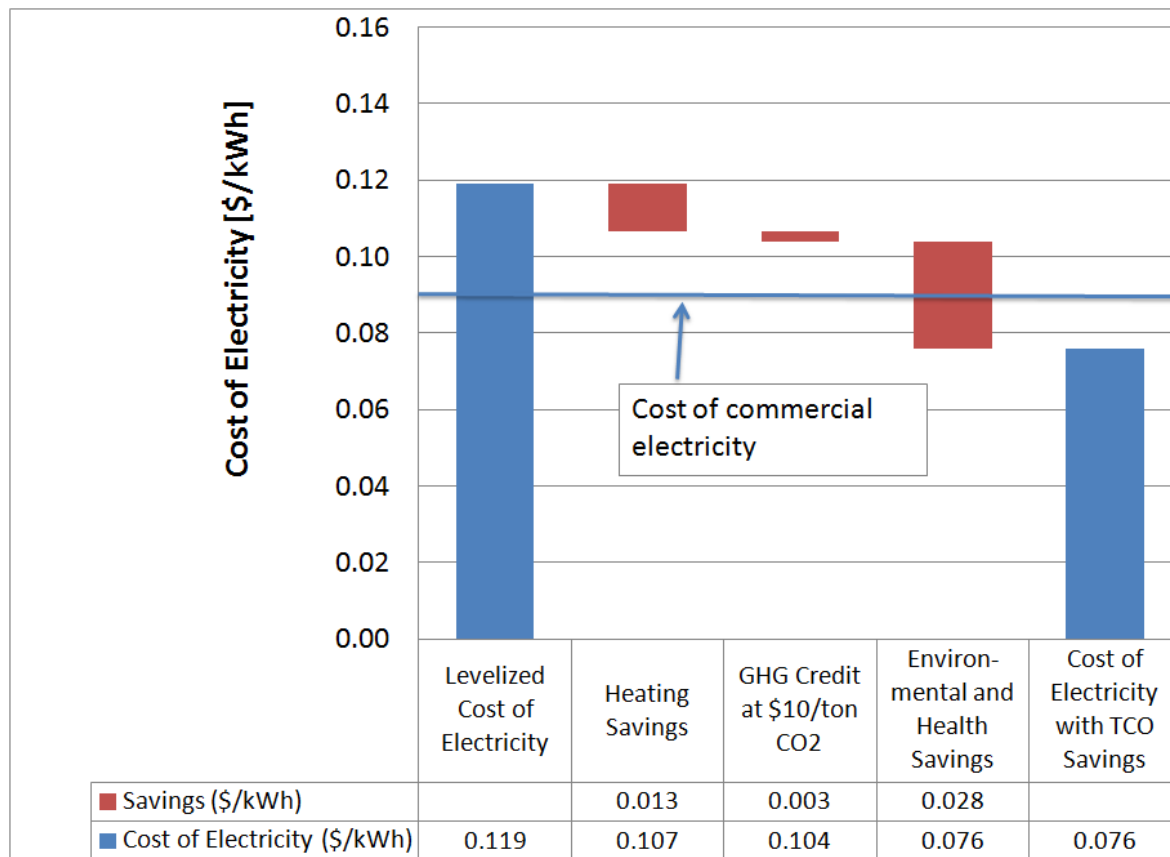


Figure 7.5. Waterfall plot of the cost of electricity from the 50-kWe SOFC fuel cell system for a small hotel in Chicago.

Table 7.10 shows the levelized cost of electricity with total cost of ownership savings for a 10-kWe SOFC FCS for a small hotel. In this case, the total cost of electricity is favorable or very comparable in all cases. Fuel savings per kWh are very comparable across cities. As before, Minneapolis and Chicago have the highest credit from health and environmental savings at \$0.018/kWh to \$0.028/kWh of fuel cell delivered electricity, respectively.

Table 7.10. Levelized cost of electricity with total cost of ownership savings for a 10-kWe SOFC Fuel cell system with the fuel cell system providing both water and space heating and assuming \$2500/kWe installed cost.

Output results from use-phase model for small hotel (10 kW FC system)										
Output	Phoenix, AZ		Minneapolis, MN		Chicago, IL		NYC, NY		Houston, TX	
	No FCS	Fuel Cell	No FCS	Fuel Cell	No FCS	Fuel Cell	No FCS	Fuel Cell	No FCS	Fuel Cell
FC System Utilization		100%		100%		100%		100%		100%
Total Electricity Demand (kWh/yr)	576,668	576,668	419,590	419,590	424,147	424,147	369,661	369,661	497,656	497,656
Total Space Heating Demand (kWh/yr)	23,307		174,743		135,869		135,869		0	
Total Water Heating Demand (kWh/yr)	76,954		127,112		118,971		116,075		83,071	
Annual Generated Power by FC (kWh)		84,096		84,096		84,096		84,096		84,096
FC fraction of Electricity Demand		15%		20%		20%		23%		17%
Annual Generated Heat by FC (kWh)		31,282		34,339		34,230		34,212		31,390
Capital Cost (\$/yr)		2409		2409		2409		2409		2409
O&M Cost (\$/yr)		2523		2523		2523		2523		2523
Scheduled Maintenance (\$/yr)		500		500		500		500		500
Fuel Cost for Fuel Cell (\$/yr)		5052		3652		4142		4697		3727
Fuel Cost for Conv. Heating (\$/yr)	3574	2413	7779	6857	7449	6407	8352	7171	2185	1325
Purchased Electricity Energy Cost (\$/yr)	47305	40333	45374	35998	32104	25495	61530	46949	39414	32476
Demand Charge (\$/yr)	5445	3635	3422	3125	6021	3460	16959	8882	15489	9422
Fixed Charge, Electricity (\$/yr)	150	150	131	131	348	348	1241	1241	295	295
Total Electricity Cost (\$/yr)	52899	54602	48927	48338	38473	38877	79730	67200	55198	51352
Total Cost of Electricity (\$/kWh)	0.092	0.095	0.117	0.115	0.091	0.092	0.216	0.182	0.111	0.103
Purchased Electricity Cost (\$/kWh)	0.092	0.090	0.117	0.117	0.091	0.086	0.216	0.200	0.111	0.102
LCOE of FC power (\$/kWh)		0.125		0.108		0.114		0.120		0.109
Fuel savings from conventional heating (\$/yr)		1161		922		1042		1181		860
Fuel savings per kWh (\$/kWh)		0.014		0.011		0.012		0.014		0.010
LCOE of FC power with fuel savings (\$/kWh)		0.111		0.097		0.101		0.106		0.099
GHG credit at \$10/ton CO ₂ (\$/kWh)		0.000		0.004		0.003		0.000		0.000
Health, Environmental Savings (\$/kWh)		0.002		0.018		0.028		0.008		0.002
LCOE with TCO Savings for Fuel Cell Power (\$/kWh)		0.109		0.075		0.071		0.099		0.096
LCOE with TCO Savings for FC and Purchased Power, (\$/kWh)		0.092		0.109		0.083		0.177		0.101

Finally, the LCOE with TCO savings is shown for the case of a 250-kWe SOFC FCS in a hospital in Table 7.11. The total cost of electricity is lower for the FCS case in New York and Houston and slightly higher in Minneapolis and Chicago, with the largest externality credit from health and environmental impacts in the latter two cities as before.

Table 7.11. Levelized cost of electricity with total cost of ownership savings for a 250-kWe SOFC FCS in a hospital with the FCS providing both water and space heating and assuming \$1600/kWe installed cost

Output results from use-phase model for hospital (250 kW FC System)												
Output	Phoenix, AZ		Minneapolis, MN		Chicago, IL		NYC, NY		Houston, TX		San Diego, CA	
	No FCS	Fuel Cell	No FCS	Fuel Cell	No FCS	Fuel Cell	No FCS	Fuel Cell	No FCS	Fuel Cell	No FCS	Fuel Cell
FC System Utilization		100%		100%		100%		100%		100%		94%
Total Electricity Demand (MWh/yr)	9,140	9,140	7,331	7,331	7,852	7,852	7,624	7,624	9,533	9,533	2166.4	2166.4
Total Space Heating Demand (MWh/yr)	2,689		3,633		3,682		4,311		2812		528.8	
Total Water Heating Demand (MWh/yr)	140		230		215		210		151		75.5	
Annual Generated Power by FC (MWh)		2,102		2,102		2,102		2,102		2,102		1965
FC fraction of Electricity Demand		23%		29%		27%		28%		22%		91%
Annual Generated Heat by FC (MWh)		837		875		875		875		836		552
Capital Cost (\$/yr)		35976		35976		35976		35976		35976		35976
O&M Cost (\$/yr)		63072		63072		63072		63072		63072		58940
Scheduled Maintenance (\$/yr)		3000		3000		3000		3000		3000		3000
Fuel Cost for Fuel Cell (\$/yr)		126179		91210		103456		211177		93086		90762
Fuel Cost for Conv. Heating (\$/yr)	100839	70110	99554	76358	107637	81329	142913	113102	77905	55265	16759	1031
Purchased Electricity Energy Cost (\$/yr)	628966	478999	449323	315087	593645	428409	1269001	904475	754975	581527	186343	10951
Demand Charge (\$/yr)	63848	52624	147992	119111	87490	71101	260526	210542	215513	178937	67485	23511
Fixed Charge, Electricity (\$/yr)	6367	6367	341	341	516	516	1241	1241	295	295	2794	2794
Total Electricity Cost (\$/yr)	699181	766216	597656	627796	681651	705530	1530768	1429482	970783	955893	256622	225935
Total Cost of Electricity (\$/kWh)	0.076	0.084	0.082	0.086	0.087	0.090	0.201	0.188	0.102	0.100	0.118	0.104
Purchased Electricity Cost (\$/kWh)	0.076	0.076	0.082	0.083	0.087	0.087	0.201	0.202	0.102	0.102	0.118	0.185
LCOE of FC power (\$/kWh)		0.109		0.092		0.098		0.149		0.093		0.096
Fuel savings per kWh (\$/kWh)		0.0146		0.0110		0.0125		0.0142		0.0108		0.0080
LCOE of FC power with fuel savings (\$/kWh)		0.094		0.081		0.085		0.135		0.082		0.088
GHG credit at \$10/ton CO ₂ (\$/kWh)		0.0000		0.0030		0.0030		0.0000		0.0003		0.0002
Health, Environmental Savings (\$/kWh)		0.0013		0.0170		0.0280		0.0080		0.0018		0.0016
LCOE with TCO Savings for Fuel Cell Power (\$/kWh)		0.093		0.061		0.054		0.127		0.080		0.086
LCOE with TCO Savings for FC and Purchased Power, (\$/kWh)		0.080		0.077		0.078		0.181		0.097		0.095

7. Conclusions

Bottom-up DFMA costing analysis for fuel cell stack components in this work shows that, for stationary applications, SOFC fuel cell stacks alone can approach a direct manufacturing cost of \$170 per kWe of net electrical power at high production volumes (e.g. 50-kWe or 100-kWe CHP systems at 50,000 systems per year). Overall SOFC system costs including corporate markups and installation costs are estimated to be about \$3,200/kWe (\$1500/kWe) for 10-kWe (100-kWe) CHP systems at 1,000 systems per year, and \$2,200/kWe and \$1,200/kWe at high volume (50,000 systems per year), respectively.

All fuel cell stack components (EEA, plate, frame, and stack assembly) are assumed to be manufactured in-house with high throughput processes and high yield (>95%) assumed for all modules at high manufacturing volumes. The assumed yield rates are a key uncertain variable in estimating fuel cell stack manufacturing costs. While it was not in the scope of this work to do a detailed yield feasibility analysis, well established methodologies exist for improving yield using similar process modules in other industries, and learning-by-doing and improvements in yield inspection, detection, and process control are implicitly assumed. Most system balance of plant components were assumed to be purchased from suppliers as they are generally available as commercial products.

Balance of plant costs including the fuel processor make up over 60% of total direct costs across the range of production volumes and are thus a key opportunity for further cost reduction. In general, the BOP has a lower rate of decrease in cost as a function of volume as the fuel cell stack in part because many components are already manufactured in reasonable volume and do not benefit in the same way from increased economies of scale as the fuel cell stack. This result is also influenced by the different methodologies applied to stack vs. BOP costing: a DFMA analysis was applied to the stack, whereas BOP costs were estimated based on purchased components and vendor price quotes.

The cost of electricity with and without total cost of ownership (TCO) credits for a fuel cell CHP system has been demonstrated for buildings in six U.S. cities. This approach incorporates the impacts of offset heating demand by the FCS, carbon credits, and environmental and health externalities into a total levelized cost of electricity (\$/kWh). This LCOE with total cost of ownership credits can then be compared with the baseline cost of grid electricity. This analysis combines a fuel cell system use-phase model with a life-cycle integrated assessment model of environmental and health externalities. Total cost of electricity is dependent on the carbon intensity of electricity and heating fuel that a FC system is displacing, and thus highly geography dependent.

For the subset of buildings considered here (small hotels and hospitals) and 100MWe annual production volume (e.g., 10-kWe at 10,000 systems per year or 50-kWe at 2,000 systems per year), overall costs of fuel cell CHP systems relative to grid power and conventional heating are competitive in some cities. In regions of the country with higher carbon intensity grid electricity, fuel cell systems further benefit from including TCO credits. Health and environmental externalities can provide large savings if electricity or heating with a high environmental impact are being displaced.

Overall, this type of total cost of ownership analysis quantification is important to identify key opportunities for direct cost reduction, to fully value the costs and benefits of fuel cell systems in stationary applications, and to provide a more comprehensive context for future potential policies.

Bibliography and References

- Akanda, S. R. (2011). Mechanical characterization of oxide coating–interconnect interfaces for solid oxide fuel cells. *Journal of Power Sources*, 210, 254-262.
- Asthana, R., Kumar, A., & Dahotre, N. B. (2006). *Materials Processing and Manufacturing Science*. San Diego: Academic Press(Elsevier).
- Aurel Automation. (2015). www.aurelautomation.com. Retrieved June 12, 2015, from <http://www.aurelautomation.com/new-products/aurel-automation-chip-resistor-line/>
- Battelle Memorial Institute. (2014, February 7). *Department of Energy (DOE)*. Retrieved March 10, 2015, from http://energy.gov/sites/prod/files/2014/06/f16/fcto_battelle_cost_analysis_apu_feb2014.pdf
- BNP Media. (2015). *Ceramic Industry*. (B. Media, Ed.) Retrieved 07 15, 2015, from <http://www.ceramicindustry.com/articles/88246-tape-casting-advanced-materials>
- Borglum, B. (2009). Development of Solid Oxide Fuel Cells at Versa Power Systems. *ECS Transactions*, 17(1), 9-13.
- Borglum, B. (2009). Solid Oxide Fuel Cell Development at Versa Power Systems. *ECS Transactions*, 17(1), 9-13.
- Brock, T., Groteklaes, M., & Mischke, P. (2000). *European Coatings Handbook*. KG: Vincentz Network GmbH & Co.
- Burggraaf, A., & Cot, L. (1996). *Fundamentals of Inorganic Membrane Science and Technology*. Amsterdam: Elsevier.
- Carlson, E. J., Yang, Y., & Fulton, C. (2004, April 20). *Solid oxide fuel cell manufacturing cost model: simulating relationships between performance, manufacturing and cost of production*. National Energy Technology Laboratory: NETL. Retrieved from National Energy Technology Laboratory.
- Carter, C., & Norton, M. (2013). *Ceramic Materials: Science and Engineering* (2 ed.). New York: Springer Science & Business Media.
- De Florio, D. Z., Fonseca, F. C., Muccillo, E. N., & Muccillo, R. (2004). Materiais cerâmicos para células a combustível (Ceramic materials for fuel cells). *Cerâmica*, 50(316), 275-290. doi:10.1590/S0366-69132004000400002
- Delahaye, T., & Rieu, M. (2012). *Patent No. PCT/EP12/57117*. United States.
- Doherty, W., Reynolds, A., Kennedy, D. (2015) Process Simulation of Biomass Gasification Integrated with a Solid Oxide Fuel Cell Stack. *Journal of Power Sources* 2015;277:292-303. <http://dx.doi.org/10.1016/j.jpowsour.2014.11.125>
- DOE (2012). U.S. Department of Energy and Environmental Protection Agency. Combined Heat and Power- A Clean Energy Solution. http://archive.epa.gov/sustainablemanufacturing/web/pdf/chp_clean_energy_solution.pdf
- DOE (2014). U.S. Department of Energy. Fuel Cell Technologies Office Multi-Year Research, Development, and Demonstration Plan, Chapter 3.4 Fuel Cells, 2012 (Updated November 2014) http://energy.gov/sites/prod/files/2014/12/f19/fcto_myRDD_fuel_cells.pdf
- EG&G Technical Services, I. (2004, November). *Fuel Cell Handbook* (VII edition). Retrieved June 2015, from Fuel Cell Handbook (VII edition): <https://www.netl.doe.gov/File%20Library/research/coal/energy%20systems/fuel%20cells/FCHandbook7.pdf>

- EPA (2015). U.S. Environmental Protection Agency Combined Heat and Power Partnership. Catalog of CHP Technologies. http://www.epa.gov/sites/production/files/2015-07/documents/catalog_of_chp_technologies.pdf
- Fergus, J., Hui, R., Li, X., Wilkinson, D., & Zhang, J. J. (2009). *Solid oxide fuel cells : materials properties and performance*. London, NY: CRC Press.
- Ghezelayagh, H. (2014, July 22). *Advances in SOFC Development at FuelCell Energy: SOFC Systems with Improved Reliability and Endurance*. Retrieved March 03, 2015, from 15th Annual SECA Workshop: <http://www.netl.doe.gov/File%20Library/Events/2014/2014%20SECA%20workshop/Hossein-Ghezelayagh.pdf>
- Greene, David L., K.G. Duleep, Girish Upreti, (2011). Status and Outlook for the U.S. Non-Automotive Fuel Cell Industry: Impacts of Government Policies and Assessment of Future Opportunities. Oak Ridge National Laboratory ORNL/TM-2011/101. http://cta.ornl.gov/cta/Publications/Reports/ORNL_TM2011_101_FINAL.pdf
- Haberl, J. S. (1994). *Economic Calculations for ASHRAE Handbook*. Texas A&M University: Dept. of Mechanical Engineering. Retrieved from <https://oaktrust.library.tamu.edu/bitstream/handle/1969.1/2113/ESL-TR-93-04-07.pdf?sequence=1&isAllowed=y>
- Hotza, D., & Greil, P. (1995). Review: aqueous tape casting of ceramic powders. *Materials Science and Engineering, A*(202), 206-217.
- Hsu, W., Lee, H.-l., Lee, H.-l., Shong, D.-n., & Chen, S.-f. (2011). *Patent No. 20110135531*. Taiwan.
- Iannone, R., & Nenni, M. (2013). Managing OEE to Optimize Factory Performance. In M. M. Schiraldi, *Operations Management* (pp. 31-50). InTech: Open Access Publisher. doi:10.5772/45775
- F.P. Incropera, D.P. DeWitt, T.L. Bergman, A.S. Lavine, *Fundamentals of Heat and Mass Transfer*, 2007. doi:10.1016/j.applthermaleng.2011.03.022.
- James, B. D. (2010, September 30). *Mass Production Cost Estimation for Direct H2 PEM Fuel Cell System for Automotive Applications: 2010 Update*. Retrieved April 2015, from http://www1.eere.energy.gov/hydrogenandfuelcells/pdfs/dti_80kwW_fc_system_cost_analysis_report_2010.pdf
- James, B., Spisak, A., & Colella, A. (2012, September 7). *Manufacturing Cost Analysis of Stationary Fuel Cell Systems*. Retrieved April 12, 2015, from <https://www.sainc.com/service/SA%202012%20Manufacturing%20Cost%20Analysis%20of%20Stationary%20Fuel%20Cell%20Systems.pdf>
- Jung, G.-b. (2013). *Yuan Ze University: SOFC Science and Technology*. Retrieved April 20, 2015, from <http://www.enedu.org.tw/files/DownloadFile/20131010130452.pdf>
- Kidner, N., Seabaugh, M., Chenault, K., Ibanez, S., & Thrun, L. (2011, October 19). *High Performance Oxide Protective Coatings for SOFC Components*. Retrieved 07 15, 2015, from Nextech Materials: <http://www.nextechmaterials.com/energy/images/pdfs/MST2011.pdf>
- Kishimoto, M., Miyawaki, K., Iwai, H., Saito, M., & Yoshida, H. (2013). Effect of Composition Ratio of Ni-YSZ Anode on Distribution of Effective Three-Phase Boundary and Power Generation Performance. *Fuel Cells*, 13(4), 476-486.
- Koleske, J. V. (1995). *Paint and Coating Testing Manual*. Philadelphia: ASTM International.

- Li, X., & Imran, S. (2005). Review of bipolar plates in PEM fuel cells: Flow-field designs. *International Journal of Hydrogen Energy*, 30(4), 359-371.
- Lipman, Timothy E., Jennifer L. Edwards, and Daniel M. Kammen, "Fuel Cell System Economics: Comparing the Costs of Generating Power with Stationary and Motor Vehicle PEM Fuel Cell Systems," *Energy Policy* 32(1): 101-125 (2004)
- Liu, Q., Fu, C., Chan, S., & Pasciak, G. (2011). Preparation and Characterization of Anode-Supported YSZ Thin Film Electrolyte by Co-Tape Casting and Co-Sintering Process. *IOP Conference Series: Materials Science and Engineering*, 18(Symposium 9B). doi:10.1088/1757-899X/18/13/132006
- Magdefrau, N. J. (2013). "Evaluation of Solid Oxide Fuel Cell Interconnect Coatings: Reaction Layer Microstructure, Chemistry and Formation Mechanisms. *Doctoral Dissertations. Paper 106., 106.*
- Mahadevan, K., Contini, V., & Goshe, M. (2010). *Economic Analysis of Stationary PEM Fuel Cell Systems*. Retrieved April 03, 2015, from http://hydrogenoev.nrel.gov/pdfs/review10/fc050_mahadevan_2010_p_web.pdf
- Mason, T. O. (2015). *Encyclopedia Britannica Inc*. Retrieved March 26, 2015, from <http://www.britannica.com/technology/advanced-ceramics>
- Mattox, D. M., & Andrew, W. (2010). *Handbook of Physical Vapor Deposition (PVD) Processing*. Albuquerque: Elsevier.
- Mazumder, S., Acharya, K., & Haynes, C. (2004). Solid-OxidFuel-Cell Performance and Durability:Resolution of the Effects of Power-Conditioning Systems and Application Loads. *IEEE TRANSACTIONS ON POWER ELECTRONICS*, 19(5).
- Menzler, N. H., Tietz, F., Uhlenbruck, S., Buchkremer, H. P., & Stöver, D. (2010). Materials and manufacturing technologies for solid oxide fuel cells. *Journal of materials science*, 45(12), 3109-3135.
- Mistler, R., Runk, R., & Shanefield, D. (1978). Tape casting of ceramics. In G. Onoda, & L. Hench, *Ceramic Fabrication Processing Before Firing* (pp. 411-448). New York: John Wiley & Sons.
- Mitchell, B. S. (2004). *An Introduction to Materials Engineering and Science for Chemical and Materials Engineers*. New Jersey: John Wiley & Sons.
- Monov, V., Sokolov, B., & Stoenchev, S. (2012). Grinding in Ball Mills: Modeling and Process Control . *CYBERNETICS AND INFORMATION TECHNOLOGIES*, 12(2), 51-68.
- Moreno, R. (2012). Chapter 4: Colloidal Methods. In N. P. Bansal, & A. Boccaccini, *Ceramics and Composites Processing Methods* (pp. 147-182). New Jersey: The American Ceramic Society (John Wiley & Sons Eds).
- Moreno, V., Bernardino, M., & Hotza, D. (2014). Mechanical Behavior of Yttria-Stabilized Zirconia Aqueous Cast Tapes and Laminates. *Journal of Ceramics*, 2014.
- Mubarak, A., Hamzah, E., & Toff, M. (2005). REVIEW OF PHYSICAL VAPOUR DEPOSITION (PVD) TECHNIQUES FOR HARD COATING . *Jurnal Mekanikal* (20), 42-51.
- Muller, N.Z., and R.O. Mendelsohn, "The Air Pollution Emission and Policy Analysis Model (APEEP): Technical Appendix" [online]. Yale University, New Haven, CT. December 2006. Available at: https://segueuser132les.middlebury.edu/nmuller/APEEP_Tech_Appendix.pdf
- National Energy Technology Laboratory (NETL). (2007, April 2). *The Impact of Scale-up and Production Volume on SOFC Manufacturing Cost*. Retrieved April 7, 2015, from <https://www.netl.doe.gov/File%20Library/research/coal/energy%20systems/fuel%20cells/JT-Manufacturing-Study-Report-070522.pdf>

- National Energy Technology Laboratory (NETL). (2009). Natural Gas-Fueled Distributed Generation Solid Oxide Fuel Cell Systems, Report Number: R102 04 2009/1
- National Energy Technology Laboratory (NETL). (2013, September 29). *Assessment of the Distributed Generation Market Potential for Solid Oxide Fuel Cells*. Retrieved July 13, 2015, from http://netl.doe.gov/File%20Library/Research/Energy%20Analysis/Publications/FINAL_DG_SOFC.pdf
- National Research Council. Hidden Costs of Energy: Unpriced Consequences of Energy Production and Use. The National Academies Press: Washington, D.C., 2010.
- Neikov, O. D., I Murashova, .. B., Yefimov, N. A., & Naboychenko, S. (2009). *Handbook of Non-Ferrous Metal Powders: Technologies and Applications*. Oxford: Elsevier.
- Nguyen, T., Kobayashi, K., Honda, T., & Limura, Y. (2004). Preparation and evaluation of doped ceria interlayer on supported stabilized zirconia electrolyte SOFCs by wet ceramic processes. *Solid State Ionics*, 174(1), 163-174.
- Norsk, J., Olsen, C., Nielsen, J. U., & Erikstrup, N. (2008). *Patent No. US 20080014492 A1*. Denmark.
- Pan, J., Tonkay, G. L., & Quintero, A. (1998). Screen Printing Process Design of Experiments for Fine Line Printing of Thick Film Ceramic Substrates. *Proceedings of International Symposium on Microelectronics*, 264-269.
- Peng, L. F., Liu, D. A., Hu, P., Lai, X. M., & Ni, J. (2010). Fabrication of metallic bipolar plates for proton exchange membrane fuel cell by flexible forming process-numerical simulations and experiments. *Journal of Fuel Cell Science and Technology, Transactions of the ASME*, 7(3). doi:031009-1~9
- Phillips, J. C. (2008). *SignalTrend Inc*. Retrieved March 15, 2015, from <http://www.forecast-chart.com/forecast-inflation-rate.html>
- K.D. Rafferty, Heat Exchangers, (1998) 261–277. <http://www.oit.edu/docs/default-source/geoheat-center-documents/publications/heat-exchangers/tp54.pdf?sfvrsn=2>.
- Rahaman, M. N. (2003). *Ceramic Processing and Sintering*. New York: CRC Press.
- Rahaman, M., & Rahaman, M. (2006). *Ceramic Processing*. Boca Raton, FL: CRC Press.
- Rehg, T., Guan, J., Montgomery, K., Verma, A., & Lear, G. (2007). *Patent No. US 20070111069 A1*. New York.
- Reitz, T., & Xiao, H. (2006). Characterization of electrolyte–electrode interlayers in thin film solid oxide fuel cells. *Journal of Power Sources*, 161, 437-443.
- Reitz, T., & Xiao, H. (2006). Characterization of electrolyte–electrode interlayers in thin film solid oxide fuel cells. *Journal of Power Sources*, 161(1), 437-443.
- Richards, M., Tang, E., & Petri, R. (2011, August 11-12). *Solid Oxide Fuel Cell Manufacturing Overview. Hydrogen and Fuel Cell Technologies Manufacturing R&D Workshop*. Retrieved 03 28, 2015, from http://www1.eere.energy.gov/hydrogenandfuelcells/pdfs/mfg2011_jia_richards.pdf
- Ried, P., Lorenz, C., Bronstrup, A., Graule, T., Menzler, N. H., Sitte, W., & Holtappels, P. (2008). *Journal of the European Ceramic Society*, 28(1801).
- Rock, J. (2003). *Patent No. US 20020119358 A1*. Michigan(US).
- Rooijen J.V. “A Life Cycle Assessment of the PureCell™ Stationary Fuel Cell System: Providing a Guide for Environmental Improvement”. A report of the Center for Sustainable Systems, Report No. CSS06-09. June 30th, 2006Salt River Project. Accessed August 2013. <http://www.srpnet.com/about/facts.aspx#ownership>

- Sanson, A., Pinasco, P., & Roncari, E. (2008). Influence of Pore Formers on slurry composition and microstructure of tape cast supporting anodes for SOFCs. *Journal of the European Ceramic Society*, 28(6), 1221-1226.
- Schafbauer, W., Menzler, N., & Buchkremer, H. P. (2014). Tape Casting of Anode Supports for Solid Oxide Fuel Cells at Forschungszentrum Julich. *International Journal of Applied Ceramic Technology*, 11(1), 125-135.
- Selinger, B. (2011). *Building Costs*. Illinois: DCEO.
- Shanefield, D. J. (2013). *Organic Additives and Ceramic Processing: With Applications in Powder Metallurgy, Ink, and Paint*. New York: Springer Science & Business Media.
- Shangai Shibang Machinery Co.,Ltd. (2015). www.sinoquarrycrusher.com. Retrieved July 15, 2015, from <http://www.sinoquarrycrusher.com/products/ball-mill.html>
- Siler-Evans, K.; Lima Azevedo, I.; Morgan, M.G. "Marginal Emissions Factors for the U.S. Electricity System." *Environ. Sci. Technol.* 2012. 46, 4742-4748.
- Singhal, S. C. (2007). Solid Oxide Fuel Cells. *The Electrochemical Society Interface*, 16(4), 41-44. Retrieved July 2015, from Solid Oxide Fuel Cells: http://www.electrochem.org/dl/interface/wtr/wtr07/wtr07_p41-44.pdf
- Singhal, S., & Kendall, K. (2003). *High temperature solid oxide fuel cells: fundamentals, design, and applications*. Oxford, UK: Elsevier Science Ltd.
- Sinha, J. (2010). *Direct Hydrogen PEMFC Manufacturing Cost Estimation for Automotive Applications*. Retrieved May 2015
- Stadler, Michael, Marnay, C., Gonçalo Cardoso, G. et. al. "The Carbon Dioxide Abatement Potential of California's Mid-Sized Commercial Buildings." California Energy Commission, PIER Program. CEC-500-2010-050 (2011).
- Stevenson, J. (2003, 07 8). *NETL: SECA Core Technology Program: SOFC Seal Meeting*. Retrieved June 25, 2015, from <http://www.netl.doe.gov/File%20Library/Research/Coal/energy%20systems/fuel%20cells/proceedings/OverviewStevenson.pdf>
- Sun, C., Hui, R., & Roller, J. (2010). Cathode materials for solid oxide fuel cells: a review. *J Solid State Electrochem*, 7, 1125-1144.
- Taroco, A., Santos, J., Domingues, R., & Matencio, T. (2011). *Ceramic Materials for Solid Oxide Fuel Cells, Advances in Ceramics - Synthesis and Characterization, Processing and Specific Applications*. doi:10.5772/18297
- Tax-rates.org. (2015). *Tax-rates.org*. Retrieved March 17, 2015, from <http://www.tax-rates.org/taxtables/property-tax-by-state>
- Terpstra, R., Pex, P., & de Vries, A. (1995). *Ceramic Processing*. Dordrecht: Springer Science & Business Media.
- Thorel, A. S. (2010). Tape Casting Ceramics for high teperature Fuel Cell Applications. In W. Wunderlich, *Ceramic Materials* (pp. 49-68). Sciyo.
- Trading Economics . (2015). www.tradingeconomics.com. Retrieved 03 20, 2015, from <http://www.tradingeconomics.com/united-states/mortgage-rate>
- U.S. Department of commerce. (2015). *Bureau of economic analysis*. Retrieved March 17, 2015, from http://www.bea.gov/scb/account_articles/national/wlth2594/tableC.htm
- U.S. Stoneware. (2015). *Jar, Ball and Pebble Milling*. (I. (Operating Division of ER Advanced Ceramics, Ed.) Retrieved 05 15, 2015, from <http://www.usstoneware.com/PDF/Theory%20and%20Practice.pdf>

- Verrey, J. (2006). Manufacturing cost comparison of thermoplastic and thermoset RTM for an automotive floor pan. *Composites Part A: applied science and manufacturing*, 37, 9-22.
- Wang, D.-Y., & Weng, K.-W. (2001). Deposition of CrN coatings by current-modulating cathodic arc evaporation. *Surface and Coatings Technology*, 137, 31-37.
- Wei, M., Lipman, T., Mayyas, A., Chien, J., & Chan, S. (2014, August). *A Total Cost of Ownership Model for Low Temperature PEM Fuel Cells in Combined Heat and Power and Backup Power Applications*. Retrieved 03 25, 2015, from http://energy.gov/sites/prod/files/2014/11/f19/fcto_tco_model_low_temp_pem_fc.pdf
- Weil, K. S., Coyle, C. A., Darsell, J. T., Xia, G. G., & Hardy, J. S. (2005). Effects of thermal cycling and thermal aging on the hermeticity and strength of silver-copper oxide air-brazed seals. *Journal of Power Sources*, 152, 97-104.
- Weil, S. K. (2006, August). *The State-of-the-Art in Sealing:Technology for Solid Oxide Fuel Cells*. Retrieved July 15, 2015, from Pacific Northwest National Laboratory: http://availabletechnologies.pnnl.gov/media/233_710200724950.pdf
- Weimar, M., Chick, L., & Whyatt, G. (2013). *Cost Study for Manufacturing of Solid Oxide Fuel Cell Power Systems*. Pacific Northwest National Laboratory: (PNNL).
- Whitesides, R. W. (2012). *Process Equipment Cost Estimating by Ratio and Proportion, PDH Course G127*. Retrieved June 8, 2015, from <http://www.pdhonline.org/courses/g127/g127content.pdf>
- Woodward, H. K. (2003, May). *A performance based, multi-process cost model for solid oxide fuel cells*. Retrieved March 19, 2015, from <https://www.wpi.edu/Pubs/ETD/Available/etd-0428103-235205/unrestricted/hwoodward.pdf>
- Yang, Z., Xia, G., & Stevenson, J. W. (2005). Mn_{1.5}Co_{1.5}O₄ Spinel Protection Layers on Ferritic Stainless Steels for SOFC Interconnect Applications. *The Electrochemical Society, Solid-State Letters*, 8(3), A168-A170.
- Ye, G., & Ju, F. C. (2005). Low-cost single-step co-firing technique for sofc manufacturing. *The Electrochemical Society*, 2005(07), 451-459.
- Yong, K. J., Hardy, J. S., & Weil, K. S. (2005). Novel metal-ceramic joining for planar SOFCs. *Journal of the Electrochemical Society*, 152(6), J52-J58.
- Zhang, Z. (2013). Three-Dimensional CFD Modeling of Transport Phenomena in a Cross-Flow Anode-Supported Planar SOFC. *Energies* 2014, 7(1), 80-98. doi:10.3390/en7010080